

# MORPHOLOGY OF OLEFINIC THERMOPLASTIC ELASTOMER BLENDS

*A comparative study into the structure-property  
relationship of EPDM/PP/oil based TPVs and  
SEBS/PP/oil blends*



This research described in this thesis was financially supported by the Dutch polymer Institute (DPI).

Morphology of Olefinic Thermoplastic Elastomer Blends

*A comparative study into the structure-property relationship of EPDM/PP/oil based TPVs and SEBS/PP/oil blends*

By Pratip Sengupta

PhD. Thesis, University of Twente, Enschede, The Netherlands 2004

ISBN 90 365 2108 4

Cover design: by Pratip Sengupta

Cover illustration:

Front. - Transmission electron microscopic image of EPDM/PP/oil TPV (top-left) and SEBS/PP/oil blend (bottom-left). A Transmission electron microscope is also shown on the right.

Back. - Examples of some products prepared from these blends.

Copyright © Pratip Sengupta 2004

All rights reserved

Printed by Print partners Ipskamp, Post Box 333, 7500 AH Enschede, the Netherlands



# **MORPHOLOGY OF OLEFINIC THERMOPLASTIC ELASTOMER BLENDS**

***A COMPARATIVE STUDY INTO THE STRUCTURE-PROPERTY RELATIONSHIP OF  
EPDM/PP/OIL BASED TPVs AND SEBS/PP/OIL BLENDS***

## **DISSERTATION**

to obtain  
the doctor's degree at the University of Twente,  
on the authority of the rector magnificus,  
prof. dr. F.A. van Vught,  
on account of the decision of the graduation committee,  
to be publicly defended  
on Wednesday, 1<sup>st</sup> December 2004 at 15:00 hrs

by

**Pratip Sengupta**

born on 9<sup>th</sup> February 1975  
in Nagpur, India

This dissertation has been approved by:

Promoter : prof. dr. ir. J.W.M. Noordermeer

Assistant promoter : dr. A.K. Talma

"Unity in variety is the plan of the creation"  
- Swami Vivekananda

*dedicated to my parents*

# Contents

## 1. General Introduction

1.1 Introduction	1
1.2 Motivation of the thesis	2
1.3 Aim of the thesis	5
1.4 Structure of the thesis	5
1.5 References	6

## 2. Structure – Property relationship in TPE Blends

2.1 Introduction	8
2.2 EPDM/PP TPVs	10
2.3 SEBS/PP/Oil blends	22
2.4 Application of TPVs and SEBS/PP/oil blends	27
2.5 Summary of literature survey and objective of the thesis	29
2.6 References	30

## 3. Optimization of Technique for Microstructural Characterization of Oil extended TPE Blends

3.1 Introduction	35
3.2 Principles of electron microscopy and atomic force microscopy	37
3.3 Experimental	41
3.4 Results and Discussions	44
3.5 Conclusion	55
3.6 References	56

## 4. A Comparative Study of the Structure-Property Relationship in Dynamically Vulcanized EPDM/PP/oil Blends and SEBS/PP/oil Blends

4.1 Introduction	58
4.2 Experimental	59
4.3 Results	63
4.4 Discussions	83
4.5 Conclusion	88
4.6 References	90

## **5. Modeling the Mechanical Properties of Ternary TPV and SEBS/PP/oil Blends**

5.1 Introduction	93
5.2 Model considerations	94
5.3 Modeling approach	101
5.4 Results	104
5.5 Discussions	122
5.6 Conclusions	124
5.7 References	126

## **6. Effect of Mixing Times and Evolution of Blend Morphology in EPDM/PP/oil TPVs and SEBS/PP/oil TPOs by Compounding in a Twin-Screw Extruder and Internal Mixer**

6.1 Introduction	128
6.2 Theory	129
6.3 Experimental	132
6.4 Results	136
6.5 Discussions	149
6.6 Conclusions	152
6.7 References	153

## **7. The Effect of Different Compounding and Processing Conditions on the Morphology and Properties of TPVs and SEBS/PP/oil Blends**

7.1 Introduction	155
7.2 Experimental	157
7.3 Results	163
7.4 Discussions	181
7.5 Conclusions	183
7.6 References	185

<b>Summary</b>	186
----------------	-----

<b>Samenvatting</b>	190
---------------------	-----

List of symbols	195
-----------------	-----

Abbreviations	196
---------------	-----

Curriculum vitae	197
------------------	-----

Acknowledgements	198
------------------	-----

---

# **Chapter 1**

## **General Introduction**

---

### **1.1 INTRODUCTION**

From grips on power tools to tooth brushes, from seals on car windows to syringes, from components in the car interior to residential window gaskets, wire and cable jacketing, thermoplastic elastomers (TPEs) are slowly replacing conventional vulcanized rubbers and many leading plastic materials. This is because of their good crosslinked rubber like properties, superior processability and ability to recycle scrap. These materials are being used on a large scale in everyday life, without the public being aware of the fact that they are actually TPEs and are different from the rubbers they see in the tyres of their car.

TPEs have a number of practical advantages over conventional rubbers:

1. No vulcanization and little compounding required;
2. Thermoplastic processing methods like injection molding, extrusion, blow molding and thermoforming are possible;
3. Scrap can be recycled;
4. Properties can be easily adjusted within certain limits, by changing the ratio of the components;

TPEs have been in the market for some 30 years<sup>[1]</sup> and are still experiencing a high growth rate in their usage. Five main families of TPEs are commercially important.<sup>[2]</sup> These are:

1. Styrenic block copolymers (SBCs);
2. Thermoplastic elastomer blends: (This includes thermoplastic olefinic blends (TPOs), and thermoplastic vulcanizates (TPVs);
3. Polyurethane based block copolymers (TPUs);
4. Polyether based block copolymers (TPEts);
5. Polyamide based block copolymers (TPAs);

For most TPE families, new generation materials are constantly being developed to meet the demands of customers, a large number of which are mainly automobile manufacturers. This is, because TPEs can easily meet the physical, chemical and aesthetic requirements of several automotive products and provide cost advantages and design flexibility to the automotive engineer.

Intra-TPE competition is emerging now, as broader families of these materials are becoming more familiar to a wider range of potential customers. Soft-touch applications such as mobile phone grips, computer accessories, pen and toothbrush handles, knobs and sports goods are targets for soft-touch TPVs, styrene-(ethylene-butylene)-styrene block copolymers (SEBS) and TPUs. Similarly in the automotive sector, driver-side airbag covers and instrument panel skins are targets for TPO, TPV, and TPU materials, depending on the models and the motor company's requirements and philosophy towards design, style and comfort.

## **1.2 MOTIVATION OF THE THESIS**

Thermoplastic elastomer blends of rubber and plastic, which cover about 50 % of the market share in TPE business,<sup>[1]</sup> are clearly the most exciting among TPE families. TPEs made this way have gained considerable importance in recent years, because the blends give rise to certain properties that cannot be attained by other means or from individual components. Blends with two or more phases can be organized into a variety of morphologies. The mechanical properties of the blends critically depend on the nature of this arrangement of the phases. These properties are mainly the mechanical and rheological characteristics. So morphology is generally considered to be a key parameter that must be tailored to achieve the desired mechanical properties of polymer blends.

In this thesis two different rubber blends with polypropylene are compared, which show similar properties despite having dissimilar morphologies. The resulting blends are very popular TPE materials. One of them is a blend of dynamically vulcanized ethylene-propylene rubber (EPDM) with isotactic polypropylene (PP) in which the EPDM phase is vulcanized using a phenolic resin cure system. This blend belongs to the family of TPVs. Although TPVs can be made from different combinations of rubber and plastics, in this thesis the term TPV is used to imply crosslinked EPDM/PP/oil blends. The other one is a blend of styrene-(ethylene-butylene)-styrene block copolymer (SEBS) with isotactic PP, belonging to the family of TPOs. In this thesis the term TPO is sometimes used to refer the SEBS/PP/oil blends. The difference between TPVs and TPOs is that the rubber phase is chemically crosslinked during mixing in a TPV and not in a TPO. In addition to the rubber and PP component, both blends also contain a significant amount of paraffinic oil, added mainly for reasons of processability and to vary the hardness of the compounds. The EPDM/PP TPVs are reported to have a dispersed EPDM phase in a PP matrix.<sup>[3]</sup> The SEBS/PP blends are reported to have a co-continuous morphology.<sup>[4]</sup> The similarity in the properties of these two blends makes them competitive materials for similar sorts of applications and, at the same time very interesting materials for studying the complex relationship between morphology, rheology and properties of rubbery polymer blends.

TPVs based on dynamically vulcanized EPDM and PP are already commercially available from the 1970's.<sup>[1]</sup> Dynamic vulcanization implies that the EPDM phase is vulcanized during the process of its melt mixing with PP. The vulcanizing agent can be sulfur, a phenolic resin system or organic peroxide. Studies on the structure-property relationship in these systems, especially when using phenolic resin as curative agent for the EPDM phase, are not totally new.<sup>[5-7]</sup> However, some fundamental questions related to the morphology of these systems are still not understood. The dispersed nature of the EPDM phase in blends with high rubber and oil content is questionable. Electron microscopy images of TPVs having EPDM contents larger than 60 vol.-% are very difficult to interpret. They give an impression of a continuous rubber phase: Figure 1.1. If this is true, how it is possible for such a blend to demonstrate thermoplastic processability? Some other questions that need to be addressed are: How sensitive are the mechanical properties to the morphology in these blends? What are the influences of composition, shear rates, preparation methods (batch versus continuous process), melt flow index of PP, screw configuration (twin-screw extruder) on the morphology of these blends? How is the morphology related to rheology and processability?

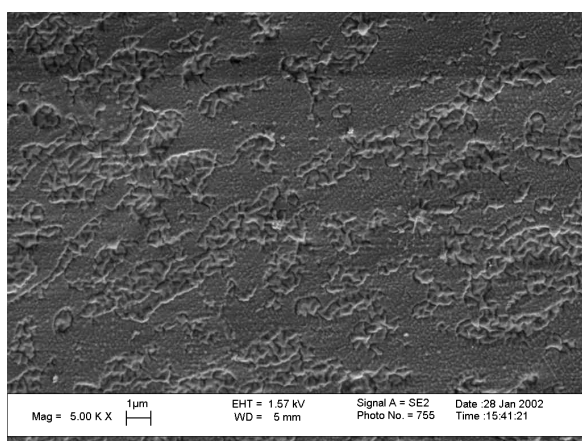


**Figure 1.1** Scanning electron microscopy of an EPDM/PP/oil TPV blend.

Blends of SEBS rubber with PP are relatively new as compared to TPVs and practically little information is known about them. SEBS itself is a thermoplastic elastomer, in which rubbery ethylene-butylene blocks are sandwiched between two polystyrene blocks: Figure 1.2. They belong to the family of styrenic block copolymers, abbreviated as SBCs. The polystyrene phase and ethylene-butylene phases in SEBS are phase separated. Below the glass transition temperature of the polystyrene blocks (around 100°C), the polystyrene blocks are physically crosslinked into clusters of 20 nm, which provide elasticity to the network: Figure 1.3. These are



comparable to the chemical crosslinks in the EPDM phase in TPVs. Adding PP to SEBS increases the processability of SEBS.<sup>[8]</sup> Further, the upper service temperature and solvent resistance is improved. Much higher strength is obtained and the blends are optically transparent.

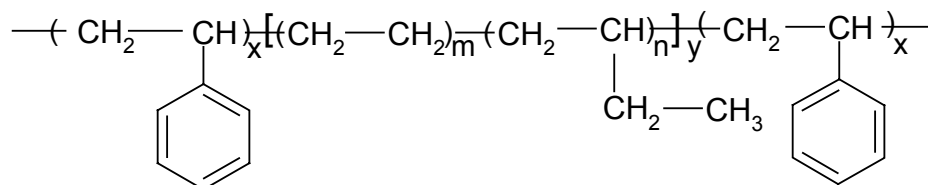


**Figure 1.2** Molecular structure of SEBS block copolymer.

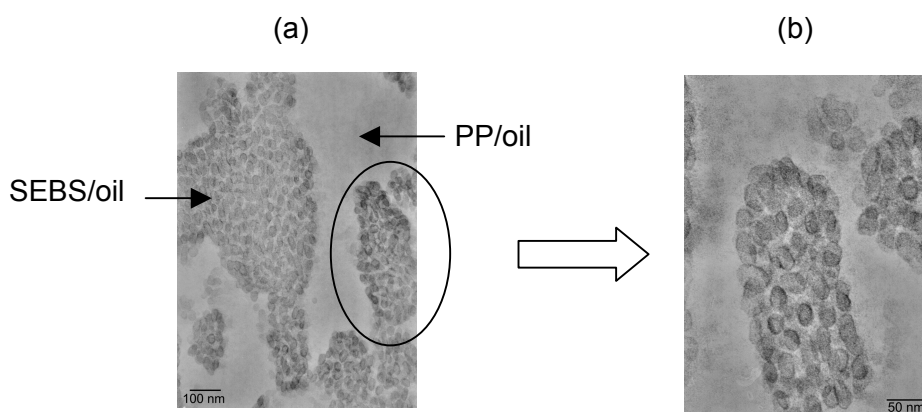


**Figure 1.3** TEM images of (a), SEBS/PP/oil blends; (b), magnified image of SEBS phase

Open literatures on the structure-property relationship of SEBS/PP/oil blends are rare. The reason for their resemblance in properties with TPVs is largely unknown. A major issue is the role of oil in these TPE blends. It is possible to make olefinic TPEs with different hardness by varying the PP-rubber ratio. The softness of a TPE is generally increased by lowering the PP content and adding oil or by both. Besides reducing the hardness, the oil also serves as processing aid allowing the blend to flow smoothly during extrusion and injection moulding. Although oil-amounts as high as 200 parts per hundred rubber are sometimes added to these TPE formulations, its role in the properties of a TPV is poorly understood. Some of the vital questions in this respect are: (a) How is the oil distributed between the phases in the melt and in the solid state? (b) Does it change the morphology? (c) How does it change the rheology and other properties?

Both types of products are presently making inroads as potential replacements for vulcanized rubbers. The melt flow properties and surface appearances, as influenced by melt fracture phenomena, are major points of concern. This processability is determined by the particular morphological structures of these compounds under processing conditions. The

technological approach taken by most companies is to solve these problems in an empirical way, by optimizing the choice of the raw materials. A morphological study linked with rheological characterization of the blends under processing conditions will greatly help in the understanding of the underlying mechanisms. This can provide new leads to optimization of these blends in view of their intended use.

### **1.3 AIM OF THE THESIS**

This thesis will investigate the inter-relationship between morphology, rheology and mechanical properties of oil extended EPDM/PP TPVs and SEBS/PP TPOs. The primary goal is to investigate how the properties of these TPE blends are determined by the properties of the component polymers and by the blend morphology that is created during the melt mixing process by changing the composition and processing conditions. The use of different microscopic techniques for the study of the morphology of these systems and the possibility of extending from 2D-imaging to 3D-imaging will be explored. Further different possibilities to alter the morphology of these blends and studies on the effect on the rheology and mechanical properties will be reported.

### **1.4 STRUCTURE OF THE THESIS**

The necessity of comparing the structure-property relationship of these two TPEs must be stated first. Chapter 2 will cover the background of each TPE with special emphasis on the analogy in the mechanical properties of these systems. A short review of the morphology and deformation behavior of these blends is also given.

The use of different microscopic tools, like scanning electron microscopy (SEM), low voltage scanning electron microscopy (LVSEM), atomic force microscopy (AFM) and transmission electron microscopy (TEM) for morphological studies on these systems will be examined in Chapter 3. The pros and cons of each technique normally associated with oil extended blends will be discussed. This will be useful to optimize a suitable characterization technique for the blend morphology. Further, extension from 2D-imaging, to 3D-imaging using electron tomography, a traditionally biological technique, will be covered.

Chapter 4 will show a one-to-one comparison of the mechanical properties of oil-extended dynamically vulcanized EPDM/PP TPVs and SEBS/PP blends. Studies on the compositions of each blend type differing in PP and oil content, prepared using internal mixer and twin-screw extruder will be reported. The studies will cover the stress-strain, thermal, dynamic mechanical and compression set properties in addition to morphology of these blends.

The stress-strain properties of these blends must somehow be related with the properties of individual phases in the blends. The correlation between morphology and mechanics of deformation will be explored in Chapter 5. The modeling of the stress-strain behavior of these TPE blends, using data about oil distribution between the components and stress-strain data of binary oil blends, will be presented.

Chapter 6 will investigate the evolution of morphology in an internal mixer and twin-screw extruder. This will be useful to interpret the morphology images presented in the previous chapter and will lead to ways for changing the morphology of these blends.

Different possibilities to alter the morphology of these blends will be explored in Chapter 7. Factors like melt flow index (MFI) of PP, shear rate of mixing, temperature and time of mixing, compression moulding conditions and their effects on the morphology and properties of these blends, will be reported.

Finally, in Chapter 8 conclusions will be drawn on the findings of all previous chapters and suggestions will be made as to the directions of any further research, which may be undertaken.

## 1.5 REFERENCES

1. P. Dufton, *"Thermoplastic Elastomers"*, RAPRA Technology Ltd., Shawbury, (2002).
2. S. K. De, A. K. Bhowmick, *"Thermoplastic Elastomers from Rubber-Plastic Blends"*, Ellis Horwood Ltd., Chichester, West Sussex (1990).
3. A. Y. Coran and R. Patel, *Rubber Chem. Technol.*, **53** (1980) 141.
4. B. Ohlsson, H. Hassender and B. Tornell, *Polym. Eng. Sci.*, **36** (1996) 501.
5. H.J. Radusch and T. Pharm, *Kautsch. Gummi Kunsts.*, **49** (1993) 249.
6. O. Chug and A. Y. Coran, *Rubber Chem. Technol.*, **70** (1997) 781.
7. F. Goharpey, A. A. Katbab and H. Nazockdast, *J. Appl. Polym. Sci.*, **81** (2001) 2531.
8. G. Holden and N. R. Legge, *"Thermoplastic Elastomers-A Comprehensive Review"*, Ed. N. R. Legge, G. Holden and H. E. Schroeder, Hanser Gardner Publication, New York (1997).

---

## Chapter 2

### Structure - Property relationship in TPE blends

---

The available know-how on the structure-property relationships of EPDM/PP TPVs and SEBS/PP/oil blends is reviewed. Although there is quite some open literature on morphology, mechanical and thermal properties, rheology and processing of TPVs, comparable information on SEBS/PP/oil blends is very limited. TPVs have undergone an evolutionary change in the design of curing system, compounding techniques and method of production aiming at higher elasticity, thermal stability and better processability. New researches in TPVs have focused on understanding the oil distribution between the phases, deformation mechanisms and evolution of morphologies during blending. Studies on soft TPVs containing a high volume percent of rubber and oil are however limited. The morphologies of these blends appear to be co-continuous, which is in contradiction to their thermoplastic processability. The properties of these compositions are close to that of SEBS/PP/oil blends, which make them both suitable for a lot of common applications in automobiles, soft-touch goods, medical applications etc.

Research on SEBS is mainly focused on its use as a compatibilizer and impact modifier for brittle thermoplastics. SEBS/PP/oil blends as a potential alternative to vulcanized EPDM rubber have been developed only in the early 1990's. Preliminary research on these blends has given some insight into their morphology, mechanical and thermal properties, rheology, processing and oil distribution. More fundamental studies on understanding their deformation mechanism, oil distribution in the melt and morphology evolution are still not reported.

The present chapter gives a comprehensive overview of the various research works in the field of TPVs and SEBS/PP/oil blends reported so far.

## 2.1 INTRODUCTION

Polymer blends are a smart and economical way to combine the properties of two or more polymers into a single product. Due to positive entropy of mixing, most polymer blends are however immiscible and show phase separation. The phases in immiscible polymer blends can arrange themselves in three types of morphologies: (a) dispersed phase morphology, (b) stratified morphology, (c) co-continuous morphology.

The morphology is determined by several factors: (a) nature of the polymers, (b) interfacial tension, (c) the ratio of the viscosities of the components, (d) volume fraction of the components, (e) processing conditions – both the mixing equipment and the process factors are important. The mechanical properties of these blends are very much dependent on morphology. Dispersions of droplets of the minor phase in a matrix of the major phase are most common. These types of blends are used in rubber modification of brittle polymers to improve the impact properties.<sup>[1-4]</sup> The minor phase can also be dispersed as fibers: in these blends the properties are mainly improved in the direction of the fibers.<sup>[5-7]</sup> Blends with stratified structure enhance barrier properties<sup>[8]</sup> and co-continuous morphologies show a combination of the characteristics of both polymer components.<sup>[9-11]</sup> The transfer of load and energy between the components depends on the arrangement of the phases and the extent of adhesion between them. In case of poor adhesion, a compatibilizer is necessary.

Apart from influencing the solid-state properties, the morphology also influences the rheological properties of the blends. The opposite is also true for many polymer blends. i.e. the morphology can change during processing operations. This has far reaching implications. These blends are processed through different techniques like injection molding, extrusion, blow molding and compression molding in the course of their fabrication into useful products. Since the morphology of immiscible blends is intricately related to the flow behavior during processing and this morphology determines the end-use properties, understanding the relationship between these factors is necessary for successful design of a product. The complex interrelationship between morphology, rheology and processability is shown schematically in Figure 2.1.

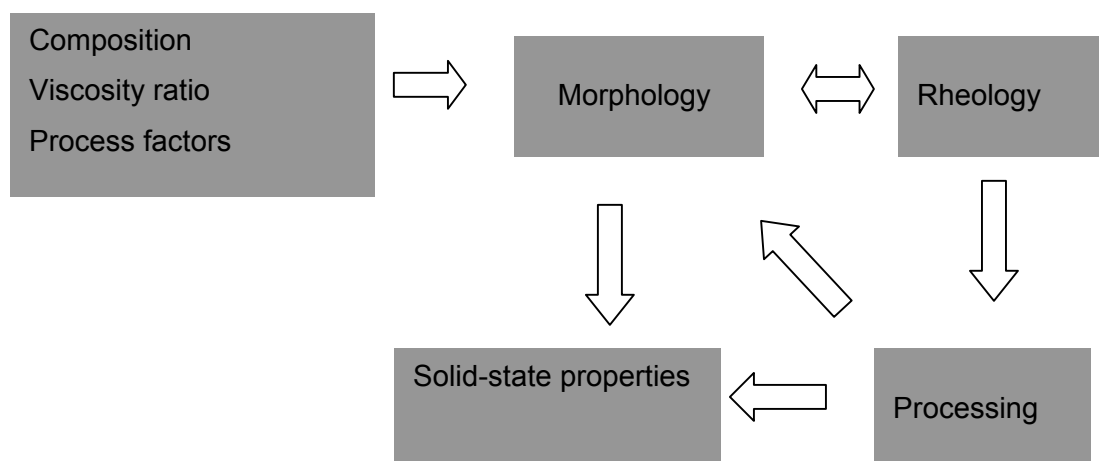


**Figure 2.1** Schematic representation of the relationship between morphology, rheology and properties in polymer blends.

Thermoplastic elastomer compounds based on blends of isotactic polypropylene and rubber are designed to provide thermoplastic processability and rubber-like properties in a single product. Rubbers that have been successfully blended with polypropylene to give technically useful thermoplastic elastomer blends are natural rubber (NR)<sup>[12]</sup>, ethylene propylene-diene rubber (EPDM)<sup>[12]</sup>, acrylonitrile-butadiene rubber (NBR)<sup>[12]</sup> and styrene-(ethylene-butylene)-styrene rubber (SEBS).<sup>[13]</sup> The best elastomer-PP blends are those in which the solubility parameters of the polymers are matched, entanglement molecular length of the elastomer is low, and when the PP is 15 - 30% crystalline.<sup>[11]</sup> For polymers differing in solubility parameter (ex. PP and NBR), one must resort to compatibilization techniques.<sup>[14,15]</sup> The relationship between morphology-rheology-properties of rubber-PP blends has been the subject of extensive research. This has led to significant understanding of the fundamental principles governing the properties of these blends, resulting in versatility in product design and performance.

The objective of this chapter is to get a comprehensive insight into what is known on the structure-property relationships of dynamically vulcanized EPDM/PP blends and unvulcanized blends of SEBS with PP. Unfortunately, the amount of open literature about SEBS/PP blends is very limited as compared to EPDM/PP TPVs. Except for the papers of Ohlsson<sup>[16]</sup> and Veenstra<sup>[17]</sup> there is hardly any other paper that has directly addressed the structure-property relationship of these blends. Therefore the present review on SEBS/PP/oil blends is mainly based on findings of these two investigations.

This chapter is divided into two sections. In the first section, literature on TPVs will be illustrated. Blends of SEBS with PP will be reviewed next.

## 2.2 EPDM/PP TPVs

### 2.2.1 General product definition

EPDM/PP TPVs are different from conventional blends of EPDM/PP, structurally and property wise. In TPVs, the EPDM phase is crosslinked during mixing with PP under dynamic shear, a process known as dynamic vulcanization. Although the content of EPDM usually exceeds that of PP, after dynamic vulcanization the soft EPDM phase is dispersed in the hard PP matrix. Historically, Uniroyal Chemical Corporation was the first company to introduce dynamically vulcanized EPDM/PP blends. This was based on the work of W.K. Fisher<sup>[18]</sup> who filed patent applications in 1971 on his discovery of partially crosslinking the EPDM phase of EPDM/PP blends with peroxide. Since peroxide degrades PP during mixing, Fisher limited the amount of peroxide in his compositions, resulting in partially crosslinked TPVs. These blends came into focus in 1978, after the detailed study by Coran and Patel<sup>[19,20]</sup> on the morphology, tensile properties, compression set and solvent swelling characteristics of sulfur cured EPDM/PP blends. Investigations made by Coran *et al.*<sup>[20]</sup> revealed that:

1. As compared to conventional non-vulcanized EPDM/PP blends, significant improvement in permanent set, mechanical properties, fatigue resistance, oil resistance, and temperature resistance can be achieved by dynamic vulcanization.
2. Best values of tensile strength, modulus, hardness and tension set are obtained when the elastomer particles in the blends are small enough (1-1.5  $\mu\text{m}$ ) and if they are fully vulcanized.

The initial studies by Coran and Patel delineated the scope and potential utility of these TPVs. Further research was carried out to study the interrelationship between the nature of the base polymers, curing systems, morphology, rheology, production methods and properties of TPVs. This section provides leading references for an introduction to TPV materials.

### 2.2.2 Influence of PP and EPDM grades

The grade of EPDM can have a pronounced influence on the properties of TPVs. The influence of ethylene content, diene content and molecular weight of EPDM, on the morphology,

crosslink density, tensile properties and compression set of TPVs has been studied by Datta,<sup>[21]</sup> using factorial design of experiments. The experiments showed that the requirements of EPDM for better tensile properties and compression set properties are diagonally opposite. Low molecular weight EPDM with low ethylene and diene content results in TPVs with better rubber properties, like improved compression/tension set. According to Legge<sup>[22]</sup> these grades are also better in low temperature properties. High molecular weight EPDM grades with a high weight ratio of ethylene and diene content result in TPVs having high tensile and tear properties.<sup>[21]</sup> The experiments showed that a reduction in diene content results in an increase in crosslink density.<sup>[21]</sup> The reason for this peculiar observation was related to the rate of curative diffusion. If the number of double bonds are too high, a highly crosslinked shell is formed around a lightly crosslinked core, and so curative diffusion to the core is difficult. Low molecular weight EPDM gives a weaker composition - lower E-moduli and tensile strength - than high molecular weight EPDM at similar amount of curative. According to Sabet *et al.*<sup>[23]</sup>, these EPDM grades also required higher amounts of curatives to achieve similar crosslink densities as high molecular weight EPDM.

Although the soft phase is important for elastic properties, most TPV properties are dominated by the hard matrix phase. In addition to processing temperatures, key properties such as thermal softening, heat deflection temperature and physical properties at elevated temperatures are directly influenced by the PP phase.<sup>[24]</sup> The amount of open literature on this subject is limited. According to Ellul<sup>[25]</sup>, TPVs with improved elastic properties, both in the solid state and melt, can be prepared if long chain branched PP is used instead of linear PP. The improved elasticity comes from a different deformation mechanism in which the EPDM phase is deformed first, almost independent of PP.

### 2.2.3 Influence of curative system

The choice of crosslinking system is important in TPVs, because apart from imparting elasticity, they influence the wetting characteristics and interfacial adhesion of the EPDM and PP phases as they are being mixed, with a resulting influence on the mechanical properties. Sulfur curing of EPDM results in TPVs with poor compression set properties.<sup>[23]</sup> This is because, sulfur crosslinks of any unsaturated rubber, including EPDM often result in structures of the following type (Figure 2.2a), where x and y are about 1-2 for efficient vulcanization systems and 2-4 for conventional systems:<sup>[26]</sup>



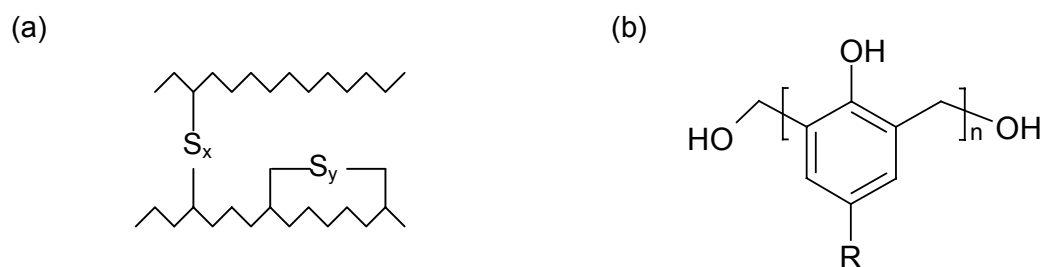


**Figure 2.2** (a), Typical structure of sulfur bridges in sulfur cured elastomers; (b), Typical structure of resol ( $R$ = iso-octyl and  $n = 1-3$ ).

The sulfur present in the cyclic ring ( $y$ ) and the excess sulfur in the crosslinks ( $x$ ) contribute to the poor compression set properties. The TPVs swell considerably in aliphatic, aromatic or chlorinated hydrocarbons. Additionally, sulfur cured EPDM/PP TPVs show poor surface appearance during extrusion or injection molding.

Significant improvements in the compression set, oil resistance and processing characteristics of these TPVs were obtained by Abdou–Sabet and Fath in 1977.<sup>[27]</sup> They used a cure package consisting of a resol phenolic resin (dimethyloctylphenol), cure activator (stannous chloride dihydrate) and zinc oxide instead of sulfur. The typical structure of the resol is shown in Figure 2.2b. Zinc oxide acts as hydrogen chloride or bromide scavenger and promotes the reaction of phenolic resin. According to these investigations, the phenolic resin reacts only with the EPDM phase i.e., there is no substantial quantity of graft formation between the polyolefin resin and the EPDM rubber. The reactivity depends on the type and amount of diene present in the EPDM. Ethylidene-Norbornene (ENB) diene contents in amounts higher than 2.5 wt.-% are sufficient to completely cure the EPDM phase in TPVs.<sup>[27]</sup> The rubber is said to be completely cured, when it is vulcanized to the extent that no more than about three-percent of the rubber is extractable in cyclohexane at 23 °C or no more than about five percent of the rubber of the blend is soluble in boiling xylene.<sup>[27]</sup>

Various mechanisms have been proposed to interpret phenolic-diene cure. In some models, dienes are consumed leading to a saturated backbone during cure<sup>[28]</sup>, while in others, double bonds are preserved.<sup>[29]</sup> Recent experiments by Ellul *et al.*<sup>[30]</sup> suggest that some but not all of the double bonds are consumed during curing with the phenolic resin curative, indicating that more than one curing mechanism could be present.

TPVs cured with resol often stain painted surfaces. The presence of stannous chloride also makes them hygroscopic, which necessitates a pre-drying step before extrusion and injection

molding. The extent of staining can be reduced if the phenolic resin curatives are esterified, - e.g. acetylated, tosylated, silylated or phosphorylated - before using as a curative.<sup>[31]</sup>

Peroxide/coagent curing of TPVs is not so common because of its degrading effect on PP. So preparing TPVs with high crosslink density is difficult using peroxide cure. Recently, some advances have been made in this direction by use of an EPDM with vinylidene norbornene as the diene.<sup>[25]</sup> Naskar *et al.*<sup>[32]</sup> studied the effect of different peroxides on the mechanical properties of TPVs. Dicumyl peroxide (DCP) curing assisted with triallyl cyanurate (TAC) as coagent gave the best combination of properties, because of better solubility parameter match with EPDM. A major problem with the DCP/TAC combination is the smell and bloom caused by side products of the vulcanization.<sup>[33]</sup> Recently, use of multifunctional peroxides combining peroxide and coagent functionality in one single molecule are reported which give properties comparable to DCP/TAC combinations in TPVs and without the aforementioned negative effects.<sup>[33]</sup>

Novel curing agents based on organosilane have been reported for TPVs as well. Synthesis and mechanical properties of TPVs based on these organosilanes are reported by Fritz *et al.*<sup>[34]</sup>

The crosslink density of the EPDM phase in TPVs is difficult to estimate. In one approach it was assumed that PP does not change the crosslink density of the EPDM phase, i.e. there is little or no resin interaction with the PP.<sup>[11]</sup> In that case, samples of EPDM vulcanized under conditions, selected to simulate the conditions of dynamic vulcanization, can be used. Crosslink densities of these samples can then be measured with solvent swelling using the Flory Rehner equation.<sup>[11]</sup> However, static vulcanization of EPDM is not equivalent to dynamic vulcanization due to lack of high shear and longer time scales, which translate to different cure efficiency. Other methods based on the use of Proton Nuclear Magnetic Resonance Spectroscopy (<sup>1</sup>H-NMR) and Dynamic Atomic Force Microscopy (AFM) are discussed by Ellul *et al.*<sup>[35]</sup> An increase in crosslink density shows up as broadening of the peak base in <sup>1</sup>H-NMR and an increase of force modulation amplitude in dynamic AFM. The results are influenced by the presence of PP, fillers, inhomogeneities in the magnetic fields, and therefore a comparison of the crosslink density among TPV samples with different PP and filler contents cannot be made. In addition, the <sup>1</sup>H-NMR experiments are difficult to perform, because the spectrometer conditions must be kept the same and experiments should be done with the same shimming parameters. Another option is to use Electron Spin Resonance (ESR) spin probe as reported by Marinovic *et al.*<sup>[36]</sup> In this method a probe (2,2,6,6-tetramethyl-4-oxopiperidinoxy) is incorporated in the EPDM phase. The probe partitions into two motionally different environments in the EPDM domains above T<sub>g</sub>, depending

on the density of crosslinks. The ratio of the amount of motionally slow component to the amount of fast component increases with increase in crosslink density.

The most common procedure used to evaluate the state of cure consists of determining the amount of rubber soluble in cyclohexane or boiling xylene. As explained before, the rubber is regarded as fully cured when it is cured to the extent that no more than about three percent of the rubber is extractable in cyclohexane at 23 °C or no more than about five percent of the rubber in the blend is extractable in boiling xylene.<sup>[27]</sup> Using a phenolic resin and stannous chloride curative package, fully cured TPV compositions can be obtained.

#### 2.2.4 Production methods

Thermoplastic vulcanizates of EPDM/PP are produced using either batch or continuous mixing techniques. The most common batch mixers are internal intensive mixers, such as the Banbury mixer. In the internal mixer, usually the EPDM and PP are first melt-mixed and afterwards vulcanizing agents are added. If the curatives are added after the rubber and molten plastic are thoroughly mixed and intimately dispersed, crosslinking of the rubber usually occurs after the polymers are thoroughly mixed. If vulcanizing agents are added in the beginning together with the polymers, a part of the vulcanization occurs before melting and mixing of the plastic with the rubber. Later, with further mixing, the rubber domains are broken down by the shearing action of the mixer or mill. Experiments by López-Manchado *et al.*<sup>[37]</sup> show that these differences have no influence as such on the tensile properties of TPVs.

Continuous mixing techniques can be performed in co-rotating twin-screw extruders. Till recently, the dynamic vulcanization processes were not entirely satisfactory for making soft compositions because, as the rubber level rises, the resulting compositions become less processable. For example, the compositions give poor extrudates and, sometimes, cannot be extruded at all. Accordingly, there is a need for processes for preparing soft, extrusion-processable, thermoplastic elastomeric compositions. According to a patent from Abdou-Sabet *et al.*<sup>[38]</sup>, the properties of the extrudate can be improved if the plastic and the rubber are subjected during vulcanization to a shear rate of about 2500 to 7500 s<sup>-1</sup>. The thermoplastic elastomer compositions so produced exhibit superior tensile properties, including higher tensile strength and greater elongation at break and also exhibit better processability. The compositions prepared under low shear rate conditions in a Banbury mixer (about 360 s<sup>-1</sup>) are not satisfactorily processable by extrusion.

### 2.2.5 Morphology

As already mentioned, TPVs are characterized by a rubber phase dispersed in the form of small particles in a PP matrix. The dispersed EPDM phase may contain trapped PP.<sup>[39]</sup> Similarly, the matrix PP phase might contain a small amount of rubber.<sup>[39]</sup> Typical rubber particle sizes for phenolic cured TPVs are within 1-5 microns. Such dispersed phase morphology has not been widely accepted, especially when it came to explaining the true elastomeric properties of the soft elastomer products, i.e. 64 and 55 Shore A hardness products. Interaction among the rubber particles, leading to a network of vulcanized elastomer phase that gives the appearance of two co-continuous networks, has been proposed.<sup>[22]</sup> Studies focused on establishing the dispersed phase morphology of TPVs were made by Sabet *et al.*<sup>[23]</sup> His experiments showed that the EPDM phase was dispersed even in a 80/20 EPDM/PP blend.

The particle size of EPDM in TPVs can be altered by different methods. A high mismatch in melt viscosity between the EPDM and PP phase results in larger EPDM particles.<sup>[21]</sup> The second option is to increase the EPDM/PP ratio. If carbon black filled EPDM is used as starting materials for the preparation of TPVs, larger particles are obtained after dynamic vulcanization as compared to TPVs with corresponding unfilled EPDM.<sup>[40]</sup> The curing system also influences the particle size. Sulfur curing results in a larger particle sizes as compared to phenolic resin cured TPVs. This is because the sulfur links can exchange among themselves, a capability that would cause the rubber particles to coalesce.<sup>[22]</sup> The amount of curative affects the particle size distribution. An increase in curative content results in narrower EPDM domain size.<sup>[41]</sup>

The development of morphology of these blends has been documented by several authors.<sup>[23, 42]</sup> Since morphological changes are very fast, special sampling devices<sup>[43]</sup> are necessary to quickly take out a sample from the mixer and cold-quench it with little chance of coalescence. The initial morphology, i.e. the morphology before the addition of curing agent varies both with the viscosity ratio of the components and the blend composition. In most cases, the rubber phase is found to be dispersed in the PP-matrix. In case the viscosities are close, the morphology becomes co-continuous, which then undergoes phase inversion.<sup>[43]</sup> Whatever might be the initial morphology, upon addition of the crosslinking agent, it changes into dispersed phase morphology of EPDM in PP.

Usually, TPVs based on EPDM/PP do not need compatibilization. This is because the solubility parameters are close to each other. The mechanical properties can be further improved

if the blends are in-situ compatibilized by ultrasonic treatment prior to dynamic vulcanization or first dynamically vulcanized and then ultrasonically treated.<sup>[44]</sup>

### 2.2.6 Rheology

The viscosities of both EPDM and PP are highly shear-sensitive, with significant drops at high shear rates. At high shear rates the viscosity difference between EPDM and PP is reduced, which is desired to decrease the size of the dispersed rubber particles.<sup>[2]</sup> The effect of dynamic vulcanization on the viscoelastic properties of EPDM/PP blends was reported by Coran *et al.*<sup>[19]</sup>, Katbab *et al.*<sup>[40]</sup> and Steeman *et al.*<sup>[45]</sup> Experimental studies show that TPV melts behave similarly to filled polymer systems. The TPVs show a higher viscosity as compared to corresponding unvulcanized blends. The rheological behavior further depends on the applied stress. Unlike PP, at low stresses the materials shows a yield stress, which is attributed to the presence of an interacting network of rubber particles. The presence of a yield stress was experimentally proved by Han and White.<sup>[46]</sup> At higher stress, passing the yield stress, this network is broken and the material flow behavior follows a power law model. As the concentration of EPDM phase increases with respect to PP, the shear viscosities of the TPVs increase as well and the blend viscosities show much higher values at lower stress. The yield stresses also increase sharply with increasing rubber content. Moreover, unlike for PP, the Cox-Merz rule stating the equivalence between the dynamic viscosity and steady state viscosity is not obeyed.<sup>[47]</sup> This means that complex viscosity data cannot be used to predict the steady state response of the polymer melt.

Studies on the dynamic properties of TPVs - dynamic modulus of elasticity and viscosity, over a wide range of frequency and strain amplitude - have been reported by Marinovic *et al.*<sup>[36]</sup> The storage and loss moduli decrease gradually with increasing strain. Such behavior resembles that of rubbers with active fillers such as carbon black or silica. The decrease in dynamic functions in filled polymers is commonly quoted to be caused by the breakdown of the secondary filler network.<sup>[34]</sup> In TPVs the secondary structure is represented by molecules of PP being anchored in EPDM particles. The drop of storage modulus with increasing strain is fastest for samples with the highest degree of crosslinking. Initially, the storage modulus is higher than the loss modulus, i.e. the material exhibits more elastic behavior. With increasing deformation the TPVs become progressively more viscous and the two curves intersect.

A usual way to quantify the molecular weight of PP is by its melt flow index (MFI). In this test the amount of material extruded from a capillary at 230°C/2.16 kg is measured. This experiment was found unsuitable for TPVs, because the low L/D ratio of the capillary does not allow for fully developed flow. Moreover the L/D ratio of the capillary is in the range of the Bagley correction for TPVs and so the melt flow index not only depends on the viscosity of the polymer, but also on the entrance pressure drop. However, in our opinion the test is not suitable for TPVs due to the presence of a yield stress that makes it difficult to flow. In this study the die swell and draw down ratio of a 60 Shore A TPV material was also investigated.<sup>[47]</sup> A relatively low level of die swell was observed, which was accounted for by the fact that the vulcanized rubber particles reduce the mobility of the chains under the influence of applied shear stress. The melt draw ratio, although low, was found to be high enough for use in blow molding and foaming applications.

Studies on the shear and uniaxial elongational viscosity of TPVs have been reported by Han and White.<sup>[46]</sup> While the elongational viscosity of PP is roughly constant as a function of shear rate, for TPVs, both viscosities are decreasing functions of shear rate. The elongational viscosity is roughly three times larger than the shear viscosity.

### 2.2.7 Properties

Stress-strain plots of TPVs are extensively reported in publications. A typical stress-strain plot of TPVs is shown in Figure 2.3 below.

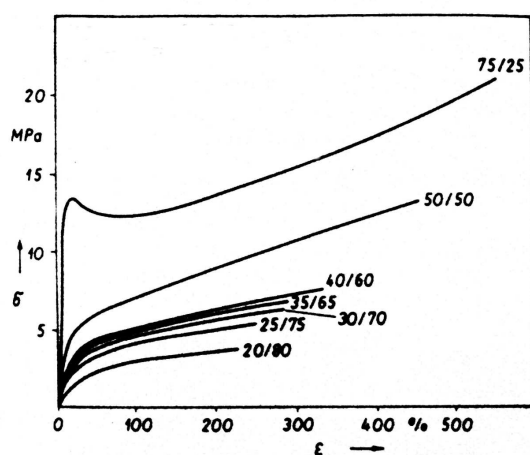


**Figure 2.3** Stress-strain curves of EPDM/PP TPVs at different compositions of EPDM/PP. <sup>[48]</sup>

The stress increases sharply with strain and then gradually, after passing through the yield point of the PP. The yielding process undergoes changes with increase in EPDM content, such that the yield peak disappears at a composition ratio of 80/20 wt.-% EPDM/PP. The tensile behavior shifts towards that of vulcanized EPDM. The tensile strength of the TPVs is higher than that of the corresponding unvulcanized blends. The tensile strength of TPVs shows an inverse relationship with increasing EPDM content, which is explained by the increase in the concentration of semi crystalline PP as the continuous phase.<sup>[42]</sup> The tensile strength and elongation at break values are an inverse function of elastomer particle diameter.<sup>[20]</sup> In general, TPVs do not require much compounding to achieve the desired combination of properties. Usual additives are oil, clays, pigments and stabilizers. Fillers like carbon black impart better tensile properties than unfilled samples.<sup>[40]</sup>

Thermal properties of TPVs were reported by Xiao *et al.*<sup>[49]</sup> Their results show that, in TPVs with increase in curative concentration, the crystallization temperature and the degree of crystallinity of the PP phase decreases whereas the melting temperature of PP increases. The influence of cooling rate on the crystallization behavior and subsequent structure development of the PP-matrix in TPVs was investigated by Scharnowski *et al.*<sup>[50]</sup> They concluded that the rubber phase influences the structural development of the PP-matrix by hindering the crystal growth, resulting in smaller spherulites. On the other hand, the rubber phase acts as a nucleating agent, which leads to formation of more stable crystals. Interestingly, these authors suggest that the stannous chloride added to the phenolic resin cured TPVs acts as a nucleating agent for PP.

Reprocessability studies of TPVs and reproducibility of measured solid state and melt properties were reported by Marinovic *et al.*<sup>[36]</sup> Their results indicate that melt viscosity, tensile strength and elongation at break of the TPV remain almost constant (varying within 2-9%) even after three cycles of repeated preheating and extrusion.

### 2.2.8 Deformation behavior of EPDM/PP TPV

The conventional picture of a TPV consists of cured rubber particles dispersed in a matrix of thermoplastic polymer. In such morphology it is expected that the ductile nature of the thermoplastic will dominate during deformation, giving rise to poor elastic behavior and high compression set values. However, the TPVs are able to shrink back from their highly deformed state just like a vulcanized elastomer even though the matrix consists of ductile polymer. Thus

the bulk properties of TPVs are not governed by the ductile nature of the matrix, but mostly by that of the elastic dispersed phase.

Various workers<sup>[51-56]</sup> have carried out studies on the deformation mechanism of EPDM/PP-TPVs. The results of current modeling approaches are in stark contrast with one another. According to the two-dimensional model of Kikuchi *et al.*<sup>[51]</sup> at least 70% of the PP matrix is deformed beyond its yield point when the material is stretched. The rest 30% PP are present at the particle poles and are unyielded due to lower stress concentration. The unyielded polar ligaments connect the rubber domains and allow for elastic recovery. This model fails to explain how the elastic forces in the EPDM-phase can pull back such large amounts of plastically deformed PP. According to the model suggested by Kawabata,<sup>[52]</sup> the adhesion between the particles and the matrix is very weak apart from a few points on the interface, so that large amounts of voids are formed when the TPV is deformed. These voids allow the rubber to deform mechanically independent of the matrix, while the small areas in which the rubber particles are still connected to the matrix hold the material together. How adhesion and debonding can occur on the same particle-matrix interface is not explained in this model.

Recent studies by Boyce and coworkers<sup>[53,54]</sup> showed that most of the matrix PP does not yield at all but undergoes rigid body motion, which is opposite to the assumptions made by Kikuchi.<sup>[51]</sup> WAXD patterns of oil extended TPVs as investigated by Ying Yang *et al.*<sup>[39]</sup> showed negligible PP orientation at strains where pure PP shows a strong orientation. This has been related to a different morphology of PP crystallites in TPVs compared to pure PP. Only thin PP ligaments between the particles yield while the rubber domains shear around the undeformed PP regions creating a pseudo-continuous EPDM phase.

The schematic representation of this phenomenon explaining the deformation behavior was given by Soliman (Figure 2.4).<sup>[55]</sup> According to her model the adhesion between the particles and the matrix is assumed to be good. At low strains, both the matrix and the rubber phase deform elastically and the applied deformation is almost fully recoverable. At higher strains, the semi-crystalline polymer in the continuous phase will be strained on an average well beyond its yield strain and thus will undergo plastic deformation. This will initiate and concentrate on those areas where the matrix is thinnest. Areas that are directed transversely to the applied tension direction will bend or buckle while those under tension yield and draw. Even at higher strains the thicker regions will be at lower strains or remain even unyielded and will act as rigid blocks that hold the rubber particles together. The thinner regions of the matrix will be at strains, which are



much higher than the applied strain and which are intrinsically not recoverable. Upon unloading, the highly stretched thin areas can undergo some reverse plastic deformation under the elastic force of the rubber phase, but are more likely to buckle because of the asymmetry of the local loading.

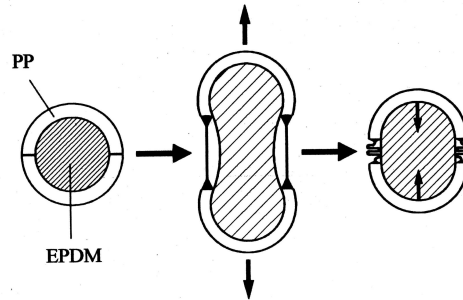


**Figure 2.4** Schematic representation of TPV deformation.<sup>[55]</sup>

Huy *et al.*<sup>[56]</sup> have used infrared dichroism to investigate the deformation mechanism of TPVs. The orientation of the EPDM phase was found to be higher than that of the PP phase. The orientation of the EPDM phase depends on the strain but not on the PP content. Interestingly, the orientation of the PP phase increased not only with increasing strain but also with crosslink content. With respect to the total strain of the material, the orientation in the PP phase of the dynamic vulcanizates was found to be lower and in the EPDM-phase higher than the corresponding orientations of the pure components. The deformation process was explained on the basis of the Takayanagi model.<sup>[56]</sup> The experiments also showed that the deformation is mainly concentrated in the EPDM particles and not in the matrix. So most of the matrix is not deformed. Similar experiments by Soliman *et al.*<sup>[55]</sup> showed that the total amount of deformed PP can be reduced by presence of a mineral oil.

A novel approach based on microcellular modeling has been proposed by Wright *et al.*<sup>[57]</sup> In this model the TPV is considered to be a filled foam: the foam struts are regions of PP and the foam interstices are “filled” EPDM rubber. This model, which takes into account the cure state of

the rubber phase, could accurately predict the yield stress and permanent set of TPVs as a function of PP concentration, but is independent of morphological terms such as the domain size of the EPDM.

To conclude, the deformation mechanism of EPDM/PP TPVs is still not clear. In the view of recent advances, constitutive micro-mechanical models seem to be much more closer to the actual mechanism, as compared to traditional approaches in explaining this process.

### 2.2.9 Oil distribution

The distribution of oil within the EPDM and PP phases under processing conditions and in the rubbery state is difficult to quantify. Such an estimate is necessary for the rational design of TPVs with optimal processability. The oil is generally believed to be present in the EPDM phase in the rubbery state. In addition, some oil can reside in the amorphous regions of PP, which improves the processability.<sup>[29]</sup> An attempt to study this distribution at processing temperatures was made by Winters *et al.*<sup>[58]</sup> using solid state  $^{13}\text{C}$ -NMR. Both TPVs with and without talcum were studied. Unfortunately, about 30% of the added oil could not be traced back in the TPV loaded with talcum filler, because the paramagnetic  $\text{Mn}^{2+}$ -ions present in the talcum filler suppressed a substantial amount of response from the oil. These experiments however indicated, that the oil is not confined to the EPDM phase at processing conditions. Upon melting, it diffuses out of the EPDM and forms a separate phase. This effect contributes to lowering the viscosity at processing temperatures.

A novel approach to study the oil distribution has been proposed by Sengers.<sup>[59]</sup> In this work, dielectric relaxation spectroscopy (DRS) was used to determine the oil distribution in the solid state. N,N-dibutyl amino nitrostilbene was used as a probe molecule. The oil distribution in the melt was measured by comparing the storage and loss moduli of ternary blends with those of binary PP-oil and vulcanized EPDM-oil blends and making use of empirical models. Results show that in solid state and in the melt the oil prefers the elastomer phase. The distribution coefficient  $K$ , defined as the ratio of the concentration of the oil in the PP phase to the one in the elastomer phase, has values smaller than 1. In the melt,  $K$  depends strongly on composition- it increases with increasing oil content and decreasing PP content. At ambient conditions the average value of  $K$  is about 0.63.  $K$  increases slightly with increasing PP content and remains constant by changing the oil content.

## 2.3 SEBS/PP/OIL BLENDS

### 2.3.1 General product definition<sup>[13]</sup>

Styrene-(ethylene-butylene)-styrene block copolymers (SEBS) belong to the family of styrenic block copolymers (SBCs), which are seen as high-volume workhorses in comparison with other TPE materials. The other two major types of SBCs are: styrene-butadiene-styrene block copolymers (SBS), and styrene-isoprene-styrene block copolymers (SIS). SBS and SIS block copolymers are prepared by anionic copolymerisation of butadiene or isoprene with styrene, in presence of an initiator. The polybutadiene mid-segment in SBS is produced as a random mixture of two structural forms of the molecule, called the 1,4- and 1,2- isomers. SEBS is prepared from SBS by subjecting the later to selective hydrogenation. Kraton polymers are the largest supplier of SEBS based materials and the polymers are marketed as Kraton G. A schematic representation of SEBS block copolymer is shown in Figure 2.5.

The polystyrene and ethylene butylene segments in SEBS are incompatible and form a two-phase system, which persists even in the melt below a certain temperature. Many arrangements of the two-phase system are possible, depending on the styrene to ethylene-butylene ratio.<sup>[60, 61]</sup> The polystyrene domains tend to cluster as hard domains in the soft ethylene-butylene matrix. These tie down the ends of the ethylene-butylene rubber chains to give an interconnected network or physical crosslinking. On heating, these domains soften and the copolymer becomes fluid; on cooling the domains become hard again, the network regains its strength and the polymer becomes elastic again. SEBS as such is a stiffer material as compared to SBS and SIS due to a higher number of chain entanglements in the polyethylene-butylene midblocks. Due to the saturated backbone, SEBS offers much higher ozone and UV resistance, resp. heat resistance as compared to SBS and SIS.

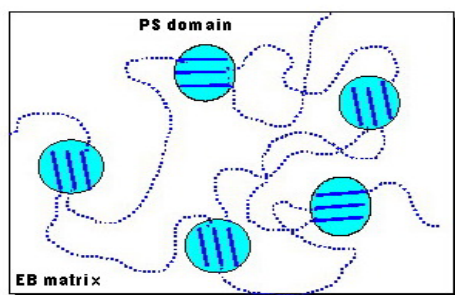


**Figure 2.5** Schematic representation of SEBS block copolymer.

Block copolymers like SBS, SIS and SEBS are characterized by an order – disorder temperature (ODT) or microphase transition temperature (MST). This is the temperature at which the microphase-separated state changes into a single-phase state. The extent of microphase separation for a given block copolymer composition is determined by the overall degree of polymerisation ( $N$ ) and the Flory-Huggins parameter ( $\chi$ ). The ODT is characteristic for a given combination of  $cN$ .<sup>[62]</sup> It has been shown experimentally that symmetrical triblock copolymer systems become ordered when the product of  $cN$  is equal to 18.<sup>[63, 64]</sup>

SEBS is never used as pure material. The 2-phase structure allows the formulator two areas in which to modify the materials for an appropriate balance of properties. Oils and resins can be added to the elastomeric phase to soften or tackify the polymer. Aromatic end block resins can be added to the polystyrene end-block regions to harden and strengthen compounds.

Blends of SEBS with PP and oil are relatively new TPE materials. Polypropylene as an additive acts in two different ways to improve the properties of compounds. First, it gives the compounds better processability. Second, when the compounds are processed under high shear and then quickly cooled, (e.g., in injection molding or extrusion), the polypropylene and the SEBS/oil mixture forms two co-continuous phases. Polypropylene is insoluble at service temperature and has a relatively high crystalline melting point of about 165°C. Thus, the continuous polypropylene phase significantly improves both the solvent resistance and the upper service temperature of these compounds.

SEBS has a high melt viscosity, which makes it extremely difficult to process. Therefore, it is always blended with large amounts of process oils. The oils can be added without the risk of bleeding out, allowing very soft compounds to be produced. Paraffinic oils are preferred, because they are more compatible with the EB center segments than the naphthanic oils used with similar SBS based compounds. Oils with high aromatic content are not compatible with the EB-block. The structure of SEBS-oil gels is described by Mischenko *et al.*<sup>[65]</sup> and Laurer *et al.*<sup>[66]</sup> Similar studies on styrene-(ethylene-propylene)-styrene block copolymer (SEPS) and SIS block copolymers have been reported by Laurer *et al.*<sup>[67]</sup>

Unlike TPVs the amount of open literature on SEBS/PP/oil blends is very limited. Several studies on the use of SEBS as a component in blends with thermoplastic polymers have been published.<sup>[68]</sup> Most of these studies focus on the use of SEBS as compatibilizer.<sup>[69-72]</sup> Use of SEBS in toughening of polyethylene, ionomers, polypropylene<sup>[73,74]</sup>, polystyrene<sup>[75]</sup> and poly(2,6-dimethyl-1,4-phenylene oxide) has also been reported.<sup>[76]</sup>

### 2.3.2 Influence of PP and SEBS types

SEBS being a block copolymer can exhibit different morphologies and properties depending on the polystyrene to ethylene butylene ratio.<sup>[77, 78]</sup> For example, the higher the ratio of hard polystyrene vs. rubber phase, the harder and stiffer the resultant copolymer.

A comparative study of syndiotactic PP and isotactic PP in blends with SEBS was reported by Setz *et al.*<sup>[79]</sup> Compositions with syndiotactic PP were found to be softer with inferior mechanical properties as compared to corresponding blends with isotactic PP. The morphology of the blends were found to be similar in both cases. The molecular weight of PP might have an influence on the blend morphology. However, the morphologies of SEBS/PP/oil blends having composition 34.5 wt.-% SEBS, 34.5 wt.-% PP and 31 wt.-% oil, prepared using PPs with MFI's of 1.5 and 20, were both found to be 100% co-continuous. Thus the degree of co-continuity was not affected by variations in PP molecular weight.<sup>[79]</sup>

### 2.3.3 Production methods

The blends can be prepared by solvent casting or melt blending. Solvent casting method for the preparation of a SEBS/PP blend is described by Setz *et al.*<sup>[79]</sup> In this method SEBS and PP were dissolved in boiling toluene to get a clear solution, which was then precipitated, in methanol. The influence of casting temperature on the morphology of the SEBS film is described by Wang *et al.*<sup>[80]</sup>

Melt blending is performed in an internal mixer or twin-screw extruder. Experiments with a twin-screw extruder and an internal mixer showed that the mixing technique affected the composition range in which the polymers formed a co-continuous structure. In a blend with 75 wt.-% PP, 13.3 wt.-% SEBS and 11.7 wt.-% oil, the SEBS phase was found to be dispersed in a twin-screw extruder. Only 28% of the SEBS phase could be extracted from this blend. However when the same blend was prepared in an internal mixer, 60% of the SEBS phase was extractable. This shows that the degree of co-continuity was higher when prepared in the internal mixer.<sup>[16]</sup>

### 2.3.4 Morphology

Blends of SEBS with PP and oil were reported to form a co-continuous morphology in a composition range from 10 to 55 % by weight of PP.<sup>[16]</sup> A co-continuous morphology is more difficult to characterize compared to a dispersed phase morphology. Different characterization methods for analysing co-continuous structures are reported by Li and Favis.<sup>[81]</sup> In most cases, co-continuous morphologies are detected using a combination of electron microscopy and solvent extraction studies.<sup>[82,83]</sup> The reason for the broad range of co-continuity in the SEBS/PP/oil blends is not fully understood. According to Ohlsson<sup>[16,84]</sup> the reason for this continuity is the miscibility between the EB blocks of SEBS and PP in the melt. In a composition range in which the SEBS matrix can take up all of the polypropylene and oil without breaking up the polystyrene junctions, crystallization of PP should lead to the formation of solid blends with a co-continuous two-phase structure.

A more fundamental study of the formation and stability of co-continuous SEBS/PP blends was performed by Veenstra *et al.*<sup>[85,86]</sup> Their study showed that the stability of the co-continuous structure is related to a complex combination of parameters, i.e.:

1. low interfacial tension between PP and SEBS (0.9 mN/m);
2. presence of physical crosslinks via the styrene phase during melt blending with PP.

The range of co-continuity is related to the temperature of blending. Stable co-continuous morphologies were found over a wide range of compositions when the blending temperature was below the ODT of SEBS. The morphology was stable even after annealing. Blending at temperatures above the ODT also lead to a reasonably wide range of co-continuity, but when annealing was performed at these temperatures the range of co-continuity decreased significantly.

The mechanism of formation and stability of co-continuous structures was investigated by Willimse<sup>[82,83]</sup> and Veenstra<sup>[85,86]</sup> According to these authors, formation of co-continuous morphologies demands stable interconnected elongated structures that do not show breakup or retraction, whatever their origin might be. There is some discussion in the literature, whether the formation of polymer blends proceeds via a droplet deformation/breakup mechanism<sup>[87, 88]</sup> or by a sheet forming mechanism.<sup>[89,90]</sup> A co-continuous morphology can be depicted by an interconnection of these stable elongated structures. The presence of physical crosslinks stabilizes these structures and the stress generated due to differences in interfacial tension

causes break-up of these structures. Veenstra<sup>[85,86]</sup> also studied the breakup mechanism of threads of different polymers imbedded in a SEBS matrix at different temperatures. The polymer with least difference in the interfacial tension was found to be most stable to breakup. This shows that co-continuous morphologies in SEBS/PP blends are stable over a wide range of compositions and processing conditions mainly due to low interfacial tension.

### 2.3.5 Rheology and processing

The flow behavior of pure SEBS is described by Ohlsson<sup>[84]</sup> and Veenstra.<sup>[85,86]</sup> Depending on the grade of SEBS, the storage moduli can show a sharp drop with increase of temperature. The change in the slope signifies the transition of a phase-separated melt to a single phase melt. The melt shows a yield stress, which is attributed to the presence of physical crosslinks in the polystyrene blocks. The shear rate dependence of the viscosity shows power law behavior above a shear rate of  $100 \text{ s}^{-1}$ . Adding oil to SEBS reduces the viscosity significantly, e.g., by a factor of three. This effect may be due to the combined effect of a decrease in the viscosity of the EB matrix and an increased tendency of the PS domains to break up at high shearing forces.

The addition of PP to the SEBS/oil mixture leads to a further pronounced reduction in viscosity. In contrast to TPVs, the Cox-Merz rule can be applied to these systems.<sup>[84]</sup> With some compositions a viscosity like that of pure PP can be obtained and even lower. According to Ohlsson *et al.*,<sup>[84]</sup> the rheological behavior is controlled by a PP-rich liquid phase, which because of the presence of oil has lower viscosity than the pure PP melt. This is technologically very important for injection molding and extrusion.

The injection molding and extrudability of these blends were also studied by Ohlsson.<sup>[84]</sup> Solid extrudates from a capillary rheometer were rich in PP and free from large domains of the SEBS. Injection molded plates had a similar surface morphology although in this case, larger domains of the elastomeric phase were found. This shows that the blend undergoes flow-induced phase-segregation during mold filling. Weld lines in injection molding test pieces prepared from blends with co-continuous morphologies had no noticeable effect on the stress-strain properties or impact strength.

### 2.3.6 Properties

Studies of Ohlsson<sup>[84]</sup> showed, that blends in which the SEBS and PP phase are co-continuous, behave differently than blends in which one of the phases is discontinuous. For example in a blend of 56.8 wt.-% PP, 22.7 wt.-% SEBS and 20.5 wt.-% oil, only 56 wt.-% of the SEBS phase was found to be extractable by xylene, which shows that the SEBS phase was dispersed. The stress-strain curve of this blend showed a typical yield point and necking. Compositions in which the SEBS and PP phase were co-continuous showed rubber like behavior. The storage moduli could be modeled using a Davies model.<sup>[91]</sup>

The crystallinity of PP in the blends was found to be independent of the blend structure. The melting point of PP decreased with decreasing PP content. This decrease was thought to be the result of two factors: a) interaction of PP with oil; b) miscibility of PP with SEBS and oil in the molten state to form a homogeneous phase.<sup>[84]</sup>

### 2.3.7 Oil distribution

The oil distribution between the SEBS and PP phase was calculated by Ohlsson *et al.*<sup>[16]</sup> by comparing the shifts in the glass transition temperature of the ternary blends with those of binary PP-oil and SEBS-oil blends. The calculations showed that the distribution coefficient between PP and SEBS had an average value of 0.35 in the rubbery state. The distribution coefficient is slightly composition dependent, e.g. from 0.47 at 90 % PP to 0.33 at 10 % PP.

Sengers<sup>[59]</sup> used dielectric spectroscopy to determine the distribution of oil at ambient temperatures. The calculations showed that the distribution coefficient is in the order of 0.57-0.63. The distribution coefficient slightly increases with increasing PP content and similar to the EPDM/PP/oil TPVs remains constant with changing oil content.

## 2.4. APPLICATIONS OF TPVS AND SEBS/PP/OIL BLENDS<sup>[92]</sup>

TPEs based on TPVs and SEBS/PP/oil blends are increasingly used in many automotive applications. The properties of these materials, although different, are well within the specification requirements for many applications. A comparative summary of a few selected properties is shown in Table 2.1. Some applications wherein these materials are used are given below:



1. Airbag doors (or covers), rack and pinion boots, brake cable covers, steering column covers, tie rod end seals, air management ducts, and windscreen washer reservoir seals, to be used in automotives. Injection molding, extrusion and blow molding are all used to make these applications. Styrenic TPEs were initially not considered for these applications, because of the upper service temperature requirements. The plethora of SEBS developments have changed the situation;
2. Vehicle interiors - the look, soft-feel and sound within automotive interiors can be tailored by both sorts of TPEs. For some of these applications polyamide bondable grades are necessary, which are available within both TPE families;
3. Automotive weather seals. An average car uses about 10 kg seals, which are still mainly made from vulcanized EPDM. Use of TPVs can result in a 5-10% reduction in cost compared to vulcanized rubber. The process is simpler, faster and a 25% lower specific gravity reduces the weight of the part. SEBS compounds are also considered to be potential alternatives for these applications;
4. Soft-touch applications like grips on power tools, knobs etc;
5. Hoses and tubes. The requirements are chemical resistance and low gas permeability.

**Table 2.1 Properties of EPDM/PP/oil TPVs and compounds of styrenic block copolymers (SBCs)**

	Specific gravity	Shore hardness	Low temperature limit	High temperature limit (continuous)	Compression set at 100 °C	Price ratio relative to SBS
EPDM/PP/oil TPVs	0.9-1.0	35A-50D	-60 °C	135 °C	good	2.5-3.0
Compounds of SBCs	0.9-1.1	3A-60D	-70 °C	120 °C	fair	1-3.6

## 2.5 SUMMARY OF THE LITERATURE SURVEY AND THE OBJECTIVE OF THE THESIS

An overview of the available literature on TPVs and SEBS/PP/oil blends shows, that these blends are morphologically different. This difference is however not well defined. Apparently, the rubber phase is dispersed in TPVs and continuous in SEBS/PP/oil blends. However, there is no direct microscopic evidence of these morphologies, especially in blends containing an excess of the rubber phase.

The role of oil in these blends is not fully clear yet. Most of the earlier studies on TPVs were conducted on compositions without oil. So a lot of questions related to the function of oil, its distribution between the rubber and PP phases, during processing and end-use conditions are still to be answered.

The properties of TPVs and SEBS/PP/oil based compositions are close enough to be considered for similar sorts of applications. The rheological properties also show similarities. A TPV melt can be pictured as an assembly of vulcanized EPDM islands suspended in PP. By analogy, the SEBS/PP/oil melt can be pictured as an assembly of SEBS islands suspended in PP. The chemical crosslinks within the EPDM particles can be compared to physical crosslinks in the SEBS domains that persists even in the melt. The resemblance in melt structure, proximity of mechanical properties but differences in solid-state morphology are all very puzzling. In most polymer blends, the properties are dependent on the morphologies and so the question is: why is it different in this case? The information available so far is not enough to answer these questions. For a proper answer a detailed study of the morphology, rheology and properties of these two blends prepared under similar conditions is necessary.

Based on these considerations the research described in this thesis will primarily focus on the following subjects:

1. Look for more direct evidence, on visualizing the morphology of TPVs and SEBS/PP/oil blends, for compositions containing abundant rubber and oil. A comparative study of different two-dimensional imaging techniques will be conducted and the possibility to extend from two-dimensional imaging to three-dimensional imaging will be explored.

2. A comparative study of the structure-property relationships in TPVs and SEBS/PP/oil blends prepared under identical conditions by two different production processes, viz.: internal mixer and co-rotating twin-screw extruder;
3. Attempt to model the influence of oil distribution on the stress-strain properties.
4. Evolution of the blend morphologies in an internal mixer and a co-rotating twin-screw extruder.
5. Influence of different material and process parameters.

## 2.6 REFERENCES

1. D. R. Paul, S. Newman, "Polymer Blends", Vol. 1,2: Academic Press, New York, 1978.
2. S. Wu, Polymer, **26** (1985) 1855.
3. Y. Seo, S. S. Hwang, K. U. Kim, Polymer, **34** (1993) 1667.
4. R. J. M. Borggreve, PhD thesis, University of Twente, The Netherlands (1986).
5. A. G. C. Machiels, K. F. J. Denys, J. van Dam, P. de Boer, Polym. Eng. Sci., **36** (1996) 2451.
6. H. Verhoogt, R. C. Willimse, J. van Dam, A. Posthuma de Boer, Polym. Eng. Sci., **34** (1994) 453.
7. B. Y. Shin, S. H. Jang, I. J. Chung, B. S. Kim, Polym. Eng. Sci., **32** (1992) 73.
8. M. B. Nir, A. Ram, J. Miltz, Polym. Eng. Sci., **35** (1995) 1878.
9. H. Q. Xie, J. Xu, S. Zhou, Polymer, **32** (1991) 95.
10. W. P. Gergen, Kautsch. Gummi Kunstst., **37**(1983) 284.
11. W. P. Gergen, R. Lutz, S. Davison, "Thermoplastic elastomers: A comprehensive review", Ed. N.R. Legge, Carl Hanser, Munich, (1987).
12. S. K. De, A. K. Bhowmick, "Thermoplastic Elastomers from Rubber - Plastic Blends" Ellis Horwood Limited Chichester, West Sussex, (1990).
13. G. Holden, "Understanding Thermoplastic Elastomers". Hanser Publications, Cincinnati, OH, (2000).
14. A. Y. Coran, R. P. Patel, Rubber Chem. Technol., **56** (1983) 1045.
15. A. Y. Coran, R. P. Patel, D. Williams, Rubber Chem. Technol., **55** (1985) 116.
16. B. Ohlsson, H. Hassender, B. Tornell, Polym. Eng. Sci., **36** (1996) 501.
17. H. Veenstra, B. J. J. van Lent, J. van Dam, A. P. de Boer, Polymer, **40** (1999) 6661.
18. W. K. Fisher, U.S. patent 3,806,558 (1974).
19. A. Y. Coran, B. Das, R. P. Patel, U.S. patent 4,130,535 (1978).
20. A. Y. Coran, R. P. Patel, Rubber Chem. Technol., **53** (1980) 781.

21. S. Datta, in 157th Spring Technical Meeting of the American Chemical Society, Rubber Division (2000), Dallas, Texas.
22. N. R. Legge, Rubber Chem. Technol., **62** (1989) 539.
23. S. Abdou-Sabet, R. P. Patel, Rubber Chem. Technol., **64** (1991) 769.
24. S. Abdou-Sabet, C. P. Rader, "Two-phase elastomeric alloys, in *thermoplastic elastomer from rubber-plastic blends*", S. K. De, A.K. Bhowmick, Ed., Ellis Horwood Limited, Chichester, West Sussex, (1990).
25. M. D. Ellul in 160th Fall Technical Meeting of the American Chemical Society, Rubber Division, (2001). Cleveland, OH.
26. M. Morton, "Rubber technology". third ed, Dordrecht, Kluwer academic publishers, Dordrecht, (1994).
27. S. Abdou-Sabet, M. A. Fath, U.S. patent 4,311,628 (1982).
28. R. P. Lattimer, R. A. Kinsey, R. W. Layer, C. K. Rhee, Rubber Chem. Technol., **62** (1989) 107.
29. M. van Duin, A. Souphamthong, Rubber Chem. Technol., **68** (1995) 717.
30. M. D. Ellul, Rubber Chem. Technol., **71** (1998) 244.
31. R.E. Medsker, R. Patel, S. Abdou-Sabet, U.S. patent 5,750,625 (1997).
32. K. Naskar, J. W. M. Noordermeer, Rubber Chem. Technol., **76** (2003) 1001.
33. K. Naskar, PhD thesis, University of Twente, The Netherlands (2004).
34. H. G. Fritz, R. Anderlik, Kautsch. Gummi Kunstst., **46** (1993) 374.
35. M. D. Ellul, A. H. Tsou, W. Hu, Polymer, **45** (2004) 3351.
36. T. Marinovic, Z. Susteric, I. Dimitrievski, A. Kranj, A. Veksli, Kautsch. Gummi Kunstst., **51** (1998) 189.
37. M. A. Lopez-Manchado, M. Arroyo, J. M. Kenny, Rubber Chem. Technol., **74** (2001) 211.
38. S. Abdou-Sabet, K. Shen, U.S. patent 4,59,4390 (1982).
39. Ying Yang, T. Chiba, Hiromu Saito, Takakhi Inoue, Polymer, **39** (1998) 3365.
40. A. A. Katbab, H. Nazockdast, S. Bazgir, J. Appl. Polym. Sci., **75** (2000) 1127.
41. M. D. Ellul, A. H. Tsou, W. G. Hu, Polymer, **45** (2004) 3351.
42. H. J. Radusch, T. Pharm, Kautsch. Gummi Kunstst., **49** (1996) 249.
43. A. Y. Coran, O. Chug, P. Laokijcharoen, Kautsch. Gummi Kunstst., **51** (1998) 342.
44. W. L. Feng, A. I. Isayev, Polymer, **45** (2004) 1207.
45. P. Steeman, W. Zoetlief, in ANTEC (2000) Orlando, USA.
46. P. K. Han, J. L. White, Rubber Chem. Technol., **68** (1995) 728.
47. Internal information DSM Research B.V., The Netherlands.
48. H. J. Radusch, E. Lammer, Th. Lupke, L. Hausler, Kautsch. Gummi Kunstst., **44** (1991) 1125.
49. H. W. Xiao, S.Q. Huang, T. Jiang, S.Y. Cheng, J. Appl. Polym. Sci., **83** (2002) 315.
50. D. Scharnowski, S. Piccarolo, H. J. Radusch in *International Rubber conference*, (2001) Prague.
51. Y. Kikuchi, T. Fukui, T. Okada and T. Kikuchi, J. Appl. Polym. Sci.: Appl. Polym. Symp., **50** (1992) 261.
52. S. Kawabata, S. Kitawaki, H. Arisawa, Y. Yamashita and X. Guo, J. Appl. Polym. Sci., Appl. Polym. Symp., **50** (1992) 245.

53. M.C. Boyce, K. Kear, S. Socrate and K. Shear, *J. Mech. Phys. Sol.*, **49** (2001) 1073.
54. M.C. Boyce, K. Kear, S. Socrate and K. Shear, *J. Mech. Phys. Sol.*, **49** (2001) 1323.
55. M. Soliman, M. van Dijk, M. Van Es and V. Schulmeister, paper presented at ANTEC, May 1999, New York.
56. T.A. Huy, T.Luepke, H.J. Radusch, *J. Appl. Polym. Sci.*, **80** (2001) 148.
57. K. J. Wright, K. Indukuri, A. J. Lesser, *Polym. Eng. Sci.*, **43** (2003) 531.
58. R. Winters, J. Lugtenburg, V.M. Litvinov, M. van Duin, H.J.M. de Groot, *Polymer*, **42** (2001) 9745.
59. W. Sengers, PhD thesis, Technical University Delft, The Netherlands, to be published
60. G. Cho, A. Natansohn, *Can. J. Chem.* **72** (1994) 2255.
61. M. Kakugo, H. Sadatoshi, M. Yokoyama K. Kojima, *Polym. Commun.* **29** (1998) 288.
62. R. M. Patel, S. F. Hahn, C. Esneault, S. Bensason, *Advanced materials*, **12** (2000) 1813.
63. A. M. Mayes, M. J. Olvera, de la Cruz, *J. Chem. Phys.*, **91** (1989) 7228.
64. M.D. Gehlsen, K. Almdal, F. S. Bates, *Macromolecules*, **25** (1992) 939.
65. N. Mischenko, K. Reynders, K. Mortensen, R. Scherrenberg, F. Fontaine, R. Graulus, H. Reynaers, *Macromolecules*, **27** (1994) 2345.
66. J. H. Laurer, R. Bukovnik, R. Spontak, *Macromolecules*, **29** (1996) 5760.
67. J. H. Laurer, S. A. Khan, R. Spontak, *Langmuir*, **15** (1999) 7947.
68. F. Picchioni, M. Aglietto, E. Passaglia, F. Ciardelli, *Polymer*, **43** (2002) 3323.
69. A. N. Wilkinson, L. Laugel, M. L. Clemens, V. M. Harding, M. Marin, *Polymer*, **40** (1999) 4971.
70. M.C. Schwarz, J. W. Barlow, D. R. Paul, *J. Appl. Polym. Sci.*, **37** (1989) 403.
71. A. K. Gupta, K. R. Srinivasan, *J. Appl. Polym. Sci.*, **53** (1993) 167.
72. K. R. Srinivasan, A .K. Gupta, *J. Appl. Polym. Sci.*, **53** (1994) 1.
73. A. K. Gupta, S. N. Patel, *J. Appl. Polym. Sci.*, **29** (1984) 1545.
74. H. T. Chiu, Y. G. Shiau, W. M. Chiu, S. S. Syau, *J. Polym. Res.*, **2** (1995) 21.
75. Y. Agari, A. Ueda and S. Nagai, *J. Appl. Polym. Sci.*, **47** (1993) 331.
76. P. S. Tucker, J. W. Barlow and D.R. Paul, *J. Appl. Polym. Sci.*, **34** (1987) 1817.
77. Information brochure from Kraton Polymers B.V. (2004).
78. J. Rosch, R. Mulhaupt, *Macromol. Chem. Rapid Commun.*, **14** (1993) 503.
79. S. Setz, F. Stricker, J. Kressler, T. Duschek, R. Mulhaupt, *J. Appl. Polym. Sci.*, **59** (1996) 1117.
80. Y. Wang, J. S. Shen, C. F. Long, *Polymer*, **42** (2001) 8443.
81. J. Li, B. D. Favis, *Polymer*, **42** (2001) 5047.
82. R. C. Willimse, A. P.de Boer, J. van Dam, A. D. Gotsis, *Polymer*, **40** (1999) 827.
83. R. C. Willimse, A. P. de.Boer, J. van Dam, A. D. Gotsis, *Polymer*, **39** (1998) 5879.
84. B. Ohlsson, B.Tornell, *Polym. Eng. Sci.*, **36** (1996) 1547.
85. H. Veenstra, J.van Dam, A. P. de Boer, *Polymer*, **40** (1999) 1119.
86. H. Veenstra, PhD thesis, Delft University of Technology, The Netherlands (1992).

- 
87. G. I. Taylor, Proc. Roy. Soc., **A146** (1934) 501.
  88. G. I. Taylor, Proc. Roy. Soc., **A138** (1932) 41.
  89. U. Sundararaj, C. W. Macosko, R. J. Rolando, H. T. Chan, Polym. Eng. Sci., **32** (1992) 1814.
  90. C. E. Scott, C. W. Macosko, Polymer, **36** (1995) 461.
  91. W. F. A. Davies, J. Phys. D (1971) 4318.
  92. P. Dufton, "Thermoplastic Elastomers", RAPRA technology Ltd., Shawbury, (2002).

---

## Chapter 3

### **Optimization of Techniques for Microstructural Characterization of Oil Extended TPE blends**

---

*Microscopic methods such as light microscopy (LM), scanning electron microscopy (SEM), transmission electron microscopy (TEM) or atomic force microscopy (AFM) are often used to visualize the morphology of polymer blends. These methods are based on observations of surfaces or thin sections that show a cross section of the three dimensional structure. Hence, in a binary blend of polymers, if one of the phases is in excess but still remains dispersed in the second phase, the morphology becomes quite difficult to identify experimentally. If, in addition, the blend contains a high volume percent of a diluent such as paraffinic oil, obtaining good microscopic images becomes very challenging.*

*This chapter gives a relative comparison of different microscopic methods that can be used to identify the morphology of highly oil extended thermoplastic elastomer (TPE) blends based on a soft rubber phase and isotactic polypropylene (PP). TPE blends of two different rubbers with PP were selected for this study: A dynamically vulcanized blend of EPDM-rubber, PP and oil, and a blend of SEBS-rubber, PP and oil.*

*Low Voltage Scanning Electron Microscopy (LVSEM) and Transmission Electron Microscopy (TEM) proved to be far superior over Scanning Electron Microscopy (SEM) and Atomic Force Microscopy (AFM) in obtaining good quality images of the morphology of these blends. In SEM experiments, samples with high oil content charged up badly and in AFM experiments the scanning probe picked up oil from the samples, resulting in blurry images. LVSEM and TEM investigations showed that the rubber phase is dispersed in TPV, but continuous with the PP phase in SEBS/PP/oil blends. In an attempt to visualize the 3D-morphology, electron tomography was carried out on these blends for the first time and models of the three dimensional morphology were constructed. The potential of electron tomography as an important tool for constructing 3D-models of polymer blends with a resolution higher than any other method currently available, is exhibited.*

---

Part of this chapter has been orally presented by the author at the International Rubber Conference 2002, Prague, 1-4 July, and also published in *Elastomer*, The Korean Institute of Rubber Industry, **38** (2003) 27.

### 3.1 INTRODUCTION

Understanding the morphology of polymer blends is important in order to determine relationships between the structure and properties of these materials. Microscopic methods such as light microscopy (LM), scanning electron microscopy (SEM), transmission electron microscopy (TEM) and atomic force microscopy (AFM) can detect details, ranging from the millimeter to the subnanometer scale, and are therefore popular tools for visualizing blend morphology: see Table 3.1. In spite of several spectacular developments in instrumental techniques, determination of polymer blend structure remains a formidable challenge. This is, because most electron microscopic methods are based on observations on surfaces or thin sections that show a cross section of the three dimensional structure. Cross sections are at best two-dimensional projections of what is a three dimensional structure, in essence discarding a third or all the spatial information that the specimen may contain. Any specimen variation in the third dimension can be minimised by careful sample preparation, sectioning a specimen in a specific orientation to reveal the features under study and/or by preparing two specimens from mutually perpendicular axes. These approaches work best for specimens with microstructures that are structurally simple, such as a single-phase alloy, or whose structure can be predicted due to specific orientational relationships, such as an epitaxially grown semiconductor device. For most specimens however, two-dimensional projections lead to some uncertainty as to their true 3D structure. There are an increasing number of systems whose functions are closely controlled by a complex 3D microstructure. In such cases two-dimensional projections can be at best inadequate, at worst misleading. Because of these reasons, a single 2D – microscopic method is not sufficient for unambiguous identification of the blend morphology and in the absence of suitable 3D microstructure visualisation techniques combinations of several two dimensional microscopy techniques are required.



**Table 3.1 Characterization techniques: size ranges<sup>[1]</sup>**

Technique	Resolution
Wide angle X-ray scattering (WAXS)	0.01nm - 1.5 nm
Small angle X-ray scattering (SAXS)	1.5 nm - 100 nm
Transmission electron microscopy (TEM)	0.2 nm - 0.2 mm
Scanning probe microscopy (STM, AFM)	0.2 nm – 0.2 mm
Scanning electron microscopy (SEM)	4 nm – 4 mm
Optical microscopy (OM)	200 nm - 200 $\mu$ m
Light scattering (LS)	200 nm – 200 $\mu$ m
Electron tomography	3 nm -20 nm

In a blend of two polymers, if the major phase is dispersed in the minor phase, the morphology becomes quite difficult to identify experimentally. Such situations are quite common in soft rubber-thermoplastic blends where the rubber phase is in excess of the plastic phase. If, in addition the blends contain a high volume percent of diluent such as paraffinic oil, which is often added as a softener and processing aid, obtaining good microscopic images becomes very difficult.

Soft rubber-plastic blends, especially those based on PP as the plastic, are quite common thermoplastic elastomer materials.<sup>[2]</sup> Compounds of these blends are very popular materials for soft-touch applications such as grips on tools, sports goods, automotive and medical applications, because the properties of the rubber and the PP phase can be easily tailored into a single product. Understanding the structure-property relationship in these materials is vital for making blends with tailored properties. Studies into these relationships are however rather limited, because visualizing the blend morphology in these systems turned out to be rather difficult.

The present chapter gives a relative comparison of different microscopic methods that can be used to identify the morphology of high oil extended thermoplastic elastomer (TPE) blends based on a soft rubber phase and isotactic polypropylene (PP).

TPE blends of two different rubbers with PP were selected for this study. One of them was a dynamically vulcanized blend of EPDM-rubber and PP, and the other a blend of SEBS-rubber and PP. To address the problem of identifying the morphology in the case of high loading of rubber along with high loading of oil, all the compositions selected for this study have a rubber content larger than 80 wt.-% and oil contents higher than 100 wt.-% with respect to PP.

The basic objective of this work was to optimize a characterization technique in order to study the morphology in an attempt to make a correlation with the mechanical properties of thermoplastic olefinic blends in the later chapters. The principles of the different microscopy techniques are described briefly first. The experimental setup and results are then discussed. In an attempt to visualise the 3D morphology, electron tomography was carried out on these blends and models of the three dimensional morphology were constructed. The potential of electron tomography as an important tool for constructing 3D-images of polymer blends, with a resolution higher than any other method currently available, is demonstrated.

## **3.2 PRINCIPLES OF ELECTRON MICROSCOPY AND ATOMIC FORCE MICROSCOPY**

### **3.2.1 Electron microscopy**

An electron microscope accelerates electrons to or through a specimen, allowing resolutions as high as 0.2 nm and a magnification 1000 times higher than achievable with a light microscope. In an electron microscope, electrons originating from the electron gun are accelerated towards the anode, a positively charged region attracting the negatively charged electrons: Figure 3.1. Depending upon the negative voltage of the anode, electrons move faster, allowing the microscope to view even thick sections with clarity and resolution. These electrons however, must be guided and focused by electromagnets and condenser lenses through which the electrons pass. Two condenser lenses focus the size of the electron stream as well as its direction. Without these lenses, the image would be blurry, as the condensers focus the electrons towards the object, functioning with the same principle, as do the lenses in light microscopes when they focus light onto an object. Once the electrons have reached their target and penetrated, they are focused into several lenses by an objective lens. Every time the electron stream passes through a lens, the image is magnified.

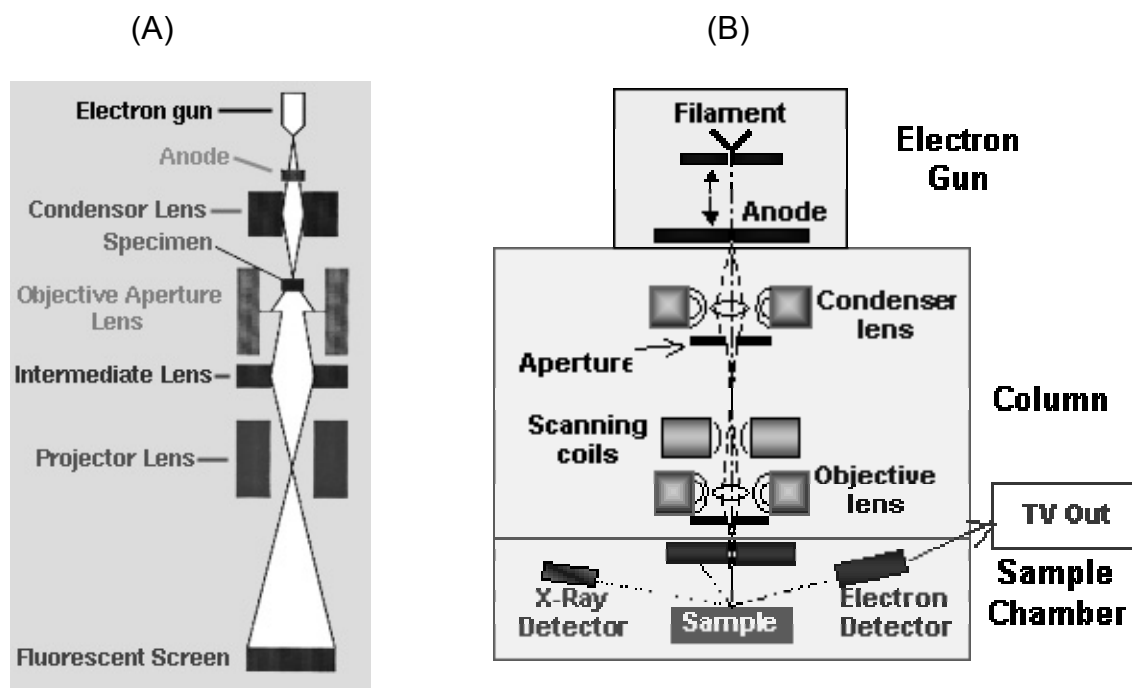


**Figure 3.1** Diagram of (A),Transmission electron microscope; (B),Scanning electron microscope.

### 3.2.2 SEM and TEM<sup>[1]</sup>

There are two kinds of electron microscopes that function using different principles. One is the scanning electron microscope (SEM) and the other is the transmission electron microscope (TEM). In the TEM: Figure 3.1A, the electrons pass through the specimen and arrive at a phosphor screen, whereupon visible light is created. Electrons that pass through less dense parts of the specimen and parts where the atomic number of the particles is low, are not scattered to a large extent, and so hit the screen in greater numbers, creating more light. Electrons that pass through dense areas of the specimen, and areas where the atomic number of the particles are high are left in lower amounts, as many are scattered. Hence light areas of the image represent less dense areas of the specimen, where particles are of a low atomic number; and dark areas of the image represent dense areas of the specimen, where the particles have higher atomic numbers. Underneath the phosphor screen is a camera that captures the images and displays them on a TV monitor for viewing.

SEMs instead scan over a surface with the point of a convergent electron beam and from the secondary electrons that are detected from the analysed positions an image of the surface is reproduced: Figure 3.1B. SEM-observation of non-conductive samples is

not possible without a metallic or carbon conductive layer on their surface. Such coatings are not necessary if one uses low voltage scanning electron microscopy (LVSEM). These microscopes operate at voltages below 5 kV and give increased spatial resolution and lower charging as compared to conventional SEM.

SEMs are therefore able to produce three-dimensional images of the surface of an object, whereas TEM produces detailed two-dimensional images. Although TEM is primarily a two-dimensional technique, the two-dimensional images can be converted into three-dimensional models through electron tomography.

### 3.2.3 Electron Tomography<sup>[3-5]</sup>

Transmission electron microscopy projects a three-dimensional object along the axis of the electron microscope lenses onto the plane of the recording medium. Hence an image is a superposition of all structures within the three-dimensional object along the electron beam trajectory. Obviously one needs to recover the spatial information in the direction of the electron beam in order to retrieve the three-dimensional structure. This can be done by imaging the sample from different angles in a way similar to computer axial tomography.

The principle of tomography is based on the central section theorem<sup>[6]</sup>, which states that the Fourier transform of a parallel beam of two-dimensional projection images is equal to the central section of the three-dimensional Fourier transform of the object. There are four steps in the process of tomography. The first step is acquisition of a set of views of the specimen from different directions. The views are obtained by tilting the specimen with the help of a goniometer. If the images are recorded in a film the micrographs are digitized. The second step is alignment of these two-dimensional images to a common origin with the help of a fiducial alignment algorithm. 10-20 nm gold particles are put on the top of the samples for this purpose. Computer programs track the fiducials and calculate the least square fit on the fiducial markers. In the third step the aligned data set is then back projected to create the tomogram. In this step, a Fourier transform of each two-dimensional projection is calculated and using the central section theorem a set of planes with a common axis in the Fourier space is obtained. The last step consists of analysis and visualization of the tomogram that is the final product of tomography. Original TEM images are often difficult to interpret, but when reconstructed along the “z” axis (third-dimension) provide better understanding of the material. A schematic diagram of the instruments

involved showing the steps involved in an electron tomographic experiment is depicted in Figure 3.2

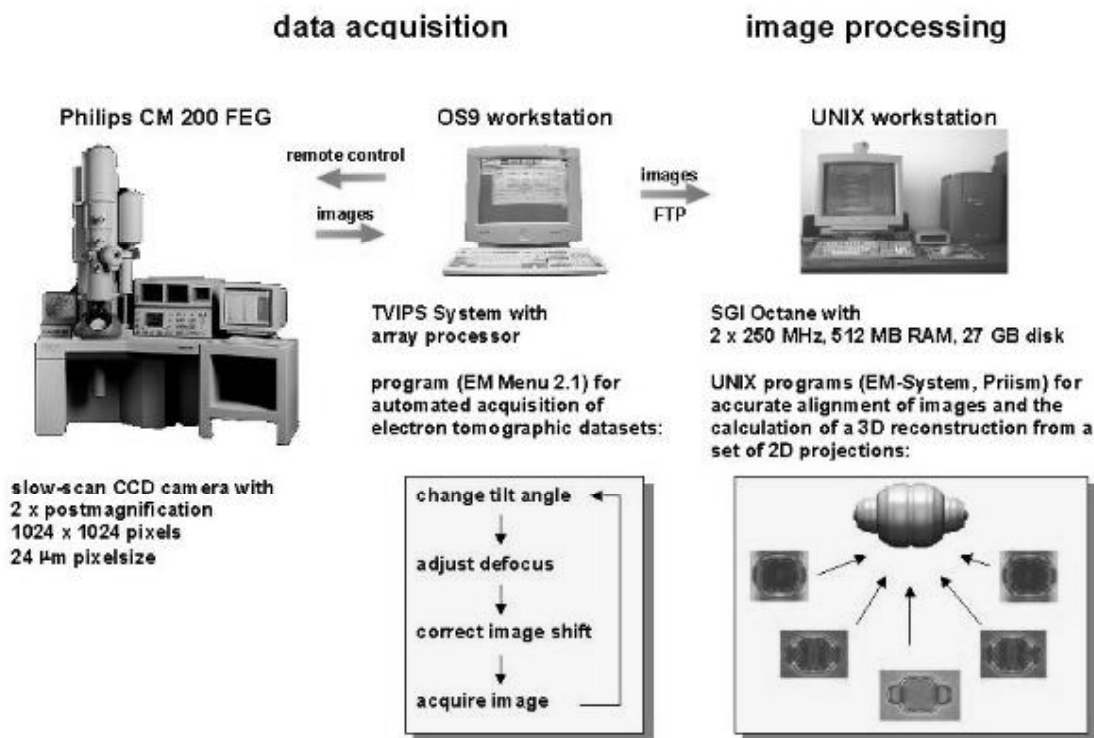


**Figure 3.2.** Experimental setup for electron tomography.

The resolution of electron tomography is 2 to 10 times higher than of conventional TEM. There are several factors that affect the resolution. The number of tilt angle projections will increase the detail and completeness of the final result. The angle increments between tilt angle projections also affect the precision of the surfaced volume. Lower angle increments and a higher number of tilt angle projections will increase the 3D resolution. The thickness of each individual section and alignment of these sections with regard to the tilt angles also affect three-dimensional resolution. A rule-of-thumb for the achievable resolution equals three times the thickness of the sample divided by the number of images.<sup>[5]</sup>

During the last decade, the application of electron tomography has gained pace. With the advent of computer-controlled microscopes, large-scale digital cameras and high-performance desktop computing power, it is possible to implement automated procedures for the acquisition of tilt series containing hundreds of views. Simultaneously, several computer program packages for alignment, reconstruction and manipulation of large

volumetric data sets are presently available to the scientific community. Typically, carrying out an electron tomography experiment with the first generation of automated systems takes a day, and the actual data collection 2-4 hours.

### **3.2.4 AFM<sup>[1]</sup>**

Contrary to electron microscopy the principle of atomic force microscopy is slightly different. In atomic force microscopy a sharp probe attached to a compliant cantilever scans a sample surface at a distance over which atomic forces act. The forces between tip and sample cause the cantilever to deflect. A photo detector measures the cantilever deflection and from this information a map of the sample topography can be created. There are two basic AFM modes - contact mode and tapping mode.

In contact mode, the cantilever with tip is dragged across the surface, which may cause damage to soft samples. In the tapping mode, a piezoelectric driver oscillates the cantilever at or near its resonance frequency at a high amplitude. The tip lightly taps the surface, touching the sample through the absorbed fluid layer during each oscillation. As the oscillating cantilever scans the surface, the amplitude of the oscillation is changed. The change in amplitude is used to measure the surface topography. As the changes in amplitude are used to make a topographic map of the surface phase signal changes are used to map regions of different composition. Phase shifts are registered as bright and dark regions in phase imaging, comparable to the way changes in height are registered in height imaging. The latter technique is successfully used for biological samples and for polymers, since damaging frictional forces are avoided.

## **3.3 EXPERIMENTAL**

### **3.3.1 Materials**

The polymers used in the present study were ethylene-propylene-diene terpolymer rubber (EPDM; DSM Elastomers B.V.; 63 wt.-% ethylene, 4.5 wt.-% 5-ethylidene-2-norbornene (ENB) termonomer) and extended with 50 wt% (100 parts per hundred rubber) of paraffinic oil; polypropylene (PP; Stamylan® P11E10 DSM Polypropylenes B.V.) and styrene-(ethylene-butylene) based triblock copolymer (SEBS; Kraton® G 1651, Kraton™ Polymers). The PP used was an extrusion grade with a melt flow index (at 230 °C, 2.16 kg) of 0.3 g/10 minute. SEBS had a styrene to ethylene-butylene ratio of 32/68 wt.-%. The oil used was a non-aromatic mineral oil containing paraffinic and naphthenic hydrocarbons. For the EPDM formulation a phenolic resin was used as curing agent along with stannous chloride

dihydrate ( $\text{SnCl}_2 \cdot 2\text{H}_2\text{O}$ ; Merck) as catalyst and zinc oxide (rubber grade; Merck) as acid scavenger during dynamic vulcanization. Additionally, stabilizers Irganox 1076: a primary hindered phenolic type antioxidant (Ciba Geigy) and Irgafos 168: a secondary phosphite type antioxidant, (Ciba Geigy) were used.

### **3.3.2 Sample preparation and application of various microscopic techniques**

Ternary blends with a composition of EPDM- or SEBS-rubber/PP/oil were prepared using a Brabender Plasticorder type 350S with a mixer chamber volume of 390 ml and fitted with Banbury type rotors. Mixing was carried out at 180°C at a rotor speed of 80 RPM. The mixing time was 12 minutes for TPVs and 20 minutes for the SEBS/PP/oil blends.

After mixing the materials were compression molded at 200°C for 3 minutes under a pressure of 10 MPa and then cooled under pressure to about 30°C. The molded sheet thickness was about 2 mm.

After compression molding small samples were taken for electron microscopic examination. Sample preparations for the different microscopic techniques used in this work are described below.

#### **3.3.2.1 SEM.-**

Samples for SEM were microtomed at -130°C using a diamond knife mounted on a Leica Ultramicrotome. The samples were then fixed using double sided tape onto a specimen stub. In order to increase the electron density contrast between the rubber and PP phase, the samples were vapor stained for 30 minutes using a 1 wt.-% solution of ruthenium tetroxide. Conductive paints such as carbon suspensions were dabbed onto the tape and base of the specimen to provide contact with the specimen stub. The samples were then coated with a thin gold layer. The coating was necessary in order to provide an electrically conducting layer, to suppress surface charging, to minimize radiation damage, and to increase electron emission during SEM. The SEM experiments were performed on a Hitachi S800 scanning electron microscope operating at a voltage of 6 kV.

### 3.3.2.2 LVSEM.-

The LVSEM experiments were performed using a Leo 1550 scanning electron microscope at an operating voltage of 1kV and lower. The LVSEM was equipped with an in-lens secondary electron detector (SE) and a back scattered electron detector (BSE). The SE detector gives images based on topography while the BSE detector gives images based on phase contrast using higher voltages. Samples to be studied with the SE detector were prepared by two different techniques. First, the samples were cryomicrotomed using similar conditions as for conventional SEM. Second, the samples were fractured under liquid nitrogen conditions. Both samples were stained with ruthenium tetroxide vapors for 30 minutes. For obtaining good BSE images the sample must have a flat surface to suppress contributions from the topographic image. So, samples for studying with BSE detector were cryomicrotomed.

### 3.3.2.3 TEM.-

Samples for TEM characterization were prepared by cryomicrotoming to 50 nm thin sections at  $-130^{\circ}\text{C}$ . The sections were vapor stained using ruthenium tetroxide for 30 minutes. TEM measurements were performed on a Philips CM 30 transmission electron microscope.

### 3.3.2.4 3D –Tomography.-

Samples for tomography were prepared by cryomicrotoming to 50 nm thin sections at  $-130^{\circ}\text{C}$ . The sections were vapor stained with ruthenium tetroxide for 30 minutes. Tomography measurements were performed on a Technai 20 Field Emission Gun Scanning Tunneling electron microscope. The images were collected digitally with a slow speed charged coupled device (CCD) camera. A series of two-dimensional TEM images was obtained by tilting the specimen over various tilt angles. The data was corrected for lateral shift and change of defocus, after taking an image. This cycle was repeated, typically, over  $\pm 65$  degrees, with 2 degree tilt increments. After the acquisition of a prealigned data set, the data series was aligned more accurately with the help of fiducial markers. Gold beads were previously sprinkled on the TEM grids to aid as markers. After the alignment of the data series the 3-dimensional construction was computed using the IMOD image processing and modeling software. The outer surface of the rubber phase was used to build up a contour 3-dimensional model of the rubber phase in each blend.



### 3.3.2.5 AFM.-

Samples for AFM were smoothed at  $-130^{\circ}\text{C}$  by using a cryomicrotome. The cut surfaces were analysed using a NanoScope III multimode atomic force microscope (Digital Instruments, Santa Barbara, CA, USA) in the tapping mode with phase imaging under ambient conditions. The instrument was equipped with an E-scanner. A Standard Si Nanosensor probe was used to conduct the measurements.

## 3.4 RESULTS AND DISCUSSION

### 3.4.1 SEM

Conventional SEM images of a TPV and SEBS/PP/oil blend are shown in

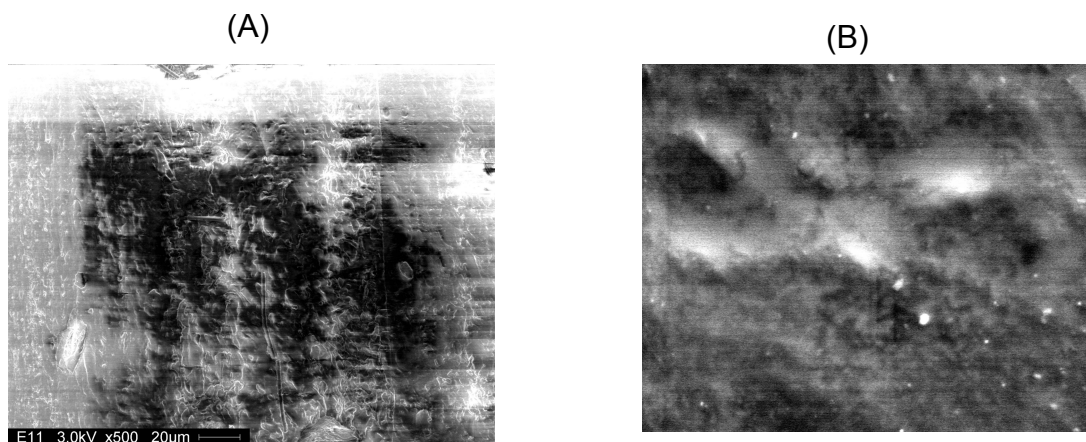


**Figure 3.3** SEM image of 28/33/39 wt.-% rubber/PP/oil blend showing poor image contrast between the rubber and PP phase; (A), TPV; (B), SEBS/PP/oil.

Figures 3.3(A) and 3.3(B), respectively. The rubber/PP/oil compositions in these images are 28/33/39 wt.-%. The oil is distributed on a molecular level between the rubber and amorphous part of PP and therefore is not visible in these images. The images show poor contrast between the rubber- and PP-phases. The image is blurred and the different features are hardly visible. The image quality even deteriorates with increasing amount of oil. This problem is caused by sample charging and some beam damage. Charging effects such as bright spots in the image arise due to build-up of an electric charge on the specimen surface. Besides, oil being a liquid and electrical non-conductor, is very unstable under an electron beam. This means, that with a high accelerating voltage, electrons cannot reach earth. Thus a charge cloud builds up around the sample surface causing a whitening effect. These problems are common in SEM analysis of biological, hydrated or

organic samples and have been well documented in literatures.<sup>[6,7]</sup> Charging can be avoided by working at low acceleration voltages (LVSEM), also known as crossover voltages, where the number of electrons leaving the sample surface is just enough to compensate for the incoming ones.

### 3.4.2 LVSEM

Low Voltage SEM images of a TPV and SEBS/PP/oil blend are shown in Figures 3.4(A) and 3.4(B), respectively. The rubber/PP/oil composition in this image is 28/33/39 wt.-%, the same as in Figure 3.3. The samples were microtomed and stained using

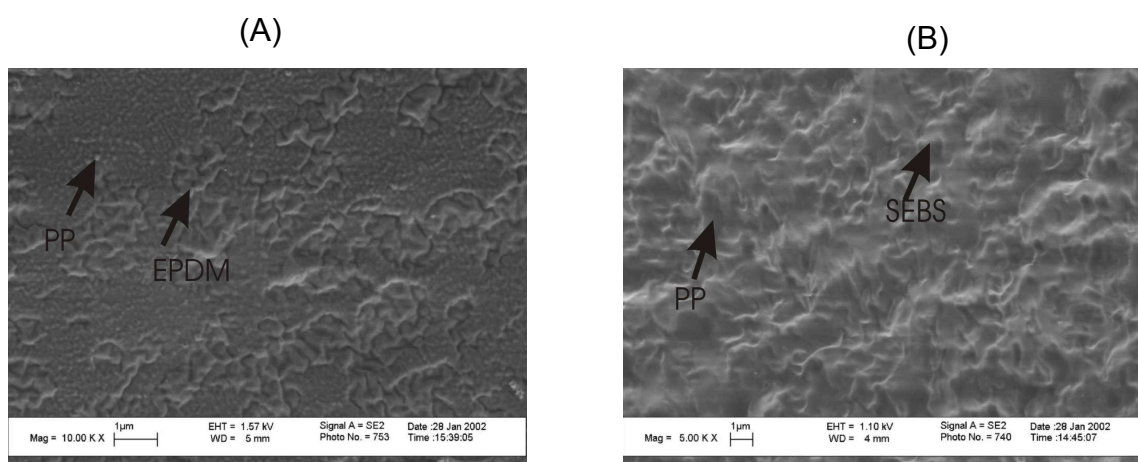


**Figure 3.4** LVSEM image of 28/33/39 wt.-% rubber/PP/oil blend showing poor image contrast between the rubber and PP phase; (A), TPV; (B), SEBS/PP/oil.

ruthenium tetra oxide vapors, as described in the experimental paragraph. The micrograph shown in Figure 3.4(A) provides a perfect view of the EPDM-phase distributed in the PP-matrix. The EPDM-domains appear to be elongated and touching each other. The rubber and polypropylene phases in the blend were identified after comparison with the SEM-micrographs of the individual components. The charging problem previously seen with conventional SEM is not experienced with this technique. This is because the images were taken at around 1 kV; quite low as compared to the voltages used in conventional SEM.

In addition to differences in morphology, Figure 3.4 also shows the influences of microtoming on the morphology. Microtome sectioning of the sample has resulted in a very flat surface in the region of the PP-matrix, while a pronounced relief is observed in the regions of dispersed rubber inclusions. Although the EPDM-domains show a topological

contrast different from the PP-matrix and the rubber is preferentially stained with  $\text{RuO}_4$ , there is little difference in the grey scales. The small difference in the grey scale levels is most probably due to the similar electron densities of the two phases resulting from poor bulk staining of the sample. If the bulk is relatively poorly stained as compared to the surface, the number of electrons coming out of the rubber- and PP-phases is grossly comparable. The topological contrast is due to a different surface topography of the rubber-phase from the PP-phase at the temperature of observation. The contrast originates from a different coefficients of thermal expansion of the rubber- and PP-phases, as the material is warmed up from  $-130\text{ }^\circ\text{C}$  to room temperature after microtome sectioning.<sup>[8]</sup> This implies that the difference in thermal expansion coefficient can be used to advantage by fracturing the samples instead of microtoming to increase the contrast in the images.

LVSEM-images of fractured TPV and SEBS/PP/oil blends are shown in Figures

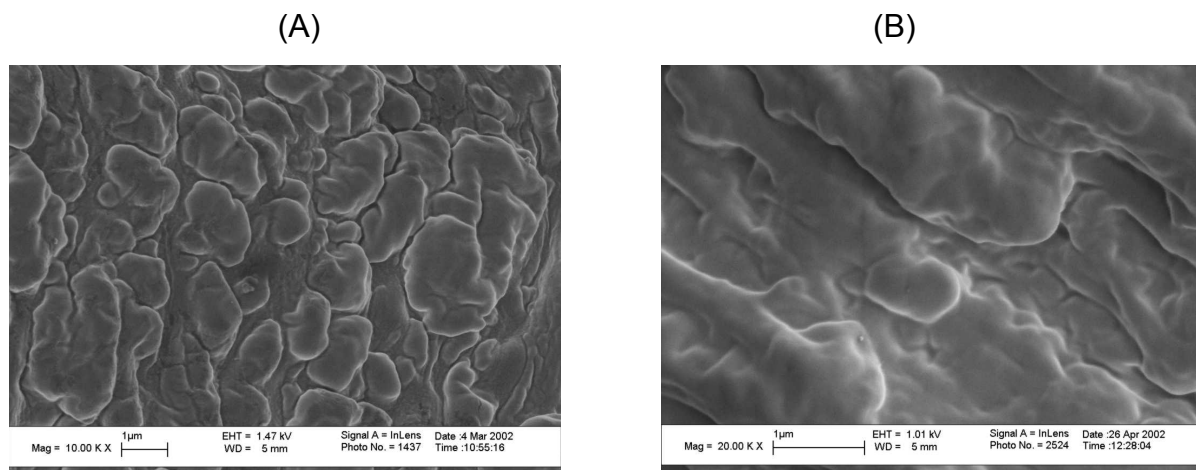


**Figure 3.5** LVSEM images of cryogenically fractured sample. The rubber/PP/oil composition is 31/25/44 wt.-%. (A), TPV; (B), SEBS/PP/oil.

3.5(A) and 3.5(B) respectively. The rubber/PP/oil is 31/25/44 wt.-%. In Figure 3.5(A), the contrast between the EPDM- and PP-phase is significantly higher, than was previously observed. Even the boundaries between EPDM-particles are clearly visible. Although the rubber particles overlap each other, they clearly appear to be dispersed in PP-phase.

LVSEM reveals many interesting features of the TPV-morphology. The particle size and shape of the EPDM-phase is not uniform. In Chapter 4 it will be shown that the particle size distribution of EPDM depends on total shear applied to the melt during blending. According to Jayaraman *et al.*<sup>[9]</sup> the particle shape is related to the melt flow index

(MFI) of the PP. In blends with low MFI of PP, the EPDM particles appear elliptical and when the MFI increases the particles appear to be more spherical.

The SEBS/PP/oil blend, Figure 3.5(B), shows a different type of morphology. The SEBS- and PP-phases appear to be co-continuous: it is impossible to distinguish the SEBS-phase from the PP-phase. Comparatively more contrast is obtained from LVSEM of extracted blends as shown in Figure 3.5(C). The SEBS- and the oil-phases are soluble in toluene at room temperature, leaving the PP-matrix. The amount of SEBS-phase soluble in toluene can further be used to measure the degree of continuity. If all of the SEBS-phase can be extracted, the SEBS-phase must have been continuous. If the PP then remains in one piece and has the same shape as the original sample, the PP- phase must also have been continuous.

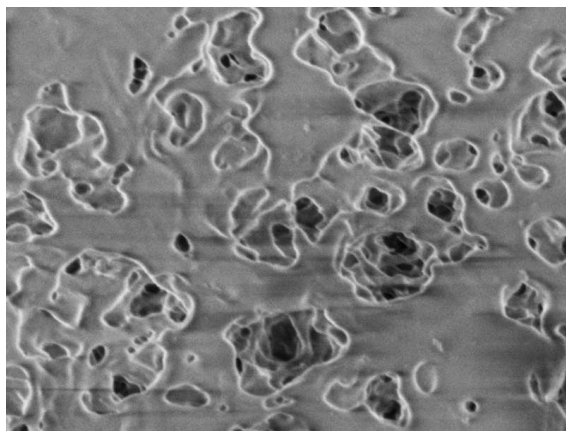


**Figure 3.5(C)** LVSEM of an extracted SEBS/PP/oil blend, showing the holes left over after the SEBS/oil phase has been extracted. The rubber/PP/oil composition is 31/25/44 wt.-%.

In Figure 3.5(C), the holes correspond to the removed SEBS-oil phase. The remaining phase is PP. A lot of holes appear to be interconnected along the third dimension, suggesting continuity of the SEBS phase. Other holes, however, appear to be dispersed. This suggests, that the SEBS-phase is not fully co-continuous. There is a limited degree of connectivity between the SEBS domains, which can be used for quantitative description of the morphology of these blends.

There are several reasons behind the enhanced contrast with LVSEM as compared to conventional SEM. The penetration depth of low secondary energy electrons ( $< 1$  kV) is less than 50 nm in most materials. The image information consequently comes more from regions close to the surface, which are higher stained, than the bulk. Besides,

modern day LVSEMs have improved field-emission cathodes, which provide narrower probe beam diameters at low, as well as high electron energies as compared to conventional SEM. In addition, the new in-lens detector in LVSEM makes it possible to work at small working distances and, as a consequence with a high resolution at low electrons current. This results in improved spatial resolution and minimal sample charging and damage.

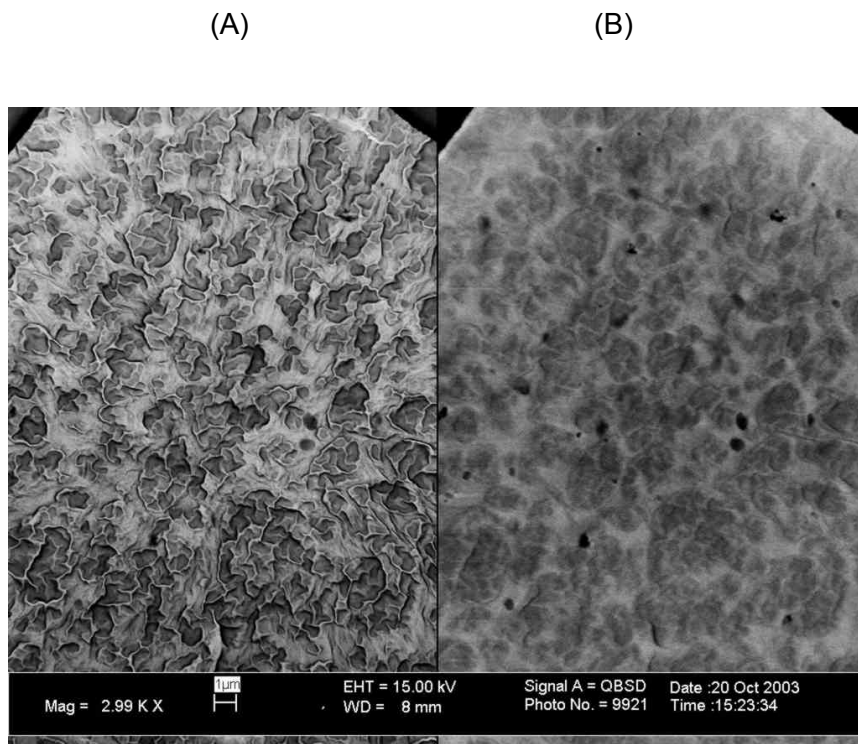


**Figure 3.6** Comparative LVSEM images of a TPV obtained using (A), a secondary electron detector; (B), a back scattered electron detector. The rubber/PP/oil composition is 31/25/44 wt.-%.

A comparative study of the secondary electron contrast and back-scattered contrast is given in Figures 3.6(A) and 3.6(B), respectively. The sample is an EPDM/PP/oil TPV of composition 31/25/44 wt.-%. The resolution of the back-scattered image is lower than the secondary-electron (SE) image. Back-scattered (BS) electrons are emitted from the primary beam and react elastically with the sample's atoms. Chemical elements that have high atomic number (high positive load of the atomic core) produce more back scattered electrons than the elements with a low atomic number. Areas of the sample with a high atomic number (here stained EPDM-domains) thus

appear whiter than areas with a low atomic number. They tend to give more phase information when compared to secondary electrons. They have higher energy than the secondary electrons and they originate from the bulk of the sample. However the resolution obtained by back-scattered electron is quite low.

Secondary electrons are emitted when the primary beam, upon losing a part of its own energy, excites atoms in the sample. They are relatively easy to detect in large numbers with the help of the in-lens detector. They give images with a good signal-to-noise ratio. The image obtained, however, shows the topography of the sample with very little phase contrast. For blends of TPVs, SE imaging was found to be more useful than back scattered imaging, because of the high contrast between the phases was necessary to study the particle size distribution.

### 3.4.3 TEM

TEM-images of TPV and SEBS/PP/oil blends are shown in Figure 3.7(A) and 3.7(B). The dark phase represents the rubber phase and the white phase is PP. This technique proves to be the best for visualizing the morphology of these blends.

The image on the left shows EPDM domains dispersed in the PP-matrix. The same seems to happen for the SEBS phase in the image shown on the right. A higher magnification image of the SEBS phase shows distinct polystyrene domains (see Figure 1.3) more or less clustered together, and phase separated from the ethylene-butylene matrix. The PP phase is more evenly distributed within the SEBS phase as compared to the EPDM phase in the left image, which hints in the direction of co-continuous morphology. The contrast between the rubber and the PP-phase is very high as compared to the one seen with LVSEM. The thickness of ultrathin sections (~ 50 nm) and staining time (~ 30 minutes) and the concentration of the staining agent (1% solution of  $\text{RuO}_4$ ) was crucial to obtaining good images with this technique.

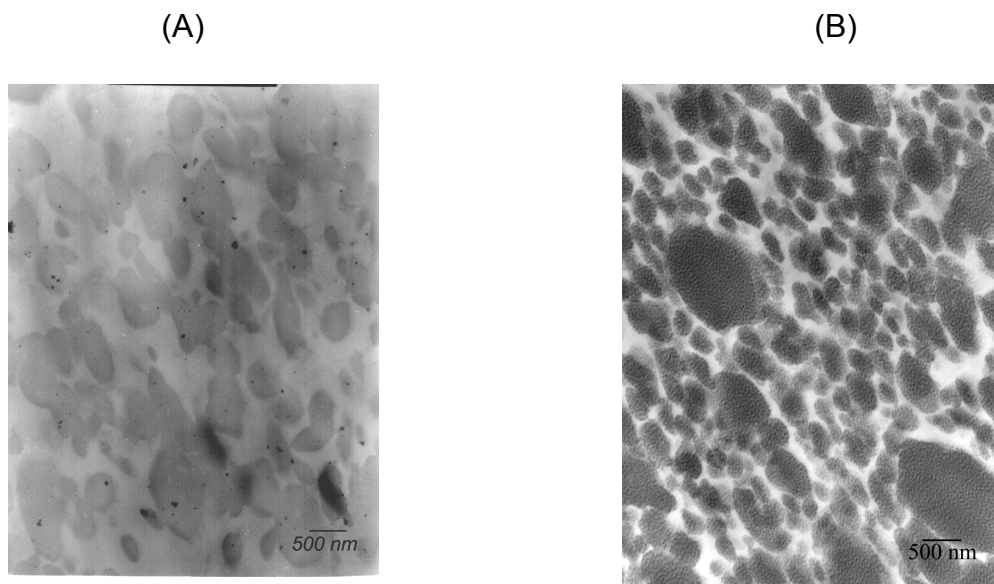


**Figure 3.7** TEM images of (A), TPV;(B), SEBS/PP/oil blend. The Rubber/PP/oil composition is 28/33/39 wt.-%.

The reason why TEM-images could reveal the finest morphological details as compared to LVSEM can be explained by the fact, that the TEM image involves detecting all electrons transmitted through a sample, whilst SEM involves detection of secondary electrons emitted from the surface of the sample. The voltage used in our TEM is between 200 and 300 kV while with low voltage SEM it is around 1 kV or less. The amount of secondary electrons produced in LVSEM is too low to be useful in creating high-resolution images. Detecting transmitted electrons in TEM demands a very thin section:  $\sim 50$  nm and they are mounted on carbon coated copper grids. This also reduces sample charging at high acceleration voltages, because the charge build up can easily be grounded.

#### 3.4.4 Tomography

Most microscopic methods like scanning electron microscopy and transmission electron microscopy are at best two-dimensional projections of a three-dimensional structure, and thus they discard some vital spatial information, which the specimen may contain in the third dimension. Any specimen variation in the third dimension can be minimized by careful sample preparation, sectioning a specimen in a specific orientation to reveal the features under study and/or by preparing two specimens from mutually perpendicular axes. These approaches work best for specimens with microstructures that are structurally simple, such as polymer blends with a small amount of the dispersed

phase, or whose structure can be predicted due to specific orientational relationships. For most specimens however, two-dimensional projections lead to some uncertainty as to their true 3D structure. This is illustrated in Figure 3.8. The TEM image of a 41/18/41 wt.-% EPDM/PP/oil TPV, shown in Fig. 3.8(A), gives an impression of a continuous EPDM phase. This is obviously an artefact of TEM, because a continuous crosslinked EPDM phase will not lead to thermoplastic processability. The reason for this artefact is exhibited in the schematic diagram showing image formation in TEM: Fig. 3.7(B).

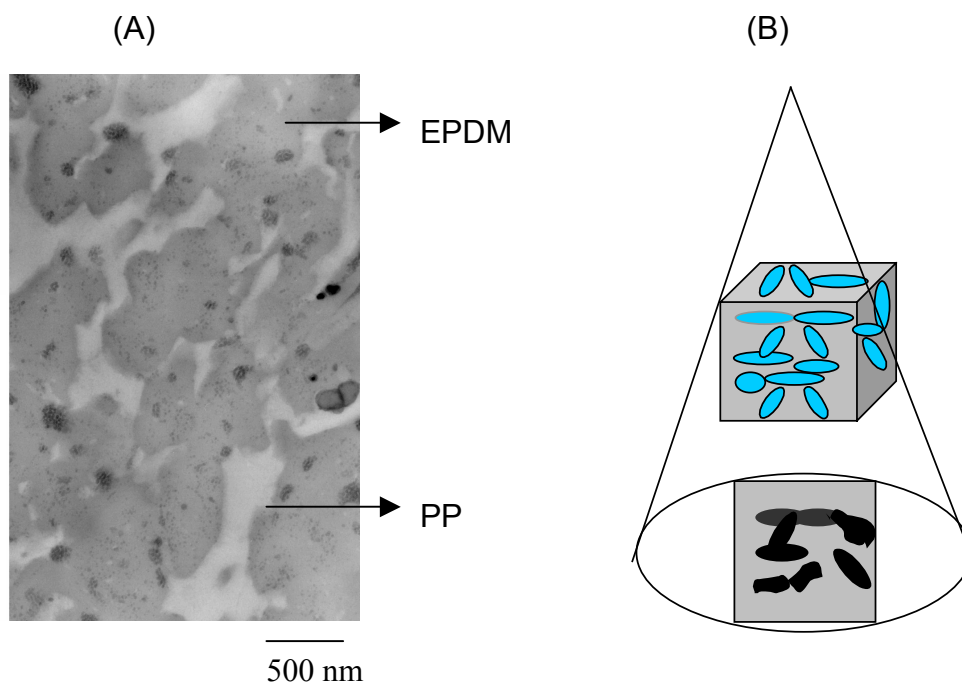


**Figure 3.8** (A), Representative TEM image of 41/18/41 wt.-% of EPDM/PP/oil –TPV. The EPDM phase appears to be co-continuous with PP; (B), Schematic representation of image formation in TEM.

In TEM, one merely projects a shadow of all features lying along the direction of the common axis on a two-dimensional screen. So in case of polymer blends, if the major phase is dispersed in the minor one, two-dimensional projection of nearby particles will overlap, giving the impression of a continuous structure.

To investigate the potential of electron tomography in differentiating between EPDM domains at high weight percentage of the dispersed phase, a TPV blend with



composition 28/33/39 wt.-% EPDM/PP/oil was imaged. In the series of 2D-TEM images the EPDM phase appears as the dark phase. The other phase is PP and oil.

Representative two dimensional TEM images of the TPV blend obtained at different tilt angles of the specimen are shown in Figure 3.9(A)–(C). In Fig. 3.9A, the EPDM domains appear to touch each other (as marked by the black circle) giving an

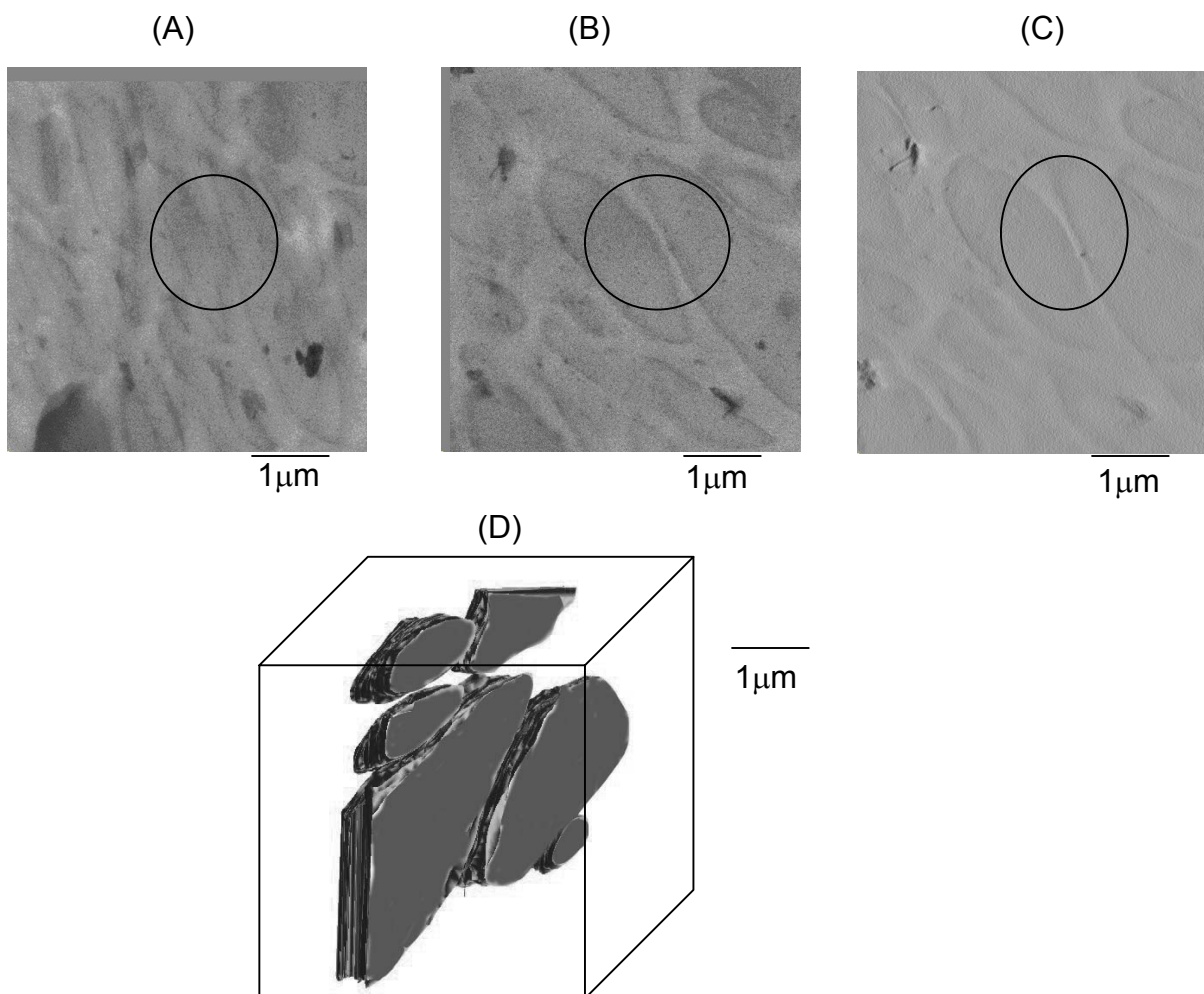


**Figure 3.9** Representative 2D-TEM images of an oil extended 41/18/41 wt.-% EPDM/PP/oil – TPV. (A), At + 45° tilt angle; (B), No tilting; (C), – 45° tilt angle; (D), 3D-model of the blend showing EPDM particles.

impression of a continuous phase.

Tilting the sample gives a different direction of view: Figures 3.9(B) and 3.9(C), which show that the particles are separated. The 3D tomographic model obtained by backprojecting these 2D-TEM images is shown in Figure 3.9(D). This model gives a

perfect view of the 3D structure of the EPDM domains and clearly shows that the EPDM domains in the TPV are dispersed, although they may touch each other if interparticle distances are small. Only few domains from the original 2D image are shown in the reconstructed 3D model for shortness sake. The domains are elongated having a major axis length in the range of 1-4 microns. The thickness of each domain depends on the number of TEM images taken for reconstruction.

The application of electron tomography in constructing 3D-images is not restricted to polymer blends with dispersed phase morphology. Figure 3.10 shows the contour of a styrene-(ethylene-butylene)-styrene block copolymer (SEBS) in a blend with isotactic polypropylene and oil, constructed using electron tomography. A TEM image of a 28/33/39 wt.-% SEBS/PP/oil blend with composition is shown in Fig 3.10(A). In the image the SEBS - domains appear black and the PP-phase appears white. It is quite difficult to judge whether the SEBS - domains are dispersed or continuous with the PP phase. The three-dimensional model of this blend obtained using electron tomography is shown in Figure 3.10(B). The model shows a SEBS-contour that resembles a

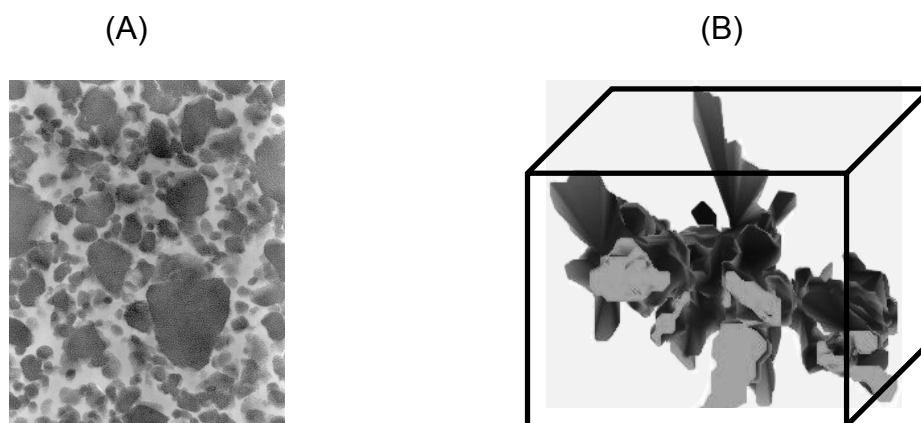


**Figure 3.10** (A), TEM of SEBS/PP/oil blends; (B), 3D reconstruction model of the continuous SEBS phase in an 28/33/39 wt.-% SEBS/PP/oil blend.

complicated double gyroid structure. This is a stronger evidence of the co-continuity of the SEBS-phase, as compared to any other microscopic technique. Until today no other microscopic technique is available, which can characterize the 3D-structure of these blends at such high resolution.

The tomographic models shown above offer the possibility to perform three-dimensional imaging of polymer blend morphology. The computing power necessary for

handling electron tomographic reconstruction is very large. A tilt-series of 60 floating points 512 x 512 pixel projections is 62 megabytes in size and the 3D reconstruction from such a data set will require some 512 megabytes. Operations such as reconstruction on such data sets require significant computing resources. With enormous improvement in present days computing power, these requirements are easy to meet.

Despite the great advantages of tomography over TEM, it was not further used in our study. This is because of the following two reasons:

- (a) Restricted availability of the equipment;
- (b) The information obtained from TEM, LVSEM and solvent extraction was sufficient to describe the morphology.

#### **3.4.5 AFM**

AFM images of TPV and SEBS/PP/oil blends are shown in Figure 3.11(A) and 3.11(B). The rubber/PP/oil percentages are 28/33/39 wt.-%. In these images the darker grey areas correspond to the rubber phase and the white areas correspond to the PP. Both images show artefacts due to contamination of the AFM-tip by oil. Such artefacts in the AFM-image were observed before in oil-extended blends of s-SBR/BR filled with silica.<sup>[10]</sup> The oil that is present in the compound is squeezed out of the polymer and ends up at the surface, where it is spread out by the AFM-tip. These problems are particularly pronounced at oil contents of more than 100 phr.

The image on the left for TPV shows elongated rubber particles, some of which are completely surrounded by PP-matrix, giving the impression that the EPDM-phase is indeed dispersed. The image on the right for the SEBS/PP/oil-blend, shows two phases, but it is impossible to determine whether the phases are co-continuous. Because of these limitations, AFM was not further pursued for morphological studies of our blends.

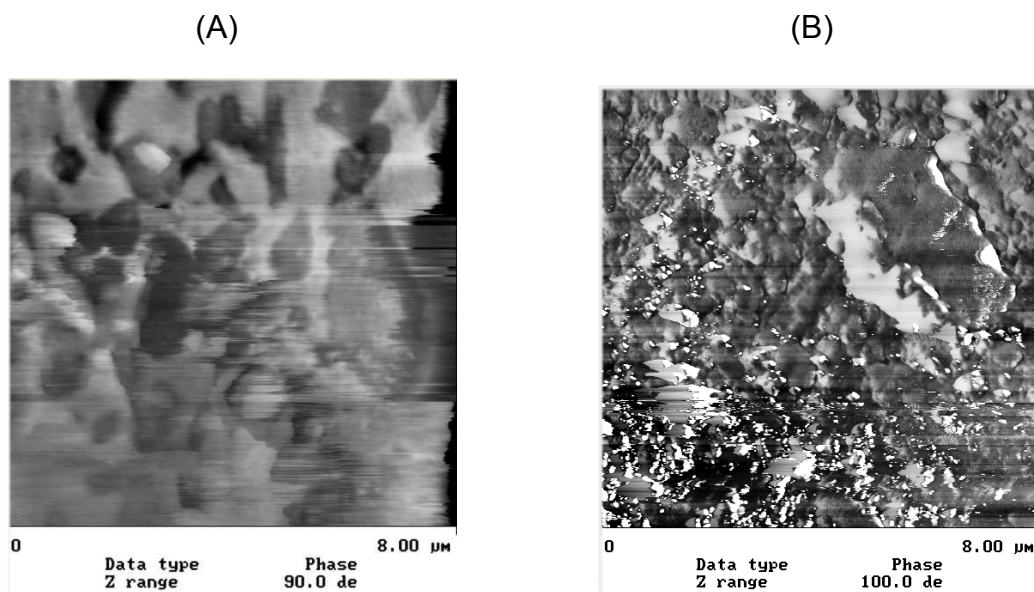


**Figure 3.11** AFM image of TPE blends. (A), TPV; (B), SEBS/PP/oil. The rubber/PP/oil composition is 28/33/39 wt.-%.

### 3.5 CONCLUSIONS

Analysis of the morphology of TPV and SEBS/PP/oil blends using a variety of techniques leads us to the conclusion that TEM is the best method for studying the morphology of these blends. The blend features are clearly resolved and very fine details of the sample can easily be visualised. The information obtained in these images can sometimes be misleading. Information from TEM must be supplemented with images obtained from LVSEM. LVSEM of fractured and stained samples gives valuable additional topological information.

Identifying a co-continuous morphology is more difficult than a dispersed phase morphology. For blends with co-continuous morphologies more information is obtained if one of the phases is removed by solvent extraction prior to LVSEM visualization. The degree of co-continuity of the phases can be calculated from solvent extraction data and correlated to microscopic images.

Conventional SEM is not suitable for analysis of soft TPE-blends due to sample charging effects. The reason is most probably the presence of a diluent such as paraffinic oil, which in large amounts builds up a static electric charge on the sample.

AFM is not so useful in investigating the morphology of highly oil extended samples, as in the present case, because the tip picks up the oil during scanning giving poor images.

Tomography gives new three-dimensional information on objects that cannot be obtained with traditional TEM. The latter gives wrong information due to the fact that the principle of image formation is based on projections. The resolution of tomography is 2 to 10 times higher than TEM. Presently it is mostly restricted to biological samples. However it has the potential to become a very valuable tool in three-dimensional structure determination of polymer blends.

### 3.6 REFERENCES

1. L. C. Sawyer, D.T. Grubb, Chapter 1, *"Polymer microscopy"*, second edition, Chapman and Hall, London (1996).
2. S. K. De, A. K. Bhowmick, *"Thermoplastic Elastomers from Rubber-Plastic Blends"*, Elis Horwood Ltd., New York (1990).
3. A. J. Koster, U. Ziese, A. J. Verkleij, A. H. Janssen, K. P. Jong, *Stud. Surf. Sci. and Catal.*, **130** (2000) 329.
4. A. J. Koster, U. Ziese, A. J. Verkleij, A. H. Janssen, K. P. Jong, *J. Phys. Chem. B*, **104** (2000) 9368.
5. U. Ziese, PhD thesis, University of Utrecht (2002), The Netherlands.
6. R. A. Crowthers, L. A. Amos, J. T. Finch, D. J. de Rosier, A. Klug, *Nature*, **226** (1970) 421.
7. V. Dudler, M. C. Grob, D. Merian, *Polym. degr. stab.*, **68** (2000) 373.
8. D. L. Vezie, W. W. Adams, E. L. Thomas, *Polymer*, **36** (1995) 1761.
9. F. Lednicky, J. Hromadkova, Z. Pientka, *Polymer*, **42** (2001) 4329.
10. K. Jayaraman, G. Kolli, M. D. Ellul, paper presented at the International Rubber Conference, Prague, (2002) July 1-4.
11. L. A. E. M Reuvekamp, PhD thesis, University of Twente (2003), The Netherlands.

---

## Chapter 4

### **A Comparative Study of the Structure-Property relationship in Dynamically Vulcanized EPDM/PP/oil-Blends and SEBS/PP/oil-Blends**

---

*This chapter presents a comparative study of the morphology and structure related properties of thermoplastic elastomer blends based on dynamically vulcanized ethylene-propylene-diene rubber (EPDM) / isotactic polypropylene (PP)/ oil, and of thermoplastic olefinic blends of styrene-(ethylene-butylene)-styrene rubber (SEBS) / PP/ oil prepared under identical conditions. Different compositions of each blend type were made in an internal mixer and co-rotating twin-screw extruder. Morphological characterization using different microscopic techniques showed droplet-matrix morphology for the TPV blends and in combination with solvent extraction, co-continuous morphology for the SEBS/PP/oil blends. The particle size distribution of the EPDM phases in the TPVs, prepared in the internal mixer, was narrower than for the twin-screw extruder. No difference in the morphology was observed for the SEBS/PP/oil blends prepared in the internal mixer and twin-screw extruder. The elongation at break values were found to be significantly higher for the SEBS/PP/oil blends as compared to the TPV blends. The gel content of the TPVs was found to be the main factor determining the stress-strain properties, as influenced by the preparation method. Also the crystallinity of the PP-phase for both TPV and SEBS/PP/oil blends was investigated and, although being dependent on the preparation method for the SEBS/PP/oil blends, did not reflect in the stress-strain properties.*

---

\*A part of this chapter has been published in Journal of Elastomer and Plastics, **36** (2004) 307, and presented at the 163<sup>rd</sup> Spring Meeting of the American Chemical Society, Rubber Division, San Francisco, CA.<sup>[1,2]</sup>

## 4.1 INTRODUCTION

Thermoplastic vulcanizates based on blends of ethylene-propylene-diene rubber (EPDM) and semicrystalline isotactic polypropylene (PP), commonly referred to as EPDM/PP TPVs, have a resemblance in properties and applications with thermoplastic elastomeric blends of Styrene-(ethylene-butylene)-styrene triblock copolymer rubber (SEBS) and PP. Both are available in a hardness range of 50 Shore A – 50 Shore D and their properties are close enough to make them both suitable for many automotive, medical and soft-touch applications.<sup>[3,4]</sup> For decreasing the hardness and improving the processability, commercial blends of these systems are often compounded with paraffinic processing oil. Although the highly oil-extended TPV blends were commercialized somewhere in the 70's already,<sup>[5]</sup> and the SEBS/PP/oil blends were commercialized in the early 90's, the scientific understanding of their resemblance in properties and how this is controlled by morphology and rheology, is incomplete. Previous studies on EPDM/PP TPVs were directed towards understanding the morphology development during processing,<sup>[6-8]</sup> influence of different curing agents<sup>[9-11]</sup> and understanding their deformation behavior.<sup>[12]</sup> Except for the works of Ohlsson *et al.*<sup>[13]</sup> and Veenstra *et al.*<sup>[14]</sup> comparative information on the SEBS/PP/oil systems is very limited. These studies have shown that the morphologies of these blends are primarily different. The TPVs are made up of EPDM-particles dispersed in a PP-matrix, while in the SEBS/PP/oil blends the two phases are co-continuous. Being morphologically different, the blends are expected to show quite different properties – a contradiction to what is observed in reality. So the question which needs to be addressed is: are the properties of these blends really independent of their respective blend morphologies?

This chapter presents a comparative study of the mechanical properties of thermoplastic elastomer blends based on dynamically vulcanized EPDM/PP/oil and SEBS/PP/oil prepared under identical conditions, in relation to their morphologies and structure related properties. Compositions of each blend type with different EPDM/PP/oil and SEBS/PP/oil ratios were made in an internal mixer. To study the effect of mixing equipment on the properties of these blends, some of the compositions were also made in a co-rotating twin-screw extruder. Both similarities and differences were observed in the stress-strain properties of the blends for both systems. In order to explain the differences, the blend morphologies were studied using transmission electron microscopy (TEM) and, wherever necessary, supplemented with Low voltage scanning electron microscopy (LVSEM) and atomic force microscopy (AFM). To further investigate the differences in the stress-strain properties, the gel content of TPVs was analyzed, the compression sets of the

blends were studied and the crystallization behavior of the PP - phase in both systems was investigated.

## 4.2 EXPERIMENTAL

### 4.2.1 Materials and blend recipes

The materials used in the present study were the same as mentioned in Chapter 3. Nine different compositions of each blend system, differing in the amount of PP and oil, were prepared in a Brabender internal mixer. As shown in Figure 4.1, the nine blends are all the combinations that can be made with three different PP/rubber weight ratios and oil/rubber weight ratios. The central compositions of these formulations, marked by circles, were also made in a co-rotating twin-screw extruder. The complete formulations in terms of weight percentage of components are shown in Table 4.1. The compounding recipes used for the preparation of TPV and SEBS/PP/oil blends are shown in Tables 4.2 and 4.3, respectively. For ease of discussion the blends are coded as follows:

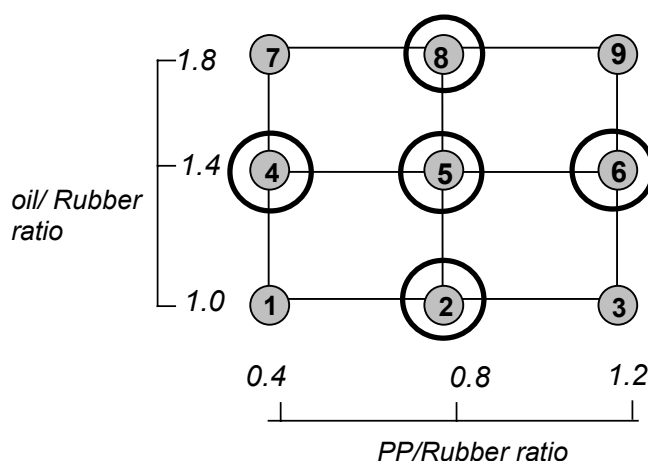


**Figure 4.1** Experimental design.

**Table 4.1** Weight composition of the blends.

Blend	% Rubber	% PP	% Oil
1	41	18	41
2	35	30	35
3	31	38	31
4	35	14	51
5	32	25	43
6	28	33	39
7	31	13	56
8	27	22	51
9	25	30	45



First letter: “B” stands for blends made in the Brabender internal mixer and “T” for blends made in the twin-screw extruder.

Second letter: “E” stands for EPDM-based TPV blends and “S” for SEBS/PP/oil blends.

Last digit: corresponds to the composition as shown in Table 4.1.

**Table 4.2 Compounding recipe of a TPV.**

Components	Composition (Parts per hundred rubber, phr)
EPDM, Keltan P597*	200
PP, Stamylan P11E10	varied
Extra Oil, Sunpar 150	varied
Phenolic resin, SP 1045	5
Stannous chloride dihydrate	1
Zinc oxide	2.5
Irganox 1076	0.5
Irgafos 168	0.5

\* Contains 50 wt.-% paraffinic oil.

**Table 4.3 Compounding recipe for SEBS/PP/oil blends.**

Components	Composition (Phr)
SEBS, Kraton G 1651	100
PP, Stamylan P11E10	varied
Oil, Sunpar 150	varied
Irganox 1076	0.5
Irgafos 168	0.5

## **4.2.2 Mixing**

### **4.2.2.1 Brabender mixing.-**

The blends were prepared using a Brabender Plasticorder type 350S, with a mixer chamber volume of 390 ml and fitted with Banbury-type rotors. A fill factor of 0.7 was used. To improve the dispersion of the large quantities of oil during mixing in the Brabender, the oil was first preblended with the rubber. Since the EPDM grade used already contained 100 phr of oil, the extra oil was added on a two-roll mill; in the case of SEBS, the oil was spontaneously soaked into the porous SEBS material without mechanical treatment.

To make the TPVs, the Brabender temperature was set at 180°C and the rotor speed at 80 rpm. The PP and stabilizers were first added in order to melt and blend these, which took about 1 minute. After this period, the EPDM/oil and zinc oxide was added. Four minutes later, the phenolic resin and stannous chloride were added. Mixing was continued for another 5 minutes. The total mixing time was 10 minutes.

For making the SEBS/PP/oil blends, the temperature and rotor speed settings were the same as for the TPVs. The PP and stabilizers were first added to the mixer and mixing was continued till they melted after about 1 minutes. The preblend of SEBS/oil was then added. Since SEBS is fluffy material and difficult to mix, the total mixing time was increased to 30 minutes.

### **4.2.2.2 Twin-screw extruder mixing.-**

The TPVs were prepared with a Werner and Pfleiderer ZSK-40 co-rotating twin-screw extruder, operated at 350 rpm. The temperature profiles were set so that the temperature in the melt ranged from 180 to 210°C. The average residence time was about 1 minute.<sup>[15]</sup> The SEBS/PP/oil blends were made in a ZSK-25 operated at 250 rpm. The SEBS was first dry blended with the oil at room temperature. The other ingredients (PP and stabilizers) were dry mixed with the oil extended SEBS to obtain all ingredients in a dry mixed state. This mixture was then fed into the extruder at a constant rate of 5-10 kg/h. The extruded strands were cooled in a water bath and pelletized.<sup>[16]</sup> Temperature profiles were similar to those used in the ZSK-40 for the preparation of the TPVs.

## **4.2.3 Morphological characterization**

After the blends had been compression molded, small samples were taken for electron microscopic examination. Two different microscopic methods – TEM and LVSEM were used to

study the morphology of both blend systems. For some SEBS/PP/oil samples AFM was also used. For TEM, the samples were microtomed at  $-130^{\circ}\text{C}$  using a diamond knife. TEM studies were performed using a Philips CM30 transmission electron microscope. In all cases the samples were vapor stained with ruthenium tetroxide. The staining time for TEM samples was 10 minutes. For LVSEM the samples were fractured in liquid nitrogen. The studies were performed using a Leo 1500 scanning electron microscope. The staining time was 30 minutes. The particle size distribution in the TEM images was analyzed using NIH imaging software.<sup>[17]</sup> AFM experiments were performed in tapping mode using a Nanoscope III scanning probe microscope (Digital instruments).

#### 4.2.4 Mechanical properties

After mixing the materials were compression molded using a WLP 1600/5\*4/3 Wickert laboratory press at  $200^{\circ}\text{C}$  for 3 minutes under a pressure of 10 MPa and then cooled under pressure to about  $30^{\circ}\text{C}$ . Sheet thickness was 2 mm. The sheets were punched into dumbbells (ISO-37, type 2) for tensile measurements.

Tensile properties were determined at room temperature according to ISO-37 using a Zwick Z020 universal testing machine equipped with a 500 N load cell. A crosshead speed of 50 mm/minute was used to measure the E-modulus and 500 mm/minute to measure the tensile strength and elongation at break. The reported results of each blend are the average of at least four measurements. The standard deviations in the whole procedure, from the mixing till the tensile properties, were generally less than 10%. The hardnesses of the compounds were measured with a Zwick hardness meter (Shore A type, ISO R868).

The compression set after 72 hrs/ $23^{\circ}\text{C}$  and 24 hrs/ $100^{\circ}\text{C}$  was measured according to ISO 815 standard.

#### 4.2.5 Solvent extraction on SEBS/PP/oil blends

In order to estimate the degree of co-continuity of the SEBS-phase in the SEBS/PP/oil blends, about 1.5 grams of SEBS/PP/oil samples were immersed in toluene at room temperature for 24 hours. The change in sample weight after extraction was compared to the amount of extractable phase originally present in the sample. This fraction is the degree of co-continuity of the SEBS phase.

#### **4.2.6 Degree of crystallinity of the PP-phase by thermal analysis**

The thermal behavior of the blends was studied by means of a Perkin Elmer DSC 7 differential scanning calorimeter (DSC). The samples, about 5-10 mg were heated at a rate of 10°C/minute from 25°C up to 200°C, maintained at this temperature for another 5 minutes and then cooled down to -100°C at the same rate. At -100°C they were kept for another 5 minutes and then reheated to 25°C at a rate of 5°C/minute. The melting, crystallization temperatures and enthalpy of fusion of PP were obtained from the cooling curve. The standard deviations in the experiments were less than 5%.

#### **4.2.7 Gel measurements on TPVs**

In order to estimate the degree of crosslinking of the EPDM phase in the TPVs, the samples were subjected to a series of solvent extractions. About 1.5 g of TPV samples were extracted for 24 hrs through stainless steel pouch in boiled acetone to remove the oil and stabilizers, followed by extraction for 48 hrs with boiling xylene to remove the PP and the soluble rubber. The amount of gel content was calculated from the weight of the residue after xylene extraction.<sup>[18]</sup>

### **4.3 RESULTS**

#### **4.3.1 Stress-strain properties of TPVs and SEBS/PP/oil blends, related to compound composition**

The study aims at understanding the mechanical properties of both systems, in terms of their morphological similarities or differences. For that reason, we will first describe the mechanical properties, as related to the compound recipes and the production methods of the blends. Secondly, the morphological and analytical characteristics of these designated blend systems will be highlighted.

The stress-strain properties of the TPV and SEBS/PP/oil blends are significantly different for identical compositions and mixing conditions. Representative stress-strain plot for blends BE5 and BS5 are shown in Figure 4.2. Both curves show a rather high modulus behavior at low elongations, to result from a continuous network of the polypropylene matrix. The SEBS/PP/oil blends show a more pronounced strain hardening effect and eventually break at higher engineering stress and strain values, as compared to the TPVs.

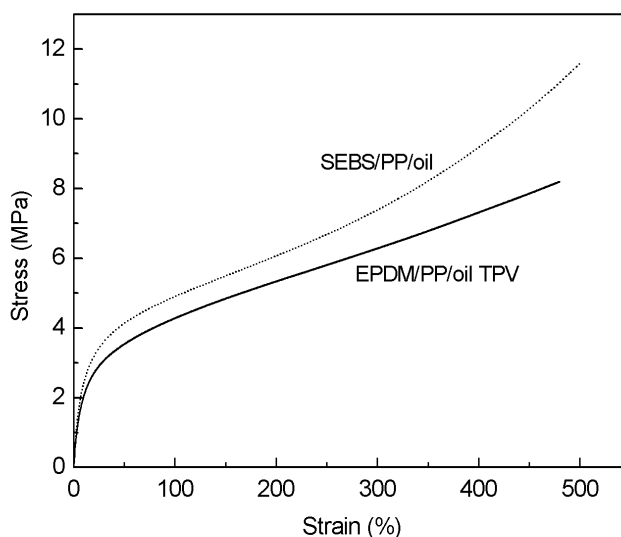


**Figure 4.2** Stress-strain plot of BE5 and BS5, as made in the internal mixer.

The conventional approach of evaluating the data of a design of experiment is, to use a multiple regression analysis (MLR). These models are commonly used for optimization problems, where one needs to find out the best combination of factors in order to maximize or minimize a response (e.g. tensile strength). In these models the effect of factors on the properties - so called responses in DOE terminology - are often weighed using centered and scaled coefficients. These mathematical transformations are useful in evaluating the effects of individual factors and their interactions on the responses. However, the physical interpretation of the centered and scaled coefficients and the correlation of these coefficients to material parameters are poorly understood. Since, in this work we are mainly interested in structure-property relationships and not in the optimization of factors, the results were not evaluated using the design of experiment approach.

The E-modulus values of both systems for different amounts of PP and oil are shown in Figures 4.3(A) and 4.3(B), respectively. The lines show the general trend of each property. The E-moduli of these blends for corresponding compositions are grossly comparable. A comparison of Figure 4.3(A) and 4.3(B) shows that E-moduli are mostly determined by the total amount of PP in the material. The variation of E-moduli due to changes due to the amount of PP are much

larger compared to changes due to the amount of oil. Although it is clear that the oil decreases the E-moduli of both blends, the decrease is less drastic in blends with high rubber content.

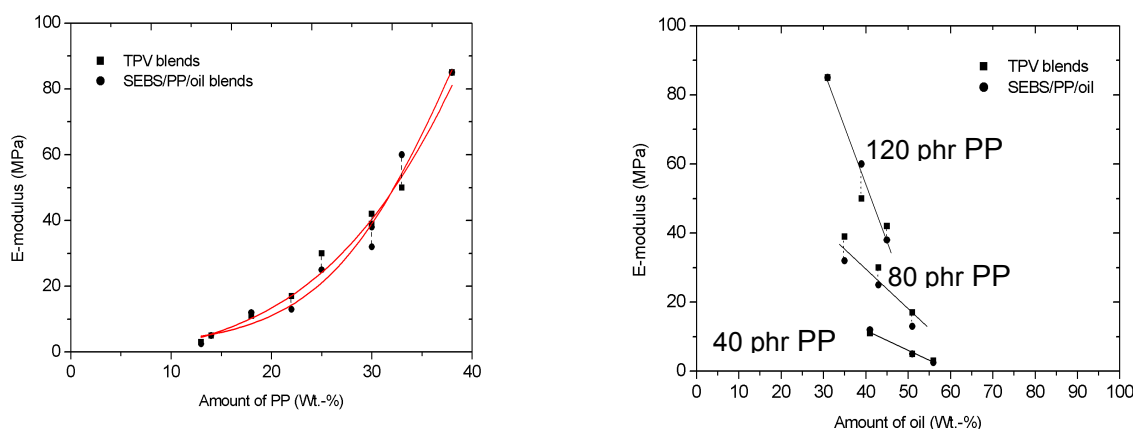


**Figure 4.3** E-modulus of TPV and SEBS/PP/oil blends with: (A), varying PP contents; (B), varying oil contents; made in the internal mixer.

The hardness of the compounds are in the range of 40-90 Shore A. The variation of hardness with the amount of PP and oil is same as in the case of E-modulus and is not reported for the sake of shortness.

The tensile strength of TPV and SEBS/PP/oil blends with increasing amount of PP and oil content is given in Figure 4.4(A) and 4.4(B), respectively. The tensile strength values are almost comparable for the two blend types at the low PP-end, but significantly higher for SEBS/PP/oil blends at the high PP-side. This shows that at the low PP-end, the rubber/oil phase in both blends has a similar contribution to the tensile properties. The large differences in tensile strength at the high PP-compositions show that, in addition to blend composition, there are more factors which influence the stress-strain behavior of these systems. Most likely factors are: blend morphology, crystallinity of the PP phase and the oil distribution between the rubber and PP phase.

From Figure 4.4(B) it is clear that oil in general decreases the tensile strength of both blends - the decrease being much faster in SEBS/PP/oil blends as compared to TPVs. This indicates that the oil has more influence on the tensile strength values of SEBS/PP/oil blends as compared to TPVs. The reason can be differences in the oil distribution between the rubber and PP phase. It can also result from differences in the deformation mechanism of the two blends due to different morphologies and crystallinity of the PP phase.

As compared to the E-modulus and ultimate tensile strength values, the differences in the elongation at break between the TPV and SEBS/PP/oil blends are large. Figure 4.5(A) suggests

that the values decrease with increase of PP-content for SEBS/PP/oil blends but increases with increasing amount of PP in TPV blends. The effect of oil on elongation at break is shown in Figure 4.5(B). A contradictory pattern is seen for TPVs and SEBS/PP/oil blends. The elongation at break values of SEBS/PP/oil increase with increasing amount of oil and that of TPV decrease. The most likely reasons for these differences lies in the deformation behavior of SEBS/PP/oil and TPVs and/or blend morphology.

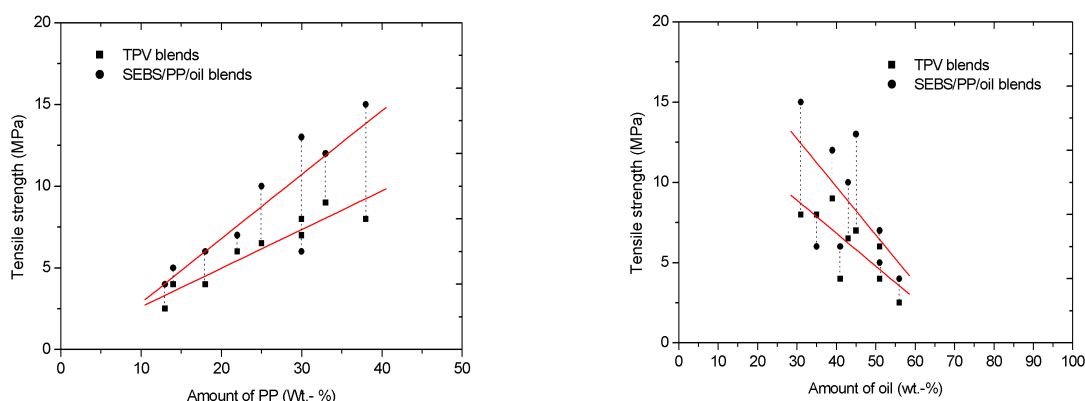


**Figure 4.4** Tensile strength of TPV and SEBS/PP/oil blends with: (A), varying PP content; (B), varying oil content; made in the internal mixer.

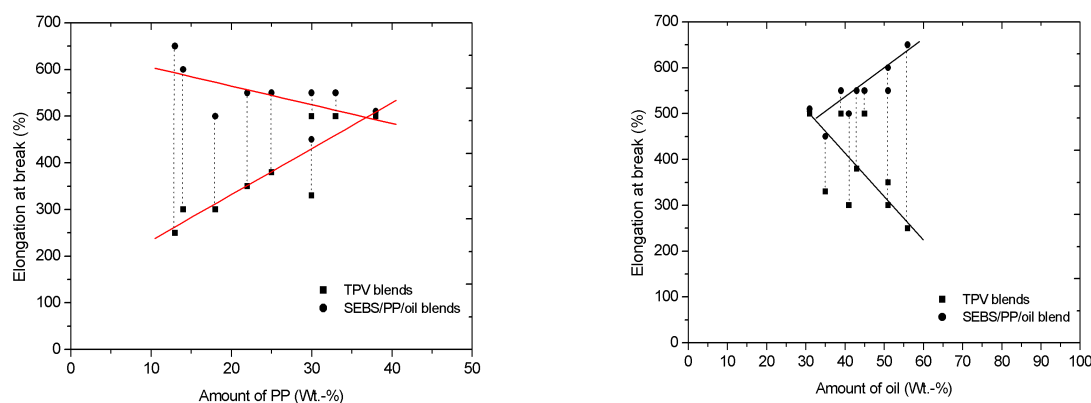


**Figure 4.5** Elongation at break of TPV and SEBS/PP/oil blends with: (A), varying amount of PP; (B), varying amount of oil; made in the internal mixer.

An overall comparison of the stress-strain behavior of the TPVs and SEBS/PP/oil blends shows that the properties of these two blend types, are in principle, different. Despite these differences, the properties are close enough to be considered for similar sorts of applications. In

order to understand these paradoxes it is necessary to study the blend morphology, oil distribution and crystallinity of the PP-phase. In addition, the properties of the binary blends of vulcanized EPDM/oil, SEBS/oil and PP/oil must be examined. The mechanism in which the binary blends couple to give the properties of the ternary blend might throw some light on this problem. These aspects will be discussed in Chapter 5.

#### **4.3.2 Effect of mixing equipment on the stress-strain properties**

##### **4.3.2.1 TPV blends.-**

The stress-strain properties of the TPV blends prepared in the two types of mixing equipment are shown in Figures 4.6 (A)-(C). The blends prepared in the twin-screw extruder show consistently higher E-moduli and tensile strengths than the blends prepared in the internal mixer. Although the differences are small especially at low PP compositions, they are based on reproducible experiments and so, should be taken for real.

##### **4.3.2.2 SEBS/PP/oil blends.-**

The stress-strain properties of the SEBS/PP/oil blends prepared in the two types of mixing equipment at different SEBS/PP/oil compositions are shown in Figures 4.7 (A)-(C). The properties of the blends are practically the same for both types of mixers except for the composition with highest amount of PP, where the E-modulus of blends made in the internal mixer is clearly higher than for the blends made with the twin-screw extruder.



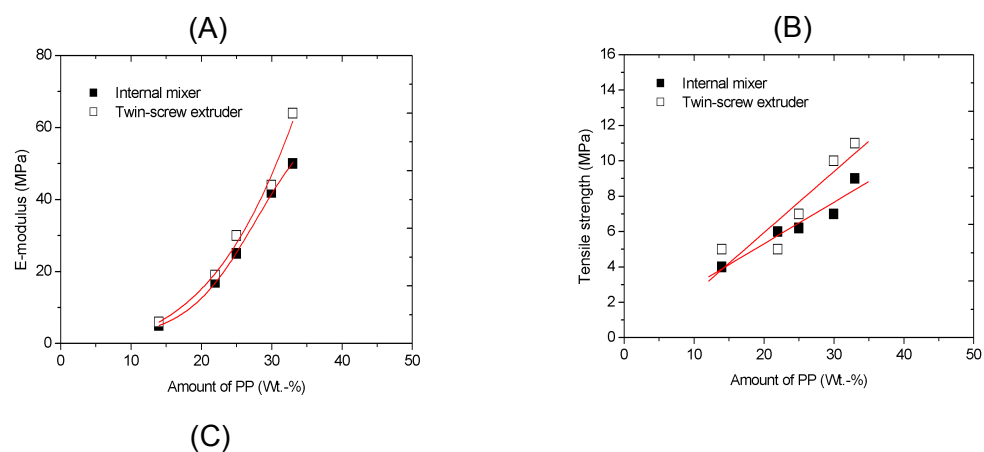


**Figure 4.6** Tensile properties of the TPV blends made in the internal mixer vs. the twin-screw extruder (A), E-moduli; (B), Tensile strength; (C), Elongation at break.

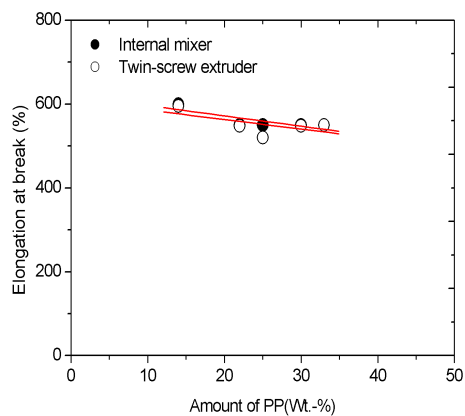
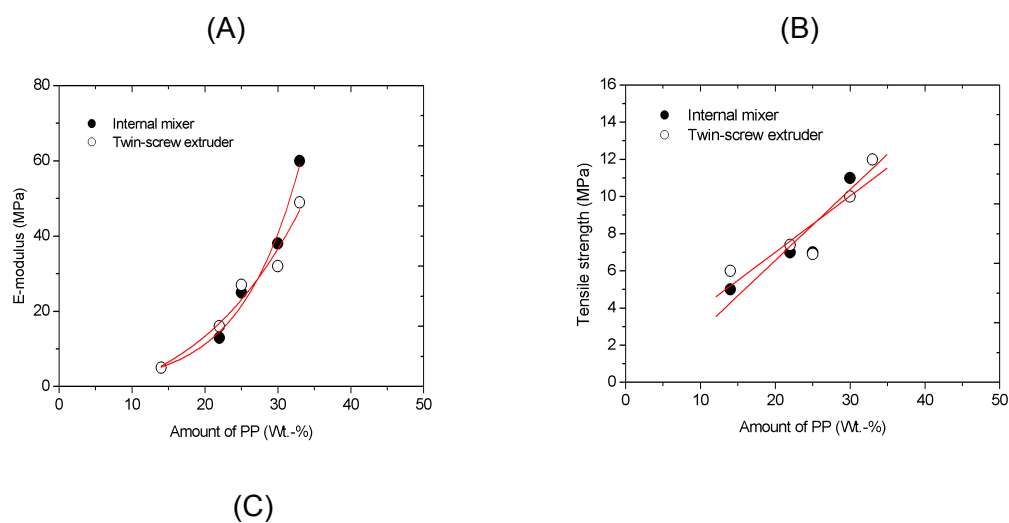
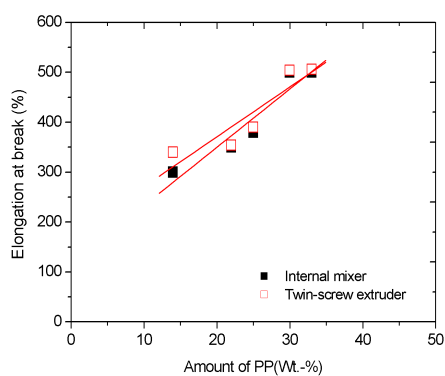


**Figure 4.7** Tensile properties of the SEBS/PP/oil blends made in the internal mixer vs. the twin-screw extruder (A), E-moduli; (B), Tensile strength; (C), Elongation at break.

The differences in the tensile properties of blends made in the internal mixer and co-rotating twin-screw extruder are significant. The mixing conditions in a ZSK twin-screw extruder are significantly different as compared to the internal mixer. The temperatures, shear rate, feeding process are different in the two mixing equipments. The results show that these factors do have an effect on the tensile properties of TPVs and SEBS/PP/oil blends.

In blends of rubber/PP, tensile properties like the E-moduli, tensile strength and elongation at break are related to structural features of the blend. The E-modulus is determined at very low deformation where only the elastic effects of the network and degree of crystallinity of the PP phase are important.<sup>[19]</sup> The ultimate tensile strength and elongation at break are determined at large deformations where, in addition to crystallinity and crosslink density of the network, the blend morphology may have an influence.<sup>[19]</sup> In order to explain the similarities as well as the differences observed in the stress-strain properties of the two blend systems, the following aspects were further studied: a) differences in morphology; b) differences in the degree of crystallinity of the PP-phase; c) differences in degree of cure of the EPDM phase in case of the TPVs: see below.

#### **4.3.3 Compression set**

The compression sets of the TPV and SEBS/PP/oil blends measured after 72 hrs at 25°C are shown in Figure 4.8. These compositions were made in the internal mixer. For all compositions studied, the compression set values are lower for SEBS/PP/oil-blends than for the TPV-blends. This is most likely due to a slight crystallinity of the EPDM-phase. If the experiments are repeated at higher temperatures e.g. 24 hrs at 100°C, the compression set of the SEBS/PP/oil blends increases much more than for the TPV blends: Figure 4.9a. This is, because at that temperature the polystyrene domains are near their glass transition temperature. These results show, that the compression sets of TPVs are much more stable to changes in temperature as compared to SEBS/PP/oil blends. The compression set values at 100°C are differentiated in three levels. If the amount of PP is expressed in terms of phr, as in Figure 4.9b, the three levels in Figure 4.9a can be correlated to the amount of PP/rubber ratio in the blends. This shows that the compression set values for both blends at 100°C is primarily determined by the PP/rubber ratio and is independent of the amount of oil.

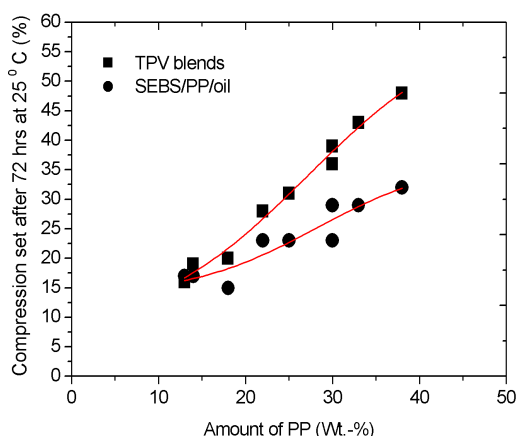


**Figure 4.8** Comparative data of the compression sets at 25°C/72 hrs of TPV and SEBS/PP/oil blends made in the internal mixer.

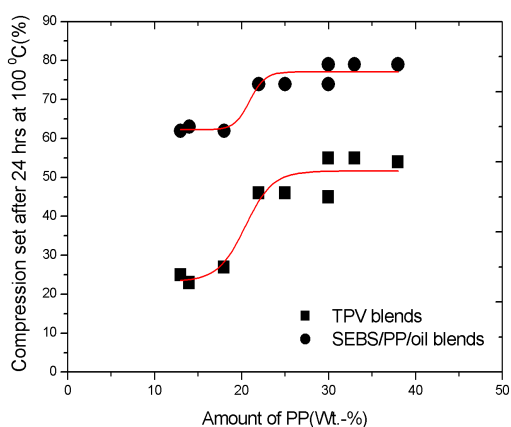


**Figure 4.9a** Comparative data of the compression sets at 100°C/24 hrs of TPV and SEBS/PP/oil blends made in the internal mixer.

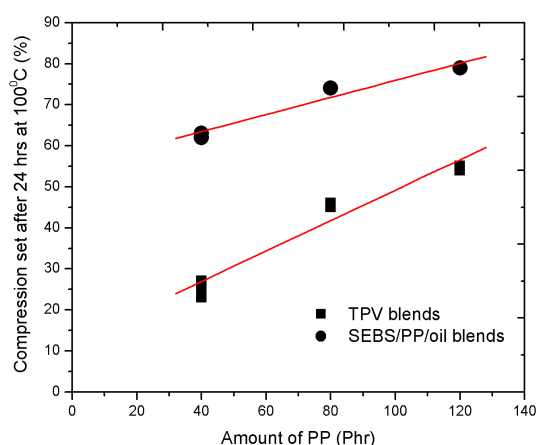


**Figure 4.9a** Comparative data of the compression sets at 100°C/24 hrs of TPV and SEBS/PP/oil blends made in the internal mixer. The data is Figure 4.9a is plotted as a function of the amount of PP in phr.

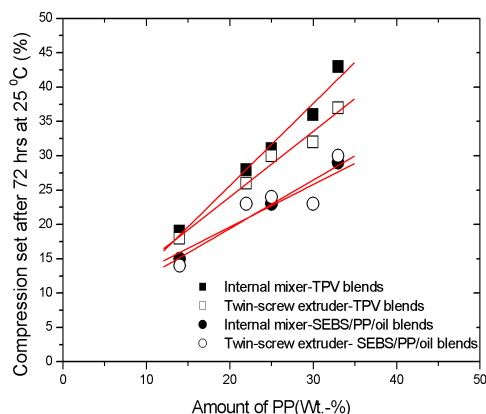


**Figure 4.10** Compression set of TPV and SEBS/PP/oil blends made in the internal mixer and twin-screw extruder.

The influences of different mixing equipments on the compression set values are shown in Figure 4.10. The TPVs made in the twin-screw extruder consistently show lower compression set values than those made in the internal mixer. Apart from the crystallinity effect of the EPDM, mentioned before, this may be due to a higher crosslink density of the EPDM phase in the TPVs made in the twin-screw extruder, as will be confirmed later: see 4.3.6 below. This result

correlates with the higher E-moduli and tensile strength values of the TPVs made in the twin-screw extruder as compared to the internal mixer. The values of compression set for SEBS/PP/oil blends were almost the same for the two mixers.

#### **4.3.4 Morphological characterization of the TPVs and SEBS/PP/oil blends**

##### **4.3.4.1 TPV blends.-**

Figures 4.11 (A)–(E) show TEM-images of the TPVs with different compositions: (A), BE1; (B), BE3; (C), BE7; (D), BE9 and (E) BE5, to represent the corner-points and center of the DOE, respectively. As a consequence of preferential staining of the EPDM phase by  $\text{RuO}_4$ , the dark phase can be assigned to EPDM domains and the white phase to PP. The oil in either phase is not visible.

The dark phases are proportional to the amount of EPDM rubber in the blends. The particles appear to be larger in TPV-blends with a low PP/rubber ratio: compare BE1 and BE3, respectively BE7 and BE9. At constant PP/rubber ratio, the EPDM particles appear larger if more oil is present in the blend: compare BE1 vs. BE7 and BE3 vs. BE9.

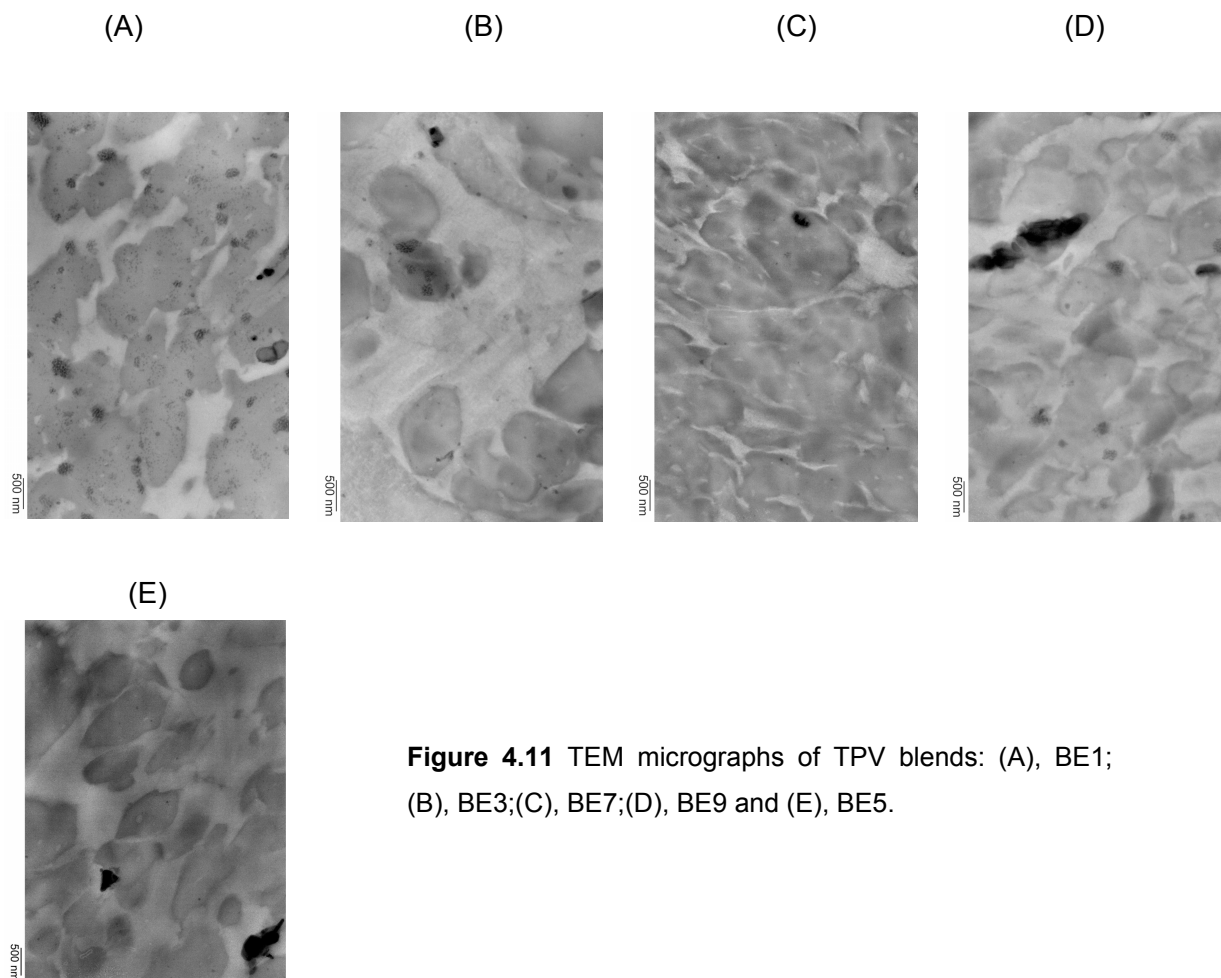


**Figure 4.11** TEM micrographs of TPV blends: (A), BE1; (B), BE3; (C), BE7; (D), BE9 and (E), BE5.

TEM-images of blends made in the internal mixer vs. the twin-screw extruder are shown in Figures 4.12 (A)–(D). In all cases the observations obtained from TEM were reconfirmed using LVSEM. In some TPVs the morphology was better revealed using LVSEM - e.g. for blends BE5 and TE5: Figure 4.13. By combining TEM- and LVSEM- data it can be seen, that for all compositions of the TPVs, the EPDM is dispersed as particles in the PP- matrix. The particle shapes are quite complicated. In TPVs prepared in the twin-screw extruder, the EPDM particles are primarily elliptical in shape. Similar elliptical shapes of EPDM particles were reported by Jayaraman<sup>[20]</sup> in EPDM/PP TPV blends. For TPVs prepared in the internal mixer, the particles are more uniform and spherical in shape. The particle size distributions for selected TPV compositions reveal, that with the exception of sample BE6, the largest amount of EPDM particles is in the range of 1-2  $\mu\text{m}$ , irrespective of the preparation method used: Figure 4.14. The particle size distribution is somewhat wider for the twin-screw extruded blends than for the TPVs produced in the internal mixer.

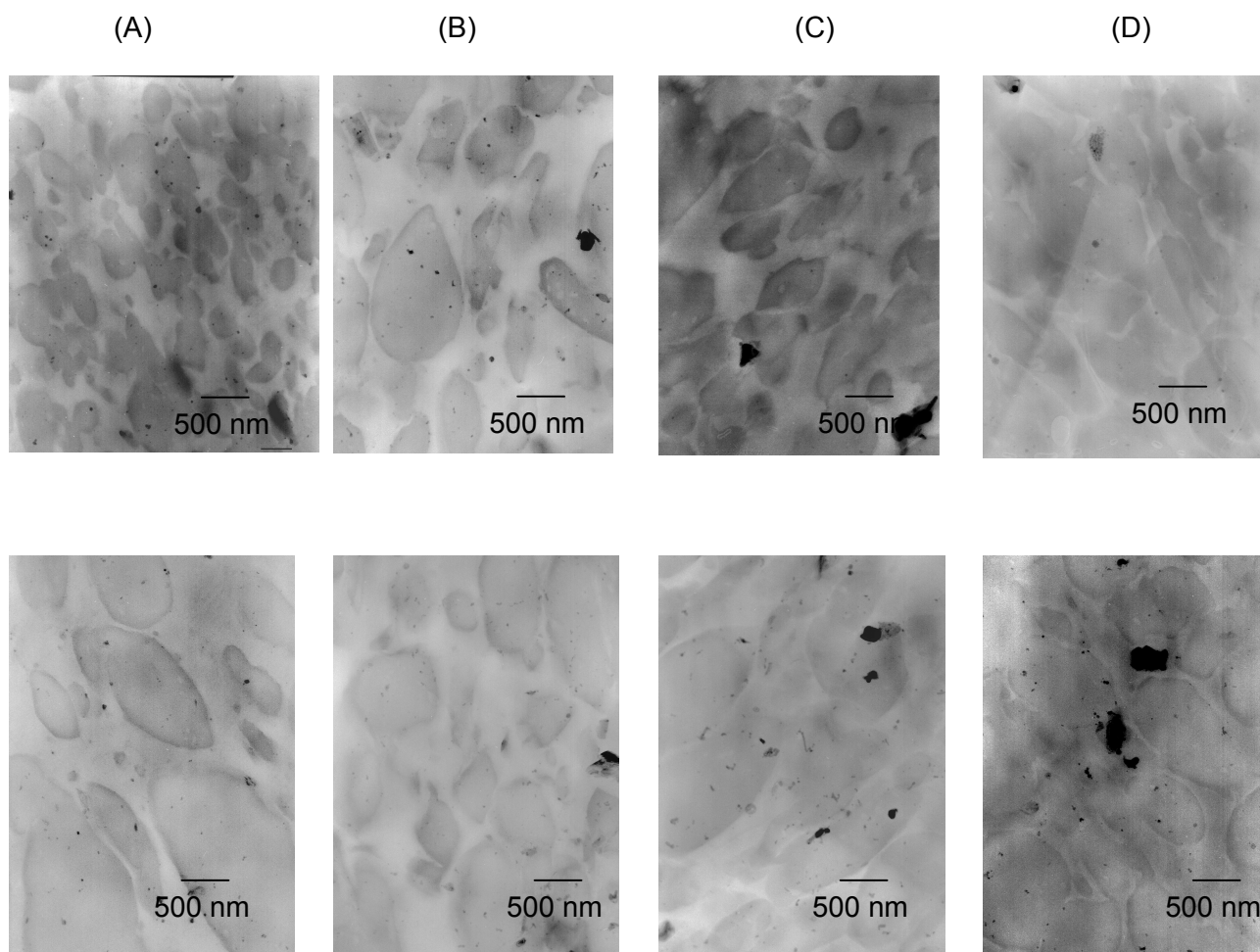


**Figure 4.12** Comparative TEM images of TPV blends made in the internal mixer (top) and twin-screw extruder (bottom): (A), BE6 vs. TE6; (B), BE2 vs. TE2; (C), BE5 vs. TE5; (D), BE4 vs. TE4.

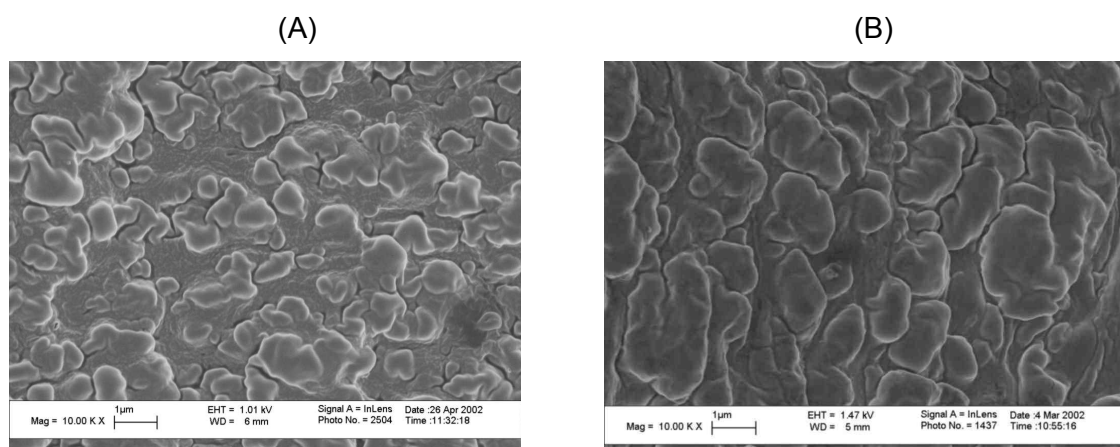


**Figure 4.13** Comparative figures of the morphology of blends made in the internal mixer and twin-screw extruder, as revealed by LVSEM: (A), BE5; (B), TE5.<sup>[2]</sup>

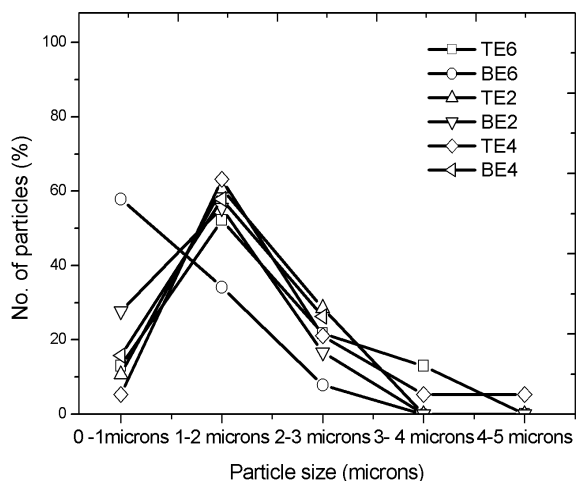


**Figure 4.14** Particle size analysis of TPVs made in the internal mixer and twin-screw extruder.

#### 4.3.4.2 SEBS/PP/oil blends.-

The differences of morphology in the SEBS/PP/oil blends due to changes in composition are similar to that observed for TPVs. However, the differences in morphology due to mixing in the internal mixer vs. the twin-screw extruder are less conspicuous than for the TPVs. Figures 4.15 (A)–(D) show the TEM-images of the SEBS/PP/oil blends at selected compositions. The TEM images for other compositions are not shown but are similar in morphologies. All the images show a pattern of rather irregular, interconnected dark domains uniformly distributed throughout the samples. As a consequence of preferential staining of the polystyrene domains in SEBS by  $\text{RuO}_4$ , the dark domains are assigned to SEBS and the white phase to PP. The oil in either phase is not visible.

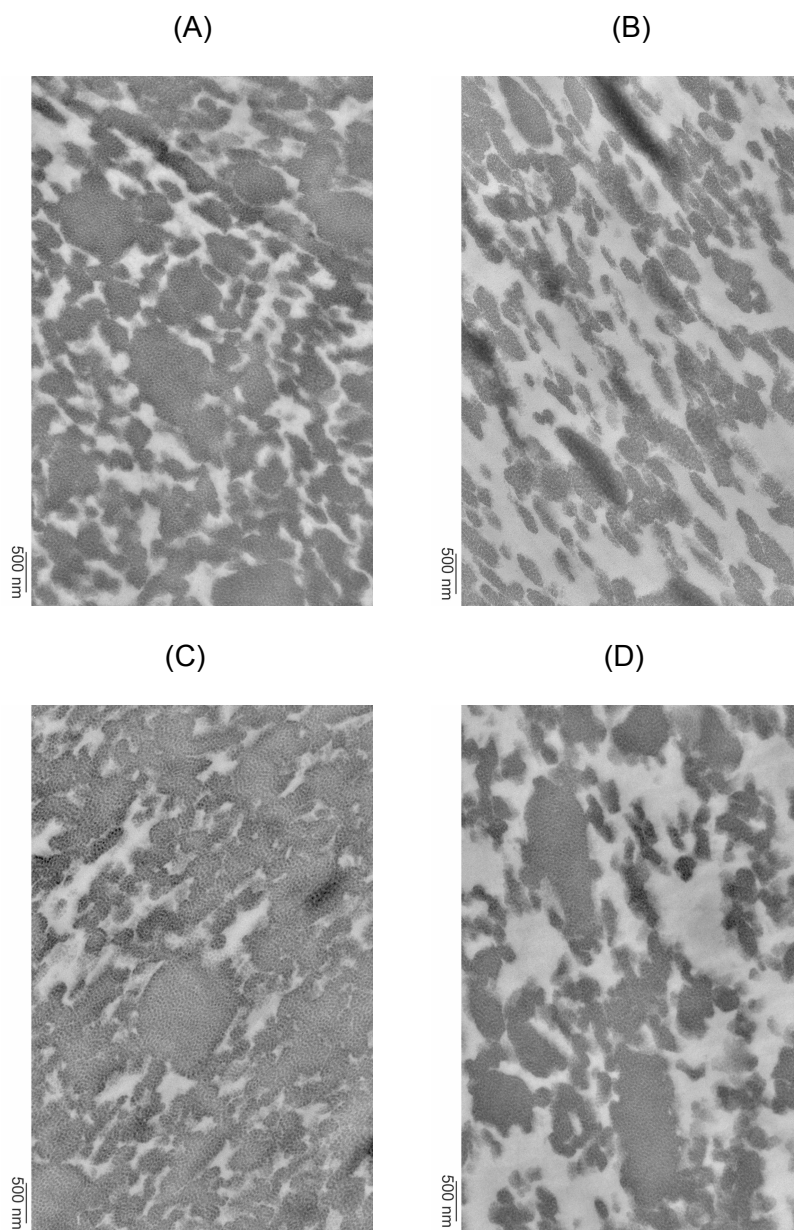


**Figure 4.15** TEM micrographs of SEBS/PP/oil samples: (A), BS1; (B), BS3; (C), BS7 and (D), BS9.

The SEBS domains appear to be larger in the blends with low PP/rubber ratio: compare BS1 vs. BS3 resp. BS7 vs. BS9. At a constant PP/rubber ratio the SEBS domains appear larger if more oil is present in the blend: compare BS1 vs. BS7 and BS3 vs. BS9. This observation is similar to what was seen in the TPVs and results from swelling of the rubber phase by oil.



TEM images of blends made in the internal mixer and twin-screw extruder are shown in Figure 4.16. The images on the top refer to the internal mixer and the corresponding twin-screw extruded blends are shown below.

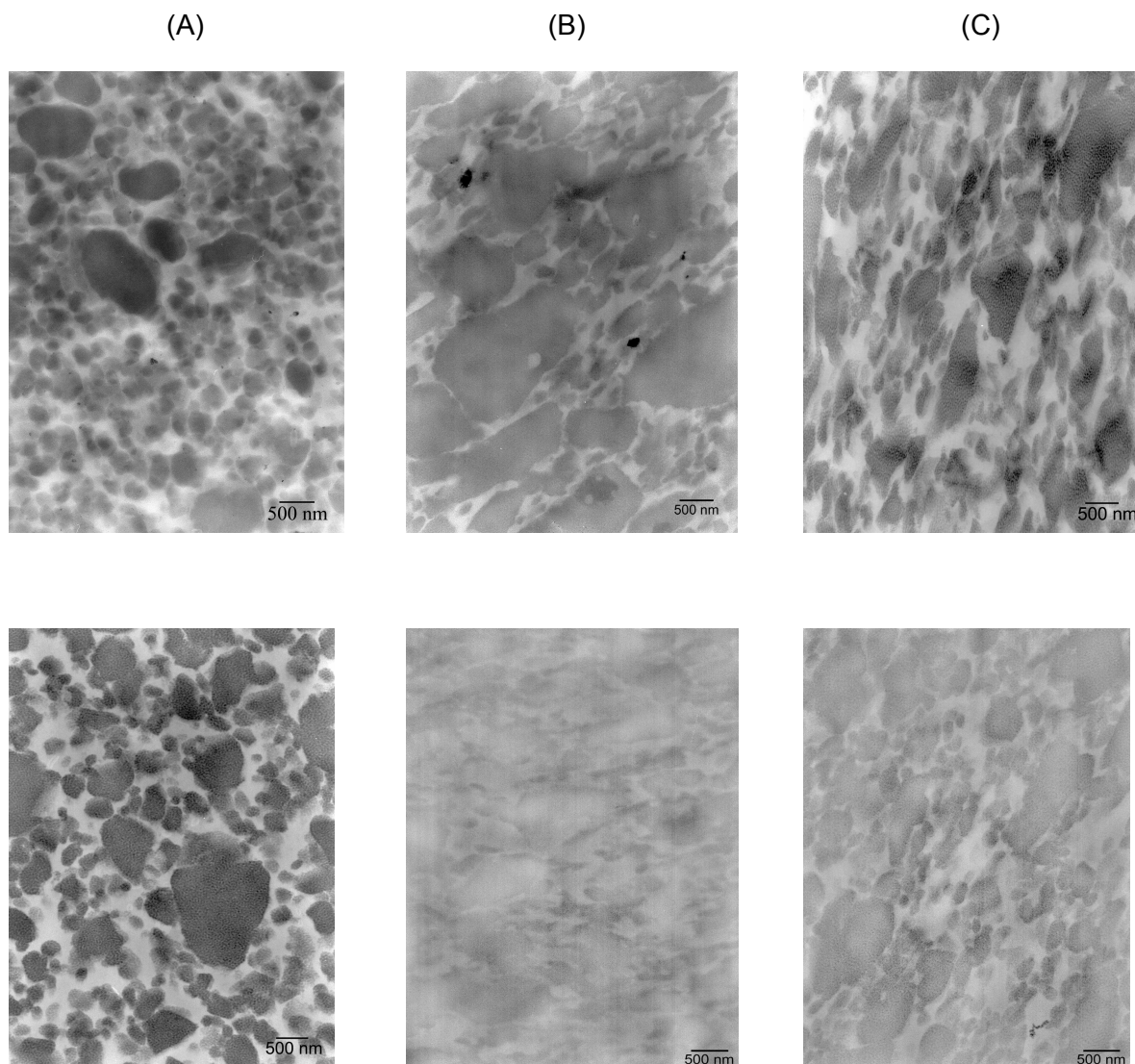


**Figure 4.16** Comparative TEM images of SEBS/PP/oil blends made in the internal mixer (top) and twin-screw extruder (bottom): (A), BS6 vs. TS6; (B), BS5 vs. TS5; (C), BS8 vs. TS8.

For all compositions, the TEM images show the SEBS- and PP-phases to form a co-continuous morphology. Detecting co-continuity differences with a single technique is difficult. The TEM images alone are insufficient for unambiguous determination of the blend morphology. For this

reason the TEM images were supplemented with LVSEM and atomic force microscopy (AFM) images. Representative LVSEM and AFM images are shown in Figures 4.17 and 4.18, respectively, for the blends BS6 and TS6. Unfortunately the contrast between the SEBS and PP phase is not high in these images either. Nevertheless it can be observed that for the composition 6, the blends made in the twin-screw extruder are less co-continuous than the corresponding blends made in the internal mixer. The SEBS domains also appear larger in TS6 than in BS6. For blends at other compositions no differences in the degree of co-continuity between the SEBS and PP phases could be detected.

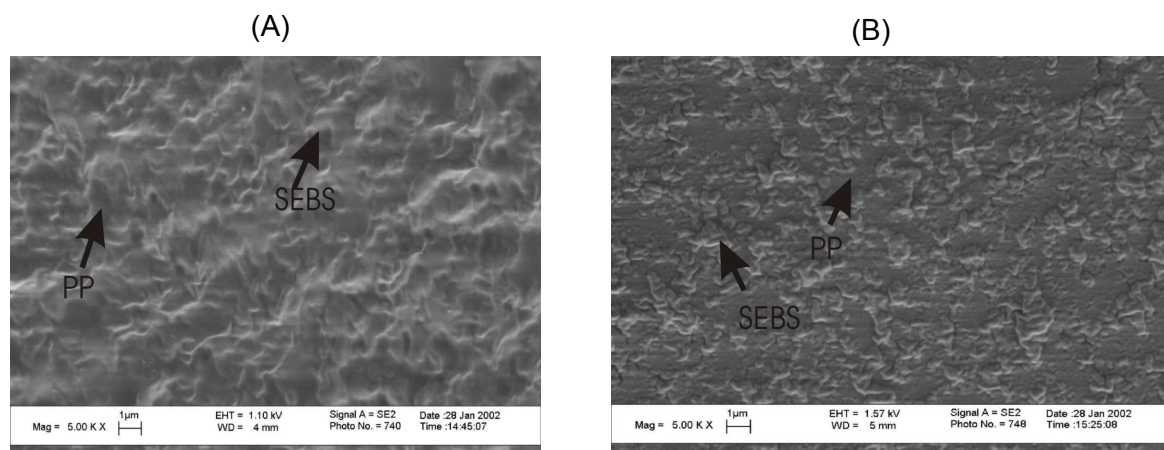


**Figure 4.17** LVSEM images of blend (A), BS6; and (B), TS6.<sup>[1]</sup>

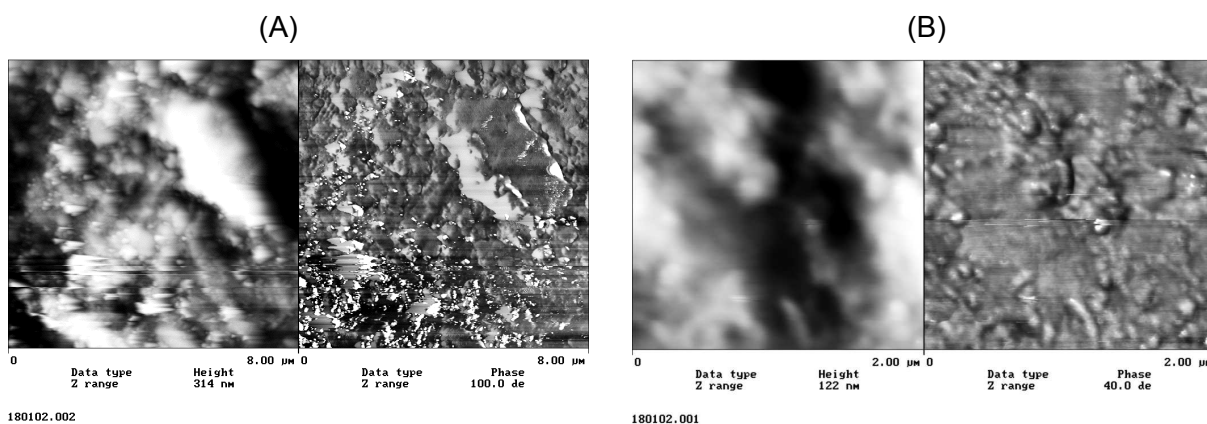


**Figure 4.18** AFM images of blend (A), BS6; and (B), TS6.<sup>[1]</sup>

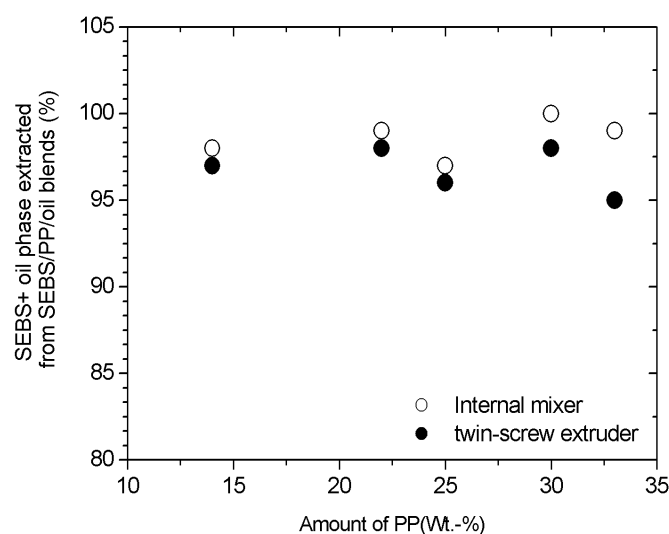


**Figure 4.19** Percentage of SEBS and oil extracted from SEBS/PP/oil blends made in the internal mixer and twin-screw extruder.

To further confirm the co-continuous morphology observed with TEM and LVSEM, the blends were extracted in toluene at room temperature for 24 hours. This resulted in complete extraction (over 95 %) of the SEBS and oil from all the blend compositions: Figure 4.19. The remaining PP-structure was self-supporting after extraction. This proves that almost all of the SEBS phase was accessible to the solvent, which is only possible if the SEBS phase is co-continuous. The amount of extractable SEBS and oil was consistently lower for the blends made in the twin-screw extruder as compared to the blends made in the internal mixer. This indicates a somewhat lower degree of co-continuity of the SEBS-phase for blends made in the twin-screw extruder, thus reconfirming the results obtained from microscopic studies for the blend compositions BS6 and TS6.

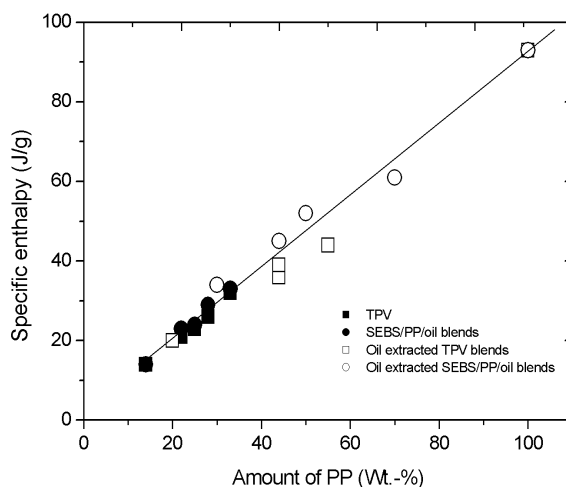


**Figure 4.20** Specific enthalpy of TPV, SEBS/PP/oil blends, oil extracted TPV blends and oil extracted SEBS/PP/oil blends made in the internal mixer.

#### 4.3.5 Crystallinity of the PP phase

Results from integrating the crystallization exotherm of polypropylene from DSC data on selected TPV and SEBS/PP/oil blends are shown in Figure 4.20. The linear relationship between PP composition and enthalpy of crystallization (or specific enthalpy) shows that the crystallinity of PP in the blends is independent of the blend composition and hence of the blend morphology. Similar results has been reported by Ohlsson for SEBS/PP/oil systems.<sup>[13]</sup>

The enthalpy of crystallization is a product of the degree of crystallinity  $X_c$  of the PP phase and heat of fusion per gram of 100% crystalline PP.<sup>[21]</sup> The degrees of crystallinity of the TPVs and SEBS/PP/oil blends prepared in the internal mixer and twin-screw extruder are shown in Figure 4.21. The values are grossly comparable for TPVs made in the two instruments. Thus, we conclude that the differences in the stress-strain properties of the TPVs having similar composition, are not due to different crystallinity of the PP phase. The SEBS/PP/oil blends made in the twin-screw extruder show consistently somewhat higher degrees of crystallinity than the blends made in the internal mixer at all compositions. However, this does not correlate with the tensile properties of these blends. This implies that, the PP-crystallinity does not have an effect on the differences in the stress-strain properties of the SEBS/PP/oil blends either.

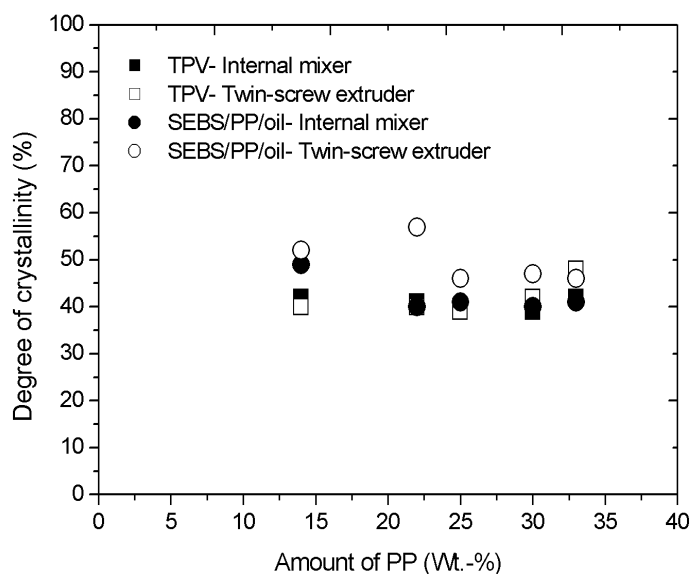


**Figure 4.21** Degree of crystallinity of TPV and SEBS/PP/oil blends.

Whereas the crystallinity of PP was independent of composition, the melting temperature of PP in these blends showed a different behavior: Figure 4.22. The shapes of these curves are the same for both TPV and SEBS/PP/oil blends. On the other hand, the crystallization temperature of the PP, shown in Figure 4.23, in these two types of blends show large differences. A depression in crystallization temperature of the PP-phase is observed in oil extended blends of both systems as compared to pure PP. The depression is higher in case of SEBS/PP/oil blends than for the TPVs, especially at the low PP-content. On extracting the oil from these blends the crystallization temperature increased in both blend types as compared to pure PP. The relative increases in crystallization temperature after oil extraction is however the same in both blend types.

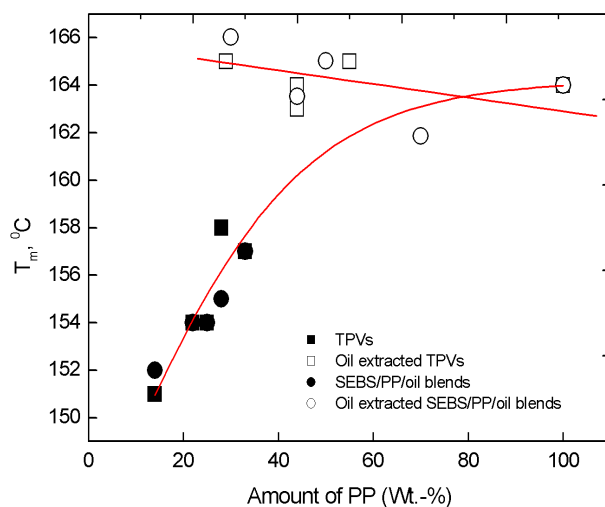


**Figure 4.22** Variation of the melting point of the PP-phase in TPVs, oil extracted TPVs, SEBS/PP/oil and oil extracted SEBS/PP/oil blends.

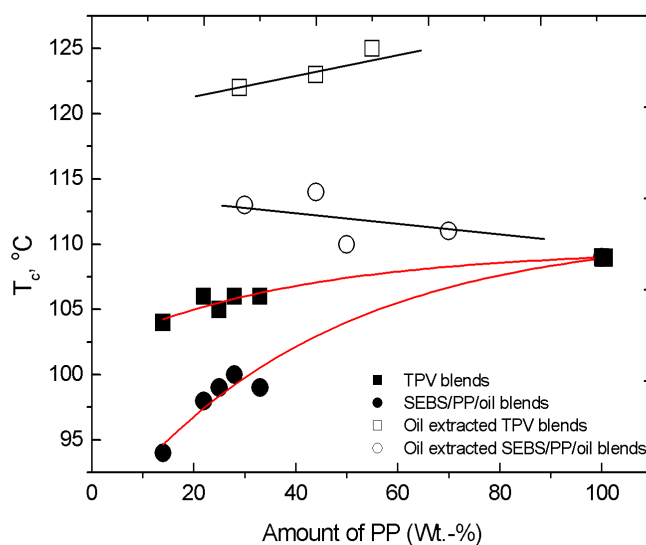


**Figure 4.23** Variation of the crystallization temperature of PP in TPVs, oil extracted TPVs, SEBS/PP/oil and oil extracted SEBS/PP/oil blends.

In TPVs, migration of stannous chloride, used as a catalyst during crosslinking may have an influence on crystallization point.<sup>[22]</sup> However, DSC experiments carried out on unvulcanized EPDM/PP/oil blends without stannous chloride and zinc oxide did not show any difference in crystallization temperature as compared to the corresponding TPV. This shows that ZnO and stannous chloride did not act as nucleating agent for PP in the blends under investigation. These differences are rather related to the nature of rubber phase.

#### 4.3.6 Gel measurements of TPVs

In order to judge the level of crosslinking of the EPDM phase in the TPVs, results from the gel measurements are given in Figure 4.24. In all cases the gel content is higher than or equal to 95%. Taking into account the experimental scatter in the gel-measurement, the result show a tendency to higher gel contents, obtained for the TPVs made in the twin-screw extruder than for those made in the internal mixer. At high gel content values, small differences in gel content relate to large differences in the degree of crosslinking.<sup>[23]</sup> This implies that the crosslink density of the EPDM phase in TPVs made in the twin-screw extruder was considerably higher – which possibly contributes to a higher E-modulus and tensile strength - than in the case of TPVs made in the internal mixer. In Figure 4.24, the largest differences in gel content are seen in between the blends, BE4 and TE4 having the maximum amount of EPDM. The smaller differences in the gel content at other compositions is probably related to the inability of the xylene to remove all the PP entrapped in the EPDM gel.

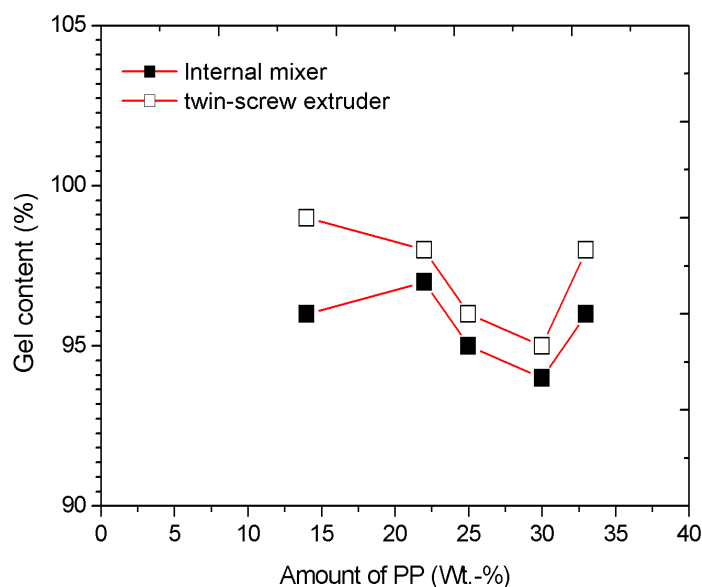


**Figure 4.24** Xylene-gel measurements on TPV blends made in the internal mixer and twin-screw extruder.

## 4.4 DISCUSSION

### 4.4.1 Stress-strain properties

The comparative study into the tensile properties of EPDM/PP/oil - TPVs and SEBS/PP/oil - blends showed several interesting features. Despite having a difference in morphology, the E-modulus values of these two blend types, are almost the same at identical blend compositions. This proves that the E-modulus in these systems is not dependent on morphology. Similar observations have also been reported by others.<sup>[24-26]</sup> The E-modulus is determined at very low deformation, where mainly the elastic effects of the network and degree of crystallinity of the PP phase are of importance. For EPDM/PP/oil TPVs our results show, that the E-modulus is primarily determined by the PP content and crosslink density of the dispersed EPDM particles – being higher for blends made in the twin-screw extruder because of a higher degree of vulcanization achieved. For SEBS/PP/oil blends the contribution of the SEB-phase to the E-modulus mainly depends on the polystyrene content of the block.<sup>[24]</sup> Since we used only one type of SEBS for all blends the contribution of the SEBS phase to the E-modulus was only proportional to its weight fraction. No dependence of the E-modulus of EPDM particle size distribution in the TPVs or of the degree of co-continuity of the SEBS-phase in SEBS/PP/oil blends was observed.



In contrast to the E-modulus, the ultimate tensile strength and elongation at break are determined at large deformations, where in addition to crystallinity and crosslink density of the network, the blend morphology may have an influence. Since the PP-phase is common in both blend types, the observed differences may relate to the strength of the chemical crosslinks in the EPDM particles versus that of the physical crosslinks in the SEBS phase. The spatial distributions of these crosslinks as influenced by the blend morphology are also important.

A better understanding of how blend morphology is related to mechanical properties is obtained by drawing analogies with mechanical models, to be discussed in the next chapter. The different phases that constitute the blend morphology, may be coupled in series or in parallel, similar to the Kelvin and Voigt models used for description of viscoelastic behavior of polymers. Because of geometric considerations one expects a lot more parallel coupling of components in a co-continuous morphology, as compared to particle-matrix type morphology. During tensile loading, especially at high volume of PP, the contributions of both components are much higher in parallel coupling as compared to series couplings. This explains the higher tensile strength of blends with co-continuous morphologies as compared to the same blends with dispersed morphologies.

The elongation at break values of TPVs decrease with decreasing PP-content of the blends. The toughness as estimated by the area under the stress-strain curve decreases with increasing rubber/oil content in these blends. This observation is similar to that reported by Lesser and Jones.<sup>[27]</sup> Based on studies on fracture properties of dynamically vulcanized EPDM/PP/oil TPVs it was reported, that both resistance to crack initiation and crack growth is poor with TPV blends containing higher amounts of rubber phase. A possible explanation of this effect can be given on the basis of differences in the EPDM particle size. In the works of Pukanszky *et al.*<sup>[28]</sup> on impact properties of EPDM modified PP it was shown that an increase in EPDM particle size leads to a gradual reduction in elongation at break values. Coran and Patel<sup>[29]</sup> also reported higher fracture properties for EPDM/PP TPV blends having smaller EPDM particle size. This implies that smaller particles result in better resistance to crack initiation and growth as compared to larger particles.

The stress-strain properties of the SEBS/PP/oil blends are mostly similar for both twin-screw extruder and internal mixer and independent of the differences in crystallinity. At higher strains, the SEBS/PP/oil blends show a more pronounced strain hardening effect with higher tensile strength and elongation at break as compared to the TPVs. The reason for this effect lies in the mechanism of tensile deformation of the PP phase that occurs in combination with the deformation of the SEBS phase. Modeling experiments by Lee *et al.* <sup>[30]</sup> showed that the strain hardening response is dominated by molecular orientations of the amorphous regions in the PP phase. Upon very large strains, whereupon the amorphous orientation has nearly reached the maximum, the crystallographic texture begins to significantly contribute to the strain hardening. For SEBS/PP/oil blends the orientation of the PP phase occurs along with the orientation of the co-continuous SEBS phase. The strain hardening response in these types of block copolymers are due to plastic deformation of hard polystyrene domains - a process that requires a large amount of energy.<sup>[31]</sup> The TEM image of fractured blend BS6, shown in Figure 4.25 confirms the deformation of the SEBS domains.

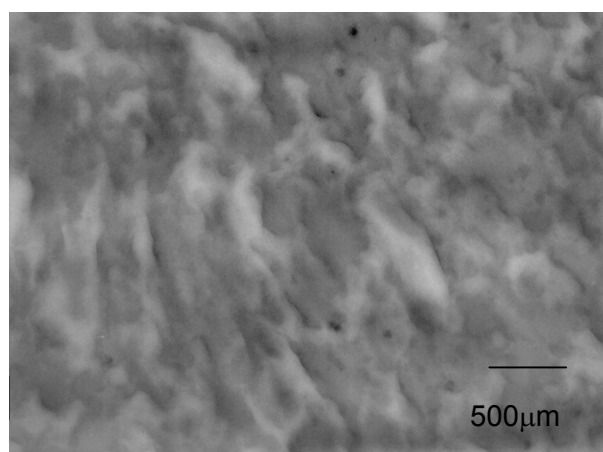


**Figure 4.25** TEM image of fractured BS6 showing deformed SEBS domains.

#### 4.4.2 Morphology

The morphological pictures show that the TPVs made in the twin-screw extruder have a wider particle size distribution than the corresponding blends made in the internal mixer. The largest amount of EPDM particles is in the range of 1-2 $\mu$ m. Whether the small morphological differences can lead to the observed differences in the stress-strain properties is not clear. However, the observed morphologies can be explained by considering the mixing conditions of the blends in the two types of mixing equipment.

Important differences between the mixing conditions in a twin-screw extruder and Brabender mixer are:

- a) Shear rate – which is much higher in a twin-screw extruder than in an internal mixer.
- b) Residence time - being higher for the internal mixer. The difference depends on the mixing time used in internal mixer. In case of TPVs the residence time in the internal mixer (10 minutes) was roughly about 10 times longer than the residence time in the twin-screw extruder (about one minute).
- c) Temperature profiles: 180°C – 210°C for TPVs made in the twin-screw extruder; in the internal mixer, the temperature of the mixing chamber was in the range 180 °C - 190 °C.
- d) Flow behavior- the relative amount of shear and deformation flow is different in the two machines due to differences in screw geometry in the twin-screw extruder or rotor design in the internal mixer.

During homogenization three main processes take place. At short mixing times large pieces of elastomer are dispersed in the melted or partially melted PP matrix the dominating process is particle break-up. With increasing mixing time the average size of the particles decreases and an equilibrium is reached between particle break-up and coalescence. SEBS particles in the SEBS/PP/oil blends can undergo coalescence but crosslinked EPDM particles in TPVs are not likely to coalesce. So in TPVs a reduction in particle size with increasing homogenization is expected.

The role of shear deformation on the break-up of particles is questionable. From theoretical calculations on Newtonian droplets it is known, that above a particular viscosity ratio it is impossible to break up a droplet by pure shear. In these situations, elongational forces are more effective in breaking the droplets than shear forces. In the internal mixer and twin-screw extruder, the particle break-up is a result of a combination of elongational and shear forces. The relative contributions of these forces in these mixers are however not known. This implies that, although

the twin-screw extruder has a higher shear rate than the internal mixer, it does not guarantee a smaller particle dispersed phase size.

The greater uniformity of EPDM particles for TPVs made in the internal mixer is probably related to the larger residence time of the blends in the internal mixer as compared to the twin-screw extruder. The larger residence time results in larger total strain (shear/elongational rate  $\times$  residence time) in the internal mixer, responsible for further breakdown of remaining larger EPDM domains into smaller uniform domains.

The study of the gel content, compression set and morphology of the TPVs shows, that the higher E-modulus and tensile strength values of the TPVs made in the twin-screw extruder vs. internal mixer are primarily governed by the PP content and crosslink density of the EPDM phase. Additionally, the morphological differences might have an influence. The blend crystallinity is grossly comparable for both mixing equipments.

While the rubber phase was dispersed in the TPVs, the SEBS phase in SEBS/PP/oil blends is co-continuous with the PP phase at similar compositions for both types of mixing devices. The reason for this must reside in the block copolymer structure of SEBS. The condition for the formation of such co-continuous morphologies is the existence of stable, elongated SEBS structures that do not show break-up or retraction in the melt. Experiments with block copolymer blends, like SEBS/PP and SEBS/PMMA, by Veenstra<sup>[14]</sup> have shown that with physical crosslinks present in the system during mixing, the break up and retraction of co-continuous structures can be severely limited or even totally stopped. The low interfacial tension between PP and SEBS and the high yield stress of SEBS further helps to stabilize these co-continuous structures.

Our experiments with the SEBS/PP/oil blends have shown that for composition 6 the blend made in the twin-screw extruder is less co-continuous than the blend made in the Brabender mixer. Such differences in the degree of co-continuity could not be detected for the other compositions. Possible reasons for such observations, especially relevant for SEBS/PP compositions with the lowest amount of SEBS - i.e. for composition 6 - are again related to the difference in residence time of the blend in the mixers. The residence time of the SEBS/PP/oil blends in the Brabender was 30 minutes, which again implies about a 30 times larger residence time than for the twin-screw extruder. A larger residence time implies more coalescence between the SEBS domains because of: (a), more number of collisions between the domains; (b), larger differences in viscosity between the SEBS and PP phases. If the residence time of the blends is less than the coalescence time like in the extruder, the blend will be less co-continuous as compared to the morphology of a similar blend prepared in the internal mixer. This process is

also composition dependent. The effect will be more manifested in blends with lower SEBS content, due to lower probability of coalescence.

A last important factor, which can influence the stress-strain properties of these blends, not further covered in this chapter, is the oil distribution between the rubber and PP phase. This will be addressed in the next chapter.

#### 4.4.3 Crystallinity of the PP-phase

The differences in the crystallization temperature of the PP-phase in TPV's as well as in SEBS/PP/oil blends, as seen in Figures 4.22 and 4.23, may be attributed to differences in the nucleating ability of the rubbers for PP-crystallization and extent of miscibility with the PP phase in melt. Although there is little experimental data in the literature on the nucleating ability of crosslinked EPDM domains or SEBS rubber on the crystallization behavior of PP, especially in blends containing over 40 wt.-% rubber phase, there are several experimental works available on EPDM/PP unvulcanized blends. In the work of Martuscelli *et al.*<sup>[32]</sup> and Jang *et al.*<sup>[33]</sup> a dramatic increase in the number of nuclei in blends, with increasing EPDM concentration was found as compared to plain PP. Through detailed studies of primary nucleation behavior in PP/EPM blends, the nucleation process was found to vary not only with the composition but also with variation of mixing time and thermal history of samples prior to crystallization. It was demonstrated that the increase of nucleation density with increasing EPM-content in the blend and with increasing mixing time is not caused by the nucleation activity of EPM on the PP crystallization, but is a result of an increased number of heterogeneous nuclei – particles of impurities and/or additives added to the polymers during blending. The low crystallization temperature of the PP phase in SEBS/PP/oil blends as compared to that in TPVs is also due to better miscibility between the SEBS and PP phase in melt.<sup>[13]</sup>

#### 4.5 CONCLUSIONS

In this study two thermoplastic elastomer blends systems have been analysed on the basis of their tensile stress-strain properties. These blends are: (1) dynamically vulcanized EPDM/PP/oil and (2) thermoplastic olefins based on SEBS/PP/oil.

While a strong influence of the composition and mixing equipment was seen on the morphologies of the blends of each type, there was a limited difference seen in the E-modulus of these two systems. This is because the E-modulus is determined at very low deformation, where only the elastic effects of the network and degree of crystallinity of the PP phase are important. Properties that involve large deformations such as the ultimate tensile strength and elongation at break are affected by parameters such as blend morphology. The stress-strain properties of the TPV blends at identical compositions depend on the mixing equipment used. Using a twin-screw extruder a higher degree of crosslinking was obtained resulting in higher E-modulus, as compared to the blends made in an internal mixer. The higher crosslinking of the EPDM phase is confirmed by xylene gel and compression set measurements. The crystallinity of the PP-phase in the TPVs is more or less comparable for both types of mixing equipment. The particle size distribution of the TPV blends made in the twin-screw extruder is wider than of the blends made in the internal mixer. This can be explained from the differences in total shear being much larger for the internal mixer than for the twin-screw extruder.

The stress-strain properties of the SEBS/PP/oil blends at identical compositions are quite independent of the mixing equipment used. For compounds with a high amount of PP, the blends made in the twin screw extruder appear to be less co-continuous than the blends made in the internal mixer. Similar to the TPVs, this can be explained on the basis of residence time differences for the blends in the two instruments. In general, the elongation at break values of the SEBS/PP/oil blends having co-continuous morphology is higher for TPVs with a dispersed EPDM phase morphology. This is due to concerted orientation of the co-continuous SEBS and PP phases.

The overall conclusion of this work is, that the dynamically vulcanized EPDM/PP/oil blends and thermoplastic olefinic blends of SEBS/PP/oil do show differences in their stress-strain properties like tensile strength and elongation at break, that are related to their different blend morphologies. So in this respect they are similar to any other immiscible polymer blends. Some other properties of these blends, like the E-modulus, are similar because they are determined more by the amount of crystallinity of the PP phase and its content but not so much by the blend morphology. Consequently, the properties of both blend systems can be tailored according to the requirements of the intended application, by changing parameters such as blend composition and preparation method.

## 4.6 REFERENCES

1. P. Sengupta, J. W. M. Noordermeer, W. G. F. Sengers and A. D. Gotsis, *Elastomer*, **38** (2003) 27.
2. P. Sengupta, J. W. M. Noordermeer, in 163 rd meeting of the American Chemical Society, Rubber Division, San Francisco, CA, (2003).
3. G. Holden, "*Understanding Thermoplastic Elastomers*", Hanser Gardner Publications Inc., New York (2002).
4. P. Dufton, "*Thermoplastic Elastomers*", RAPRA Technology: Shawbury, Shrewsbury, Shropshire, (2001).
5. S. Sabet-Abdou, "*Ullmann's Encyclopedia of Industrial Chemistry*", Ed. J. E. Bailey and M. Bonet, Wiley Interscience, West Sussex, (1998).
6. O. Chug, A. Y. Coran, *Rubber Chem. Technol.*, **70** (1997) 781.
7. F. Goharpey, A. A. Katbab, H. Nazockdast, *J. Appl. Polym. Sci.*, **81** (2001) 2531.
8. H. J. Radusch, *T. Pharm, Kautsch. Gummi Kunstst.*, **49** (1996) 249.
9. S. Abdou-Sabet, R. P. Patel, *Rubber Chem. Technol.*, **64** (1991) 769.
10. M. D. Ellul, in 160th meeting of the American Chemical Society, Rubber Division, Cleveland, OH, (2001).
11. H. W. Xiao, S. Q. Huang, T. Jiang, S. Y. Cheng, *J. Appl. Polym. Sci.*, **83** (2002) 315.
12. M. C. Boyce, K. Kear, S. Socrate, K. Shaw, *J. Mech. Phys. Solids*, **49** (2001) 1073.
13. B. Ohlsson, H. Hassender, B. Tornell, *Polym. Eng. Sci.*, **36** (1996) 501.
14. H. Veenstra, B. J. J. van Lent, J. van Dam, A. P. de Boer, *Polymer*, **40** (1999) 6661.
15. Information obtained from DSM Research B.V.
16. Information obtained from Kraton Polymers B.V.
17. A public domain image analysis programme developed at the U.S. National Institute of Health and available on the internet at <http://www.scion.com>
18. Internal procedure DSM Research B.V.
19. A. J. Brydson, "*Plastic Materials*", Vol. 7, Butterworth-Heinemann, Oxford, (1999).
20. K. Jayaraman, G. Kolli, M. D. Ellul, in International Rubber Conference, Prague (2002).
21. L. D. Orazio, C. Mancarella, C. E. Martuscelli, G. Sticotti, R. J. Ghisellini, *J. Appl. Polym. Sci.*, **53** (1994) 387.
22. E. Martuscelli, C. Silvestre, L. Bianchi, *Polymer*, **24** (1983) 1458.
23. B. Jang, D. R. Uhlmann, J. B. Van der Sande, *J. Appl. Polym. Sci.*, **29** (1984) 4377.
24. D. Scharnowski, S. Piccarolo, H. J. Radusch, in International Rubber Conference Prague (2001).
25. A. J. Charlesby, *J. Polym. Sci.*, **11** (1953) 513.
26. C. P. Rader, "*Handbook of Thermoplastic Elastomers*", Ed. V.N. Reinhold, New York (1998).
27. B. Pukanszky, F. Tudos, A. Kallo, G. Bodor, *Polymer*, **30** (1989) 1399.
28. B. Pukanszky, F. Tudos, A. Kallo, G. Bodor, *Polymer*, **30** (1989) 1407.
29. B. Pukanszky, F. Tudos, *Makromol. Chem., Macromol. Symp.*, **38** (1990) 221.

30. A. J. Lesser, A. N. Jones, J. Appl. Polym. Sci., **76** (2000) 763.
31. B. Pukanszky, I. Fortelny, J. Kovar, F. Tudos, Rubber Comp. Process. Appl., **15** (1991) 31.
32. A. Y. Coran, R. P. Patel, Rubber Chem. Technol., **53** (1980) 141.
33. B. J. Lee, A. S. Argon, D. M. Parks, S. Ahzi, Z. Bartczak, Polymer, **34** (1993) 3555.
34. J. A. Sperling, L. H. Sperling, "*Polymer blends and composites*", Platinum Press, Hayden, (1976).



---

## Chapter 5

### **Modeling the mechanical properties of ternary TPV and SEBS/PP/oil blends**

---

*This chapter investigates the influence of oil distribution on the mechanical properties of TPVs and SEBS/PP/oil blends. The oil distribution values between the PP and rubber phase are calculated based on experiments with dielectric relaxation spectroscopy (DRS). Model binary blends of PP-oil, vulcanized EPDM-oil and SEBS-oil are studied in order to understand the stress-strain properties of ternary TPVs and SEBS/PP/oil blends. The experimental values of E-moduli of the ternary blends are compared with their corresponding calculated values, obtained with the help of empirical models. Some of these models viz. Davies, Coran, Takayanagi, Veenstra D and Kolarik were found to be better than others, viz. the Halpin–Tsai, parallel and series models for predicting the E-moduli. While the E-modulus values gave a reasonably good fit with the models, the properties measured at high strains such as tensile strength and elongation at break were difficult to simulate with modeling. In addition to modeling tensile properties, cyclic deformation experiments and microscopic studies of deformed samples were carried out in order to experimentally verify the assumptions of the models. The studies showed that the deformation behavior of pure PP phase is different from the deformation of PP in tertiary blends, which partially explains why the modeling attempts to fit the tensile strength and elongation at break values were not so successful as the E-moduli. The chapter shows that, in addition to morphology and blend composition, the properties of these two blend systems are also dependent on oil distribution between the phases.*

## 5.1 INTRODUCTION

One of the attractive features of immiscible polymer blends is the possibility to tailor their properties. In order to do that, it would be of help to predict their properties with the aid of mathematical models. To make such a model for dynamically vulcanized TPVs and SEBS/PP/oil blends, various factors that influence the properties must be known. In Chapter 4 of this thesis, a comparative study of the E-moduli, tensile strength and elongation at break of these blends was presented. In order to explain the properties, (1) morphology, (2) blend crystallinity for both blend types and (3) gel content of the EPDM phase in TPVs were investigated. Despite having differences in morphology, the E-modulus values of the TPVs were similar to those of SEBS/PP/oil. The tensile strength and elongation at break values were different however for these two blend types, which could be due to differences in morphology, oil distribution or properties of constituent phases. Thus, the role of morphology in governing these tensile properties is not clear. If the properties are governed by composition only and not by morphology, it should be possible to predict them by simple composite averaging methods.

In order to model their stress-strain behavior, the ternary blends can be considered as two-phase systems in which the oil is distributed over the PP and elastomer phases. The properties of the two phases depend on the amount of oil present in each phase, which is not known beforehand. If these properties can be estimated from series of binary phases of PP-oil and elastomer-oil, then the properties of the ternary blends can be calculated from a weighed addition of the two phases.

The goal of this chapter is to investigate upto what extent the tensile properties of ternary blends can be explained purely on the basis of blend composition, corrected for the oil distribution between the phases, without taking into consideration the blend morphology. The experimentally obtained values of E-moduli, tensile strength and elongation at break are compared with those obtained theoretically from the empirical models. Some of the basic assumptions for using these models are as follows:

- (1) Each component contributes isotropically to the property corresponding to its volume fraction;
- (2) The adhesion between the phases is perfect even at large strains;

- (3) The mixing process of rubber and PP does not result in a significant change of morphology, so that the structure evolution during deformation of ternary blends is basically not different from the binary systems.

The oil distribution is calculated using the shift in glass-transition temperature of the binary blends and comparing them with the corresponding shift in ternary blends.<sup>[1]</sup> The binary oil compositions are selected such that they correspond to the oil content in the phases of the compounds. The theoretical treatment of the models used in these studies is discussed below.

## 5.2 MODEL CONSIDERATIONS

### 5.2.1 Series and Parallel models<sup>[2]</sup>

Models such as series and parallel models are often used as first approximations of the upper and lower limits, respectively, of the mechanical properties of isotropic heterogeneous materials. The parallel coupling of elements implies, that the strains of all constituents are equal and the contribution of each component to the final value of a mechanical property is given by the rules of mixing. The lines of force do not cross any interface, so that the resulting mechanical properties of the composite systems are independent of interfacial adhesion. Mathematically, parallel coupling of elements is given as:

$$M = \phi_1 M_1 + \phi_2 M_2 \quad (5.1)$$

where  $\phi_1$  and  $\phi_2$  are the volume fractions of components 1 and 2 respectively.  $M_1$  and  $M_2$  are the particular properties under consideration of the pure component 1 and 2 respectively, and  $M$  is the property of the blend.

The series coupling of components stands for the lower limit of the mechanical properties. Since all components are discontinuous in the direction of the applied force, their continuity can be regarded as zero. Contributions of constituents to a system property are then expressed by the inverted rule of mixing. As all stress is transmitted through the present interfaces, interfacial adhesion between the constituents is of primary importance. Mathematically, series coupling of elements is given as:

$$\frac{1}{M} = \frac{\phi_1}{M_1} + \frac{\phi_2}{M_2} \quad (5.2)$$

In principle, the phase structure of heterogeneous isotropic materials cannot correspond to mere parallel or series coupling of components, but models combining

both couplings are indispensable. Examples of such couplings are seen in the models of Halpin-Tsai,<sup>[3]</sup> Coran,<sup>[4]</sup> Takayanagi,<sup>[5]</sup> Davies,<sup>[6]</sup> Veenstra<sup>[7]</sup> and Kolarik<sup>[8]</sup>. Mathematical descriptions of each model are given below.

### 5.2.2 Halpin-Tsai model

Halpin-Tsai developed a well-known theory for predicting the modulus of fiber-reinforced composites as a function of aspect ratio. A general form of the model is given below:

$$M / M_1 = \frac{(1 + AB\phi_2)}{(1 - B\phi_2)} \quad (5.3a)$$

where

$$B = \frac{(M_2 / M_1) - 1}{(M_2 / M_1) + A} \quad (5.3b)$$

In this model subscripts 1 and 2 correspond to the continuous and dispersed phase, respectively. The constant  $A$  represents the shape parameter and is equal to 0.66 when elastomers form the dispersed phase in a continuous hard matrix.<sup>[9]</sup>  $M$  is the property of the blend and  $M_1$  is the property of the matrix.

### 5.2.3 Equivalent Box model of Kolarik

Kolarik's method for predicting the mechanical properties of polymer blends is based on the equivalent box model (EBM). In the EBM both phases are assumed to have a series and a parallel contribution to the property. The contributions of the corresponding components are represented by blocks. The dimensions of the blocks indicate which volume fraction,  $\phi_{ij}$ , of each constituent can be regarded as coupled in parallel or in series, so that the EBM response to loading can be equivalent to that of the modeled system. Figure 5.1 shows a schematic representation of a two-parameter model of EBM in which, out of four-volume fractions  $\phi_{ij}$ , only two are independent.

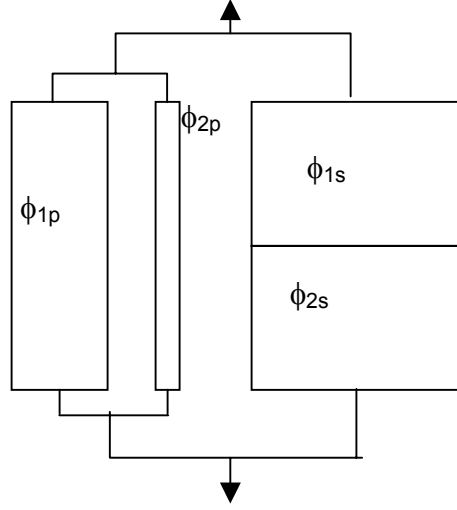


**Figure 5.1** Equivalent Box model for a model binary blend

The fractions of the components 1 and 2 couples in series (subscript s) and parallel (subscript p) are related as follows:

$$\phi_1 = \phi_{1p} + \phi_{1s} \quad (5.4a)$$

$$\phi_2 = \phi_{2p} + \phi_{2s} \quad (5.4b)$$

$$\phi_p = \phi_{1p} + \phi_{2p} \quad (5.4c)$$

$$\phi_s = \phi_{1s} + \phi_{2s} \quad (5.4d)$$

$$\phi_1 + \phi_2 = \phi_p + \phi_s = 1 \quad (5.4e)$$

The contributions of the parallel and series branches to the E-modulus of the EBM are equal to:

$$E_p = (E_1\phi_{1p} + E_2\phi_{2p}) / \phi_p \text{ and } E_s = \phi_s / [(\phi_{1s} / E_1) + (\phi_{2s} / E_2)] \quad (5.4f)$$

The resulting E-modulus of the two-component blend  $E_b$  is then given as:

$$E_b = E_1\phi_{1p} + E_2\phi_{2p} + \phi_s^2 / [(\phi_{1s} / E_1) + (\phi_{2s} / E_2)] \quad (5.4g)$$

The E-modulus is measured at low strains, typically below 1%. At higher strains the applied tensile stress is likely to exceed the linearity limit. Kolarik deduced the following equation for tensile strength in terms of the EBM visualized in Figure 5.1.

$$TS_b = TS_1\phi_{1p} + TS_2\phi_{2p} + ATS_2\phi_s \quad (5.4h)$$

where  $TS_1 > TS_2$  and  $A$  is inversely proportional to the extent of interfacial debonding. The value of  $A$  is 0 for complete debonding and 1 for strong interfacial bonding.

Calculation of  $\phi_{ij}$  for the EBM employs a universal percolation formula derived for the modulus of binary systems with negligible contribution of one component:

$$E_i = E_0(\phi_i - \phi_{icr})^{t_i} \quad (5.4i)$$

where  $i = 1, 2$ .  $E_0$  is a constant,  $\phi_{cr}$  is the critical volume fraction (percolation threshold) above which the phase becomes continuous and  $t_i$  is the critical volume exponent of the  $i^{th}$  component.  $\phi_{1cr}$  thus represents the point of phase inversion for phase “1” – here PP. Equation (5.4i) was shown to plausibly fit the modulus of a “single-component blend” with  $E_1 \gg E_2$  in the range  $\phi_{1cr} < \phi_{2cr} < 1$ . Thus equation (5.4i) can be modified into the following form:

$$E_{1b} = E_1[(\phi_1 - \phi_{1cr})/(1 - \phi_{1cr})]^{t_1} \quad (5.4j)$$

If  $E_1 \gg E_2$ , the contribution of  $E_2\phi_{2p}$  to the modulus of EBM is negligible in comparison to  $E_1\phi_{1p}$ . Consequently,  $E_1\phi_{1p}$  (or  $E_2\phi_{2p}$  for  $E_2 \gg E_1$ ) can be set equal to the apparent modulus  $E_{1b}$  (or  $E_{2b}$ ):

$$E_{1b} = E_1\phi_{1p} \quad (5.4k)$$

$$E_{2b} = E_2\phi_{2p} \quad (5.4l)$$

$\phi_{1p}$  and  $\phi_{2p}$  can be calculated from combining equation (5.4i), equation (5.4k) and equation (5.4l):

$$\phi_{1p} = [(\phi_1 - \phi_{1cr})/(1 - \phi_{1cr})]^{t_1} \quad (5.4m)$$

$$\phi_{2p} = [(\phi_2 - \phi_{2cr})/(1 - \phi_{2cr})]^{t_2} \quad (5.4n)$$

The remaining  $\phi_{1s}$  and  $\phi_{2s}$  are evaluated using equation (5.4e).

#### 5.2.4 Coran's model

Coran's model is based on an adjustment between the parallel and series models for upper and lower moduli  $M_U$  and  $M_L$ . Thus,

$$M = fM_U + (1 - f)M_L \quad (5.5a)$$

where  $f$  is an adjustable parameter, that varies between 0 and 1.  $M_U$  represents the upper limit and  $M_L$  represents the lower limit of the property. They are calculated using equations (5.1) and (5.2), respectively. The parameter  $f$  is related to the volume fraction of the components by the following equation:

$$f = \phi_1^n (n\phi_2 + 1) \quad (5.5b)$$

where  $n$  is another fitting parameter and has been related to aspects of dispersed particle shape, wetting, molecular interpenetrability, thermodynamic compatibility, interdomain interference, etc.  $\phi_1$  and  $\phi_2$  are the volume fractions of the hard and soft phases, respectively.

### 5.2.5 Takayanagi model

Takayanagi models consists of two main models: (1) and (2), and two accompanying sub-models for each main model. Figure 5.2 shows schematic diagrams of the models. The Takayanagi models regard a polymer as a hybrid material consisting of a crystalline (striped) and an amorphous (blank) phase, with either serial or parallel coupling. In the model, the mechanical properties are dominated by the content of crystalline phase, which can be continuous or discontinuous. However, the only implication of a continuous crystal phase in the model is one of mechanical continuity, and no structural continuity.

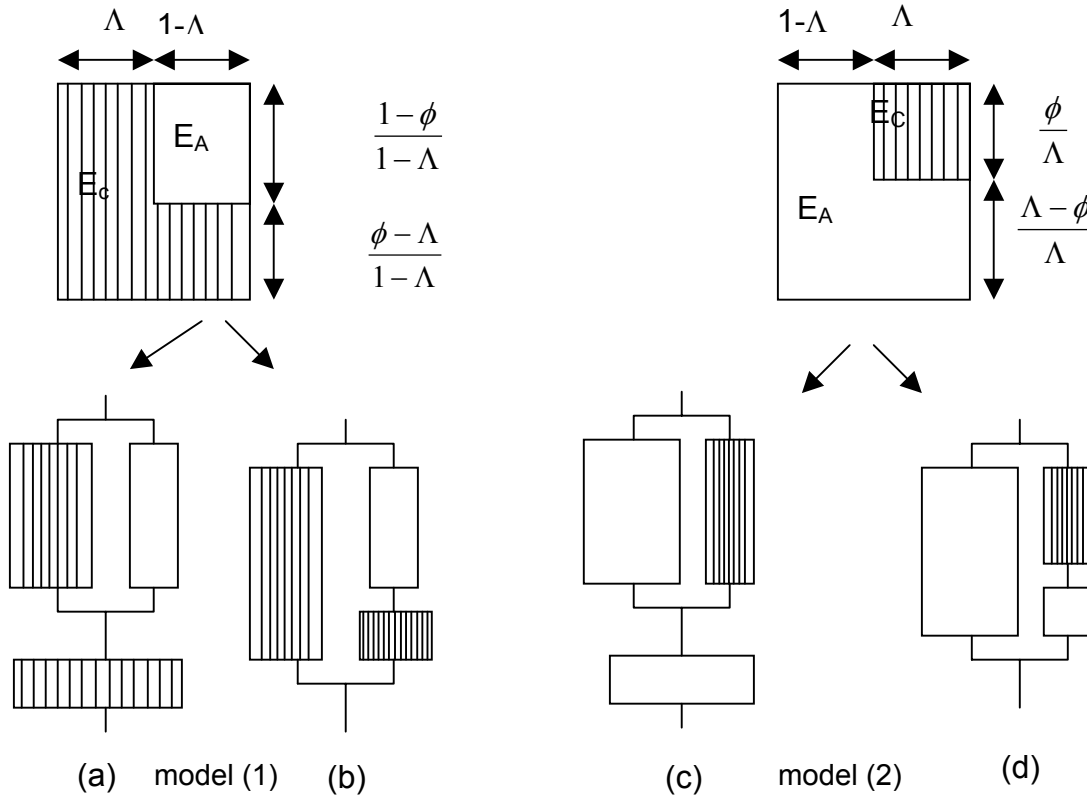


**Figure 5.2** Schematic diagram of the Takayanagi models (1) and (2), which consist of a three-component system.

Model (1) is suitable for analyzing the modulus of a continuous crystal – (or microfibril) - reinforced polymer, while model (2) is appropriate for predicting the properties of discontinuous crystal-reinforced polymers. Depending on the stress distribution in the material, models (1) or (2) may be considered with two sub-models, (a) or (b), or (c) or (d), representing the possible serial and parallel alignment of a three component system. In Figure 5.2, a unit cell in the model has an area equal 1, with a length of unity for each side. In the serial mode (a) and parallel mode (b) of model (1), continuous fibrils in the unit cell play a major role in the load-bearing properties, and dominate the composite modulus. The theoretical term ' $\Lambda$ ' derives its meaning from the continuous crystal (or fibrils) fraction in both models, which can be separated from the total crystalline (or fibrils) fraction,  $\phi$ . However, there is no continuous crystalline material in models (c) and (d) of model (2). Instead the value of  $\Lambda$  indicates a fraction of discontinuous crystalline material (fibrils) in the series mode (c) or parallel mode (d). In each case, the value of  $\Lambda$  determines the fraction of crystalline material and is the dominating factor in the mechanical properties of the composite. Thus, determination of the value of  $\Lambda$  is very important for analyzing the properties of the blend.

The theoretical properties for each model are given by the following equations:

$$\text{Model (a):} \quad M = \frac{1}{\frac{1-\phi}{(\Lambda M_c + (1-\Lambda)M_a)(1-\Lambda)} + \frac{\phi-\Lambda}{M_c(1-\Lambda)}} \quad (5.6a)$$

$$\text{Model (b):} \quad M = \Lambda M_c + \frac{1-\Lambda}{\frac{1-\Lambda}{M_a(1-\Lambda)} + \frac{\phi-\Lambda}{M_c(1-\Lambda)}} \quad (5.6b)$$

$$\text{Model (c):} \quad M = \frac{1}{\frac{\phi}{\Lambda(\Lambda M_c + (1-\Lambda)M_a)} + \frac{\Lambda-\phi}{\Lambda M_m}} \quad (5.6c)$$



$$\text{Model (d): } M = (1 - \Lambda)M_a + \Lambda / \{[(\Lambda - \phi) / \Lambda M_a] + (\phi / \Lambda M_c)\} \quad (5.6d)$$

where  $M_a$  is the property of amorphous phase and  $M_c$  is the property of crystalline phase.

### 5.2.6 Davies model

This model is usually applicable to dual phase continuity in polymer blends and is given by the equation:

$$M^{1/5} = M_1^{1/5}\phi_1 + M_2^{1/5}\phi_2 \quad (5.7)$$

### 5.2.7 Veenstra model

There are four models of Veenstra, referred as model A, B, C and D. These models are given by equations (5.8a)-(5.8d) respectively. Equations (5.8a) and (5.8b) are used for modelling blends with droplet/matrix morphology:

$$M(A) = M_1 \frac{\Psi^2 M_2 + (1 - \Psi^2)M_1}{(1 - \Psi)\Psi^2 M_2 + (1 - \Psi^2 + \Psi^3)M_1} \quad (5.8a)$$

$$M(B) = (1 - \Psi^2)M_1 + \frac{\Psi^2 M_1 M_2}{\Psi M_1 + (1 - \Psi)M_2} \quad (5.8b)$$

where  $\Psi^3 = 1 - \phi_1 = \phi_2$ .  $M(A)$  and  $M(B)$  refer to properties obtained from model A and B, respectively.

Equations (7c) and (7d) are used for co-continuous morphologies:

$$M(C) = \frac{(a^4 + 2a^3b)M_1^2 + 2(a^3b + 3a^2b^2 + ab^3)M_1M_2 + (2ab^3 + b^4)M_2^2}{(a^3 + a^2b + 2ab^2)M_1 + (2a^2b + ab^2 + b^3)M_2} \quad (5.8c)$$

$$M(D) = \frac{a^2bM_1^2 + (a^3 + 2ab + b^3)M_1M_2 + ab^2M_2^2}{bM_1 + aM_2} \quad (5.8d)$$

where  $a$  is related to the volume fraction of component 1 by the equation:

$$\phi_1 = 3a^2 - 2a^3 \quad (5.8e)$$

and  $b = 1 - a$  is related to the volume fraction of component 2 by the equation:

$$\phi_2 = 3b^2 - 2b^3 \quad (5.8f)$$

$M(C)$  and  $M(D)$  refer to properties obtained from model C and D, respectively.

Here it is assumed that the PP-phase is component 1 and the rubber phase is component 2. The Veenstra D model will be used in this thesis for co-continuous SEBS/PP/oil blends. It consists of an arrangement of two phases within an unit cube in such a way, that the dual phase interconnectivity is incorporated in three dimensions.

The Veenstra D model can also be used when the co-continuity in the morphology is not perfect. In that case the equations (5.8e) and (5.8f) will not hold exactly and  $a$  (or  $b$ ) is an adjustable parameter. The volume fractions calculated from equations (5.8e) and (5.8f) are the effective volume fractions. Their (negative) deviation from the actual volume fraction is an indication of the degree of disruption of the co-continuous structure.

### 5.3 MODELING APPROACH

Two different approaches are tried to combine the models with the experimental data. In what will be called a Type I approach, the properties of the ternary blends are calculated from the binary compositions with the model, as explained before. The calculated properties are then compared with the experimental values in order to estimate the goodness of fit. Models that are used for this approach are Series, Parallel, Halpin-Tsai, Davies and Kolarik. In a Type II approach, starting from the experimental data the free-parameters of the model are adjusted to come to a good fit. The adjusted parameters are then correlated with some features of the blends, such as blend composition or morphology. Models that were used for this approach are from Coran and Takayanagi. The Veenstra model C and D can be employed with either approach. In the Type I approach the parameter “ $a$ ” or “ $b$ ” is assumed to be dependent on the volume fraction of PP and rubber phase respectively. In the Type II approach, the parameter “ $a$ ” or “ $b$ ” is assumed to be freely adjustable. The value of parameter “ $b$ ” can be calculated and this can be used to calculate the effective volume fraction of the rubber phase:  $\phi_{eff}$ . If the model fits, then this value must show a correlation with the actual volume fraction of the rubber phase present in the model:  $\phi_2$ .

A schematic diagram of the two model approaches is show in Figure 5.3 below:

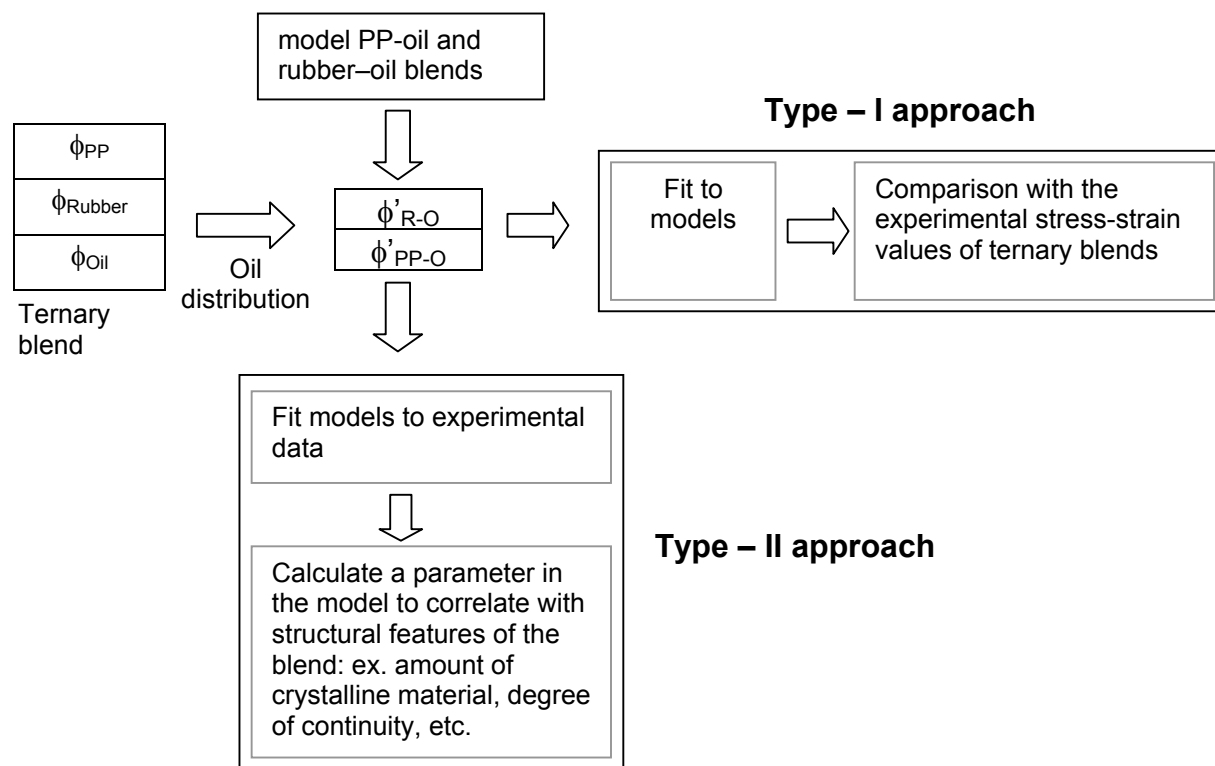


**Figure 5.3** Schematic diagrams of the two model approaches.

## 5.4 EXPERIMENTAL

### 5.4.1 Sample preparation and testing

The grades of materials and sample preparation of ternary blends are described in Chapter 3. The blend compositions are shown in Table 5.1 in the order of decreasing PP content.

Binary PP-oil mixtures were made in the internal batch mixer (Brabender Plasticorder 50 cc with Banbury rotor elements) at 180°C. SEBS-oil blends were prepared by dry blending the SEBS pellets with oil. The EPDM-oil preblends were prepared on a two-roll mill and cured during compression molding. The compositions of all binary blends are shown in Table 5.2. PP-oil binary blends containing more than 30 wt.-% oil showed phase separation after mixing in the internal mixer and so higher oil compositions were not taken into account.

**Table 5.1 Compositions of ternary blends.**  
(The blend codes are explained in Chapter 4)

Blend	% Rubber	% PP	% Oil
BE6/BS6	28	33	39
BE2/BS2	35	30	35
BE5/BS5	32	25	43
BE8/BS8	27	22	51
BE4/BS4	35	14	51

**Table 5.2 Compositions of PP-oil, SEBS-oil and vulcanized EPDM-oil blends (weight percent)**

PP	Oil	SEBS	Oil	EPDM	Oil
95	5	30	70	30	70
90	10	40	60	40	60
80	20	50	50	50	50
70	30	60	40	60	40

After mixing, the materials were compression molded using a WLP 1600/5\*4/3 Wickert laboratory press at 200°C for 3 mins under a pressure of 10 MPa and then cooled under pressure to about 30°C. Sheet thickness was 2 mm. The sheets were punched into dumbbells (ISO-37, type 2) for tensile measurements.

Tensile properties were determined at room temperature on ISO-37 type 2 dumbbell specimens using a Zwick Z020 universal testing machine equipped with a 500 N load cell. A crosshead speed of 50 mm/min was used to measure the E-modulus and 500 mm/min to measure the tensile strength and elongation at break. The standard deviations in the experiments were less than 10%.

To study the deformation mechanism of the ternary blends, the tensile samples were subjected to cyclic deformations. Two sorts of cyclic deformation experiments were used. First, the samples were subjected to multiple cyclic deformations upto a fixed strain of 100% and the hysteresis loss was measured. Second, the samples were subjected to multiple cyclic deformations in which the strain was increased by 50% after each cycle.

The deformation process was also studied using LVSEM and TEM. Samples were pre-stretched to 100% and 200% strain in the tensile tester and then clamped

firmly on a metal disc. The disc containing the sample in a stretched state was observed in LVSEM without staining. Samples for TEM examination were taken from fractured specimens. Sample preparation for TEM was the same as mentioned in Chapter 3.

## 5.5 RESULTS

### 5.5.1 Stress-strain properties of binary blends

#### 5.5.1.1 PP - oil binary blends.-

Since the PP-oil phase forms the matrix in both ternary blends, the stress-strain properties of PP and PP-oil blends can provide significant insight into the deformation behavior of ternary blends. Stress-strain plots of several PP-oil blends are shown in Figure 5.4. The plots show initial linear elastic behavior, followed by yielding and necking, and some strain hardening visible in pure PP and PP with 5 wt.-% oil. With increasing amount of oil in PP, the E-modulus, yield stress and tensile strength decrease and the extent of necking increases: Table 5.3. Samples with oil content larger than 10 wt.-% show a marked decrease in elongation at break, indicating that PP is clearly weakened by the oil. The results of the pure PP sample are in accordance with those reported by the supplier.<sup>[10]</sup>

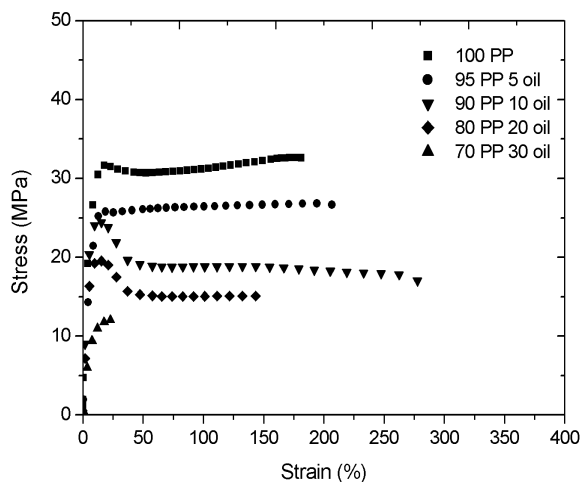


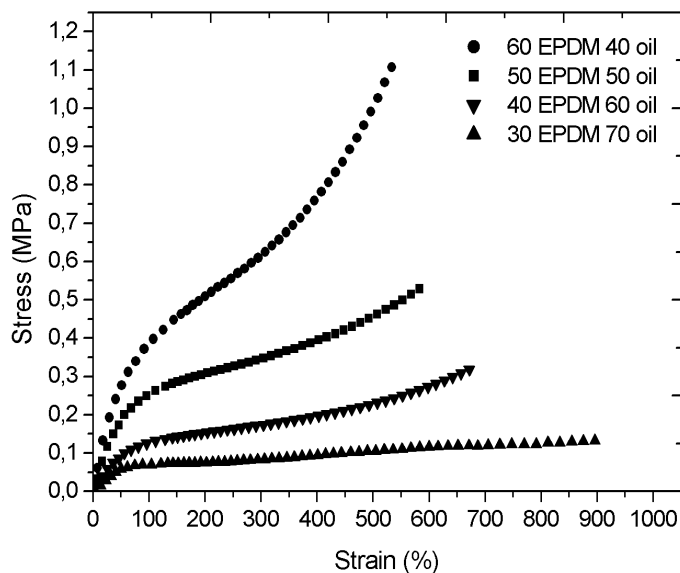
**Figure 5.4** Stress-strain curves of different PP-oil binary blends

**Table 5.3 Tensile properties of PP-oil blends**

Oil (wt.-%)	E-modulus (MPa)	Yield stress (MPa)	Tensile strength (MPa)	Elongation at break (%)
0	900	31	32	180
5	700	25	26	250
10	500	24	19	275
20	350	17	15	150
30	200	9	12	30

#### 5.5.1.2 EPDM-oil binary blends.-

Stress-strain curves for binary blends of vulcanized EPDM-oil are shown in Figure 5.5. The plots simulate the deformation behavior of crosslinked EPDM-oil particles during deformation of TPVs. The curves show a very small initial linear elastic behavior, followed by gradual flattening and later strain hardening. As expected, the E-modulus, yield stress and tensile strength decrease with increasing oil content: Table 5.4. The elongation at break values increase and the onset of strain hardening is delayed with increase of oil content.

**Figure 5.5** Stress-strain plot of vulcanized EPDM-oil binary blends

**Table 5.4 Tensile properties of vulcanized EPDM-oil blends**

Oil (wt.-%)	E-modulus (MPa)	Tensile strength (MPa)	Elongation at break (%)
40	4.8	1.1	500
50	3.5	0.5	550
60	1.5	0.3	650
70	1.0	0.1	900

### 5.5.1.3 SEBS-oil binary blends.-

Stress-strain curves for SEBS-oil binary blends are shown in Figure 5.6. The plots simulate the deformation behavior of the SEBS-oil phase during deformation of ternary SEBS/PP/oil blends.

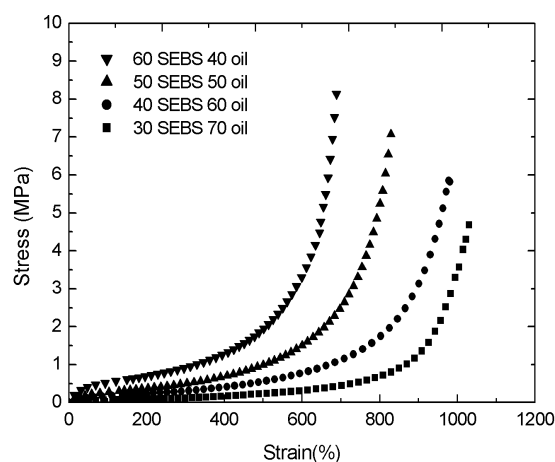


**Figure 5.6** Stress-strain curves of different SEBS-oil binary blends

Both similarities and differences with the stress-strain behavior of PP-oil binary blends are visible. A comparison of the 70-30 PP-oil and 60-40 SEBS-oil blends shows, that the E-moduli values are different by a factor of 100 and the elongation at break values are higher by a factor of 20: Table 5.5. The blends show remarkable strain hardening

phenomena, similar to vulcanized natural rubber or filled SBR.<sup>[11]</sup> The onset of strain hardening is clearly delayed by increasing the amount of oil.

**Table 5.5 Tensile properties of SEBS-oil blends**

Oil (wt.-%)	E-modulus (MPa)	Tensile strength (MPa)	Elongation at break (%)
40	5.0	8.0	600
50	4.0	7.0	800
60	2.0	6.0	900
70	1.0	5.0	1000

A comparison with the stress-strain curves of EPDM-oil blends shows that at similar oil content, the EPDM vulcanizates have much lower tensile stress as compared to the SEBS-oil blends. The E-moduli values are however close for both blends. Both tensile strength and elongation at break values are however significantly larger for the SEBS-oil blends.

### 5.5.2 Oil distribution

In the rubbery state, the oil is absorbed in the rubber phase and the amorphous regions of PP.<sup>[12]</sup> In order to relate the mechanical properties of binary blends with the properties of PP-oil and rubber-oil phases in ternary blends, the values of oil distribution must be known.

The oil has a plasticizing effect on both the PP and the elastomer. The change in glass-transition temperature with increasing amount of oil can therefore be used to prepare a calibration plot. Such plots can be used to determine an unknown oil composition of a phase in ternary blends, if the glass-transition temperature of that phase is known. Figure 5.7 shows this effect for PP-oil and rubber-oil blends, as measured with dynamic mechanical analysis by Sengers.<sup>[13]</sup> A relative comparison shows that due to addition of oil, the maximum change occurs in the  $T_g$  of the PP, followed by that of SEBS and vulcanized EPDM.

When the glass transition temperatures of the compounds are measured with common techniques, like DMA or DSC, only a single glass transition was observed. Comparing these values with the ones of the binary mixtures, the  $T_g$  of the compound



could therefore not be related to one of the phases: the glass transition dynamics of the two phases overlap in this temperature range. These methods were thus unsuitable to estimate the concentration of oil in the two phases.

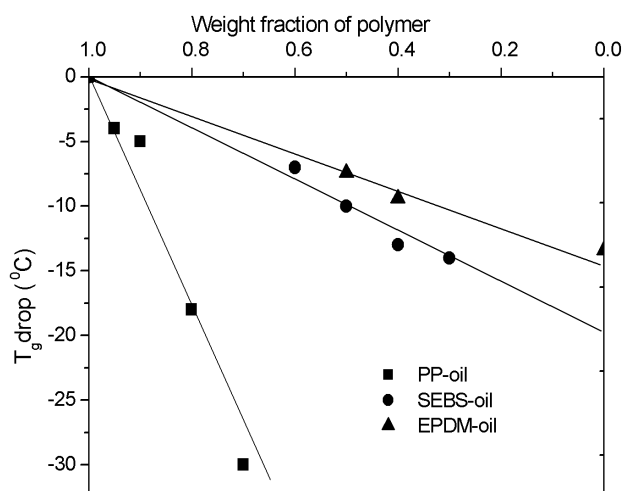


**Figure 5.7** Relative  $T_g$ -drop of PP-oil, SEBS-oil and vulcanized EPDM-oil.

Therefore, the oil distribution was determined using a new method, based on dielectric relaxation spectroscopy (DRS). In this technique a molecular probe N,N-dibutyl amino nitrostilbene was introduced into the blend in order to make them polar. DRS reveal the molecular dynamics of polymeric materials by characterizing the response of polar groups to a time-dependent electrical field. Further details of the DRS method are reported in a separate thesis.<sup>[13]</sup> Measurements under conditions spanning a wide range of frequency and temperature are thus possible. The binary blend analogues of ternary blends calculated from the oil distribution values are reported in Table 5.6. The oil distribution coefficients (K – values) are shown in Figure 5.8. In this calculation, the two polymer phases were regarded as homogeneous, i.e., the presence of polystyrene domains in the SEBS phase and crystalline domains in the PP phase was not explicitly accounted for. This simplification does not effect the present calculations because the same assumptions were also made on the binary blends.

**Table 5.6 Compositions of the binary blends, analogues of ternary blends, calculated from oil distribution values (in weight percentage).**

Code	TPV blends		SEBS/PP/oil blends	
	EPDM-oil	PP-oil	SEBS-oil	PP-oil
B6*	52-48	73-27	52-48	73-27
B2*	57-43	77-23	57-43	77-23
B5*	49-51	70-30	49-51	71-29
B8*	42-58	68-32	42-58	69-31
B4*	45-55	70-30	46-54	66-34

\* The compositions corresponding to these codes are given in Chapter 4. The letter "B" implies blends made in the internal mixer.

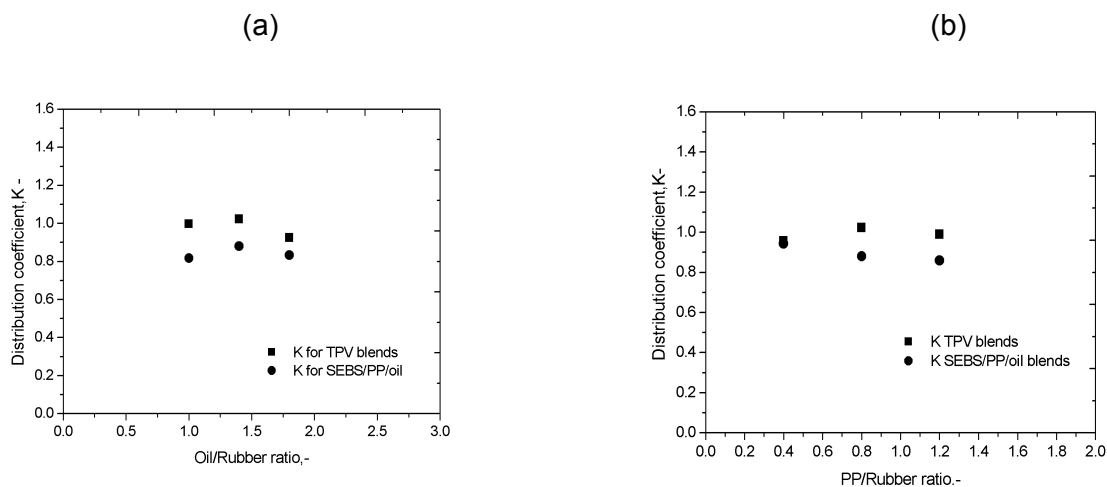


**Figure 5.8** Oil distribution coefficient for TPV and SEBS/PP/oil blends: (a), Increasing PP/rubber ratio (b), Increasing Oil/Rubber ratio.

The value for the oil distribution coefficient is about 0.55-0.60 with only a slight difference between EPDM and SEBS, indicating that the oil prefers the elastomer phase in both cases. The distribution is independent of the PP/elastomer and oil/elastomer ratios in both blend types. These results are further discussed in another study.<sup>[13]</sup> Microscopic attempts to visualize a separate oil phase using cryo-TEM were negative. So the presence of a third oil phase was not considered for the oil distribution calculations. However, the presence of small oil pockets in the regions between PP spherulites cannot be ruled out.

### 5.5.3 Fitting the E-moduli of TPVs with a Type I approach

The extrapolated E-modulus values of the binary PP-oil and EPDM-oil phases in the ternary blends are given in Table 5.7. Note, that the E-moduli of PP-oil phases do not necessarily decrease with a decrease in the amount of PP-oil phase the blend. This discrepancy is most probably due to differences in oil distribution.

**Table 5.7 E-moduli and Tensile Strengths of binary PP-oil and EPDM-oil phases in ternary blends**

Blend	$E_{PP-oil}$ (MPa)	$E_{EPDM-oil}$ (MPa)	$TS_{PP-oil}$ (MPa)	$TS_{EPDM-oil}$ (MPa)
BE6	353	3.98	12	0.72
BE2	445	4.68	15	0.88
BE5	283	3.56	11	0.63
BE8	237	2.58	9.2	0.4
BE4	283	3.0	7.3	0.5

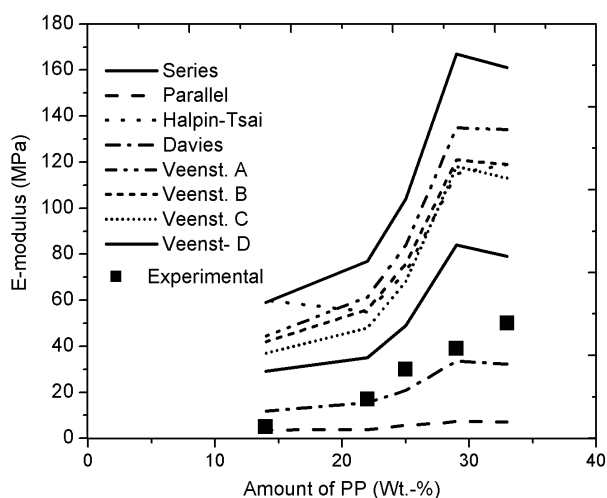


**Figure 5.9** E-moduli of TPVs as predicted by different models using type I approach vs. experimental data.

Figure 5.9 shows the E-moduli of TPV blends as calculated using different models. The properties of constituent binary phases are different at all the five compositions

investigated, because of differences in oil distribution. A comparison with the experimental data taken from Chapter 4 shows that most models are not able to predict the E-moduli properly, with the exception of Davies model. The fit with Davies model suggests that there are interactions, as interconnections between the soft domains and the rubber phase behave like a continuous network during deformation.

#### 5.5.4 Fitting the E-moduli of SEBS/PP/oil blends with a Type I approach.

Table 5.8 shows the E-moduli of the PP-oil and SEBS-oil phases as extrapolated from studies of model blends. The E-modulus of ternary SEBS/PP/oil blends as predicted by different models are shown in Figure 5.10. Except for the Davies model, which is known to hold for blends with co-continuous morphology, all type I approaches gave a poor fit to the experimental data. The Davies model does not fit at the composition with highest amount of PP.

**Table 5.8 E-moduli and Tensile strengths of binary PP-oil and SEBS-oil phases in ternary blends**

Blend	$E_{PP-oil}$ (MPa)	$E_{SEBS-oil}$ (MPa)	$TS_{PP-oil}$ (MPa)	$TS_{SEBS-oil}$ (MPa)
BS6	353	3.69	12	6.1
BS2	445	4.30	15	7.7
BS5	307	3.23	10.5	5.8
BS8	261	2.29	10	5.2
BS4	190	2.83	5.5	7

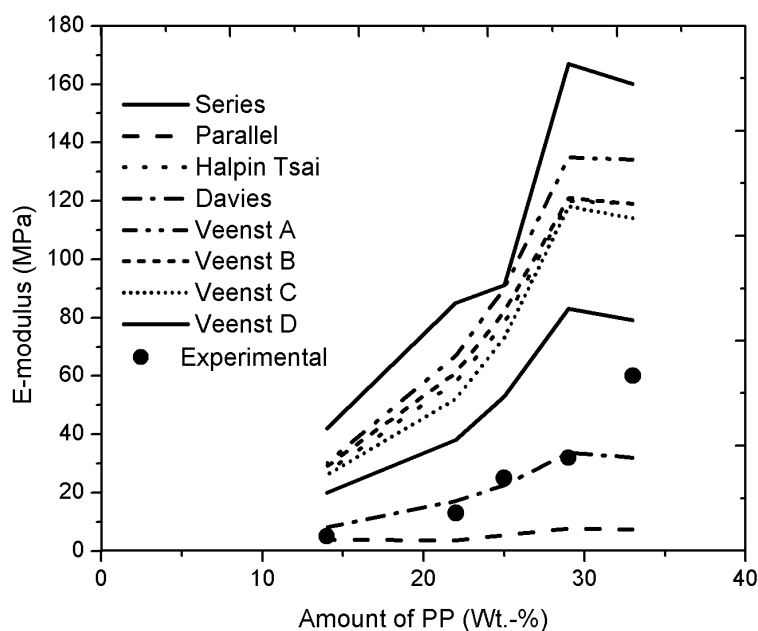


**Figure 5.10** E-moduli of SEBS/PP/oil blends as predicted by different models vs. experimental.

### 5.5.5 Fitting the physical properties of TPVs and SEBS/PP/oil blends with a Type I approach using the Equivalent Box model of Kolarik

In order to use the Kolarik's model, one can use the  $t$ 's and  $\phi_{cr}$  as free parameters: type II approach, or alternatively use the values predicted theoretically: type I approach. In the present calculations the value of  $t$  for both components was taken as 1.8 and  $\phi_{1cr} = \phi_{crPP} = 0.156$  and  $\phi_{2cr} = \phi_{crRubber} = 0.156$ , which are the theoretically dictated values for phase inversion<sup>[15]</sup>, so the type I approach.

The value of  $\phi_{1cr}$  is very crucial for the model but its physical interpretation is not clear. According to Kolarik it represents the critical volume fraction above which one of the phases becomes continuous. The model is not very sensitive to the value of  $\phi_{2cr}$  where the subscript "2" refers to the rubber phase. This is because  $E_1 \gg E_2$  and so the modulus of the ternary blend is not very sensitive to the volume fraction of the rubber.

The result of fitting the EBM to the E-moduli of TPVs and SEBS/PP/oil blends is shown in Figure 5.11.

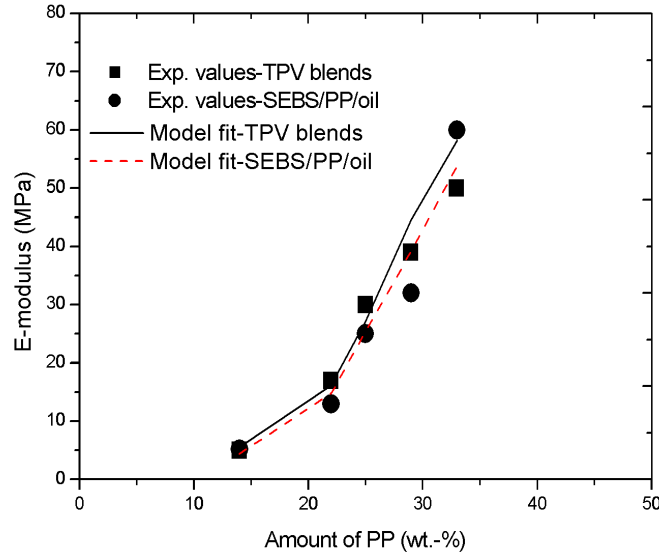


**Figure 5.11** E-moduli of EPDM/PP/oil-TPVs and SEBS/PP/oil blends.

The points represent the experimental values and the lines represent fits obtained from the EBM model. The value of  $\phi_{1cr} = 0.156$  for TPVs.

For SEBS/PP/oil blends the best fits were obtained with  $\phi_{1cr} = 0.18$ .

For experimental fitting of the E-moduli of SEBS/PP/oil blends, small variations relative to the theoretically dictated value of 0.156 are employed. Except for one composition of SEBS/PP/oil, the fit is excellent for all other compositions of both blends.

In addition to the E-moduli, the EBM can be used to model the tensile strength of TPVs. The EBM however needs to be modified to account for the yielding and plastic deformation of the matrix that occurs at higher strains. If the interfacial adhesion is assumed to be strong enough to transmit the stress between the constituents, the contribution of the series branch is added to that of the parallel branch. If two components of different tensile strengths are coupled in series, the branch is expected to fail at a stress whichever is the lower one. Thus if  $TS_2 < TS_1$  the upper bound assumes the following form:

$$TS_b = (TS_1\phi_{1p} + TS_2\phi_{2p}) + ATS_2\phi_s \quad (5.9a)$$

In the above equation, A is the extent of interfacial bonding. For weak interfacial bonding,  $A = 0$  and for very strong interfacial bonding,  $A=1$ . The experimental values of the tensile strength of both blends could be fitted reasonably well by the above equation,

if it was assumed that the PP-oil phase fails earlier than the rubber-oil phase. Mathematically this implies a modification of the above equation as stated below:

$$TS_b = (TS_1\phi_{1p} + TS_2\phi_{2p}) + ATS_1\phi_s \quad (5.9b)$$

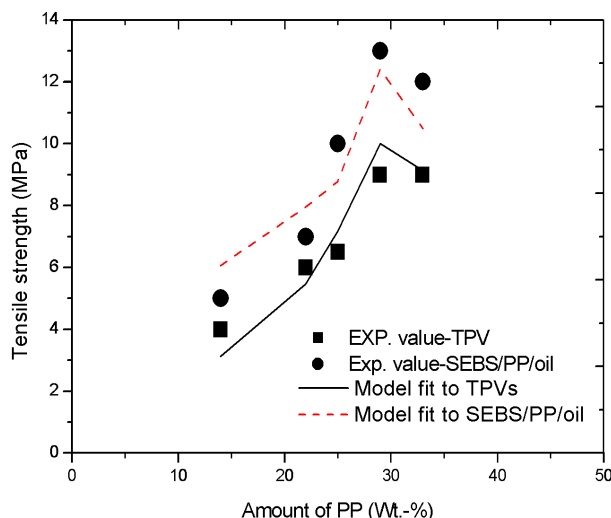


**Figure 5.12** Tensile strength of EPDM/PP/oil-TPVs and SEBS/PP/oil blends. The points represent the experimental values and the lines represent fits obtained from the EBM model. The value of  $A = 1$  in both cases.

Results obtained from fitting the modified equation to the tensile strength values are shown in Figure 5.12. A reasonably good fit is obtained in both cases. Implicitly this would mean that the PP phase fails earlier than the rubber phase.

#### 5.5.6 Fitting the E-moduli of TPVs and SEBS/PP/oil blends with a Type II approach, using Coran's model

Figure 5.13 shows the E-moduli of TPV blends as calculated from Coran's model. The symbols represent the experimentally obtained E-moduli values. Using an average value of 2.58 for the parameter "n", a reasonably good fit to the experimental data was obtained. This is close to the value of 2.63 for the E-moduli of SEBS/PP/oil blends. According to Coran and Patel<sup>[4]</sup> the parameter "n" is related to the particle shape of the dispersed phase, wetting, molecular interpenetrability, thermodynamic compatibility, interdomain interface, etc. These authors reported a value of 2 for EPDM/PP unvulcanized blends and a value of 3.1 for TPVs.

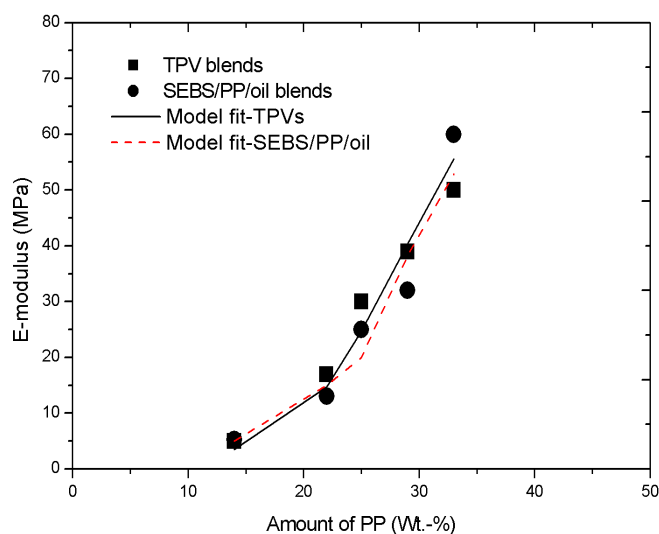


**Figure 5.13** E-moduli of EPDM/PP/Oil - TPVs and SEBS/PP/oil - blends. The points represent the experimental values and the lines represent fits obtained from Coran's model. The value of  $n = 2.58$  for TPVs, and  $n = 2.63$  for SEBS/PP/oil blends.

The variation of  $f$  with volume fraction of PP,  $\phi_1$  is given in Figure 5.14. Since  $f$  represents the amount of parallel behavior, a value of  $f$  higher than 0.5 would indicate a larger contribution of the series mode as compared to the parallel mode. As shown in Figure 5.13, for both blend types the value of  $f$  is below 0.5 which shows that the load is predominantly transmitted in series during the measurement of E-moduli and this is independent of the blend morphology. The change in  $f$  with respect to  $\phi_1$  is greatest when  $\phi_1$  is  $(n-1)/n$ . According to Coran and Patel,<sup>[4]</sup> this value represents a packing volume for blends with fixed morphology, and phase inversion for blends with variable morphology. For both TPVs and SEBS/PP/oil blends the hard phase concentration,  $\phi_1 = 0.61$ , corresponds to a maximum rate of change in  $f$  with  $\phi_1$ . However, in these blends there is no real phase inversion, because the morphology of TPVs is fixed after dynamic vulcanization and for SEBS/PP/oil the co-continuous morphology did not show any change due to alteration in the blend compositions. Similarly “ $n$ ” in these systems cannot correspond to a packing volume of the hard phase, since the hard phase forms the matrix in both blends. Thus, the physical significance of “ $n$ ” is not clear from this model.



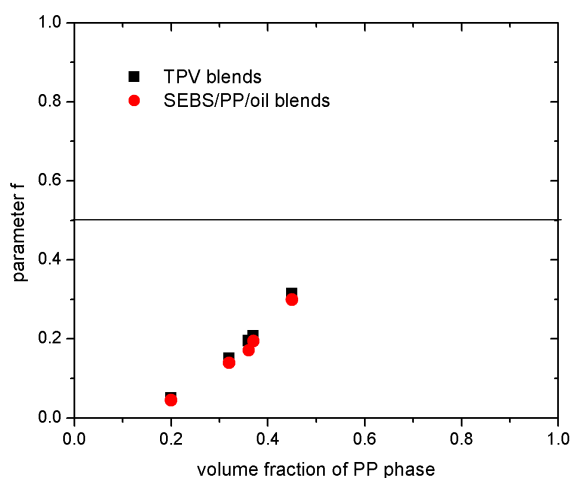


**Figure 5.14** Variation of parameter  $f$  in Coran's model with volume fraction of PP phase

### 5.5.7 Fitting the physical properties of TPVs and SEBS/PP/oil blends with a Type II approach, using the Takayanagi models

The calculated values of  $\Lambda$  obtained by fitting the equations (5.6a)-(5.6d) to the E-moduli of TPV and SEBS/PP/oil blends are given in Tables 5.9a and 5.9b, respectively. Here it is assumed that the total amount of rubber represents the amorphous phase and total amount of PP represents the crystalline phase. The volume fraction of PP reported in the table corresponds to the volume fraction of PP phase in the ternary blends, calculated while taking into consideration the oil distribution between the phases. Among the four Takayanagi models, the  $\Lambda$  values of model (d) approach that of the PP volume fraction in both ternary blends. This indicates that the PP phase is mechanically discontinuous and the discontinuous crystalline model (d) is suitable for explaining the actual modulus of both ternary blends.

Results from applying the above four models to the tensile strength values of TPVs and SEBS/PP/oil blends are given in Tables 5.10a and 5.10b, respectively. The  $\Lambda$  values obtained for the discontinuous model (d) are close to the PP volume fraction in case of TPVs, but very different from the PP volume fraction in case of SEBS/PP/oil blends. Thus the model fits very well to the tensile strength values of TPV blends but not for the SEBS/PP/oil blends. This model has also been suggested for TPVs by Radusch *et al.*<sup>[14]</sup> This difference in fit indicates that the deformation of TPVs is mainly governed by the PP phase, but in case of SEBS/PP/oil blends the deformation mechanism is also

very much influenced by the rubber phase. This is in line with the fact that the rubber phase is dispersed in TPVs, but co-continuous in SEBS/PP/oil blends. The strain hardening phenomena of SEBS in SEBS-oil blends is also reflected in the stress-strain plots of SEBS/PP/oil blends.

For both blends, the elongation at break values could not be fitted with any of the four Takayanagi equations.

**Table 5.9a Calculated  $\Delta$  values from the Takayanagi model for E-moduli of TPV blends**

	1	2	3	4	5
$E_c$ (MPa)	353	445	283	237	283
$E_a$ (MPa)	3.98	4.68	3.56	2.58	3.0
$E_{\text{experimental}}$ (MPa)	50	39	30	17	5
$\phi_{(PP)}$ (vol%)*	45	37	36	32	20
Model (a) (%)	8	5	6.5	4.2	0.4
Model (b) (%)	12	7	8.5	5.7	0.5
Model (c) (%)	48	41	39.5	36.4	48
Model (d) (%)	46.2	38.5	37.3	33.49	28

\*This represents the volume fraction of the PP phase in the analogous binary blends (i.e.  $\phi_{PP-O}$  in Figure 5.3)

**Table 5.9b Calculated  $\Delta$  values from the Takayanagi model for E-moduli of SEBS/PP/oil blends**

	1	2	3	4	5
$E_c$ (MPa)	353	445	307	261	190
$E_a$ (MPa)	3.69	4.30	3.23	2.29	2.83
$E_{\text{experimental}}$ (MPa)	60	32	25	13	5
$\phi_{(PP)}$ (vol%)	45	37	36	32	20
Model (a) (%)	10	3.9	4.5	2.56	0.55
Model (b) (%)	14.6	5.5	6.32	3.54	0.7
Model (c) (%)	47	42.1	40.7	38.92	48.38
Model (d) (%)	45.9	39	37.8	34.38	27.93

**Table 5.10a Calculated  $\Delta$  values from the Takayanagi model for tensile strength of TPV blends**

	1	2	3	4	5
TS <sub>c</sub> (MPa)	12	15	11	9.2	7.3
TS <sub>a</sub> (MPa)	0.72	0.88	0.63	0.4	0.5
TS <sub>experimental</sub> (MPa)	9	32	25	13	5
$\phi_{(PP)}$ (vol%)	45	37	36	32	20
Model (a) (%)	-	-	-	-	-
Model (b) (%)	52.06	60	59.09	65.21	40.52
Model (c) (%)	42.51	34.76	33.79	29.7	15.50
Model (d) (%)	43.9	36.19	35.22	31.29	19.13

A '-' sign implies that the value obtained was not within 0-100 %

**Table 5.10b Calculated  $\Delta$  values from the Takayanagi model for tensile strength of SEBS/PP/oil blends**

	1	2	3	4	5
TS <sub>c</sub> (MPa)	12	15	10.5	10	5.5
TS <sub>a</sub> (MPa)	6.1	7.7	5.8	5.2	7
TS <sub>experimental</sub> (MPa)	12	12	10	7	5
$\phi_{(PP)}$ (vol%)	45	37	36	32	20
Model (a) (%)	-	-	-	-	-
Model (b) (%)	23.12	12.21	19.61	6.15	-
Model (c) (%)	-	-	-	-	-
Model (d) (%)	28.68	26	20.72	27.61	5

A '-' sign implies that the value obtained was not within the range 0-100 %

### 5.5.8 Fitting the physical properties of TPVs and SEBS/PP/oil blends with a Type II approach using Veenstra model D

The Veenstra D model, which is generally used for co-continuous morphologies, can also be used as a type II approach. The model has only one unknown parameters a,

related to the volume fraction of the phases: equations (5.8e) and (5.8f). In this case "1" refers to the PP phase and "2" the rubber phase.

Figure 5.15 shows the effective volume fraction of the rubber phase, calculated from equation (5.8f), as a function of its actual volume fraction. The effective rubber volume fractions of both the TPVs as the SEBS/PP/oil compounds are all higher than the actual ones. This effect can be explained by the model used and the properties of the two phases. In both compound types the PP phase is continuous and its modulus value is about three decades higher than that of the elastomer phase. However, as can be seen in the TEM images, the morphology of both compound types does not consist of equally sized uniformly packed cubes. Thus, there are parts of the two phases that do not contribute in a continuous way, as described in the model. In the present case, the PP phase has the highest modulus and parts that are trapped in the elastomer phase do not contribute in a continuous way. This results in a higher effective volume fraction of the rubber phase and hence a lower value of the modulus, than expected.

In general, the effective volume fraction is thus a measure for the net mechanical continuity of the phase with the highest modulus. Both in the TPVs as in the SEBS/PP/oil compounds the PP phase is partially disrupted. The model results obtained from these tensile moduli are confirmed by those obtained in the modeling of the dynamic shear modulus (to be reported separately).<sup>[13]</sup>

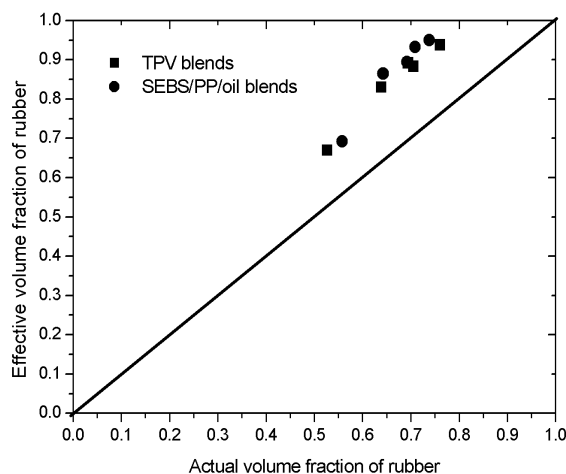


**Figure 5.15** The effective volume fraction of the rubber phase as calculated by the model,  $\phi_{2\text{ eff}}$  as compared to the actual volume fraction  $\phi_2$ .

### 5.5.9 Study of the deformation mechanism using cyclic tensile deformation and microscopy

The modeling of the failure characteristics: tensile strength and elongation at break, failed for nearly all systems and models. In order to gain additional insight into possible reasons for this failure, the deformation mechanism of SEBS/PP/oil was studied with cyclic deformation. These data were further enlarged upon with SEM- and TEM-data.

A representative stress-strain curve of SEBS/PP/oil blend - BS6 - subjected to multiple cyclic deformation upto 200% strain is shown in Figure 5.16. Similar curves for TPV blends and other compositions of SEBS/PP/oil blends are not shown for the sake of shortness. The first cycle shows a large hysteresis that gradually diminishes with increasing cycle. This can be explained by assuming that the PP phase buckles upon unloading resulting in plastic deformation. It indicates that PP phase suffers plastic

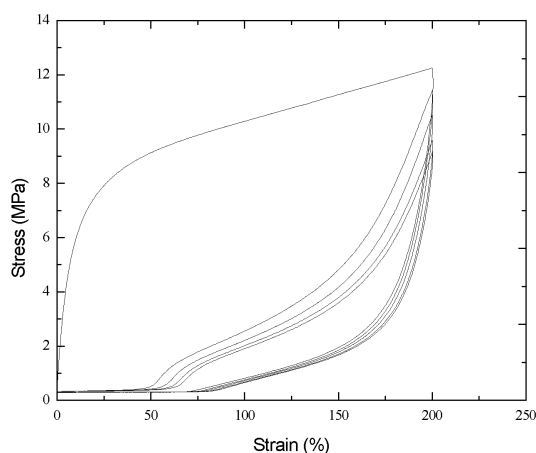


**Figure 5.16** Stress-strain curve of the 28/33/39 wt.-% SEBS/PP/oil blend subjected to multiple cyclic deformations at a fixed strain of 200 %.

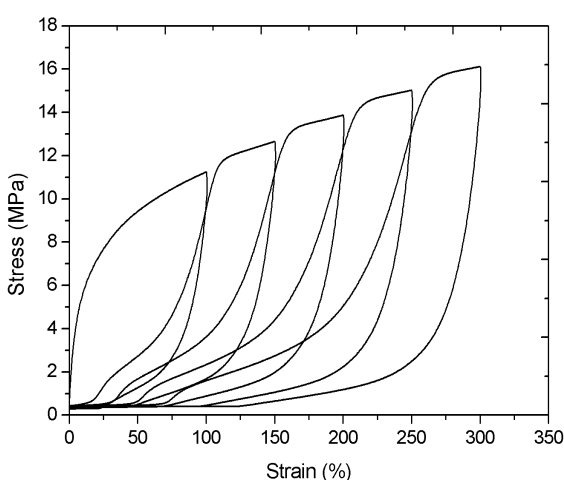


**Figure 5.17** Stress-strain curve of the 28/33/39 wt.-% SEBS/PP/oil blend subjected to multiple cyclic deformations. The strain is increased by 50% after each cycle.

deformation at low strains but it does not give evidence that it becomes discontinuous at strains larger than 100%.<sup>17</sup>

Fig 5.17 shows stress-strain plots of the sample subjected to multiple cyclic deformations. The amount of strain is increased by 50% after each cycle. The hysteresis loop after every step increase in strain does not decrease. This indicates that the PP phase does not fail even at strains as high as 300%. Thus, the deformation of the PP-oil phase in ternary blends is different from the deformation mechanism of neat PP or PP-oil binary blends.

Microscopic attempts to study the deformation of the PP and rubber phases in these blends are not conclusive either. Both materials show multiple holes with increasing deformation. A TEM image of the SEBS/PP/oil blends obtained after tensile failure at 600% shows deformed polystyrene and PP domains. These images indicate that both phases are deformed during tensile tests. During tensile deformation lots of defects are generated which can lead to catastrophic failure: Figure 5.18

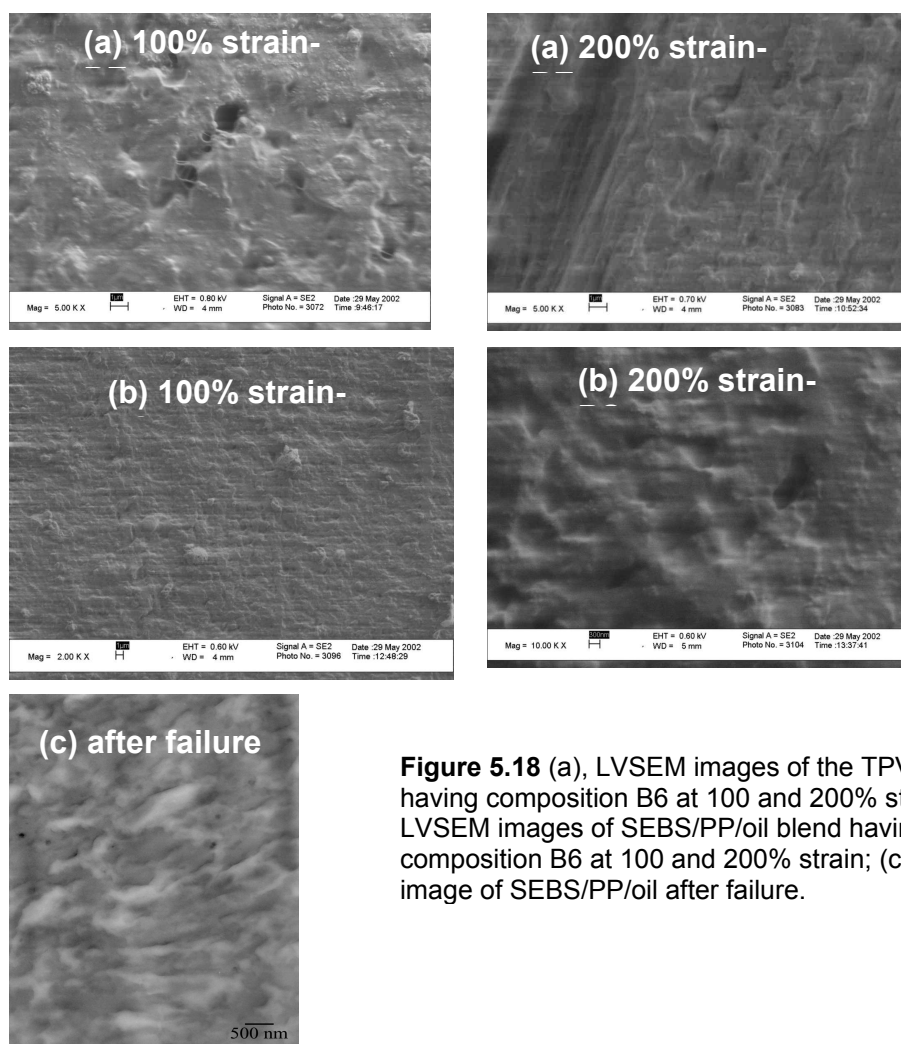


**Figure 5.18** (a), LVSEM images of the TPV blend having composition B6 at 100 and 200% strain; (b), LVSEM images of SEBS/PP/oil blend having composition B6 at 100 and 200% strain; (c), TEM image of SEBS/PP/oil after failure.

## 5.6 DISCUSSION

### 5.6.1 Deformation of the PP-oil phase

The question may be raised whether the deformation behavior of the PP-oil phase in the ternary blends is similar to the deformation of PP-oil model blends. An indication of the micro mechanics of the deformation process can be obtained from the studies of Lee.<sup>[16]</sup> Since PP is a semicrystalline material, it consists of crystalline and amorphous regions. Its yielding and necking behavior is associated with orientation of both crystalline and amorphous regions. The strain-hardening phenomenon is however mainly dominated by molecular orientations in the amorphous regions. It is not until very large strains, where the amorphous chains are nearly stretched to their maximum, that the crystallographic texture begins to significantly contribute to the strain hardening. Using IR dichroism experiments it has been proved that the presence of oil in the amorphous regions of PP delays the molecular orientation of PP chains.<sup>[17]</sup> This explains the fact that the onset of strain hardening is visible only in pure PP and PP with 5 wt.-% oil but not in other samples.

### 5.6.2 Deformation of the rubber-oil phase

A comparison of Figures 5.4-5.6 shows that the deformation behavior of rubber-oil blends is very different from that of the PP-oil blends. There are also differences between SEBS-oil and vulcanized EPDM-oil blends. The former blends exhibit much more pronounced strain-hardening as compared to the later.

The micromechanics of the deformation behavior of these rubber-oil blends has not been reported, but there are similar studies done on styrene-butadiene-styrene block copolymers (SBS).<sup>[11]</sup> Based on these studies, an explanation of the higher tensile strength and strain hardening of SEBS-oil blends as compared to vulcanized EPDM-oil blends can be obtained. At low strains, the soft ethylene-butylene chains are stretched and the polystyrene domains remain intact. These domains behave as crosslinking points. At higher strains agglomerates consisting of clustered SEBS domains of 1-5  $\mu\text{m}$  are deformed. Since the modulus of polystyrene is much higher than that of the ethylene-butylene regions, the deformation requires much larger stress which is reflected as an abrupt increase in the stress-strain curve. The strain hardening effect may also be due to orientation of the polystyrene domains.<sup>[11]</sup> Deformation of polystyrene domains in SEBS block copolymers during tensile tests has been observed in electron micrographs: see Figure 4.25. A higher resolution image showing deformation of

polystyrene domains of SBS is reported by Gergen *et al.*<sup>[11]</sup> The tensile failure is due to failure in polystyrene domains. Therefore it is reasonable to state, that the high tensile strength of SEBS-oil blends is due to the clusters formed by polystyrene domains that act in a way similar to reinforcing filler particles in conventional vulcanizates. This also explains, why the tensile strength of SEBS-oil blends shows a linear correlation with the amount of oil which, being paraffinic of nature is not likely to dissolve in the aromatic polystyrene domains. The delay in the onset of strain hardening may mean that oil reduces the orientation of both phases in SEBS, which is an effect similar to what was observed for the PP-oil blends.

### 5.6.3 Modeling

As seen in the results section, the E-moduli of the blends could well be predicted using Coran's model, Kolarik's model, the Veenstra D model and one of the Takayanagi model. Since these models assume a certain degree of oil distribution between the rubber and PP phase it is clear that the E-moduli of these blends are dependent on the oil distribution between the components. The models were not correlated to morphological parameters such as particle size of the EPDM phase or the degree of co-continuity of the SEBS phase. This is because of two reasons: (1) the E-modulus values of the TPVs and SEBS/PP/oil blends were close, which proves that morphology does not correlate strongly with the E-modulus; (2) the particle size of the TPVs showed a wide distribution. The models were not successful in predicting the tensile strength - except for the modified Kolarik model - and elongation at break values. A reason for this could be a difference in the behavior of the PP-oil phase in the ternary blends from neat PP-oil blends. This is further explained below.

### 5.6.4 Deformation behavior of the PP-phase in the ternary blends

Figure 5.19, shows a comparative stress-strain plot of PP-oil, SEBS-oil and SEBS/PP/oil blends. The oil content in the binary blends is close to the actual amounts in the PP and SEBS phases in the ternary blend. The large difference in the elongation at break of PP-oil and rubber-oil binary blends and the good fit obtained by modifying the Kolarik's model to the tensile strength suggests that the failure in ternary rubber/PP/oil blends results from failure of the PP-oil phase. If this happens at low strains, as suggested by the elongation at break values of the PP-oil blend, it should result in a disruption of the continuity of the PP phase in both blends. In case of SEBS/PP/oil



blends, the SEBS phase while being continuous will stretch the dispersed PP phase during deformation.

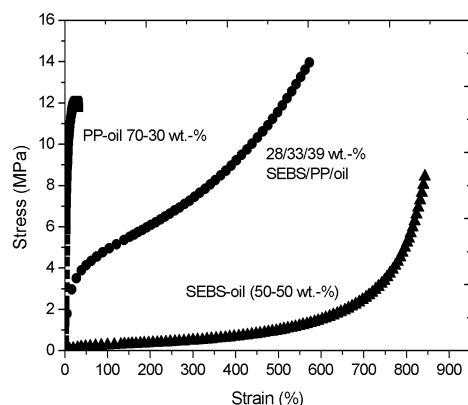


**Figure 5.19** Comparative stress-strain plots of PP-oil, SEBS/PP/oil and SEBS-oil blends.

However, the results from cyclic tensile deformation studies indicate that the continuity of PP phase is not lost during deformation of the ternary blends. Microscopic evidences of the existence of dispersed PP domains in the rubber phase were negative. In addition, finite element analysis studies reported by Boyce *et al.*<sup>[18]</sup> indicate that the majority of the PP phase remains below its elastic limit during the deformation of TPVs.

Further, from failure mechanics of polymers, it is a known phenomenon, that lowering the sample thickness enhances ductility due to a “Plane strain-Plane stress” transition.<sup>[20]</sup> The critical thickness below which the polymers undergo a transition from brittle failure to ductile failure has been modeled by Brown.<sup>[21]</sup> The PP-interstices in both blend systems obviously are far thinner than the pure PP-samples investigated here. All these evidences suggest, that the deformation behavior of the PP phase in these ternary blends is different from that of pure PP and so, any direct composite averaging method to model the deformation behavior of these blends is due to fail.

## 5.7 CONCLUSIONS

This study aimed at explaining the stress-strain properties of ternary TPV blends and SEBS/PP/oil blends on the basis of the properties of the constituent phases and oil distribution. It was assumed that, provided the same two components are involved, only their volume fractions determine the resulting properties. Several models for predicting the properties of binary polymer blends were used for this purpose. The E-moduli of the

blends can reasonably well be fitted by many of the empirical models. This property is determined in the linear regime of the stress-strain curves, the part where the initial morphology is still intact. The closest fits (Davies, Coran, Takayanagi, Veenstra D and Kolarik) are the ones which employ (partially) parallel connection of the two phases. The other models that failed (Veenstra A and B, Halpin Tsai, series and parallel) are characteristic for dispersed morphology. The fits suggest that the volume fraction of the elastomer phase is so high, that the particles can touch each other and form agglomerated or network like structures.

The fitting of the E-moduli suggests that the properties of the two blend systems at low strains are mainly composition-dependent. So it is not surprising that, although they have different morphologies, the properties are similar at equivalent compositions. The fit of the E-moduli works for both cases because:

- in both cases the PP phase is continuous and is the stiffer phase;
- in TPVs the particles can touch each other and form an agglomerated (continuous) network: it behaves as if it is continuous.

Models that have a combination of serial and parallel connections represent this dual phase continuity. When the models were applied to elongation at break values, poor fits were obtained. This shows, that it is not possible to model these properties purely on the basis of composite averaging methods. This can be due to two reasons: a) lack of parameters in the model, which relate to sample morphology; the models ignore the morphological changes occurring during deformation; b) the failure of binary oil blends is different from that of ternary blends. In Chapter 4 of this thesis it is reported that the particle sizes and interparticle distances change with composition. The properties are affected by the morphology of the system, i.e. by the juxtaposition and shape of the individual components in space, and how they are bonded together. The basic difficulty is, that one does not know *a priori* how stresses and strain are transmitted through the system, especially at high strains. Nevertheless, the results show that apart from morphology, blend composition and method of preparation, respectively the oil distribution between the PP and rubber phase also determine the stress-strain properties of these blends.

## 5.8 REFERENCES

1. W. G.F. Sengers and A. D. Gotsis, paper presented at the Polymer Processing Society Conference, September 2003, Athens, Greece.
2. R. C. Willimse, A. Speijer, A. E. Langeraar, A. Posthuma de Boer, *Polymer*, **40** (1999) 6645.
3. J. C. Halpin, *J. Compos. Mater.*, **3** (1969) 732.
4. A. Y. Coran, R. Patel, *J. Appl. Polym. Sci.*, **20** (1976) 3005.
5. S. G. Lee, S. H. Kim, *Polymer International*, **52** (2003) 698.
6. W. E. A. Davies, *J. Phys. (D)*, 4318 (1971).
7. H. Veenstra, P. C. J. Verkooijen, B. J. J. van Lent, J. Van Dam, A. P. De Boer, A. Posthuma, H.J. Nijhof, *Polymer*, **41** (2000) 1817.
8. J. Kolarik, *Polym. Eng. Sci.*, **36** (1996) 2518.
9. J. Kolarik, L. Fambri, A. Pegoretti, A. Penati, *Polymers for Advance Technology*, **11** (2000) 75.
10. Product brochure of Stamylan P11E10, SABIC Polypropylene.
11. W. P. Gergen, R. Lutz, S. Davison, "*Thermoplastic elastomers: A comprehensive review*", Ed. N.R. Legge, Carl Hanser, Munich (1987).
12. M. van Duin, A. Souphamthong, *Rubber Chem. Technol.*, **68** (1995) 717.
13. W. Sengers, PhD thesis, University of Delft, The Netherlands, to be published.
14. T. A. Huy, T. Luepke, H. J. Radusch, *J. Appl. Polym. Sci.*, **80** (2000) 148.
15. J. Kolarik, L. Fambri, *Macromol. Mater. Eng.* **283** (2000) 41.
16. B. J. Lee, A. S. Argon, D. M. Parks, S. Azhi, R. E. Cohen, **34** (1993) 3555.
17. M. Soliman, M. van Dijk, M. Van Es and V. Shulmeister, paper presented at ANTEC, May 1999, New York, NY, USA.
18. M. C. Boyce, K. Kear, S. Scorate, K. Shaw, *J. Mech. Phys. Solids*, **49** (2000) 1073.
19. K. J. Wright, K. Indukuri, A. J. Lesser, *Polym. Eng. Sci.*, **43** (2003) 531.
20. G. C. Adams, T. K. Wu, "*Failure of Plastics*", Ed. W. B. Brostow and R. D. Corneliussen, Hanser Publishers, Munich (1986).
21. H. R. Brown, *J. Mat. Sci.*, **17** (1982) 469.

## Chapter 6

### ***Effect of mixing times and evolution of blend morphology in EPDM/PP/oil-TPVs and SEBS/PP/oil-TPOs during compounding in a twin-screw extruder and internal mixer***

---

*This chapter reports the effect of mixing times on the morphology development of EPDM/PP/oil-TPVs and SEBS/PP/oil-TPOs during compounding in an internal mixer and a co-rotating twin-screw extruder. Samples were collected after mixing for different times in both equipments and immediately frozen for microscopic analysis. To study the morphology development in the twin-screw extruder, 'screw pullout' experiments were used.*

*Co-continuous morphology was observed for EPDM/PP/oil TPV blends before addition of phenolic resin in the internal mixer, which "phase-inverted" to a dispersed morphology within a few seconds after the addition. The morphology development of TPVs in the twin-screw extruder occurred within the first kneading block. No co-continuous EPDM/PP phase could be detected in this case. The crosslinked EPDM particles broke down into smaller aggregates on further mixing in both equipments. The experiments showed that in TPVs, the mixing time or screw configuration had negligible effects on the EPDM particle size after dynamic vulcanization.*

*Similar to the TPVs the process of morphology development in SEBS/PP/oil blends was also very rapid, both in the internal mixer and twin-screw extruder. However, the morphology so developed is less stable. The SEBS phase showed coalescence with increasing mixing time in both types of mixers. The screw pullout experiment in the twin-screw extruder showed that the dynamic equilibrium between coalescence and breakup of SEBS-particles shifted to increasing coalescence at the transporting blocks, respectively towards increasing breakup at the kneading blocks. The results are explained on the basis of two factors: a) the temperature effect on the viscosity ratio; b) shear versus elongational flow of the melt at different screw elements.*

*The stress-strain properties of the blends are however not influenced by the variations in mixing time in the internal mixer or residence time in the twin-screw extruder.*

## 6.1. INTRODUCTION

Mixing equipments like the internal mixer and co-rotating twin-screw extruder are commonly used in preparation of TPVs and SEBS/PP/oil blends. The influences of these mixing equipments on the morphologies and properties of these blends were presented in Chapter 4. TPVs made in the twin-screw extruder had a wider particle size distribution than the TPVs made in the internal mixer. In case of SEBS/PP/oil-TPOs, for high PP compositions, the blends made in the internal mixer had a higher degree of co-continuity than the blends made in the twin-screw extruder. It was suggested that the narrower particle size of the EPDM-phase in TPVs is related to a higher total shear strain in the internal mixer. The higher degree of co-continuity of the SEBS phase in TPOs is because of more coalescence between the SEBS particles in the internal mixer. Both these effects were considered to be the result of higher residence times in an internal mixer as compared to a twin-screw extruder.

The basic objective of this chapter is to further explore the effect of mixing times on the morphology of EPDM/PP/oil-TPVs and SEBS/PP/oil-TPOs during compounding in these two mixing equipments. To go a step further, the evolution of morphology during blending is studied. Since conditions of mixing: temperature, shear rate, melt flow pattern and feeding process are entirely different in an internal mixer from a co-rotating twin-screw extruder, it would be interesting to see if the morphology taken at different stages of mixing in these two types of equipment is different. Although comparative informations on other blend systems are available in the literature<sup>[1-4]</sup> a generalized model for this subject is yet to be developed. This is because there are many factors that can alter the morphology of an immiscible polymer blend and what is true for one blend might not hold for the other. Some of these factors are: (1) temperature, (2) mixing time, (3) rotor speed, (4) screw configuration, (5) blend composition, (6) viscosity ratio, (7) elasticity ratio, (8) interfacial tension. Another serious handicap is the lack of suitable characterization methods that can visualize the morphology in-situ.

As already mentioned, the primary focus of the present chapter is to investigate the morphological changes that occur during preparation of thermoplastic elastomer blends in an internal mixer and a twin-screw extruder. Previous works in this area have shown that the morphology develops very fast. In order to study the initial phase of morphology development, suitable sampling devices are necessary that can directly collect the samples during mixing.<sup>[5,6]</sup> The collected sample must be immediately frozen in order to preserve the morphology. Due to experimental limitations we used traditional sampling techniques to study the morphology development: stopping the internal mixer at different times or pulling out the screws after a certain time during twin-screw extrusion. Due to limitations of these methods, we were not able to detect the initial morphological changes that develop within the first few seconds of mixing. In our experiments we were rather interested in the secondary changes in morphology occurring due to effects of

temperature, screw configuration and flow patterns in the two sorts of mixing equipment. These secondary changes are more related to the mechanical properties of the polymer blends as compared to the initially developed morphology.

In the present chapter, first, the influence of mixing time in the internal mixer on the final morphology is presented. These samples also represent the morphology development in the internal mixer. In the twin-screw extruder, effects of mixing time and morphology development are studied in separate experiments. To study the effect of residence time in the twin-screw extruder, the polymers are compounded over the full length, half-length and  $1/3^{\text{rd}}$  of the length of the screw and the morphology studied for samples collected at the die. In this way the influence of screw configuration and residence time are both taken into consideration. The morphology at different positions of the screw along the screw axis are studied using screw pullout experiment. In addition, the stress-strain properties of the samples obtained at different mixing times from the internal mixer and at different residence times in the twin-screw extruder are reported.

## 6.2. THEORY

The fundamental principle behind the process of morphology formation in a blend of two immiscible polymers lies in their interfacial tension and viscoelastic properties. The deformation and breakup of droplets of one fluid dispersed in another have been extensively studied and reviewed by Jansen and Meijer.<sup>[7]</sup> The basic principles governing droplet deformation date back to the pioneering work of Taylor, who uncovered most of the features of Newtonian drop deformation and burst.<sup>[8]</sup> The breakup of a droplet can occur if the viscous forces acting on the droplet are stronger than the interfacial forces for a sufficient amount of time. The ratio of stresses that elongate the droplet, to the interfacial tension that keeps the droplet spherical, is defined by the capillary number:  $\kappa$ .

$$\kappa = \frac{\sigma D}{\nu} \quad (6.1)$$

where  $\sigma$  is the stress,  $D$  is the initial drop diameter and  $\nu$  is the interfacial tension. The condition for droplet deformation leading to breakup is, that the capillary number  $\kappa$  must be larger than a critical capillary number  $\kappa_{\text{cr}}$ . In shear, the critical capillary number is a strong function of the viscosity ratio defined as:

$$\lambda = \eta_d / \eta_m \quad (6.2)$$

where  $\eta_d$  is the viscosity of the dispersed phase and  $\eta_m$  is the viscosity of the matrix. The critical capillary number is minimum and approximately equal to 1 for  $\lambda = 1$ .<sup>[9]</sup> For a viscosity ratio larger than 1,  $\kappa_{\text{cr}}$  increases rapidly with  $\lambda$  and becomes infinite for  $\lambda > 3.8$ .<sup>[10]</sup> This means that breakup of a droplet in shear becomes impossible for  $\lambda > 3.8$ . The value of  $\kappa_{\text{cr}}$  is lower and less dependent on the viscosity ratio in stronger flow fields or in elongation.<sup>[11]</sup> Internal mixers and twin-screw extruders

usually provide a mixture of shear and elongational flows. In twin-screw extruders, shear is the predominant deformation mode in conveying elements, while both shear and elongation are present in mixing elements such as kneading blocks.

The mechanism of drop deformation and breakup in polymers is more complex than deformation of Newtonian droplets as described above. Due to their viscoelastic nature, polymer droplets also experience deformation-resisting forces arising from elasticity.<sup>[13]</sup> In a simple flow field, there is a minimum drop size below which breakup cannot be achieved.<sup>[14]</sup> Wu<sup>[15]</sup> obtained a correlation relating capillary number to viscosity ratio for twin-screw extruded blends and suggested the following equation for the final particle diameter,  $D$ :

$$D = \frac{4\nu\lambda^{\pm 0.84}}{\eta_m \dot{\gamma}} \quad (6.3)$$

where the (+) sign in the exponent applies for  $\lambda > 1$  and the (-) sign applies for  $\lambda < 1$ .  $\nu$  is the interfacial tension,  $\eta_m$  is the viscosity of the matrix,  $\dot{\gamma}$  is the shear rate and  $\lambda$  is the viscosity ratio (eq. 6.2). Van Oene developed a relation for the dynamic interfacial tension  $\nu_{12}$  between the dispersed and matrix phase:

$$\nu_{12} = \nu_{12}^0 + \left(\frac{D}{12}\right) [N_{2,d} - N_{2,m}] \quad (6.4)$$

where  $\nu_{12}^0$  is the interfacial tension in a quiescent polymer blend,  $N_{2,d}$  is the second normal stress difference of the dispersed phase, and  $N_{2,m}$  is the second normal stress difference of the matrix phase.

Coalescence of droplets can occur during morphology development, especially if the dispersed phase has a high concentration. Coalescence is caused by collision of droplets, which can be flow-driven<sup>[15]</sup> or static – caused by annealing. The relative importance of the two types of coalescence can be estimated based on Peclet number:  $P_e$ , the ratio of external flow, to the movement due to Brownian motion, where  $D$  and  $\mu$  are the particle diameter and diffusion coefficient, respectively. Flow-driven coalescence dominates when  $P_e \gg 1$ .<sup>[16]</sup>

$$P_e = D^2 \dot{\gamma} / \mu \quad (6.5)$$

The processes of break-up and coalescence are in dynamic equilibrium during the process of morphology evolution. The equilibrium may shift from one process to the other, depending on “strong” and “weak” mixing zones present inside the mixer.<sup>[17]</sup> The “strong” mixing zones represent the region in the mixer where high deformation rates are present. The droplets deform into long

threads until the capillary number equals 1. Coalescence does not occur in this region due to a short collision time of the droplets. The 'weak' zones represent the more or less quiescent zones in the mixer. The droplets will not deform here into threads, because the deforming stress is much lower than the interfacial stress. These regions stimulate higher coalescence.

The mechanism of morphology development in dynamic vulcanizates and SEBS/PP/oil - TPOs is based on the principles of particle break-up and coalescence illustrated above. Several authors have investigated the process of morphology development for TPVs made in an internal mixer<sup>[1,18]</sup>, but the process of morphology development in twin-screw extruders is still not clear. It has been reported, that the morphology before the addition of crosslinking agent is largely co-continuous. Once the vulcanization process begins, the rubber phase becomes highly viscous but the thermoplastic matrix viscosity does not change. The viscosity ratio increases to a value at which, theoretically, droplet breakup is impossible in conventional shear flows. As the rubber particles cure, they undergo shrinkage. The shrinkage of these particles in combination with shear and elongational flows causes a phase inversion, resulting in dispersion of rubber domains in the thermoplastic matrix.

Comparable information on the morphology development in SEBS/PP/oil blends does not exist. The stability of the end morphology of these blends has been investigated by Verhoogt<sup>[19]</sup> and later by Veenstra.<sup>[20]</sup> These blends were reported to exhibit co-continuous morphologies in a wide range of compositions. Formation of co-continuous morphologies in other polymer blends such as polyethylene (PE) and polystyrene (PS) has been investigated by Willemse.<sup>[21]</sup> In contrast to the work of previous investigators, his results prove that co-continuous morphologies can be obtained for a large range of compositions rather than for a single blend composition. The mechanism of morphology development in PE/PS blend was similar to that proposed by Scott and Macosco<sup>[22-24]</sup>. According to this mechanism, morphology development begins with the formation of sheets or ribbons of the dispersed phase in the matrix. Owing to the effects of flow and interfacial tension, these sheets are unstable and holes begin to form. The holes are filled with matrix phase, which surrounds the sheet on either side. When the holes in the sheet or ribbon attain a sufficient size and concentration, a fragile lace structure is formed, which begins to break into irregularly shaped pieces due to flow and interfacial forces. These pieces are approximately the diameter of the particles that are generated in the blend at long mixing times. According to these authors this proposed mechanism results in the generation of very small particles at very short timescales.



## 6.3. EXPERIMENTAL

### 6.3.1 Materials

The grades of polymers used in these experiments are the same as described in Chapter 4. The recipe used for the preparation of TPV and SEBS/PP/oil blends are shown in Tables 6.1 and 6.2.

**Table 6.1: Compounding recipe for EPDM/PP/oil - TPVs**

Components	Composition (Parts per hundred rubber, Phr)
EPDM, Keltan P597*	200
PP, Stamylan P11E10	80
Extra Oil, Sunpar 150	40
Phenolic resin, SP 1045	5
Stannous chloride dihydrate	1
Zinc oxide	2.5
Irganox1076	0.5
Irgafos 168	0.5
*Contains 50 wt.-% of paraffinic oil	

**Table 6.2: Compounding recipe for SEBS/PP/oil blends**

Components	Composition (Phr)
SEBS, Kraton G 1651	100
PP, Stamylan P11E10	120
Oil, Sunpar 150	140
Irganox 1076	0.5
Irgafos 168	0.5

The recipe used for TPVs corresponds to the center point of the experimental design – composition “5” - as shown in Figure 4.1. For SEBS/PP/oil blends however, the composition “6” of Figure 4.1 was selected, because at that composition the SEBS/PP/oil blend has shown maximum differences in the degree of co-continuity as a result of mixing in different equipments.<sup>[26]</sup>

### 6.3.2 Mixing process and sample collection procedures

#### 6.3.2.1 Effect of mixing time on morphology development of TPVs in the internal mixer.-

The process variables, viz. the feeding procedure, rotor speed and temperature settings, used for the preparation of the TPVs were the same as described in Chapter 4. At 80 rpm the maximum shear rate in the mixer was  $140 \text{ s}^{-1}$ . This was calculated on the basis of rotor speed, the gap between the rotor tip and the mixing chamber wall.

The blends were compounded for 300, 360, 420, 450 and 720 seconds of mixing. The sampling points are shown in the Figure 6.1. Time zero corresponds to the end of feeding the PP pellets to the mixer. The phenolic resin was added after 360 s in each case. So the first sample was taken before the addition of the resin and the second sample was taken immediately after adding the resin. After the specified time of mixing, the internal mixer was stopped and the mixer was opened. Samples attached to the rotors were pulled off with a set of pliers and dropped directly into a bath of liquid nitrogen to freeze the morphology. The time required between stopping the mixer and dropping the sample in liquid nitrogen bath was 10 to 15 s. The sample morphology was examined with TEM using the procedures described in Chapter 4. Further, the samples were compression molded into 2 mm sheets and their tensile stress-strain properties, and plastic deformations during cyclic tests were investigated.

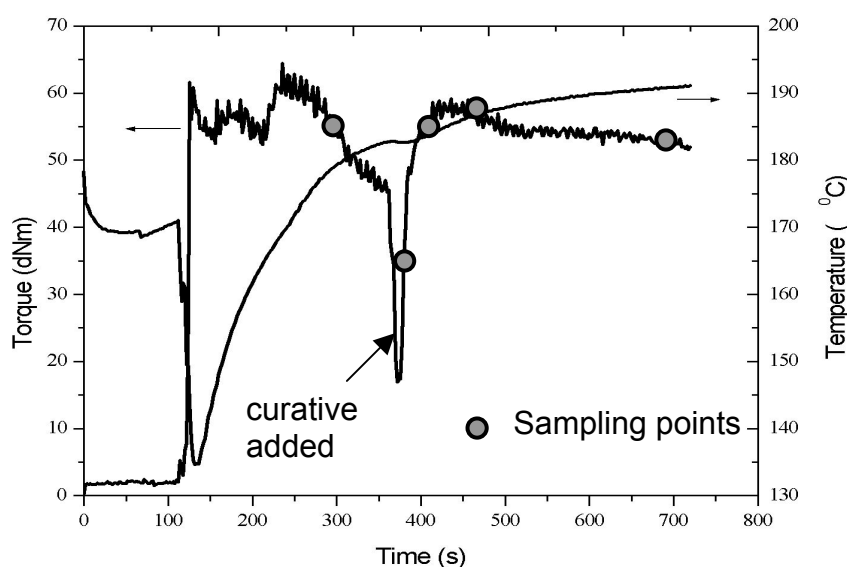


**Figure 6.1** Sampling points for studying the effect of mixing time and mechanism of morphology development for TPVs made in the internal mixer.

### 6.3.2.2 Effect of residence time on morphology development of TPVs in the twin-screw extruder.-

Melt blending of EPDM-oil/PP and extra oil was conducted using a Berstorff (ZE 25 x 33 D) co-rotating twin-screw extruder. The oil was previously premixed with the rubber on a Schwabenthan two-roll mill. The EPDM-oil premix was subsequently pelletized in a pelletizer. All the compounding ingredients, including phenolic resin and stannous chloride, were then prepared as a dry mix. This mix was then fed to the extruder at a constant rate. To investigate the effect of different residence times the feeding port was chosen in such a way, that the materials are compounded over the full length, half-length and  $1/3^{\text{rd}}$  of the length of the screw: Figure 6.2. At the end of the extruder a 2-hole strand die was attached. The screw speed was set at 150 rpm and the throughput was 4 kg/hr. The temperature used was 170°C at the feeding port and 200°C throughout the rest of the barrel. Samples meant for studying the end morphology of TPVs due to variation in mixing time were collected from the die exit.

To investigate how the morphology develops inside the screw, the compounding ingredients were fed through the first port. Once the extrusion reached a steady state, the extruder was shut

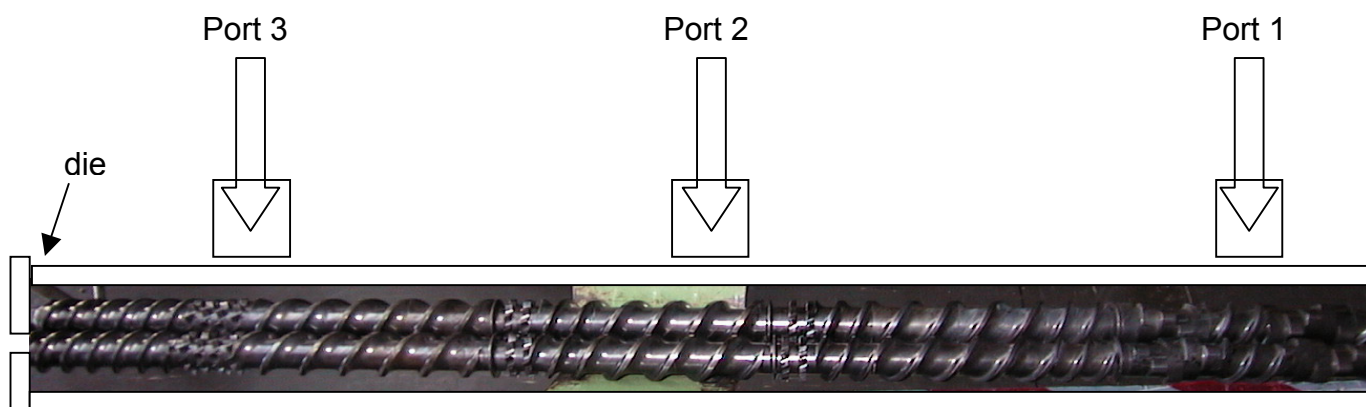


**Figure 6.2** Picture of the twin-screw extruder, showing the feeding ports.

down. Immediately the screws were taken out and placed on iron stands. Samples were quickly picked up using pliers at different positions of the screw and quenched in liquid nitrogen. The complete process took about 2-3 minutes. The morphology was subsequently studied using TEM.

### 6.3.2.3 Effect of mixing time on morphology development of SEBS/PP/oil blends in the internal mixer.-

The process variables, viz. the rotor speed and temperature settings, used for the preparation of SEBS/PP/oil compositions were the same as described in Chapter 4. The PP and the stabilizers were added together with the preblend of SEBS/oil into the hot mixer. Samples were collected after 60, 120, 180, 300 and 1200 s of mixing: see Figure 6.3 for sampling points. Time zero

corresponds to the end of feeding the premixed pellets to the mixer. The sample morphology was examined with TEM using the procedures described in Chapter 4. In addition, the degree of co-continuity of the SEBS phase in the samples was studied using a solvent extraction method also given in Chapter 4. Further, the samples were compression molded into 2 mm sheets and their tensile stress-strain properties, compression set and plastic deformation during cyclic tests were investigated.

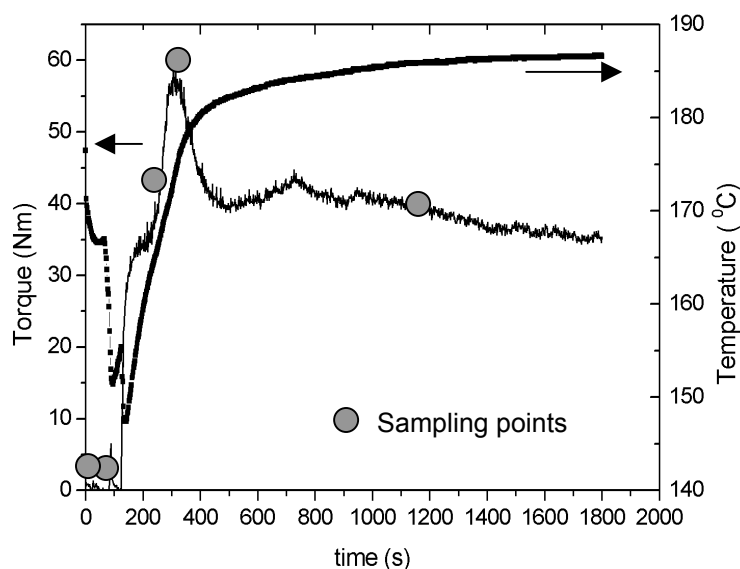


**Figure 6.3** Torque-temperature-time graph of SEBS/PP/oil blends in the internal mixer.

#### 6.3.2.4 Effect of residence time on morphology development of SEBS/PP/oil blends in the twin-screw extruder.-

The SEBS was first dry blended with the oil at room temperature. The other ingredients, PP and stabilizers, were dry mixed with the oil extended SEBS to obtain all ingredients in a dry mixed state. The SEBS/PP/oil mixture was then fed through different ports of the twin-screw extruder to vary the residence time. Samples were collected at the die exit for TEM and stress-strain analysis. To study the morphology at different positions of the screw, the experimental procedures were exactly similar to that described for TPVs.

## 6.4. RESULTS

### 6.4.1. Effect of mixing time on morphology evolution of TPV blends in the internal mixer

Figure 6.4 shows the effect of mixing times and the evolution of morphology in TPV blends during mixing in the internal mixer. The temperature profile during mixing, the torque-time graph and the times at which the samples were collected are shown in Figure 6.1. In images shown in Figure

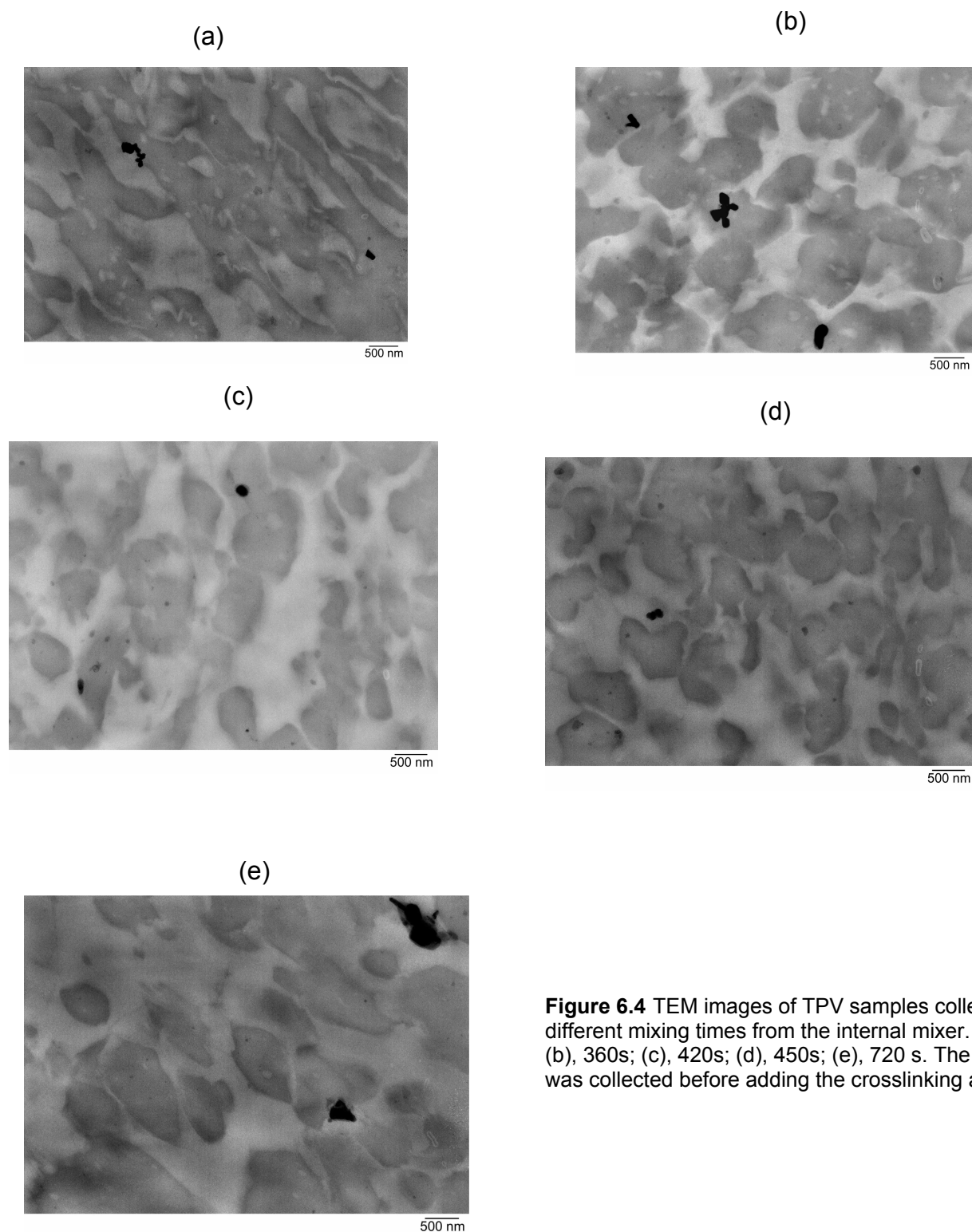


**Figure 6.4** TEM images of TPV samples collected at different mixing times from the internal mixer. (a), 300 s; (b), 360s; (c), 420s; (d), 450s; (e), 720 s. The first sample was collected before adding the crosslinking agent.

6.4, the black regions represent the EPDM phase and the other phase is PP. The oil is distributed over the two phases and is not visible in the images. The TEM image of the sample collected after 300s of mixing shows co-continuous EPDM- and PP-phases. This is seen from the interconnected ribbon-like structures of the EPDM-phase that extend throughout the PP-phase. After addition of the crosslinking agent, the co-continuous morphology changes to dispersed phase morphology. The TEM image obtained at 360s of mixing shows dispersed EPDM-phases. The EPDM-phase is broken up into irregular shaped domains. The domains are still somewhat interconnected and at some places appear to be at the point of breakdown. No significant differences in the images obtained after 360s can be detected anymore. The only visible change is still a slight improvement of the spatially homogeneous distribution of EPDM rubber particles with increasing mixing time. Image analysis, however shows a gradual narrowing of the particle size distribution with increasing mixing time.

#### 6.4.2. Effect of residence time and screw configuration on morphology evolution for TPV blends in the twin-screw extruder

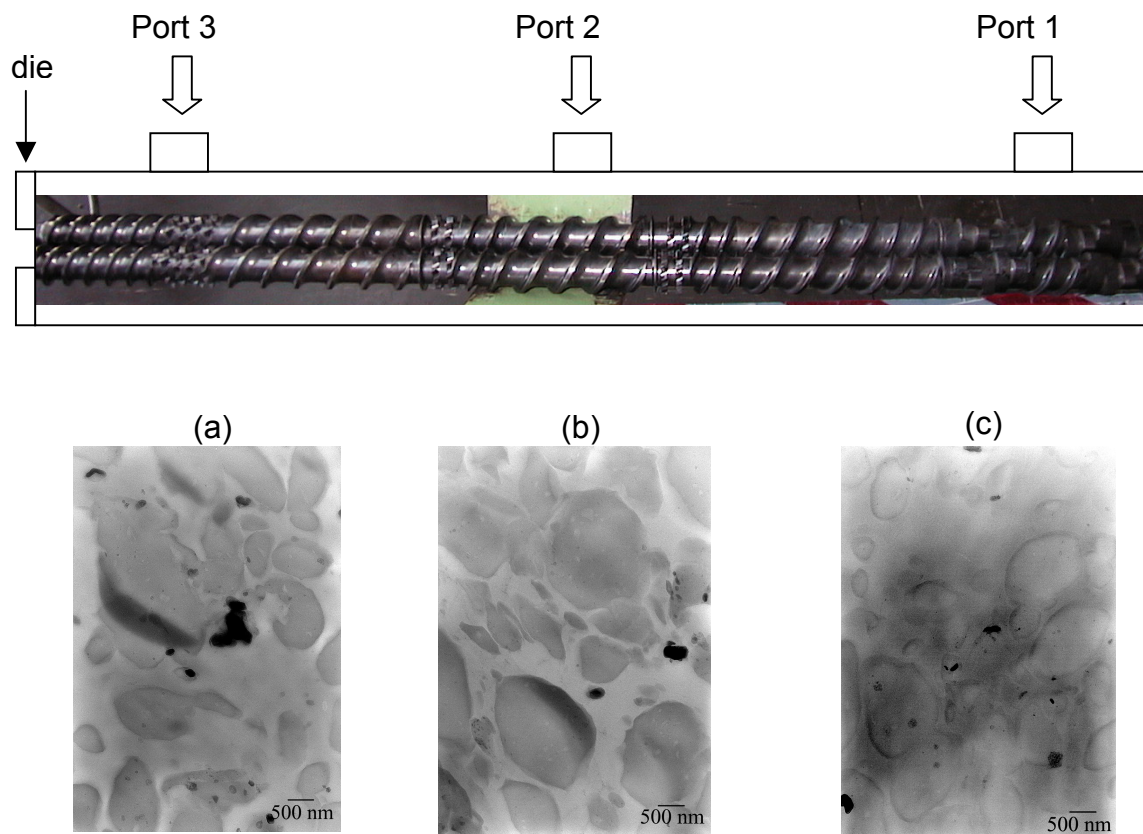


**Figure 6.5** Effect of residence time on the morphology of TPV blends made in the twin-screw extruder. (a),  $1/3^{\text{rd}}$  of the length of the screw; (b), half-length of the screw; (c), full length of the screw.

Figure 6.5 shows the TEM images illustrating the morphology of the EPDM/PP/oil TPVs as obtained after mixing for different mixing histories in the twin-screw extruder. After 1-2 minutes of mixing, resulting from feeding at port 3, the EPDM-phase is coarsely distributed in the PP-matrix, giving an impression of a wide particle size distribution. This is due to lack of kneading blocks or insufficient time of mixing. The TPV blend prepared using the half-length of the screw shows a comparatively more homogeneous particle size distribution, expected to result from the longer mixing time. Particle sizes are about 2-4  $\mu\text{m}$ . No significant changes in the particle size of EPDM

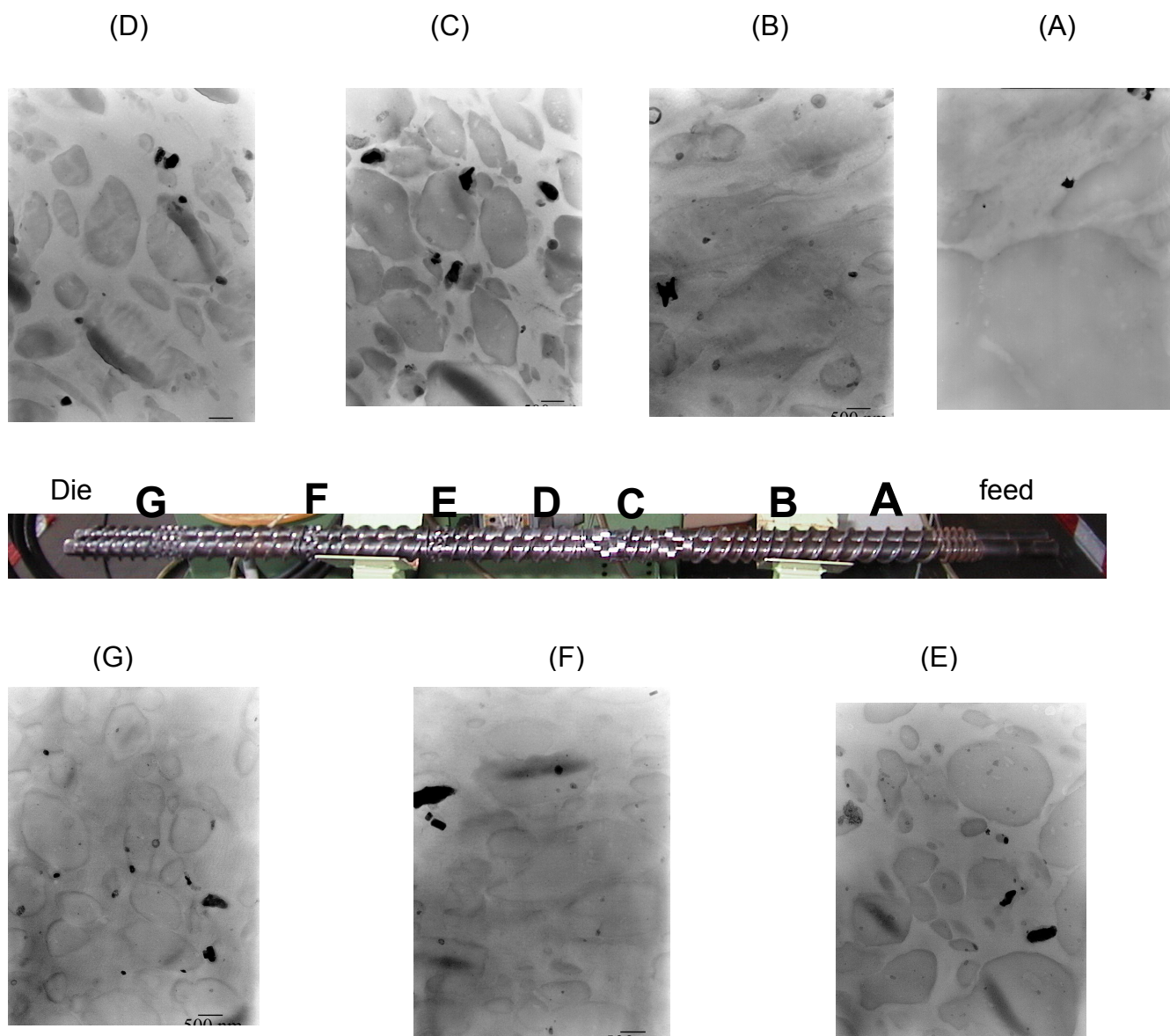


**Figure 6.6** The evolution of morphology in a EPDM/PP/oil TPV blend during compounding in a twin-screw extruder: (A), at the front end of the screw near the feed hopper; (B), near to point A; (C), first kneading block; (D), after the first kneading block; (E), after the second kneading block; (F), at the third kneading block; (G), at the tip of the screw just at the die entrance.



were detected using the full length of the screw. This result shows that the morphology of TPVs develops very fast. The morphology so developed is fixed after dynamic vulcanization, i.e. it does not change further.

Figure 6.6 shows TEM images illustrating the morphology evolution of the EPDM/PP/oil TPV blends along the extruder axis and a picture of the screw showing the positions from where the blend specimens were taken after 'screw pullout'. Visual examination of the sample taken at position A shows partially molten PP and EPDM-granules. The morphology at position A is underdeveloped, as expected. The TEM image shows rubber particles as large as 10-15  $\mu\text{m}$ , poorly distributed in the PP matrix. The image taken at position B, which is three threads to the left of position A, shows elongated EPDM-domains. Although the screw configuration is the same as in position A, the EPDM-domains are smaller in size than those observed at position A. The particle size of EPDM decreases further at the first kneading block: position C. At this position, the EPDM-particles are clearly seen to be dispersed in the PP-matrix. So the phase inversion is complete. No significant changes in particle sizes of the EPDM-phase are observed anymore in TEM images obtained at positions D, E, F and G. These results show that the morphology of TPVs in the twin-screw extruder is already developed at the first kneading block and remains unchanged over the rest of the screw.

#### **6.4.3 Comparative study of the morphology development of TPVs in the internal mixer and twin-screw extruder**

The sequence of morphology development for TPVs made in the internal mixer is similar to that reported by others.<sup>[1,27]</sup> A comparison of the morphology development for EPDM/PP TPVs prepared in the internal mixer and the twin-screw extruder shows several interesting features. The morphology development is very fast in both types of equipment. In the internal mixer it occurs within one minute after the addition of the crosslinking agent. In the twin-screw extruder it occurs at the first kneading block. One important difference between the two equipments is the feeding procedure. In the internal mixer the PP and EPDM was premixed to a certain degree of mixing before the resin was added. On the other hand, in the twin-screw extruder all the ingredients including the resin were added together. This explains why a co-continuous EPDM/PP morphology was observed in the internal mixer before adding the resin, but not in the twin-screw extruder. In spite of differences in the mixing conditions, in the melt flow mechanism and melt temperatures in the two equipments, the final morphology of the TPVs is found to be the same in both types of



equipment. The particle size distribution of the TPV blends made in the internal mixer and twin-screw extruder after different mixing times are shown in Figure 6.7 (a)-(d). Most particles are less than 3  $\mu\text{m}$  irrespective of the blend preparation method used. A comparison of percentage of the number of particles- Figure 6.7(a) and (b) - indicate that there is a gradual diminishing of particle size in either machine, till overall somewhat smaller in the internal mixer. The percentage of particles with a particle size less than 1  $\mu\text{m}$  is higher for the internal mixer as compared to the twin-screw extruder. This difference in EPDM particle size distribution is in agreement with what was observed in Chapter 4.

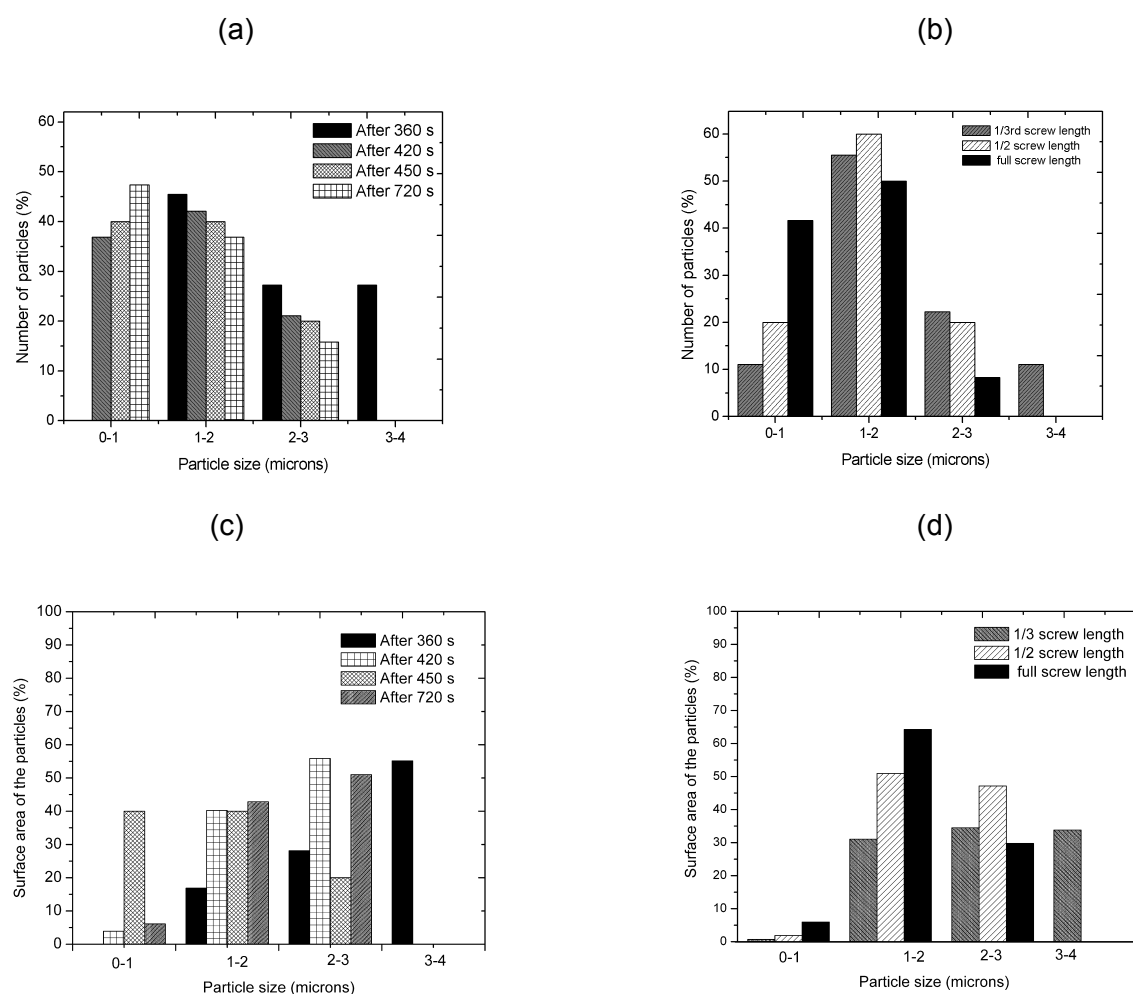


**Figure 6.7** Relative comparison of EPDM particle size distribution in TPV blends (a), made in the internal mixer; (b), made in the twin-screw extruder. If instead of number of particles, the surface areas of the particles are calculated, a different distribution is obtained. Plots (c), made in the internal mixer; (d), made in the twin-screw extruder

However if the surface area covered by these particles are taken into consideration a different picture is obtained - Figure 6.7(c) and (d). In this case the particle-size distribution is more narrow in the twin-screw extruder using the full length of the screw as compared to the

corresponding blend in the internal mixer mixed for 720s. Thus, although the average particle size might be smaller in the internal mixer, the mixing is more homogenous in the twin-screw extruder.

#### 6.4.4 Effect of mixing time on morphology evolution of SEBS/PP/oil blends in the internal mixer

Figure 6.8 illustrates the evolution of the morphology of the SEBS/PP/oil blend during mixing

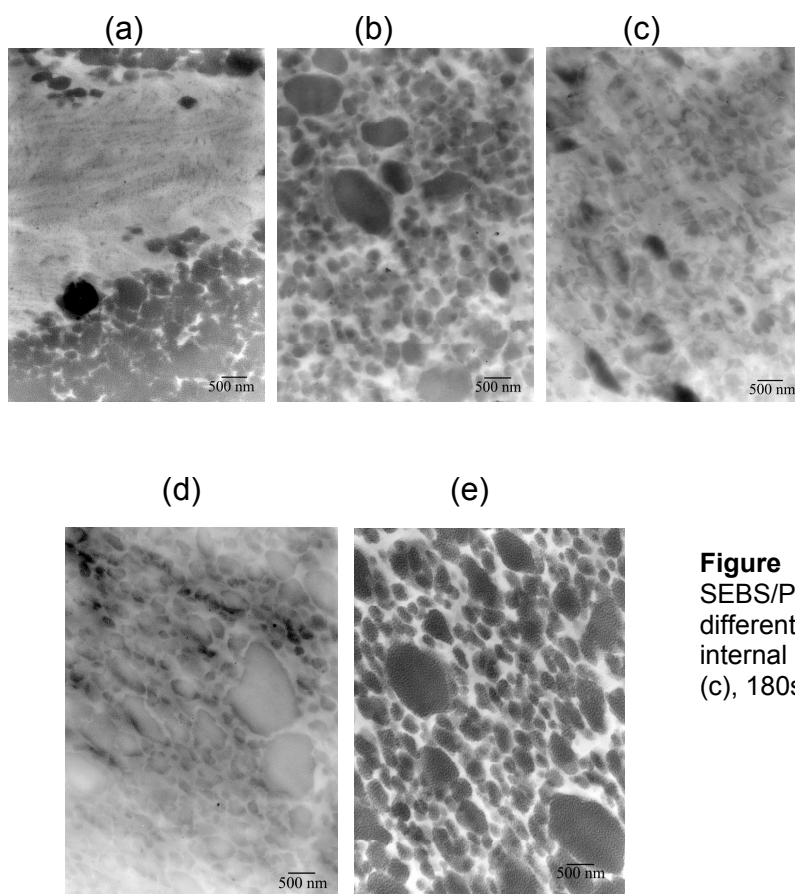


**Figure 6.8** TEM images of SEBS/PP/oil samples collected at different mixing times from the internal mixer. (a), 60s; (b), 120s; (c), 180s; (d), 300s; (e), 1200s.

in the internal mixer. The temperature profile during mixing and the corresponding torque-time graph showing the sampling points, is given in Figure 6.3.

At the beginning cold pellets are added to the hot mixer and the mixing torque rises rapidly. The torque then falls as the temperature increases and the polymers soften. After about 400 s, the torque levels off at a reasonably constant value. A visual examination of the sample collected after 60s of mixing shows, that part of the preblend comprising SEBS and PP pellets is still not completely molten. The corresponding TEM image (Figure 6.8a) shows separate SEBS-rich and PP-rich regions, confirming poor mixing between the two polymers. After 120 s of mixing, visual examination shows no signs of pellets anymore. The corresponding TEM image shows several SEBS domains ranging from 0.1-0.2  $\mu\text{m}$ , distributed in the PP matrix. This is the result of extensive particle break-

down. No significant changes in morphology are observed anymore after 180 s and 300 s of mixing. The TEM image after 1200 s of mixing shows several SEBS domains with phase sizes similar to those observed after 300 s. Also some SEBS domains are seen, which are significantly larger than the average, possibly due to coalescence: see later. The TEM images shown are not sufficient to determine whether the SEBS phase is continuous or dispersed in the PP matrix. This is a disadvantage of TEM and is discussed in Chapter 3. The TEM images were supplemented with LVSEM experiments after solvent extraction. Two representative LVSEM images are shown in Figure 6.9. In these images the holes correspond to the extracted SEBS and oil phase. These solvent extraction studies showed that the PP phase was continuous in all blends. All the blends were found to be co-continuous to different degrees, Table 6.3: much more than seen for the TPVs: Figures 6.4-6.6.

**Table 6.3: The degree of co-continuity of the SEBS phase in SEBS/PP/oil blends obtained at different mixing times in the internal mixer.**

Time (s)	60	120	180	300	1200
Degree of co-continuity (%)	60	90	95	100	100

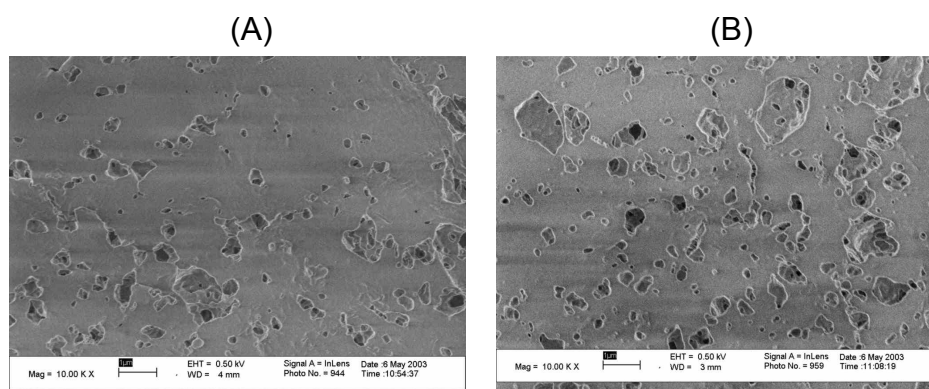


**Figure 6.9** LVSEM of SEBS/PP/oil blends from which the SEBS/oil phase has been extracted: (A), after 60 s; (B), after 1200 s.

The above results show that the mechanism of morphology development for SEBS/PP/oil blends in the internal mixer is also rapid, similar to the TPVs. The SEBS/PP/oil blend shows co-continuity already after 120 s of mixing. This shows that the phase inversion from a dispersed SEBS phase to a continuous SEBS phase is very rapid. The co-continuous morphology developed after 120 s mixing is found to be stable, even till 120 s of mixing possibly due to equilibrium between particle breakup and coalescence. The reason for increasing coalescence of the SEBS phase with increase in mixing time will be discussed later.

#### 6.4.5 Effect of residence time on morphology evolution of SEBS/PP/oil blends in the twin-screw extruder

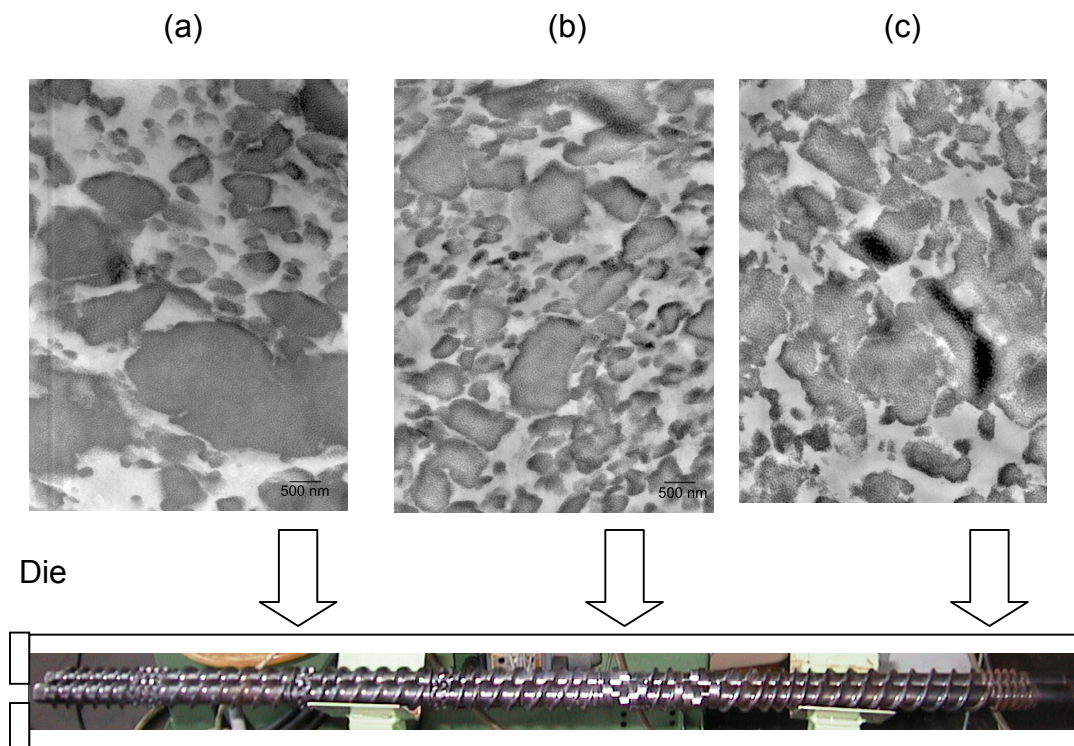


**Figure 6.10** Effect of residence time on the morphology of SEBS/PP/oil blends made in the twin-screw extruder. (a),  $1/3^{\text{rd}}$  of the length of the screw; (b), half-length of the screw; (c), full length of the screw.

Figure 6.10 shows TEM images illustrating the morphology of SEBS/PP/oil blends as obtained after mixing for different residence times. After 1-2 minutes of mixing, resulting from mixing over  $1/3^{\text{rd}}$  of the screw-length, the SEBS phase shows an inhomogeneous distribution of domain sizes. This is due to the lack of kneading blocks in this region or still too little time for proper mixing. Compounding the same polymers over  $1/2$  - screw-length, which corresponds to about 4 minutes of mixing, results in extensive breakdown of the SEBS domains. This shows, that the polymers now had enough time for good dispersive mixing. Using the full length of the screw, corresponding to about 6 minutes of mixing, the SEBS phase again shows signs of coalescence. This result is similar to what was observed after 1200 s mixing in the internal mixer.

Figure 6.11 depicts the evolution of morphology in the SEBS/PP/oil blend along the screw-axis in the twin-screw extruder. Visual examination of the sample collected at feed position A shows that a part of the preblend comprising of SEBS and PP pellets is still not completely molten.

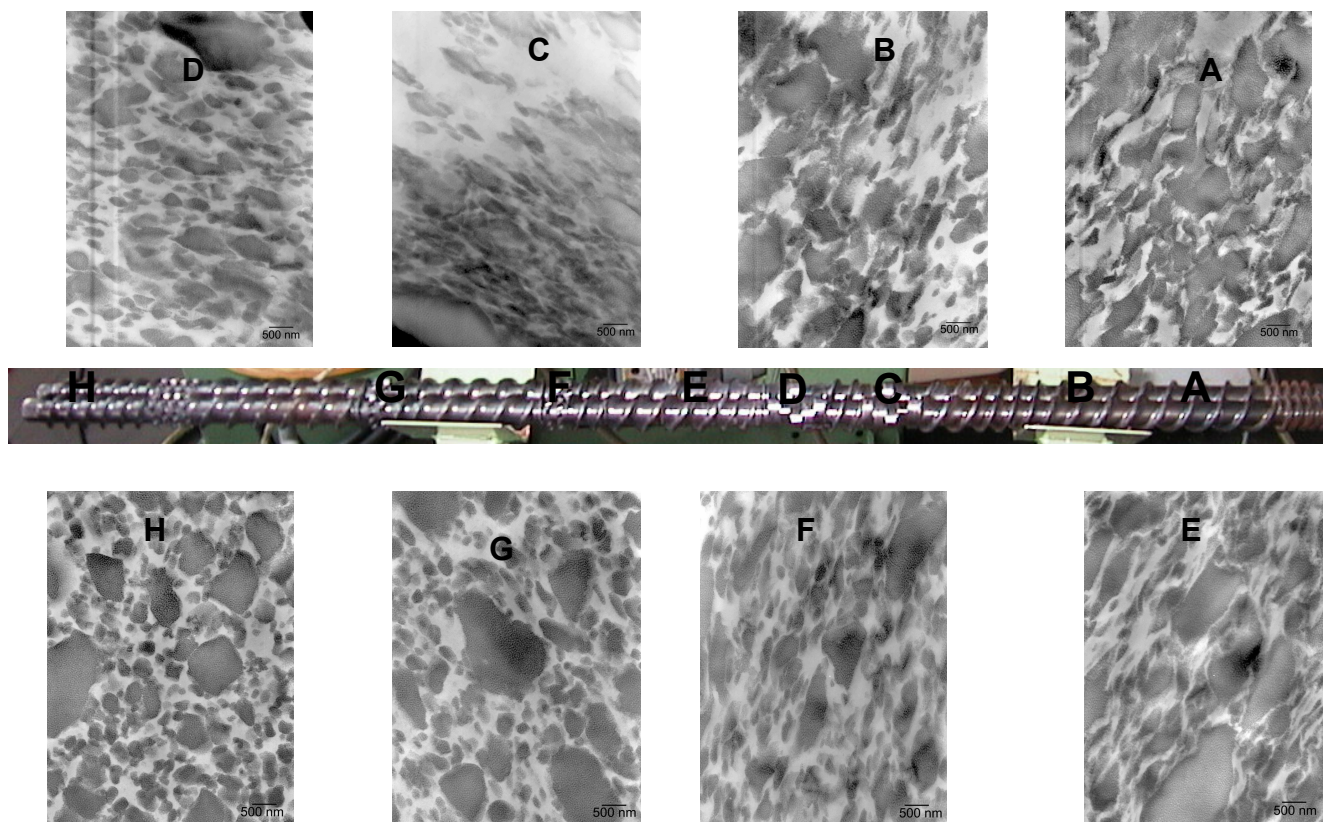


**Figure 6.11** The evolution of morphology in the SEBS/PP/oil blend during compounding in a twin-screw extruder: (A), at the front end of the screw near the feed hopper; (B), near to point A; (C), near to the first kneading block; (D), at the first kneading block; (E), in between the first kneading block and dispersion block; (F), in between the first and second dispersion block; (G), at the third dispersion block; (H), at the tip of the screw, just at the die entrance.

The TEM image of the sample collected at this point shows large SEBS domains poorly distributed in the PP. At few threads further down the twin-screw extruder, position B, the morphology looks already different. Visually the samples look molten. In the TEM images obtained from these positions a lot of SEBS domains are observed smaller in size ( $0.5\text{--}1\text{ }\mu\text{m}$ ), than seen at position A. This shows, that the SEBS phase is broken up as it passes through the transporting blocks. At the entry of the kneading block, position C, and at the exit of the kneading block, position D, the SEBS phase experiences extensive break-up. However, a TEM image taken from samples collected at position E, shows larger SEBS domains than observed at position D. This shows, that the SEBS phase does coalesce during transport from D to E. As the melt passes to position F, which is also a kneading block but much shorter than that at position D, we again see particle break-up. The SEBS



particles are still larger as compared to position D. Samples collected from positions G and H show significantly larger SEBS domains again coming from coalescence of the SEBS particles.

From the above images it is difficult to determine whether the SEBS phase is co-continuous or dispersed in the PP matrix. The degree of co-continuity was further studied using solvent extraction and LVSEM studies on extracted blends. Solvent extraction results for SEBS/PP/oil samples collected from different screw-positions are shown in Table 6.4. Extraction resulted in 100 % removal of SEBS and oil from samples collected at position A, B and H. This shows, that the SEBS phase was continuous in these samples. The degree of co-continuity was less in the middle of the screw, especially at the transporting blocks E and kneading blocks D and F. The PP film obtained after extraction of SEBS and oil was self-supporting in all cases. This proves, that the PP phase was continuous in all blends. The continuity of the PP phase is also clearly seen in the LVSEM images of the extracted films shown in Figure 6.12. In this figure the holes correspond to the extracted SEBS and oil phase. Only three images are shown here for shortness sake. These images are better representations of the interconnectivity between the SEBS domains as compared to TEM, but support the observations made by TEM.

**Table 6.4 The degree of co-continuity of the SEBS phase in SEBS/PP/oil blends measured on samples collected at different screw positions.**

Screw position	A	B	C	D	E	F	G	H
Degree of co-continuity (%)	100	100	90	93	90	88	100	100

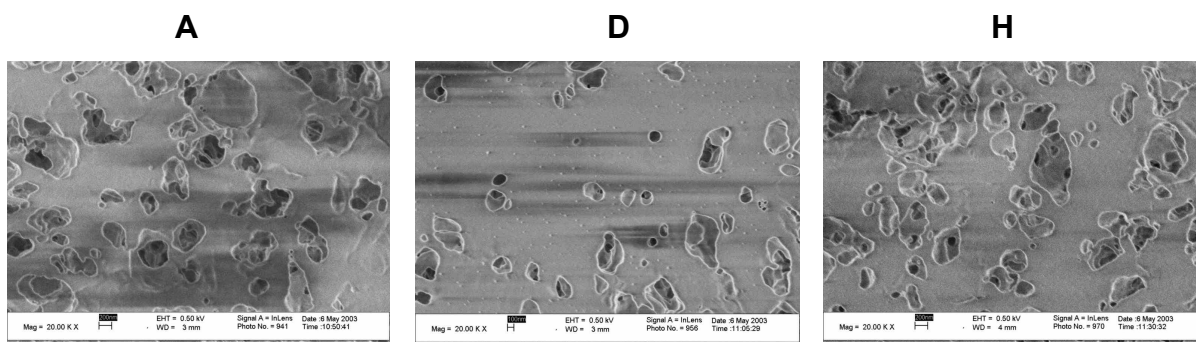


**Figure 6.12** LVSEM mages of SEBS/PP/oil blend from which the SEBS/oil phase has been extracted: (A), at the front end of the screw near the feed hopper; (D), at the first kneading block; (H), at the tip of the screw, just at the die entrance.

#### 6.4.6 Influence of the morphology on stress-strain properties

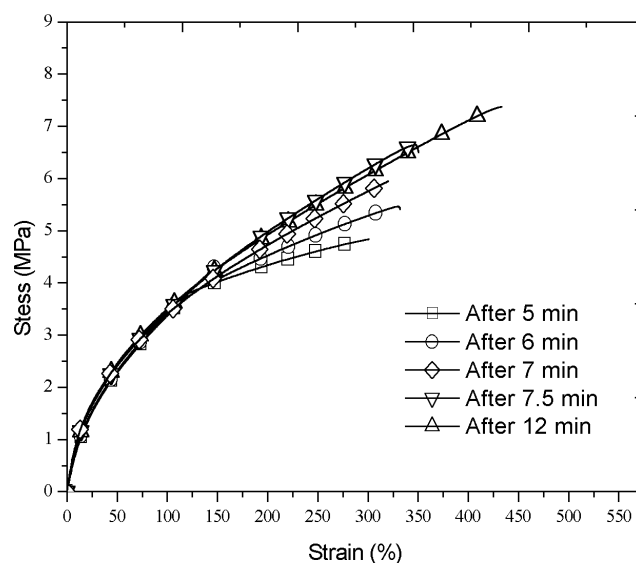


**Figure 6.13** Stress-strain properties of TPV blends obtained after different mixing times in the internal mixer.

The stress-strain properties of the different EPDM/PP/oil based TPV blends obtained after different mixing times in the internal mixer, are shown in Figure 6.13. The curves overlap upto 100 % strain. This is due to a larger contribution from the continuous PP phase, as compared to the dispersed rubber domains at these low strains. At higher strains the curves deviate and, at comparable strains show higher stress with increasing mixing time. The deviation of the curves at higher strains implies that the contributions from the dispersed rubber domains are significant. The difference in contribution of the continuous PP phase vs. the dispersed EPDM domains, is expected on the basis of morphology: a serial loading of components; and different stress-strain behavior of binary PP-oil and rubber-oil blends. The E-moduli of these blends are comparable within experimental error. In general, the tensile strength at break and elongation at break rises with increasing mixing time. Also the area under the stress-strain curve increases, implying that the blends become tougher with increasing mixing time.

These changes in the stress-strain properties of TPVs can result from two factors: 1) increase of the crosslink density of the rubber phase, and 2) reduction of the EPDM particle size.

The influence of rubber crosslink density is better manifested in cyclic stress-strain experiments. At fixed EPDM/PP/oil compositions, a more crosslinked EPDM phase should lead to lower residual plastic strain after unloading. The residual plastic strain as a function of strains for different TPV blends is shown in Figure 6.14. The curves are incidentally separated into three

groups based on the crosslink density differences of the EPDM phase. The unvulcanized blend shows the highest plastic deformation, as expected. The curves for 6 minutes and 7 minutes overlap. This implies similar crosslink densities of the two blends. The lowest plastic deformation is obtained after 7.5 minutes of mixing and this does not change anymore even after 12 minutes of mixing. This implies that under the present experimental conditions, the vulcanization reaction is essentially complete after 7.5 minutes i.e. already within 1 minute after adding the crosslinking agent.

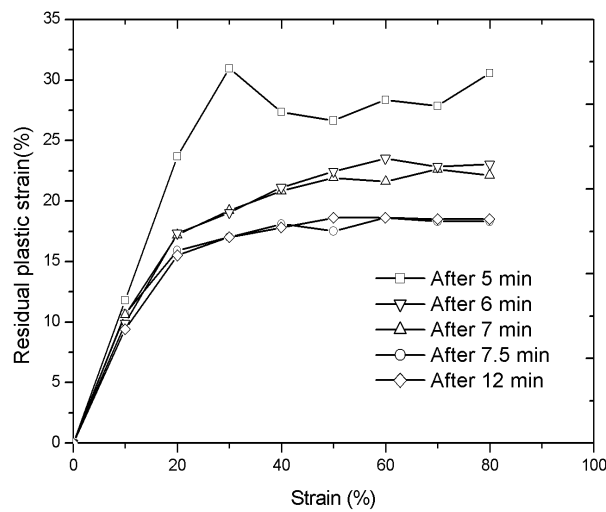


**Figure 6.14** Residual plastic strain of TPV blends for different mixing times in the internal mixer. The lines only serve as guide to the eye.

The effect of EPDM particle size on the stress-strain properties is seen in the toughness values of the TPV blends as shown in Table 6.5. Toughness here is defined as the area under the stress-strain curve. The area is proportional to the integral of the force ( $F$ ) over the distance ( $L$ ) the sample stretches before breaking.

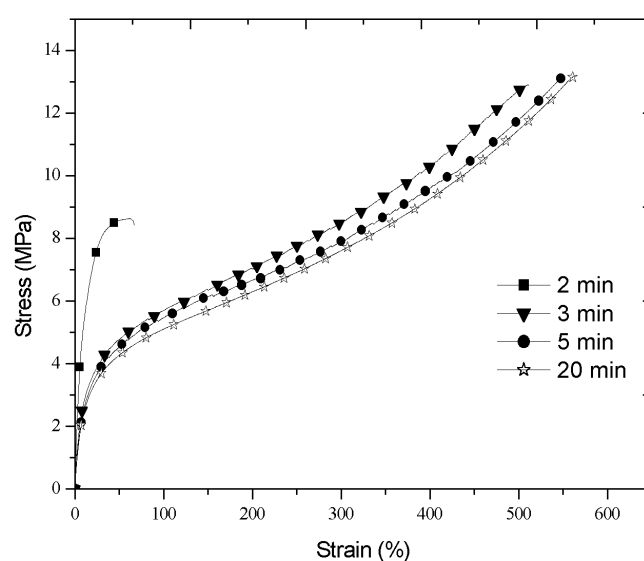
$$Area \sim \int F(L)dL \quad (6.6)$$

The integral is the work (energy) required to break the sample. Figure 6.14 shows that toughness increases with increasing mixing time. This is most likely an effect of the morphology. In literature, the increase in toughness in EPDM/PP blends has been related to smaller particle size.<sup>[27]</sup> Smaller particles result in better resistance to crack initiation and growth, as compared to larger particles.



**Table 6.5 E-modulus and toughness of TPV blends**

Mixing times (minutes)	5	6	7	7.5	12
E-mod (MPa)	12	14	14	17	18
Toughness (Nmm)	868	1967	2518	3745	4710

**Figure 6.15** Stress-strain curves of SEBS/PP/oil blends at different mixing times in the internal mixer.

The stress-strain curves for SEBS/PP/oil blends obtained for different mixing times are shown in Figure 6.15. The tensile strength and elongation at break of the blend obtained after 2 minutes mixing show low values, due to poor mixing. Although the blends show differences in the degree of continuity of the SEBS phase for longer mixing times, as seen before, the curves are quite similar. This result shows that the minor differences in the degree of continuity of the SEBS phase do not have a significant influence on the stress-strain properties.

The stress-strain properties of TPVs and SEBS/PP/oil blends prepared by varying the residence times in the twin-screw extruder are shown in Figure 6.16. The stress-strain curves overlap in both blends showing negligible effect of residence time on final properties.

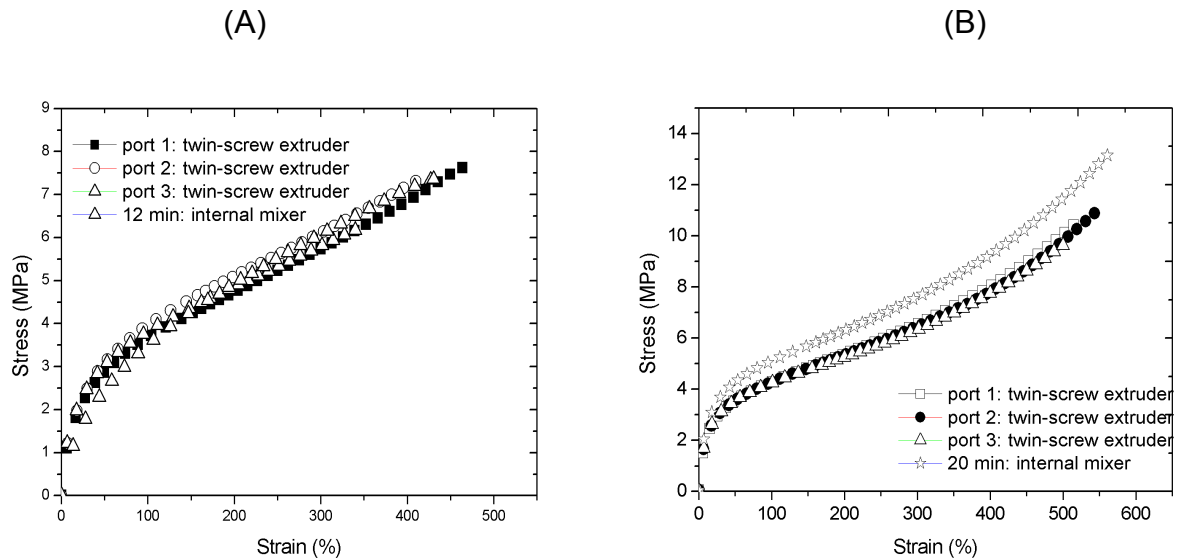


**Figure 6.16** Stress-strain properties of (A), TPV blends; (B), SEBS/PP/oil blends; made at different residence times in the twin-screw extruder.

A comparative plot of TPV and SEBS/PP/oil blends prepared in twin-screw extruder and internal mixer is also shown in Figure 6.16. While the curves for TPVs overlap, the SEBS/PP/oil blends prepared in the internal mixer show higher values of stress at comparable strains. Similar results were also reported in Chapter 4, although the twin-screw extruder used in those experiments as different from the one used here.

## 6.5 DISCUSSION

An overall comparison of the mechanism of morphology development between the TPV and SEBS/PP/oil blends shows an interesting difference. In TPV blends the morphology is fixed by the process of dynamic vulcanization, which occurs only seconds after adding the phenolic resin. Since crosslinked particles cannot coalesce, with increasing mixing time only particle breakdown can occur. The average particle sizes in TPVs prepared by both types of equipment are about 1-2  $\mu\text{m}$  and after long shearing there is a reduction in particle size, which is manifested as a gradual reduction in the surface area of the particles. On the contrary, the morphology of SEBS/PP/oil blends is not fixed after a few minutes of mixing, or at the first kneading block of the twin-screw extruder. In this blend it is the last flow environment that influences the final morphology. This has the effect of essentially wiping out the previous mixing history. This shows that, although a major reduction in phase size occurs during the melting process as shown in previous studies, it does not mean that this step controls the final particle size.

The coalescence of the SEBS phase resulting from prolonged mixing in the internal mixer can be explained from literature. Pukanszky *et al.*<sup>[28]</sup> studied the time dependence of the particle size during homogenization and the process resulting in equilibrium particle size in PP/EPDM unvulcanized blends. According to these authors, if the mixing time is short, large pieces of elastomer are dispersed in the melted or partially melted PP matrix-the dominating process is particle breakup. With increasing mixing time the average size of the particle decreases and equilibrium is reached between particle break-up and coalescence. The dynamic equilibrium can be shifted towards more coalescence by increasing the viscosity ratio, which is influenced by temperature and shear rate. A higher temperature resulting from longer mixing time – especially relevant for the internal mixer – can also result in thermo-mechanical degradation of PP, even though a stabilizer combination is used. This can be seen as a decrease in mixing torque as a function of time during blending in the internal mixer: Figure 6.3. The viscosity of the SEBS phase ( $\eta_{\text{SEBS}}$ ) is relatively less sensitive to temperature changes as compared to PP, because the physical crosslinks in the polystyrene blocks exists even at 250 °C.<sup>[20, 29]</sup> The polystyrene blocks, clustered in droplets, are dragged through the molten PP-phase. The persistence of the microphase structure at such high temperatures in SEBS is due to a big difference in the solubility parameters of the polystyrene end blocks and the ethylene-butylene end blocks.<sup>[29]</sup>

In a twin-screw extruder the viscosity ratio is influenced by local variation of both temperature and shear rate. This is demonstrated in Figure 6.17, which shows the variation of viscosity ratio  $\lambda$

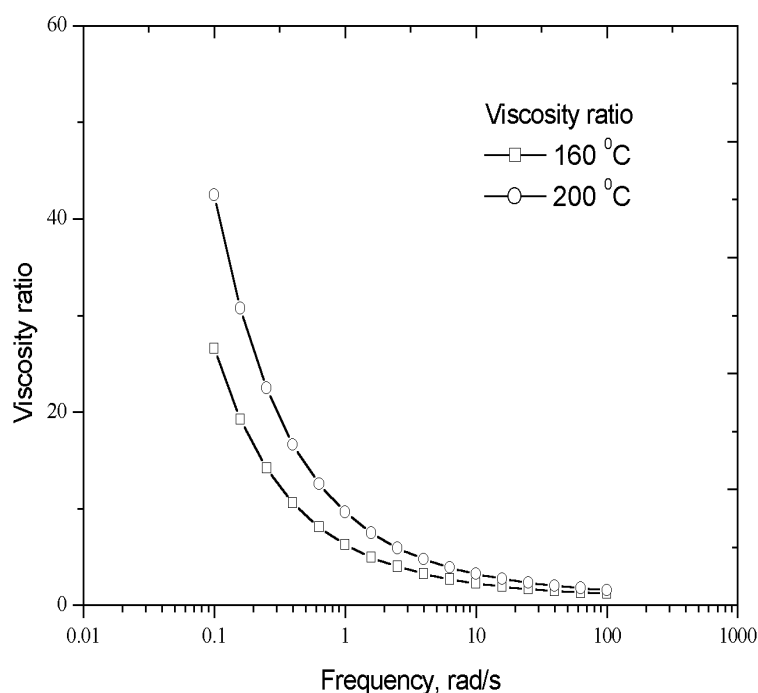


**Figure 6.17** Variation of viscosity ratio with frequency and temperature for a SEBS/PP/oil blend.

with frequency at two different temperatures: 160°C and 200°C.<sup>[30]</sup> The viscosity ratio increases with increasing temperature, but the increase is significantly higher at lower frequencies. Thus a change in frequency (or shear rate) has more effect than a change in temperature. With reference to equations (6.1) and (6.2), indicating that particle breakup is impossible in shear flow for  $\lambda > 3.8$ , vice versa coalescence is prevailing. The data in Figure 6.17 shows that the coalescence of the SEBS domains in the transporting blocks - where shear flow prevails at lower shear rates than in the kneading blocks, where also significant elongational flow is developed - is more likely to occur as a result of reduction of shear rates - corresponding with lower frequencies in Figure 6.16 - than due to changes in temperature; The lower the shear rate - lower frequency -, the higher  $\lambda$ , the more the blend will tend to coalescence.

The reason for increased tendency towards coalescence with reduction in viscosity ratio of the matrix is also explainable from the mechanism of coalescence between polymer droplets as discussed by Potente *et al.*<sup>[31]</sup> The external flow field in the mixing equipment causes collision of droplets. This collision causes a contact force to act on both drops for a specific amount of time. This flattens the drops and causes the film between the drops to drain away to finally form a critical thickness and rupture. After the film has ruptured a neck is formed between the two drops and then they unite. For coalescence to take place, the contact time of the colliding drops must be as long as film drainage time. Thin (low viscosity) films are easier to displace than highly viscous films. This implies that the time of contact, flow rate, residence time, local force fields are all crucial factors which determine the dynamic equilibrium between particle breakup and coalescence.<sup>[32]</sup>

As mentioned in Chapter 4, the stress-strain properties of these blends depend on the properties of individual phases, blend composition, oil distribution and morphology. As most of the factors except the morphology are fixed in the experiments reported in this chapter, the observed differences in stress-strain properties of the blends can be attributed to the differences in morphology. The stress-strain properties of blends with dispersed phase morphology as in TPVs, are very sensitive to changes in morphology: particle size distribution and crosslink density of the rubber phase. The stress-strain properties of blends with co-continuous morphology as in the case of SEBS/PP/oil are grossly comparable even though, depending on the blend preparation conditions, the degrees of co-continuity are significantly different. This shows that, provided other factors such as SEBS/PP ratio, crystallinity of PP, grades of base polymers and oil distribution are constant, the stress-strain properties are not noticeably dependent on the degree of co-continuity of the SEBS phase.

## 6.6 CONCLUSIONS

The morphology development of TPVs both in an internal mixer and in a twin-screw mixing extruder occurs within seconds after adding the curing resin. This very fast morphological change involves a phase inversion from a co-continuous morphology to dispersed phase morphology. The crosslinking reaction however is slower, and is essentially complete after a few minutes of mixing. This implies that the crosslinking reaction occurs within separate EPDM particles. There is no difference in the particle size of the EPDM-phase in TPV blends made in the internal mixer and twin-screw extruder. By changing the shear rate or shear strain it is possible to vary the particle size distribution of the EPDM phase. This effect is independent of the mixer type. The crosslink density of the EPDM phase influences the stress-strain properties of the TPVs, especially at strains larger than 100 %. The elastic recovery of the blends is significantly influenced by the crosslink density of the EPDM phase even though the particles are separated by a thermoplastic matrix phase.

The morphology development in SEBS/PP/oil blends during compounding in the internal mixer and the twin-screw extruder can be described as follows. When the PP and SEBS are fed together to the hot mixer (twin-screw extruder or internal mixer), the initial morphology must be a mixture of rubber dispersed in molten PP. This morphology subsequently changes very fast to co-continuous morphology with increased mixing. During this process the rubber is softened, stretched and broken down into droplets. The whole process occurs extremely fast. In our experiments we could not detect the initial morphology due to the experimental limitations on the speed of detection.

The co-continuous morphology of the SEBS/PP/oil blends undergoes further changes due to changes in temperature and screw element configurations in the twin-screw extruder. As the temperature rises with increasing mixing time, the viscosity of the PP phase drops and if at that instance the melt is in transporting blocks of the twin-screw extruder (lower shear rate) or in the internal mixer, the SEBS domains start to coalesce. If, on the other hand, the melt is in the kneading blocks, the shear and elongational forces are high enough to cause breakdown of the SEBS domains. This implies that with proper control of temperature and screw configurations the morphology can be "tailor-made". The stress-strain properties are however not influenced by these variations in the degree of co-continuity of the SEBS/PP/oil blends.

## 6.7 REFERENCES

1. H. Van Oene, in *"Polymer Blends"*, Eds, S. Newman, D. R. Paul, Academic Press, New York (1978) 295.
2. C. D. Han, T. C. Yu, *Polym. Eng. Sci.*, **12** (1972) 81.
3. C. D. Han, Y. W. Kim, *Trans. Soc. Rheol.*, **19** (1975) 245.
4. C. J. Nelson, G. N. Avgeropoulos, F. C. Weisser, G. G. A. Bohm, *Angew. Makromol. Chem.*, **60/61** (1977) 49.
5. T. Pharm, H. J. Radusch, *Kautsch. Gummi Kunstst.*, **49** (1996) 249.
6. M. van Duin, A. V. Machado and J. Covas., *Macromol. Symposia*, **170** (2001) 29.
7. J. M. H. Janssen, H. E. H. Meijer, *"Mixing and Compounding-Theory and Practice"*, in *"Progress in Polymer Processing Series"*, Ed. L.A. Utracki, Hanser Publications, Munich (1994).
8. G. I. Taylor, *Proc. Roy. Soc.*, **A 146** (1934) 501.
9. M. A. Huneault, M. F. Champagne, A. Luciani, *Polym. Eng. Sci.*, **36/12** (1996) 1649.
10. H. P. Grace, *Chem. Eng. Commun.*, **14** (1982) 225.
11. B. J. Bentley, L. G. Leal, *J. Fluid Mech.*, **167** (1986) 241.
12. L. A. Utracki, Z. H. Shi, *Polym. Eng. Sci.*, **32** (1992) 1824.
13. R. W. Flumerfelt, *Ind. Eng. Chem. Fundam.*, **11** (1972) 312.
14. S. Wu, *Polym. Eng. Sci.*, **27** (1987) 335.
15. C. M. Ronald, G. C. Bohm, *J. Polym. Sci., Polym. Phys.*, **22** (1984) 79.
16. H. Wang, A. Z. Zinchenko, R. H. Davis, *J. Fluid Mech.*, **265** (1994) 161.
17. J. M. H. Janssen, Ph.D thesis, Eindhoven University of Technology, The Netherlands (1993).
18. F. Goharpey, A.A.Katbab, H. Nazockdast, *J. Appl. Polym. Sci.*, **81** (2001) 2531.
19. H. Verhoogt, Ph.D thesis, Technical University Delft, The Netherlands (1992).
20. H. Veenstra, Ph.D thesis, Technical University Delft, The Netherlands (1999).
21. R. C. Willemse, Ph.D thesis, Technical University Delft, The Netherlands (1998).
22. C. E. Scott, C. W. Macosko, *Polymer*, **36** (1995) 461.
23. U. Sundararaj, Y. Dori, C. W. Macosko, *Polymer*, **36(10)** (1995) 1957.
24. U. Sundraraj, C. W. Macosko, R. J. Ronaldo, H. T. Chan, *Polym. Eng. Sci.*, **32** (1992) 1814.
25. P. Sengupta, J. W. M. Noordermeer, Paper presented at 163rd meeting of the ACS, Rubber Division (2003) San Francisco, CA.
26. A. Y. Coran, O. Chug, P. Laokijcharoen, *Kautsch. Gummi Kunstst.*, **51(5)** (1998) 342.
27. A. Y. Coran, R. P. Patel, *Rubber Chem. Technol.*, **53** (1980) 141.
28. B. Pukanszky, I. Fortelny, J. Kovar, F. Tudos, *Rubber Comp. Process. Appl.*, **15** (1991) 31.
29. R. M. Patel, S. F. Hahn, C. Esneault, S. Bensason, *Advanced Materials*, **12(23)** (2000) 1813.
30. W. Sengers, Ph.D thesis, Technical University Delft, The Netherlands; to be published.
31. H. Potente, M. Bastian, *Polym. Eng. Sci.*, **40(3)** (2000) 727.
32. C. E. Scott, N. B. D. Lazo, *Polymer*, **40** (1999) 5469.

---

## **Chapter 7**

### ***The effect of different compositions and processing conditions on the morphology and properties of TPVs and SEBS/PP/oil blends***

---

*This chapter reports studies on the influence of different compositions and processing conditions on the morphology and mechanical properties of TPVs and SEBS/PP/oil blends. Attempts were made to alter the morphology of the blends using the principles learnt from previous chapters. For both blend types controlled changes in melt flow index of PP and rotor speed of the internal mixer were made to vary the viscosity-ratio of the PP- to the rubber-phase and the shear rate, respectively. Statistical designs of experiments were used to determine the separate effects of each factor, including the amount of EPDM, PP and oil. For TPVs, the amount of curatives and the process of EPDM-oil preblend preparation were also varied. For TPVs prepared in the internal mixer, particle size of EPDM is influenced by the melt flow index of PP and the curative resin content. If the total shear is kept constant, the shear rate of the internal mixer has little influence on the EPDM particle size. For SEBS/PP/oil blends, although the domain size of the SEBS phase shows differences, the morphology remains co-continuous irrespective of the changes in melt flow index of the PP, the rotor speed or mixing temperature. The results demonstrate the potential of different routes to vary the morphology and its consequences for the properties of these blends.*

## 7.1 INTRODUCTION

The properties of polymer blends are to a large extent dependent on morphology, i.e., the size, shape and distribution of the phases. Factors that govern the morphology are blend composition, level of compatibility between the phases, processing conditions and rheological characteristics of the components.<sup>[1]</sup>

It has been shown in the previous chapters that the properties of TPVs and SEBS/PP/oil blends can be altered by making variations in blend composition, method of production and oil distribution. In this chapter four other factors are studied, which could have an influence on the morphology and properties. These factors are discussed below:

1) *Amount of phenolic resin (for TPVs);*

The dispersed EPDM phase in TPVs is responsible for the elastic properties of the blends. The purpose of changing the amount of phenolic resin is to alter the crosslink density of the EPDM phase and study its influence on the tensile and elastic properties. Another consequence of varying the amount of phenolic resin would be, to alter the viscosity ratio between EPDM and PP. This should have an influence on the morphology of TPVs. In fact, atomic force microscopy studies by Ellul *et al.*<sup>[2]</sup> have shown that the EPDM particle size distribution is narrowed by increasing the crosslink density of the EPDM phase.

2) *Melt flow index of PP;*

The Melt Flow Index (MFI) of PP is an important criterion that determines the processability. Blends with a low MFI are associated with high molecular weight, while a high MFI indicates a low average molecular weight. A high flow material is favourable for processing, especially for injection molding, because it facilitates the filling of intricate mold parts.

The influence of varying the MFI of PP on the morphology of these blends is not clear. According to Jayraman *et al.*<sup>[3]</sup> the aspect ratio of the EPDM particles in TPVs is altered due to changes in MFI of the PP. A consequence of varying the MFI of PP during melt blending with EPDM or SEBS is to alter the viscosity ratio between the PP and the rubber phase. This should influence the morphology and properties of both blend types.



### 3) *Different shear rates of mixing;*

The rotor speed of the internal mixer corresponds to the shear rate which the polymer melt experiences during blending. This can be calculated approximately by using equation (7.1):<sup>[4]</sup>

$$\dot{\gamma} = \frac{\pi DS}{\delta} \quad (7.1)$$

where  $\dot{\gamma}$  is the shear rate, D is the diameter of the rotor, S is the rotor speed in rpm and  $\delta$  is the gap between the rotor tip and mixing chamber. From the dimensions of our internal mixer the shear rate at a rotor speed of 80 rpm was calculated to be  $140\text{s}^{-1}$ . The influence of shear rate during mixing on the morphology of polymer blends has been reported by several authors.<sup>[5-8]</sup> On the basis of these works it is expected that an increase of shear rate will have an effect on the dispersion of the phases which, in turn, should also influence on the properties.

### 4) *Effect of oil preblending methods (for TPVs);*

TPVs and SEBS/PP/oil blends are increasingly used as materials for soft-touch applications. Such compositions usually contain a low level of PP. In order to prepare these compositions, especially in an internal mixer, it is necessary to make a preblend of oil with rubber as otherwise the oil is not incorporated completely. Preblending of oil with EPDM in amounts over 100 phr is not problematic, when preparing TPVs in a co-rotating twin-screw extruder. But in compositions made in the internal mixer such large amounts of oil cause mixing problems. There are different ways to prepare the preblends: e.g. in solution, on a two-roll mill or in an internal mixer. Each of these methods has an influence on the viscosity of the EPDM phase that might later on influence the properties and possibly the morphology of TPVs. This part of the study was only restricted to TPVs because the oil could be easily absorbed by SEBS and preblending with oil levels as high as 180 phr was comparatively easy.<sup>[9]</sup>

### 5) *Temperature of mixing (for SEBS/PP/oil blends);*

According to investigations by Veenstra the range of co-continuity of SEBS/PP/oil blends is dependent on the mixing temperature. His experiments showed that mixing at a temperature above the order-disorder temperature (ODT) of SEBS and subsequent

compression molding at a temperature above ODT results in a decrease of the continuity of the SEBS phase. The ODT is defined as the temperature above which polystyrene and ethylene-butylene phases exists as a one-phase system. The ODT is dependent on the volume fraction of the polystyrene content in SEBS and on the extent of phase separation between the polystyrene and ethylene-butylene blocks. Since the grades of SEBS used in these investigation were different from the one used in the present study, it was intriguing to know whether the mixing temperature would have an influence on the morphology of the SEBS/PP/oil blends. Therefore, the mixing temperature of the SEBS/PP/oil blends was also varied and its influence on the morphology and properties investigated.

Statistical design of experiments was used for the set up of some experiments. This was done in order to evaluate the separate effects of each factor on the blend properties. In the design two levels of each factor were varied.

## 7.2 EXPERIMENTAL

### 7.2.1 Materials

The grades of EPDM, SEBS, oil and stabilizers are the same as described in Chapter 3 of this thesis. Two different grades of PPs were used in this work: Stamylen P11E10 and three Vestolen<sup>®</sup> grades. All grades are available from Sabic Euro Petrochemicals B.V. The characteristics of the Stamylen P11E10 grades have been described before. The characteristics of the Vestolen grades are shown in Table 7.1.

**Table 7.1 Characteristics of the PP's used<sup>[10]</sup>**

Vestolen Grade	MFI [dg/min]	Mn [g/mol]	Mw [g/mol]	Mw/Mn	Crystallinity (%)	E-modulus [MPa]
P9000	0.3	77800	657000	8.4	45	1095
P8000	1.1	82000	427000	5.2	45	903
P6000	5.5	63300	316000	6.0	45	925

## **7.2.2 Blend compositions**

### **7.2.2.1 TPV blends.-**

The blend compositions used for preparation of the TPV blends are summarized in Table 7.2. For ease of description, the compositions are coded in four groups. Experiments with compositions AE1-AE5 were designed to study the influence of phenolic resin curative concentration; BE1-BE9 were designed to study the influence of MFI of the PP and CE1-CE7 were designed to study the influence of shear rate during mixing. Note that some compositions/mixing conditions occur more than once: e.g. AE3 and CE5. The composition DE1 was used to study the influence of oil-preblending methods. All the compositions of TPVs are stabilized with Irganox 1076 and Irgafos 168.

### **7.2.2.2 SEBS/PP/oil blends.-**

The blend compositions used for the preparation of the SEBS/PP/oil blends are summarized in Table 7.3. For ease of description, the compositions are coded in three groups. Experiments with compositions AS1-AS3 were designed to study the influence of temperature of mixing; BS1-BS9 were designed to study the influence of MFI of the PP and CS1-CS4 were designed to study the influence of shear rate during mixing. Note that some of the compositions occur twice to check the reproducibility.

**Table 7.2 Blend compositions used for preparation of TPV blends**

code	PP-type	PP content (Phr)	Oil content (Phr)	Phenolic resin content (Phr)	RPM
AE1	Stamylan P 11E10	40	140	0	80
AE2	Stamylan P 11E10	40	140	2	80
AE3	Stamylan P 11E10	40	140	5	80
AE4	Stamylan P 11E10	40	140	8	80
AE5	Stamylan P 11E10	40	140	10	80
BE1	Vestolen P 6000	40	100	5	80
BE2	Vestolen P 6000	40	180	5	80
BE3	Vestolen P 6000	120	100	5	80
BE4	Vestolen P 6000	120	180	5	80
BE5	Vestolen P 8000	80	140	5	80
BE6	Vestolen P 9000	40	100	5	80
BE7	Vestolen P 9000	40	180	5	80
BE8	Vestolen P 9000	120	100	5	80
BE9	Vestolen P 9000	120	180	5	80
CE1	Stamylan P 11E10	40	100	5	80
CE2	Stamylan P 11E10	40	100	10	80
CE3	Stamylan P 11E10	120	100	5	80
CE4	Stamylan P 11E10	120	100	10	80
CE5	Stamylan P 11E10	40	100	5	40
CE6	Stamylan P 11E10	40	100	10	40
CE7	Stamylan P 11E10	120	100	5	40
CE8	Stamylan P 11E10	120	140	10	40
DE1	Stamylan P 11E10	120	140	5	80

**Table 7.3 Blend compositions used for preparation of SEBS/PP/oil blends**

code	PP-type	PP content (Phr)	Oil content (Phr)	Mixing temp. (°C)	RPM
AS1	Stamylan P11E10	80	140	180	80
AS2	Stamylan P11E10	80	140	200	80
AS3	Stamylan P11E10	80	140	220	80
BS1	Vestolen P 6000	40	100	180	80
BS2	Vestolen P 6000	40	180	180	80
BS3	Vestolen P 6000	120	100	180	80
BS4	Vestolen P 6000	120	180	180	80
BS5	Vestolen P 8000	80	140	180	80
BS6	Vestolen P 9000	40	100	180	80
BS7	Vestolen P 9000	40	180	180	80
BS8	Vestolen P 9000	120	100	180	80
BS9	Vestolen P 9000	120	180	180	80
CS1	Stamylan P 11E10	80	140	180	40
CS2	Stamylan P 11E10	80	140	180	80
CS3	Stamylan P 11E10	80	140	180	120
CS4	Stamylan P 11E10	80	140	180	150

### 7.2.3 Evaluation method for two-factorial design

The influence of MFI of the PP on the properties of TPVs and SEBS/PP/oil blends: series B, was analyzed with the help of two-factorial design of experiments. A similar design was used to analyze the combined effect of PP-content, resin-content and rotor speed of the internal mixer for TPVs: series CE. In these factorial designs there are three factors and each factor was varied at two levels.

To determine the effect of the factors on the properties, the impact of all the variables (primary factors) or combinations of variables (secondary factors) is displayed in a Pareto chart.<sup>[11]</sup> To construct such a chart, the effects of each factor have to be calculated. All factors have a minimum (-) and maximum (+) value. The compositions table for investigating the effects of MFI, PP-content and oil-content can thus be described as follows: Table 7.4.

**Table 7.4 Compositions of TPV and SEBS/PP/oil blends**

Code	PP content	Oil content	MFI	PP*MFI	MFI*Oil	Oil*PP
BX1 <sup>*)</sup>	-	-	+	-	-	+
BX2	-	+	+	-	+	-
BX3	+	-	+	+	-	-
BX4	+	+	+	+	+	+
BX6	-	-	-	+	+	+
BX7	-	+	-	+	-	-
BX8	+	-	-	-	+	-
BX9	+	+	-	-	-	+

<sup>\*)</sup> "X" stands for E for TPV blends and S for SEBS/PP/oil blends

The effect of such a design is calculated by using the formula:

$$\text{Absolute effect} = \frac{\text{Sum of all (+) responses}}{\text{No. of (+) signs}} - \frac{\text{Sum of all (-) responses}}{\text{No. of (-) signs}} \quad (7.2a)$$

This method assumes a linear relationship between the maximum and minimum values of primary factors. The results are evaluated with the help of linear regression analysis. In this approach the final property, so called the response of the design, is evaluated with the help of a multi-variable equation. As an example, such an equation for hardness would look like this:

$$\begin{aligned} \text{Hardness} = & C_0 + C_1 * PP + C_2 * \text{Resin} + C_3 * RPM + C_4 * PP * RPM + C_5 * RPM * \text{Resin} + \\ & C_6 * \text{Resin} * RPM \end{aligned} \quad (7.2b)$$

$C_0, C_1, \dots, C_6$  are the coefficients of the variables, which evaluate the respective influences of each factor on the end property. Similar equations can be obtained for other properties like the E-modulus, tensile strength or elongation at break.

A chart for evaluating the effect of PP composition, resin content and rotor speed on the morphologies and properties of TPVs is shown in Table 7.5.

**Table 7.5 Compositions of TPV blends**

Code	PP content	Resin content	RPM	PP*RPM	RPM*Resin	Resin*PP
CE1	-	-	+	-	-	+
CE2	-	+	+	-	+	-
CE3	+	-	+	+	-	-
CE4	+	+	+	+	+	+
CE5	-	-	-	+	+	+
CE6	-	+	-	+	-	-
CE7	+	-	-	-	+	-
CE8	+	+	-	-	-	+

#### 7.2.4 Sample preparations and testing

The TPV and SEBS/PP/oil compositions were prepared in a Brabender Plasticorder type 350S according to procedures described in Chapter 4.

To study the effect of oil preblending methods on the properties of TPVs the composition DE1 was used. Three different preblending techniques were used to add the extra oil: on a mill, in the internal mixer and in solution. A fourth blend was made without preblending, i.e. directly adding the oil into the internal mixer along with other ingredients. The Mooney viscosities of the EPDM-oil preblends: ML (1+4) at 125°C, were measured by a 2000E Mooney viscometer from Alpha technologies.

After mixing, the materials were compression molded at 200°C for 3 min. under a pressure of 10 MPa and then cooled under pressure to about 30°C. The moulded sheet thickness was about 2 mm. Dumbbells were punched out of the sheets for tensile measurements.

Tensile stress-strain experiments were measured at room temperature according to ISO 37, using a Zwick Z020 universal testing machine equipped with a 500 N load cell. Tension set experiments was conducted on TPV samples prepared with different amounts of resin content. In these experiments the samples were stretched to a cyclic strain of 100% and the amount of irrecoverable strain was measured.

The hardness of the compounds was measured with a Zwick hardness meter (Shore A type, ISO R868).

Morphology was studied using a Philips CM30 transmission electron microscope (TEM). Low voltage scanning electron microscopic studies (LVSEM) were conducted using a Leo 1550 scanning electron microscope. The sample preparations are described in Chapter 3.

The gel-content of the samples was determined using the boiling xylene method described in Chapter 4.

## **7.3 RESULTS**

### **7.3.1 Effect of phenolic resin content on TPVs**

The influences of phenolic resin on the properties of TPVs are shown in Figure 7.1. It is clear from this figure that a higher degree of cure of the EPDM phase results in a higher E-modulus, hardness and tensile strength. Also, as seen in the tension set results, the elastic recovery is improved. The elongation at break decreases.



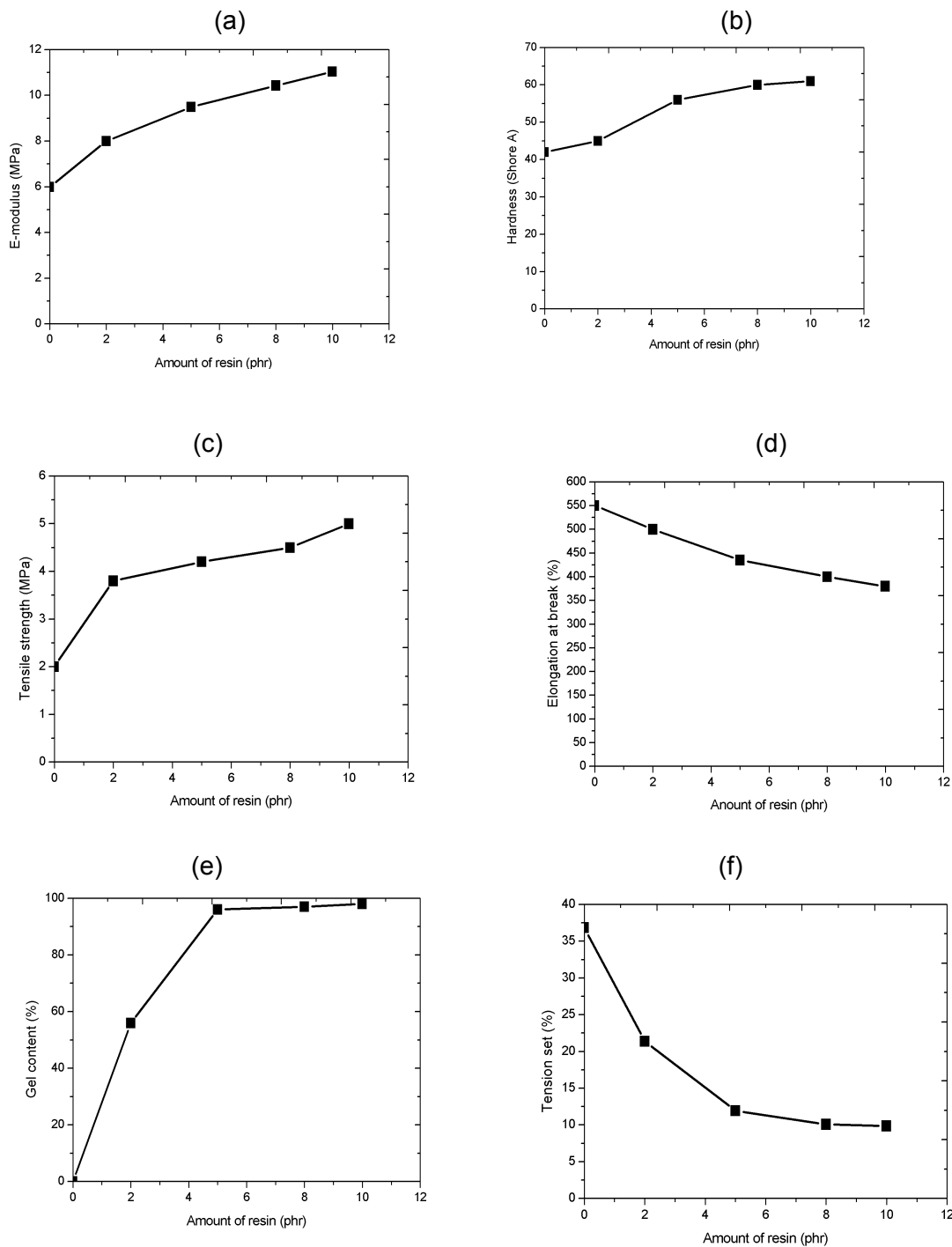


**Figure 7.1** Influence of phenolic resin content on different properties of TPVs. The EPDM/PP/oil composition is given by AE1-AE5 in Table 7.2.

The morphologies of the TPV blends having different amounts of phenolic resin are shown in Figure 7.2:

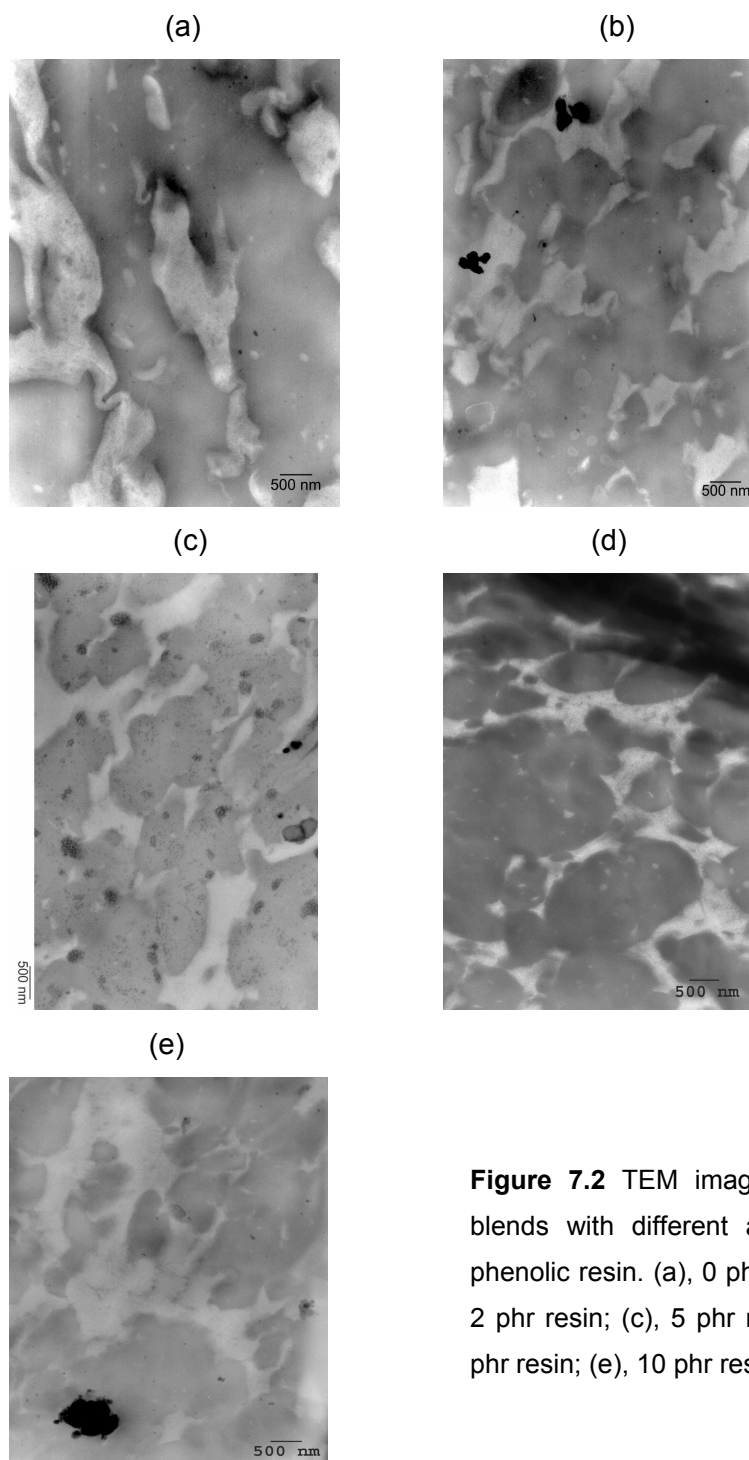


**Figure 7.2** TEM images of TPV blends with different amounts of phenolic resin. (a), 0 phr resin; (b), 2 phr resin; (c), 5 phr resin; (d), 8 phr resin; (e), 10 phr resin.

As a consequence of preferential staining of the EPDM phase by  $\text{RuO}_4$ , the dark phase can be assigned to the EPDM phase and the white to PP. The oil in either phase is not

visible. The EPDM/PP/oil blend without any phenolic resin shows two co-continuous phases. This is expected if the viscosity ratio of the EPDM and PP is close to unity.<sup>[3]</sup> The co-continuity of the rubber phase explains the high value of the elongation at break of this blend as compared to the cured TPVs. Adding 2 phr of phenolic resin to the composition results in partially cured TPVs. This TPV shows properties intermediate between those of the unvulcanized EPDM/PP/oil blend and fully cured TPV: Figure 7.1. The TEM image of this blend, as shown in Figure 7.2b, shows that the EPDM phase is still partially continuous. Partial co-continuity of the EPDM phase is also still observed in the TEM image of Figure 7.2c, which corresponds to a composition containing 5 phr phenolic resin. The gel content value at this composition shows that the EPDM phase is already completely cured.<sup>[12]</sup> The partial co-continuity as suggested by the TEM images 7.2b and c is doubtful, because at a high loading of rubber phase the TEM images can be misleading. This has been explained in detail in Chapter 3. The TEM images of the blends having 8 phr and 10 phr resin show a wide distribution of particle sizes. Most EPDM particles are between 1-4  $\mu\text{m}$  and there are particles even less than 1  $\mu\text{m}$ . An accurate estimation of the particle size distribution was not possible due to lack of clear boundaries between the particles. With increasing amount of phenolic resin, the particle shape tends to be more spherical and well defined. Attempts were made to see this distribution with LVSEM. These failed because the particles of EPDM seem to be interconnected to one another: Figure 7.3.

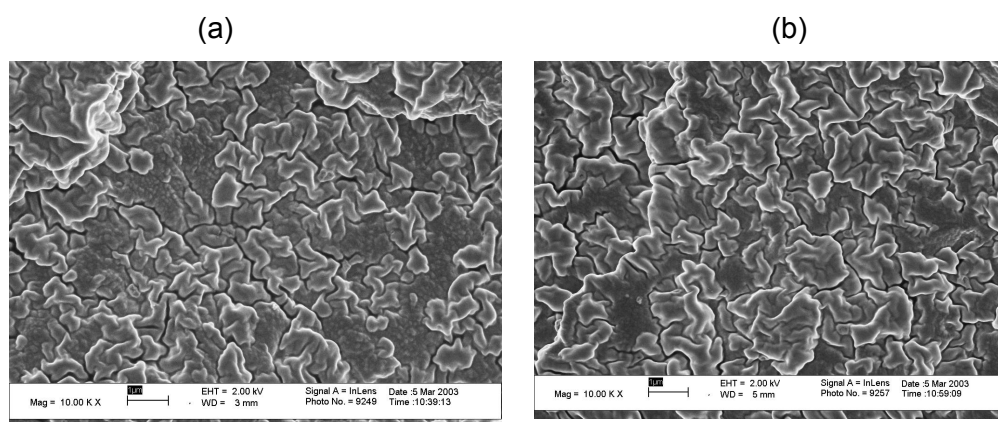


**Figure 7.3** LVSEM image of TPV blends prepared with: (a), 5 phr of resin; (b), 10 phr of resin.

### 7.3.2 Effect of MFI of PP and blend composition on the properties and morphology of TPVs and SEBS/PP/oil blends

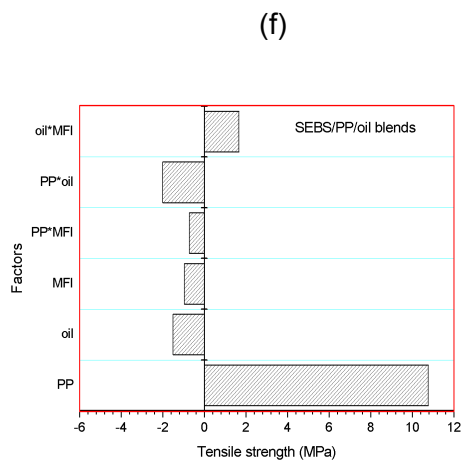
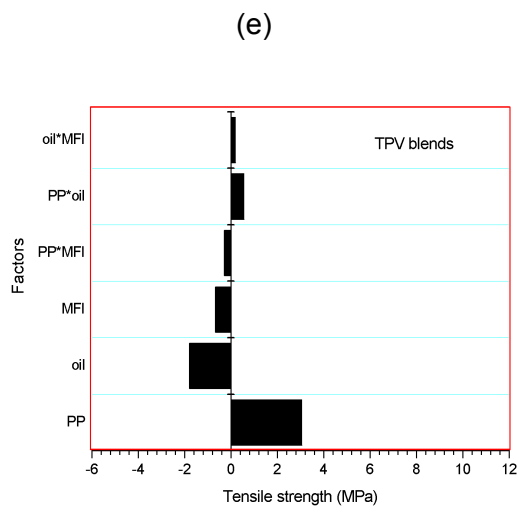
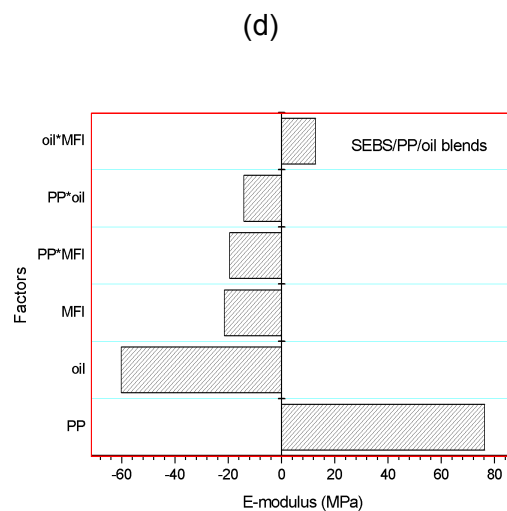
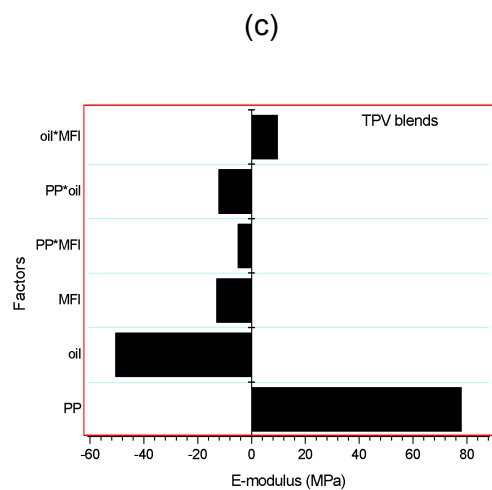
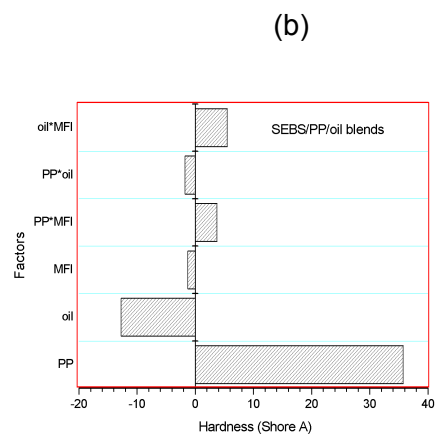
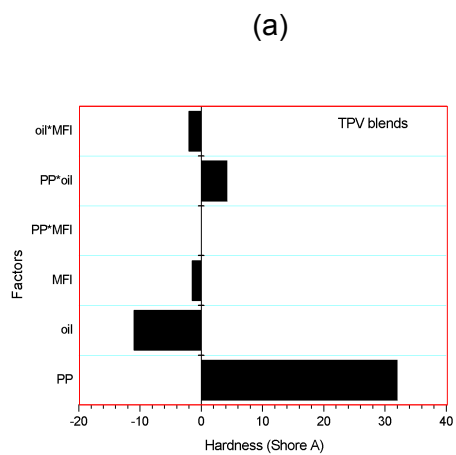
Table 7.6 summarizes the effect of increasing the MFI of PP on the properties of both blends. The Pareto diagrams of the coefficients calculated from these results according to eq. 7.2b, are given in Figure 7.4 for both blend systems.

**Table 7.6a Influence of MFI of PP, PP- and oil-content on the properties of TPV blends.**

Code	Hardness (Shore A)	E-moduli (MPa)	Tensile strength (MPa)	Elongation at break (%)
BE1	61	7.77	3.9	290
BE2	45	4.4	1.7	270
BE3	90	69	6.6	350
BE4	60	18	5.6	310
BE6	75	25.7	3.7	300
BE7	49	5.9	2.7	250
BE8	90	88	8.6	500
BE9	83	40	5.6	300

**Table 7.6b Influence of MFI of PP, PP- and oil-content on the properties of SEBS/PP/oil blends.**

Code	Hardness (Shore A)	E-moduli (MPa)	Tensile strength (MPa)	Elongation at break (%)
BS1	59	15.3	7.7	302
BS2	40	3.4	1.8	580
BS3	94	61	15.4	315
BS4	84	23.5	5.7	302
BS6	69	17.5	6.0	500
BS7	48	5.8	4.0	650
BS8	91	89	15.0	510
BS9	82	39.5	18.0	520



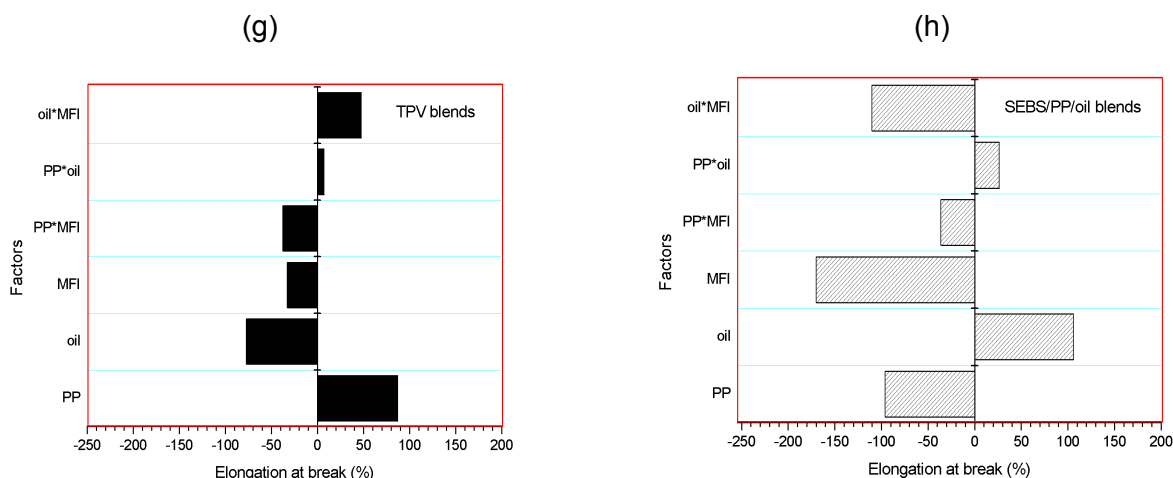


**Figure 7.4** Tensile properties of TPV and SEBS/PP/oil blends as influenced by PP-content, oil-content and MFI of the PP.

The diagrams show the influence of the various parameters and their interactions on the tensile properties of both blend systems. Hardness and E-moduli are directly correlated, as common: Figure 7.4(a) and (c), resp. 7.4(b) and (d). Both increase with increasing PP-content and decrease with increasing oil-content. The values of the corresponding factors indicate that blend composition plays an important role at low strains. MFI has a negative effect on these properties, i.e. an increase in MFI of the PP, from its low value (0.3 g/10 min) to a high value (5.5 g/10 min) resulted in a decrease of hardness and E-moduli: Figure 7.4(c) and 7.4(d). Increasing the MFI of PP also has a negative effect on the tensile strength of TPVs and SEBS/PP/oil blends: Figure 7.4(e) and 7.4(f). The largest effect is on the elongation at break. In both cases, increasing the MFI results in a significant decrease in the elongation at break values: Figure 7.4 (g) and (h).

The reason for the better properties of the blends prepared with PP having a MFI of 0.3 g/10 min, as compared to blends prepared with PP having a MFI of 5.5 g/10 min, can be explained from their morphology. The morphologies of representative TPV compositions prepared using different PP's are shown in Figure 7.5.

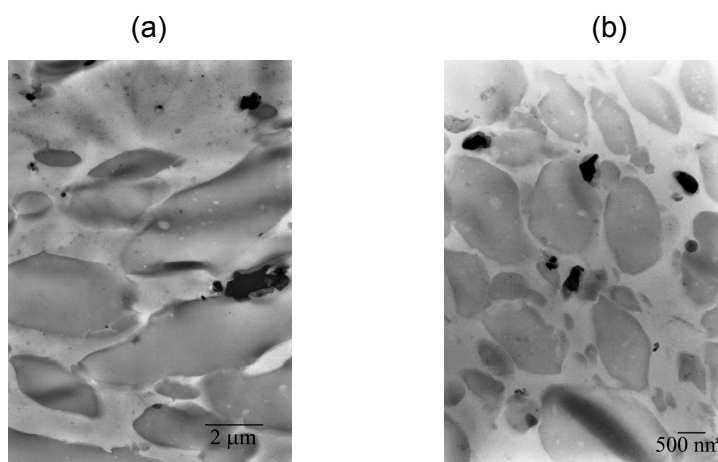


**Figure 7.5** TEM images of TPV blends having compositions: (a), BE3; (b), BE8.

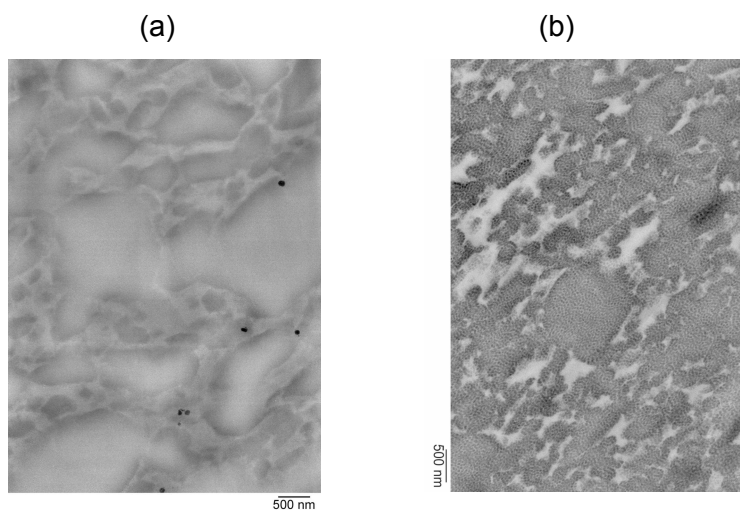


**Figure 7.6** TEM images of SEBS/PP/oil blends having compositions: (a), BS2; (b), BS7.

The EPDM particles size distribution appears coarser in the TPV blend prepared with a PP having a MFI value of 5.5 g/10 min, as compared to the TPV blend prepared with PP having a MFI value of 0.3 g/10 min. Particles as large as 6–7 μm are seen in Figure 7.5(a), whereas the maximum particle size in Figure 7.5(b) is about 3 μm.

Similar results are seen in the TEM images of SEBS/PP/oil blends as shown in Figure 7.6. Although the SEBS-phase is found to be continuous with the PP phase in both cases, the average domain size distribution is very wide in case of composition BS2 as compared to composition BS7.

These effects of composition on the properties are in accord with the results described in Chapter 4, where the properties of these blends were reported as a function of composition and blend preparation method, although prepared with a different grade of PP. Although the influence of the three factors on the Hardness and E-modulus are similar for both blend types, some features in the tensile strength and elongation at break values are strikingly different. A comparison of Figure 7.4(e)–(h) shows, that increasing the amount of oil from its low value of 100 phr to a high value of 180 phr leads to a larger reduction in the tensile strength of SEBS/PP/oil blends as compared to the TPVs. The elongation at break decreases in case of TPVs, but increases in case of the SEBS/PP/oil blends with increasing oil-content. Increasing the amount of PP from its low value of 40 phr to a high value of 120 phr increases the tensile strength and elongation at break for TPVs, whereas in case of SEBS/PP/oil blends the elongation at break is significantly decreased, although the tensile strength increases. These differences are probably due to the presence of a continuous rubber phase in SEBS/PP/oil blends, which participates equally with PP in the deformation process.

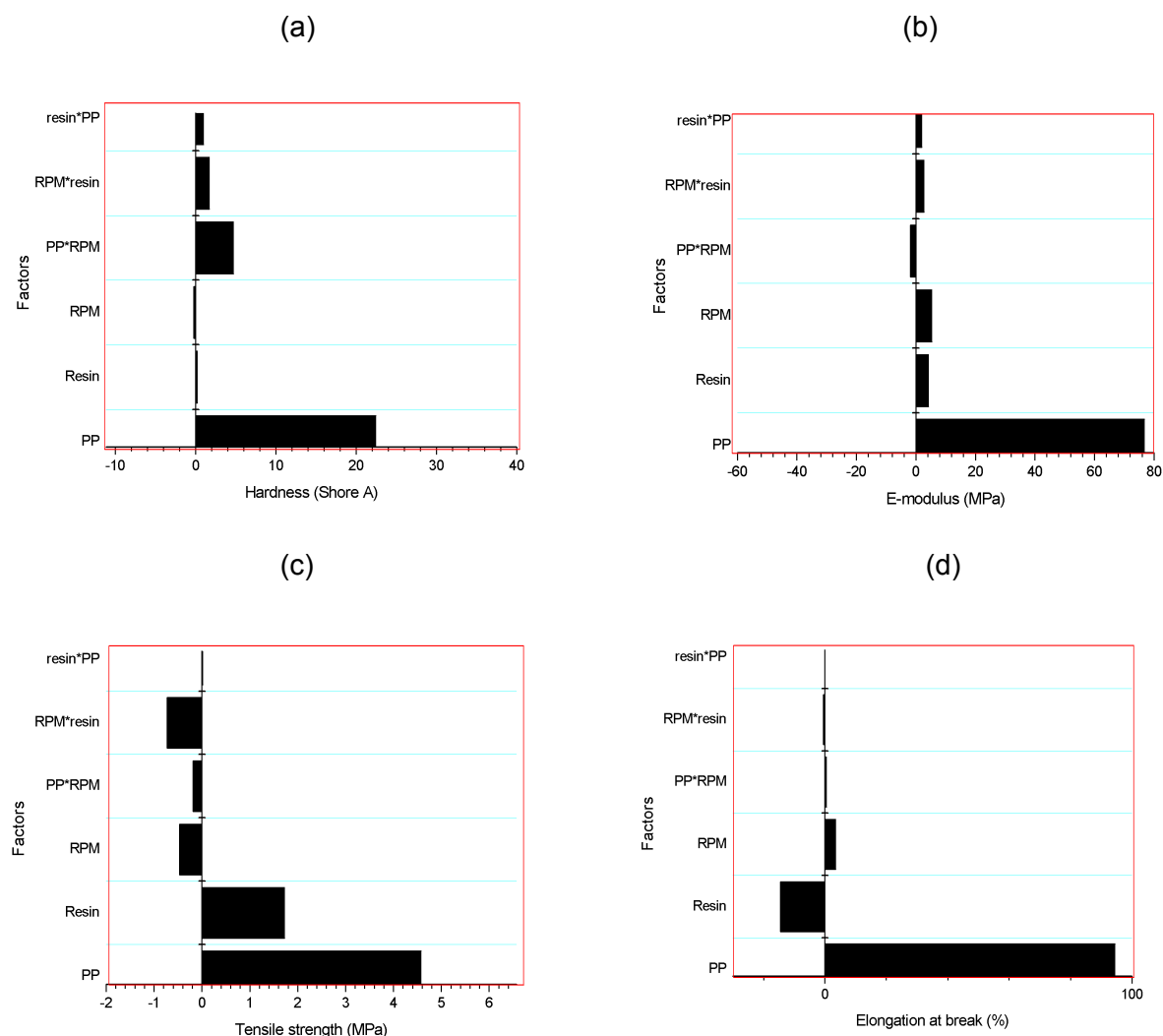
### 7.3.3 Effect of PP-content, resin-content and rotor speed of mixing on properties and morphology of TPVs

Table 7.7 summarizes the effect of PP-content, resin-content and rotor speed of the internal mixer on the properties of TPVs. The Pareto diagrams of the coefficients calculated from these tables are given in Figure 7.7.

**Table 7.7 Influence of MFI of PP, PP and oil content on the properties of TPV blends.**

Code	Hardness (Shore A)	E-modulus (MPa)	Tensile strength (MPa)	Elongation at break (%)
C1	60	18	4.7	300
C2	62	20	5.2	290
C3	87	88	8.6	400
C4	89	100	10.1	380
C5	68	10.9	4.7	297
C6	64	14.7	5.6	287
C7	83	90	8.0	395
C8	84	91	12.0	377





**Figure 7.7** Tensile properties of TPV blends as influenced by PP, amount of resin and RPM of the internal mixer.

The diagrams show the influences of the various parameters and their interactions on tensile properties. As seen before, all the properties increase with increasing PP-content. Increasing the amount of phenolic resin from 5 phr to 10 phr has a negligible effect on the hardness and E-modulus. However, it has a positive effect on the tensile strength and a negative effect on the elongation at break values. On the other hand increasing the rotor speed of the internal mixer from 40 RPM to 80 RPM, while keeping the total strain the same, has no effect whatsoever on the mechanical properties.

TEM images of the TPV blends prepared at different RPM of the internal mixer are shown in Figure 7.8. The dark phase is EPDM and the bright phase is PP.

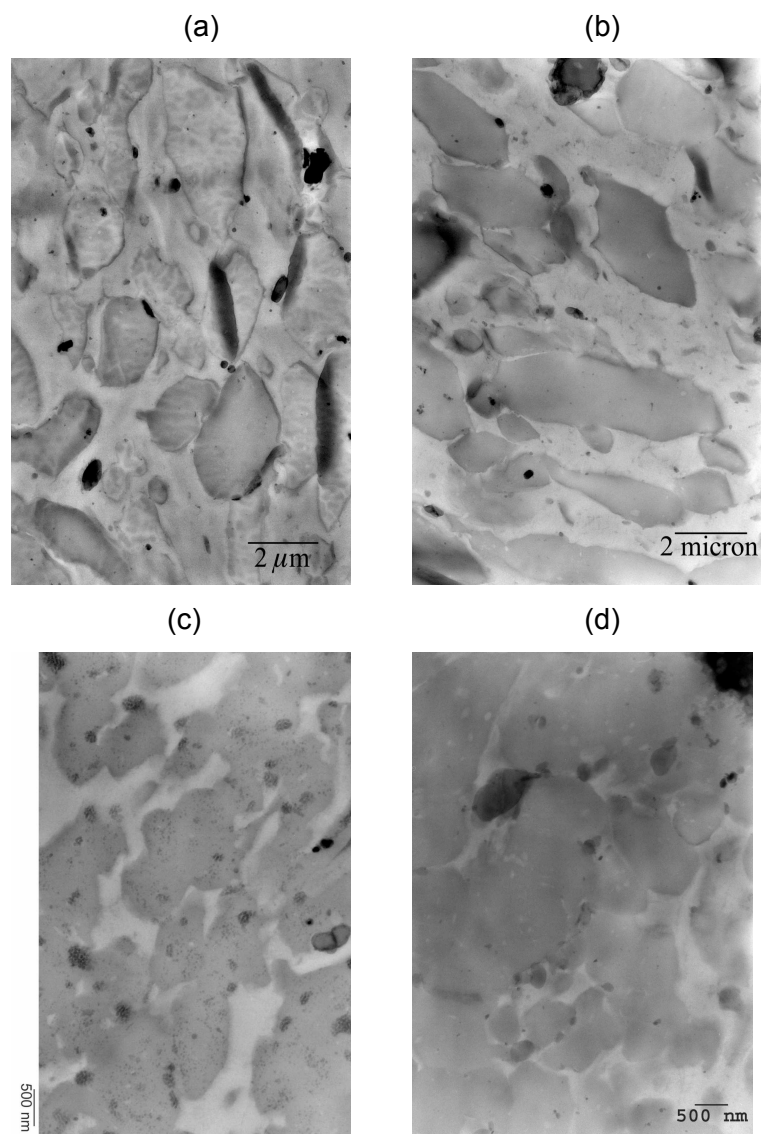


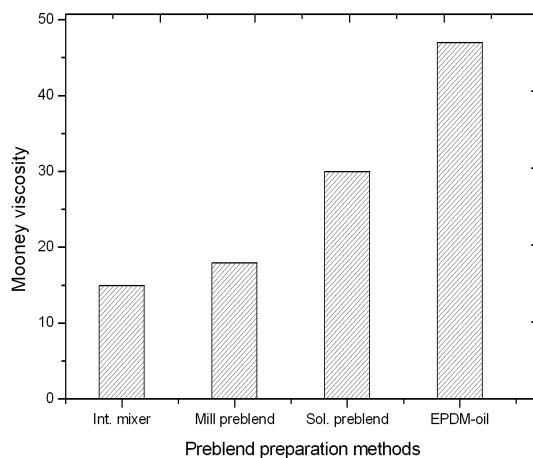
**Figure 7.8** TEM images of TPV blends having compositions: (a), CE5; (b), CE6; (c), CE1; (d), CE2.

The particles of EPDM are within 2-6  $\mu\text{m}$  in all cases. This proves that, provided the total shear and amount of resin remains the same, the particle size of the EPDM phase does not differ significantly.

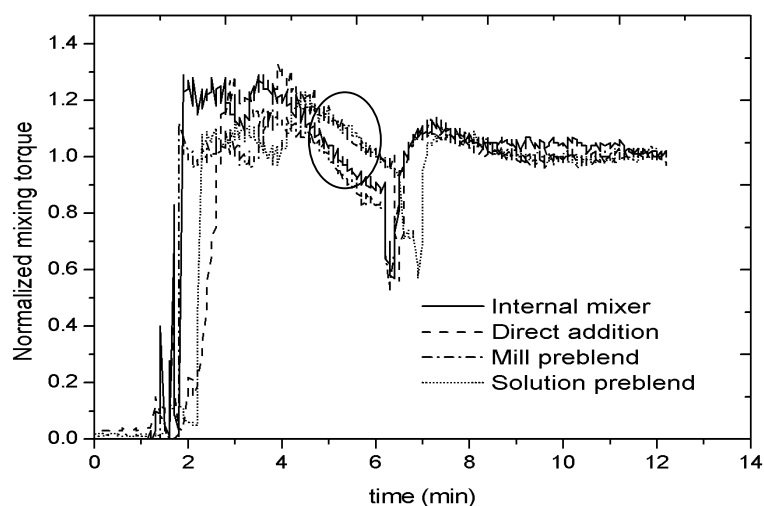
#### 7.3.4 Influence of oil preblending methods on the properties and morphology of TPVs

The effects of different preblending techniques on the Mooney viscosity of the EPDM-oil preblends are shown in the Figure 7.9. Since no molecular weight reduction should occur during solution preblending, the Mooney viscosity of the solution preblend can be considered as reference. Compared to the reference, the Mooney values dropped by 11 units during mill preblending and by 14 units during preblending in the internal mixer. Since the amount of oil incorporated in the blends during preblending is almost the same, as checked by extraction experiments, this drop in Mooney viscosity values reflects a drop in molecular weight of the EPDM-phase during the preblending process. The higher Mooney-drop in the internal mixer is probably due to the higher temperature involved during blending in that apparatus.

The effects of reduction in molecular weight of the EPDM on the viscosity of the EPDM-oil preblends are also visible from the torque curves as shown in Figure 7.10. These curves refer to the production of actual TPVs in the internal mixer. The viscosity of all these TPV blends before addition of the curatives depends on the viscosity of the EPDM/oil and PP/oil phases. As can be seen in the Figure 7.10, the blends with lower Mooney viscosity (prepared on the mill and internal mixer) also exhibit a lower torque during initial mixing in the internal mixer.

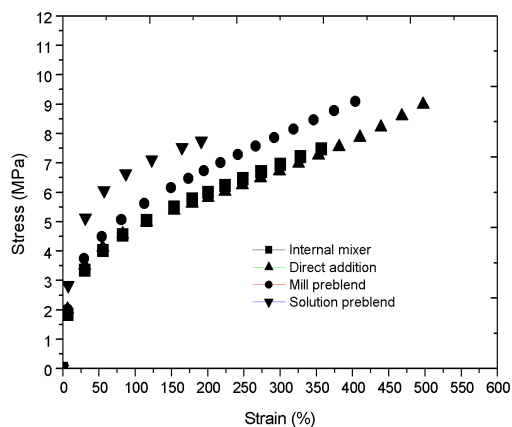


**Figure 7.9** Mooney viscosity, ML(1+4) at 125°C of EPDM-oil preblends

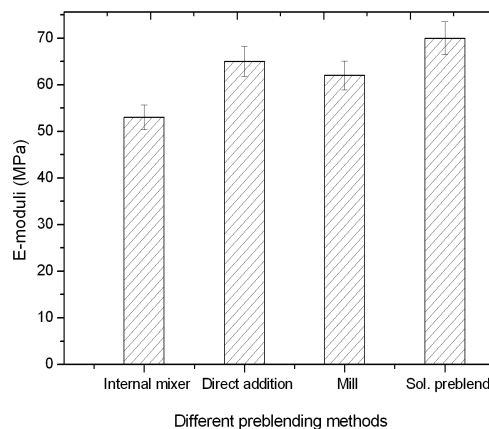


**Figure 7.10** Mixing curves in the internal mixer.

The effects of different oil preblending methods on the stress-strain properties and E-modulus of the TPVs are shown in Figures 7.11(a) and 7.11(b) respectively. As the EPDM molecular weight decreases due to the mastication effect, the E-modulus of the TPVs also decreases. The solution preblend, in which the EPDM was not masticated during preblending, shows the highest E-modulus and lowest elongation at break. The E-modulus values of the mill-preblended TPV and the direct-addition TPV are close, but the mill-preblended sample exhibits somewhat lower ultimate elongation. The preblend in the internal mixer, in which EPDM has suffered the maximum mastication, shows the lowest E-modulus and also the lowest tensile strength.

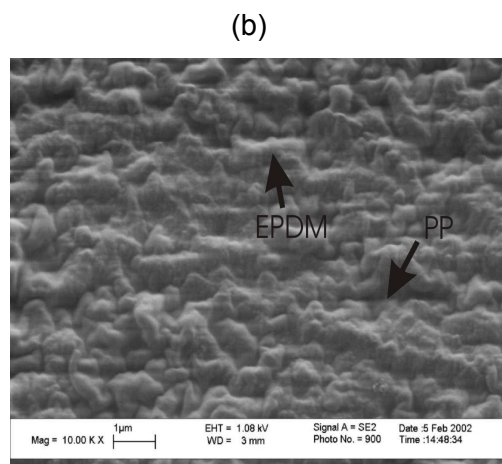
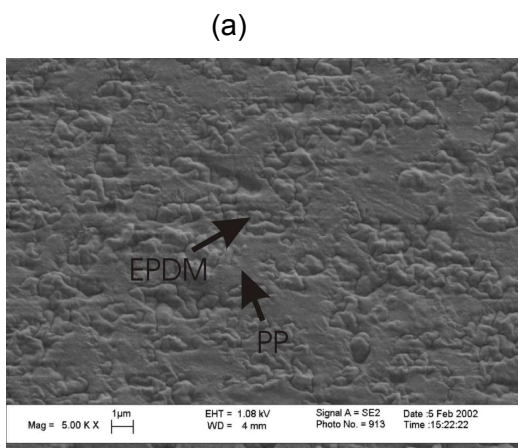


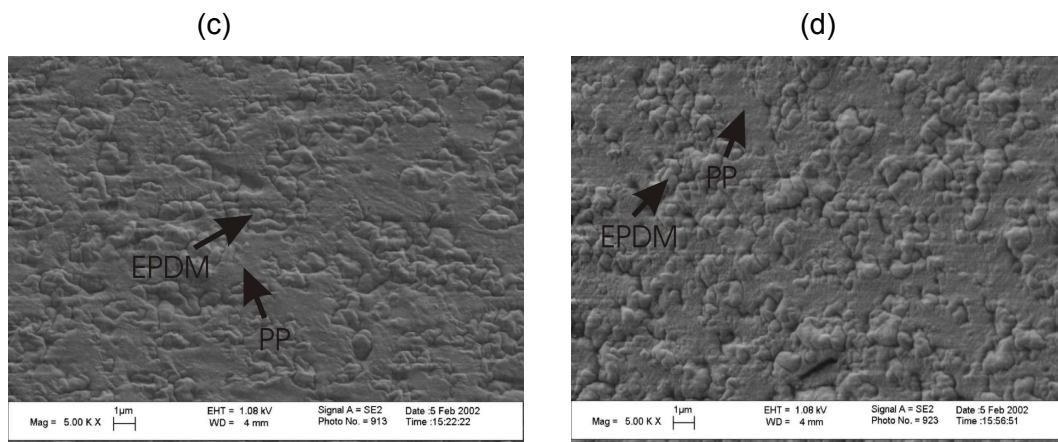
**Figure 7.11(a)** Stress-strain properties of TPVs prepared using different oil preblending methods



**Figure 7.11(b)** E-moduli of TPVs prepared using different oil preblending methods

Although the different oil preblending method has a strong influence on the stress-strain properties of the TPVs, their morphology is not affected. LVSEM images of the blends are shown in the Figures 7.12(a) – (d). The EPDM particles appear to be identical in size in all cases (1 micron in diameter) and well dispersed within the PP matrix. Any difference in the oil dispersion due to different preblending processes could not be found either.

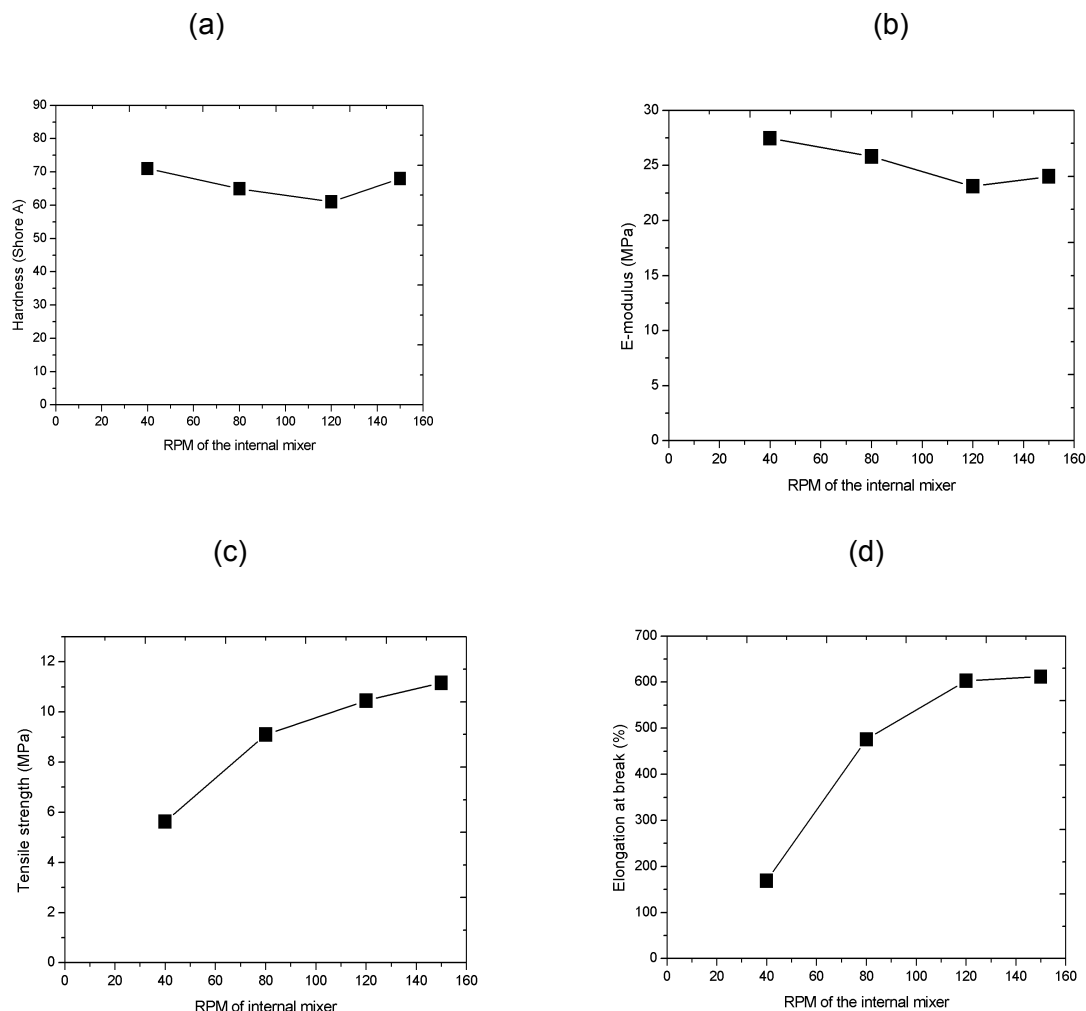




**Figure 7.12** Low voltage SEM image of TPVs prepared with different oil-preblending methods (a), Direct addition; (b), Mill; (c), internal mixer; (d), Solution preblending.

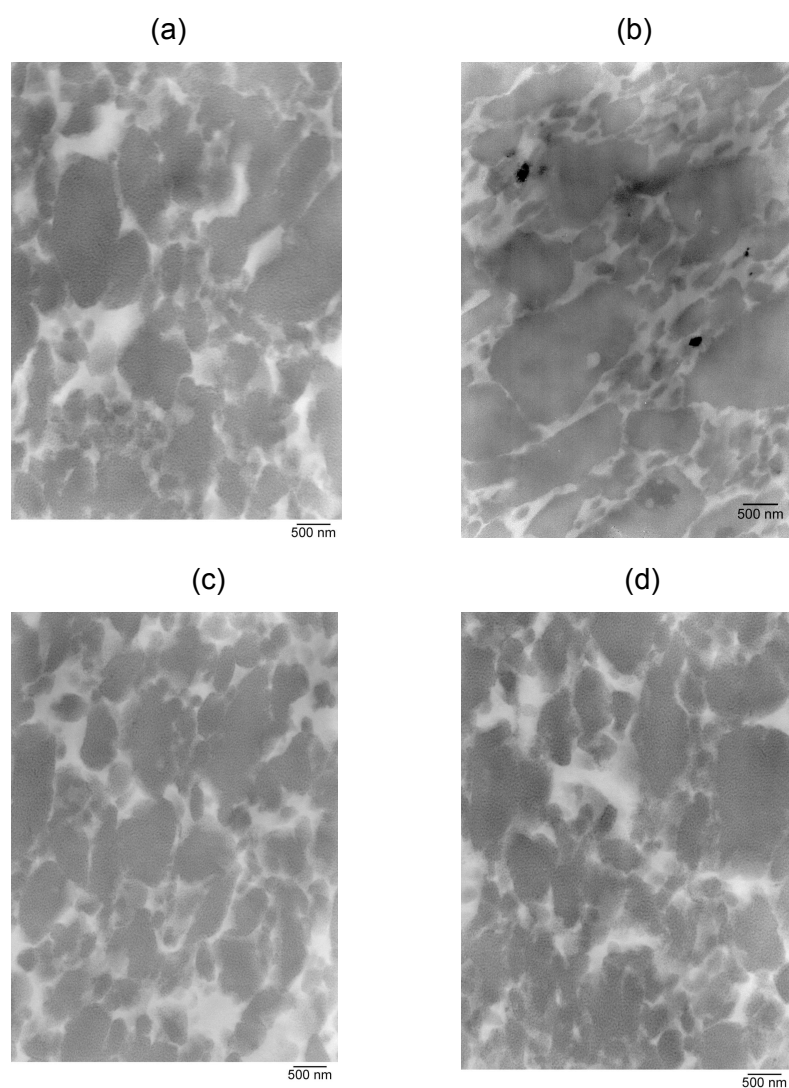
### 7.3.5 Influence of mixer rotor speed on the morphology of SEBS/PP/oil blends

Figure 7.13 shows the properties of blends - series CS1 to CS4 in Table 7.3 - prepared with different rotor speeds of the internal mixer. The E-modulus and the hardness do not change significantly with the change in RPM from 40 to 150. The tensile strength and elongation at break show a remarkable improvement. This suggests, that the degree of mixing of the SEBS- and PP-phases is improved with an increase in rotor speed.



**Figure 7.13** Tensile properties of SEBS/PP/oil blends prepared with different rotor speeds of the internal mixer.

Figure 7.14 shows the TEM-images of the blends prepared with different RPM of the internal mixer. The SEBS-phase remains fully continuous with the PP-phase in all cases. This was confirmed using the solvent extraction methods as described in Chapter 4. The SEBS domain sizes however decreases from an average of 2  $\mu\text{m}$  - Figure 7.14(a) - to an average of 0.5  $\mu\text{m}$  - Figure 7.14(d) - with increase in rotor speed.



**Figure 7.14** TEM images of SEBS/PP/oil blends having compositions prepared at: (a), 40 RPM; (b), 80 RPM; (c), 120 RPM and (d), 150 RPM.

### 7.3.6 Influence of the temperature of mixing on properties and morphology of the SEBS/PP/oil blends

The stress-strain properties of the SEBS/PP/oil blends prepared with various mixing temperatures: recipes AS1-AS3 in Table 7.3, are displayed in Figure 7.15. Although the curves obtained at 180°C and 200°C are close, the one obtained at 220°C lies below the other two. This is most probably due to degradation of the PP at high temperatures. In order to verify this effect, the same blend was prepared at 200°C without adding stabilizers. The stress-strain properties of this blend overlaps quite nicely



with that of the SEBS/PP/oil blend prepared at 220°C in the presence of stabilizers: Figure 7.15.

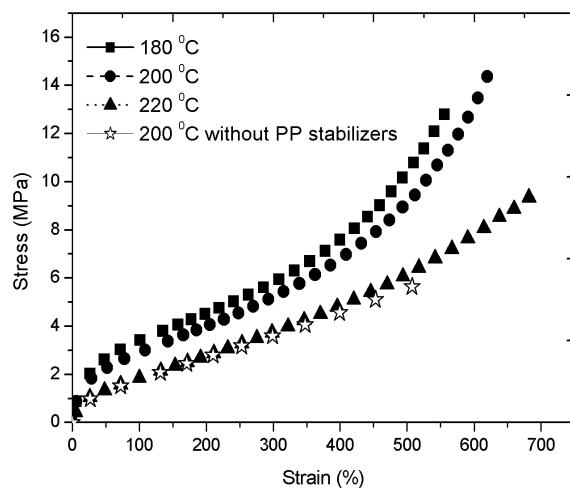


**Figure 7.15** Stress-strain curves for SEBS/PP/oil blends prepared at 180°C, 200°C and 220°C. The open symbols represent the stress strain curves of a blend without stabilizers and mixed at 200°C.

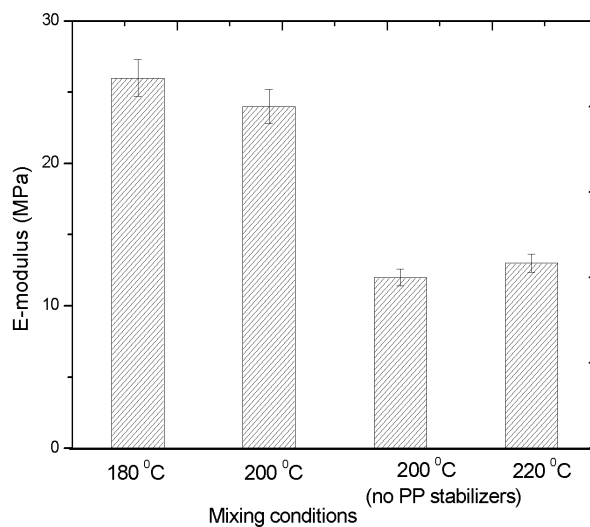


**Figure 7.16** E-moduli of SEBS/PP/oil blends prepared with different mixing temperatures.

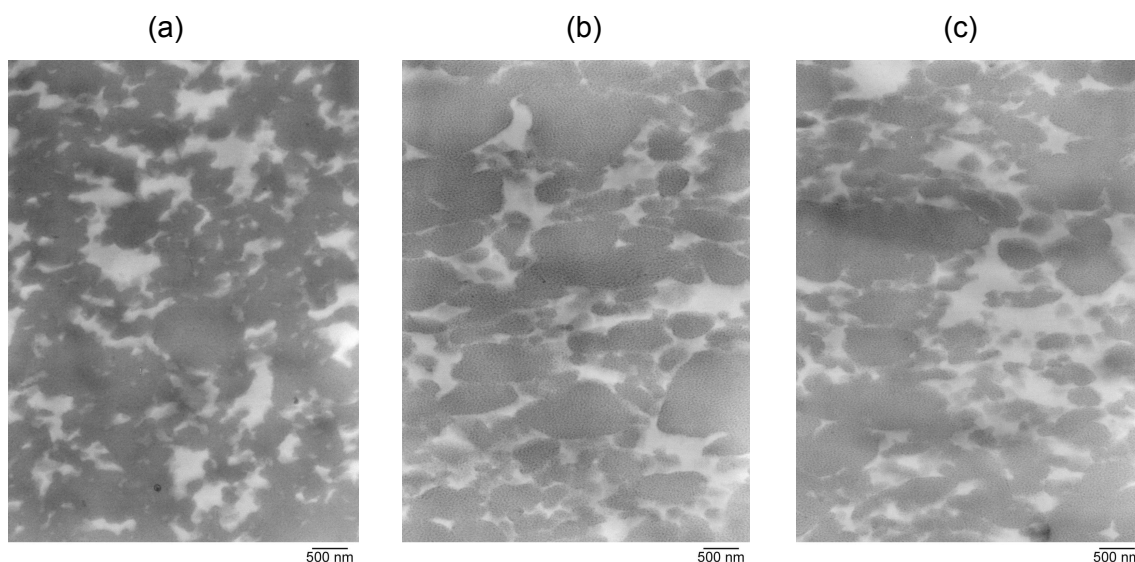


**Figure 7.17** TEM images of 31/25/43 wt.-%SEBS/PP/oil blends prepared at: (a), 180°C; (b), 200°C and (c), 220°C.

The degradation effect of temperature is also seen in the trends obtained with the E-moduli values reported in Figure 7.16. Again, the values for the SEBS/PP/oil blend at 200°C containing no stabilizers and the one at 220°C are almost the same, reconfirming that the PP phase degrades with an increase in the temperature of mixing.

Figure 7.17 shows the TEM images of the SEBS/PP/oil blends mixed at 180, 200 and 220°C. The interconnectivity between the SEBS domains deteriorates with an increase of temperature. Results from solvent extraction experiments also showed a decrease in the degree of co-continuity of the SEBS phase: Table 7.8.

**Table 7.8 The degree of continuity of the SEBS phase as measured by solvent extraction**

Temperature of mixing	180°C	200°C	220°C
Degree of co-continuity (%)	100	100	92

## 7.4 DISCUSSION

### 7.4.1 Effect of phenolic resin content on properties and morphology of TPVs

Increasing the amount of phenolic resin results in an increase of hardness, E-modulus, tensile strength and a decrease of elongation at break values and tension set of the TPVs. The changes in the mechanical properties are as expected on the basis of a higher crosslink density of the EPDM-phase. Although this EPDM-phase is dispersed

in the PP, the results show that it contributes significantly to the deformation process. According to Medintseva *et al.*,<sup>[13]</sup> a high degree of curing of the EPDM phase results in a coarse dispersion of EPDM. As a result, the PP matrix develops many defects and regions of discontinuities. This explains the reason for the lower elongation at break of TPV blends with an increase in phenolic resin content. According to morphology studies of Jayaraman *et al.*<sup>[3]</sup> and Thakkar *et al.*,<sup>[7]</sup> however, increasing the amount of curative results in a narrow particle size distribution, which is in contradiction to the observations of Medintseva *et al.* The present investigations using TEM show a tendency towards larger particle size with an increase in curative concentration: see e.g. Figure 7.2 and also Figure 7.8. However, an accurate estimate of particle size changes is difficult because of particle-particle overlap and the difficulties associated with TEM to see the particles as physically separated.

#### 7.4.2 Effect of MFI of PP on the properties and morphology of both blends

The dimensions of the rubber phase increased with an increase in the MFI of PP in both TPV and SEBS/PP/oil blends. This can be explained theoretically. According to Wu,<sup>[14]</sup> the particle size of the dispersed phase having viscosity  $\eta_d$  is given by the relation:

$$R = 4\lambda^{\pm 0.84} \frac{\nu_{12}}{\eta_m \dot{\gamma}} \quad (7.3)$$

where R is the radius of the particle,  $\lambda$  is the viscosity ratio defined as  $\eta_d/\eta_m$ ,  $\nu_{12}$  is the interfacial tension and  $\dot{\gamma}$  is the shear rate. The '+' sign in the exponent applies for  $\lambda > 1$  and the '-' sign for  $\lambda < 1$ . This relationship points out that increasing the viscosity ratio of the system results in larger particles. A minimum particle size is obtained when the ratio is close to unity. As the MFI of the PP is increased from 0.3 to 5.5 g/10 min, due to accompanying changes in molecular weight the viscosity of the PP-phase decreases. This results in an increase of the viscosity ratio, and as predicted by the equation (7.3) mentioned above, results in an increase of particle size. Note that the present results indicate that this relationship is also applicable to TPVs provided the total mixing time is kept constant.

A study of the mechanical properties of these blends shows, that the properties of both blends deteriorate with an increase of MFI. In case of TPVs, since other factors like the crystallinity of the PP, amount of phenolic resin, and mixing conditions were not

varied, this decrease in properties is most probably a consequence of increased EPDM particle size, as has been proposed earlier by Coran and Patel.<sup>[15]</sup> For the SEBS/PP/oil blends the reason for improvement must be the dispersion of SEBS domains in PP, obtained by reducing the MFI of PP.

#### 7.4.3 Effect of rotor speed on the properties and morphology of both blends

The results show that, provided the total strain is kept constant, the rotor speed does not influence the properties of the TPVs. Morphological images obtained for 40 and 80 RPM do not show differences in EPDM particle size either, where the mixing time has been adjusted to keep the total strain same. According to Medentseva *et al.*,<sup>[13]</sup> the criterion for dynamic vulcanization is:  $t_{mix} \leq t_i \leq t_{res}$ , where  $t_{mix}$  is the time of components mixing,  $t_i$  is the induction period of vulcanization and  $t_{res}$  is the residence time of the components in the mixer. The results show, that the particle size of EPDM is controlled by the total strain, i.e. the product of shear rate and residence time of the blend in the internal mixer. Note that the relationship between particle size and shear rate as proposed by Wu (equation 7.3), does not take into account the effect of total shear.

For SEBS/PP/oil blends the TEM-images show that the SEBS domain size marginally decreases with an increase in shear rate. The properties, especially the tensile strength and elongation at break, were found to increase with increasing rotor speed of the internal mixer. This most probably results from a better dispersion of the SEBS phase in the PP matrix, as evidenced by the smaller SEBS domain sizes.

### 7.5 CONCLUSIONS

The results demonstrate the different ways to alter the properties of TPV and SEBS/PP/oil blends, when prepared in the internal mixer. For TPV blends the stress-strain properties are changed by making variations in the blend composition, amount of crosslinking agent, MFI of PP and shear rate during mixing. If compositions, having oil amounts in excess of 100 phr are to be prepared, a preblending step in which EPDM is mixed with oil is necessary. The method of preblending can also influence the properties. Similarly, it is possible to vary the properties of SEBS/PP/oil blends by using PPs of different MFI, mixing at different shear rates or at different temperatures. Not all these methods have an influence on the morphology. The dispersed EPDM particle size in TPVs was found to increase by increasing the MFI of PP from 0.3 to 5.5 g/10 min. or by increasing the amount of phenolic resin from 5 to 10 phr. However, increasing the

shear rate from 40 RPM to 80 RPM or varying the method of oil addition to make a preblend, did not have a significant influence on the particle size of EPDM. The morphology of the SEBS/PP/oil blends also shows a coarsening of SEBS domains with an increase in the MFI of the PP or a decrease in rotor speed of the internal mixer. Increasing the mixing temperature resulted in loss of interconnectivity between the SEBS domains with a negative effect on the degree of co-continuity.

The separate experimental design used for TPVs can be combined with the help of Partial Least Square (PLS) model. This model can be used for predicting the mechanical properties at any desired composition or processing conditions. An example is shown in Figure 7.18(a), which shows the different possible ways to vary the hardness of a TPV: by changing the rotor speed and resin content at a fixed composition of PP (80 phr), keeping the MFI 0.3 g/10 min. fixed and the composition of oil fixed at 140 phr. Similarly, for SEBS/PP/oil blends the PLS design Figure 7.18(b) shows the influence of PP - and oil-content on hardness. Similar figures are possible for the other mechanical properties, not further pursued in the context of this thesis.

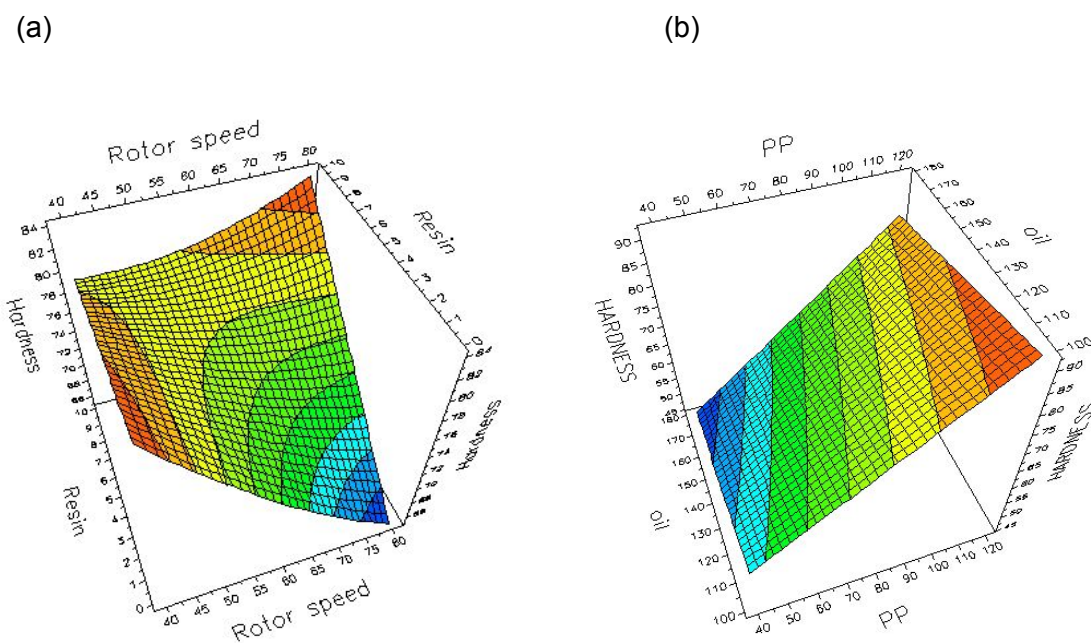


**Figure 7.18** Plots showing variation of Hardness with: (a), resin-content and oil-content for TPVs; (b), PP-content and oil-content for SEBS/PP/oil blends.

---

## 7.5 REFERENCES

1. D. R. Paul, S. Newmann, "Polymer Blends", vol. 1,2; Academic press, New York, 1978.
2. M. D. Ellul, Paper presented at 160<sup>th</sup> Fall Technical Meeting of the American Chemical Society, Rubber Division (2001), Cleveland.
3. K. Jayaraman, G. Kolli, M. D. Ellul, Paper presented at the International Rubber Conference, Prague (2002).
4. J. K. Lee, C. D. Han, Polymer, **40** (1999) 6277.
5. R. A. Shanks, B. E. Tiganis, Paper presented at ANTEC (1998), Atlanta.
6. Y. Li, H. J. Sue, B. Coleman, Paper presented at ANTEC (2001), Dallas.
7. H. Thakkar, L. A. Goettler, Paper presented at 163<sup>rd</sup> Spring Meeting of the American Chemical Society, Rubber Division, San Francisco, 2003.
8. S. M. Nachtigall, R. Baumhardt Neto, R. S. Mauler, Polym. Eng. Sci., **39** (1999) 630.
9. P. Sengupta and J. W. M. Noordermeer, Paper presented at Asia Rub. Tech. Expo (2002), New Delhi.
10. A. Vander wal, PhD thesis, University of Twente (1996), The Netherlands.
11. T. Roy in "Design and analysis in chemical research", 1st edn. Sheffield Academic Press, 2000.
12. S. Abdou-Sabet, M. A. Faith, U.S. patent 4,311,628 (1982).
13. T. Medintseva, N. Erina and E. Prut, Macromol. Symp., **176** (2001) 49.
14. S. Wu, Polym. Eng. Sci., **27** (1987) 335.
15. A. Y. Coran, R. P. Patel, Rubber Chem. Technol., **53** (1980) 781.

## **Summary**

---

Thermoplastic elastomers are materials, which combine the properties of vulcanized rubbers under ambient conditions with the processing versatility of thermoplastics. This thesis describes a study into the morphology and mechanical properties of thermoplastic elastomers based on blends of polypropylene with two different rubbers. The first rubber is EPDM and the corresponding blends are commonly known as EPDM/PP dynamic vulcanizates (TPVs). Dynamic vulcanizates are a unique category of thermoplastic elastomers in which the rubber phase is crosslinked during the process of melt mixing with a thermoplastic polymer. The second rubber is SEBS, a triblock copolymer in which poly (ethylene-butylene) blocks are sandwiched between two end polystyrene blocks. SEBS itself is already a thermoplastic elastomer. At room temperature the polystyrene heads of SEBS cluster together to form a physical network in the material. These blocks, which are typically, about 20 nm, impart elasticity to the material which makes it behave like a vulcanized elastomer. At 100 °C, the polystyrene blocks pass through their glass transition temperature, above which the material can flow. On cooling, the polystyrene blocks again solidify, and the material regains its elastic properties.

Commercial blends of EPDM/PP-TPVs and SEBS/PP are commonly extended with paraffinic oils. The oil improves processability, makes the blends softer and to a certain extent improves the elastic recovery. Often the amount of oil is over 100 phr, so that the blends can be considered as ternary blends of rubber, PP and oil.

Ternary rubber/PP/oil blends of TPVs and SEBS/PP/oil show properties that are remarkably similar for same sorts of application. For example, both blends are used in automotive under the hood applications, rack and pinion boots, airbag covers and many soft touch applications. This is surprising, because preliminary studies have shown that the blends have totally different morphologies. Since morphology is usually considered to be the most important parameter in controlling the properties of multiphase polymer blends, this paradox is difficult to understand. Another problem is, that the amount of information openly available on these blends is very little. Although TPVs are better documented than the SEBS/PP/oil blends in this respect, most studies on TPVs were conducted on relatively hard samples (higher than 60 shore A) and without oil as the third component.

The comparative study of EPDM/PP/oil based TPVs and SEBS/PP/oil blends reported in this thesis is an attempt to throw light onto this paradox. The ideal way to approach this problem is to conduct an in-depth study of the morphology, rheology and properties of these systems so as to understand the interrelationship between each parameter. In this thesis, morphology studies in relation to mechanical properties of these blends are reported; the rheological properties will be reported in a separate related additional thesis.

In recent times, several microscopic methods have become available for studying the morphology of polymer blends. Optical Microscopy, Scanning Electron Microscopy, Transmission Electron Microscopy, Atomic Force Microscopy and Confocal Scanning Laser Microscopy are all widely used in polymer science. Some of these techniques are complimentary to each other. Some have complex sample preparation techniques and some are very sensitive to the amount of oil present in the samples. Comparative studies of different microscopic techniques for characterizing the morphology of these blends are reported in Chapter 3 of this thesis. Two techniques which are especially found to be useful and will widely be used in this thesis are: Low voltage Scanning Electron Microscopy (LVSEM) and Transmission Electron Microscopy (TEM).

Most TEM images of these blends provide good enough evidence for the actual morphology of these blends. However, in some cases the TEM images are found to be misleading. This is especially so when the rubber content is relatively high relative to polypropylene as in a 70/30 EPDM/PP – TPV. TEM images of such blends often show interconnected rubber particles giving the impression of a continuous vulcanized elastomer phase, which is not to be expected from its thermoplastic processability. One way to solve this problem is to use Electron Tomography, a technique widely used in the biological sciences, but not explored yet in polymer material science. In this thesis the use of electron tomography as a tool for directly visualizing the three-dimensional morphology in polymer blends is reported.

Once the microscopic technique has been optimized, the next step was to investigate the stress-strain characteristic of these blends. Chapter 4 gives an overview of the comparative properties of the two blend types. The properties are found to vary both with the composition and blend production method, i.e. in an internal mixer or in a twin-screw extruder. The stress-strain curves are grossly comparable for both blend types, with the exception at large strains where the SEBS/PP/oil samples show pronounced strain hardening. The E-moduli are similar for both blend types, showing



that this property is little dependent on morphology. The tensile strength and elongation at break values are higher for SEBS/PP/oil blends as compared to the TPV analogues. The gel content of the TPVs is higher when prepared in the twin-screw extruder as compared to the blends in the internal mixer. Finally, the degree of crystallinity of the PP phase is slightly influenced by the blend preparation method, but this again does not correlate with the stress-strain properties.

Apart from the preparation methods, Chapter 5 shows that the stress-strain properties of the two blend types are also dependent on the oil distribution between the PP and rubber phase. In fact, the E-modulus values of both blends can be explained using empirical models from Coran, Veenstra, Takayanagi and Kolarik based on the properties of binary PP-oil and rubber-oil phases and the oil distribution values taken from the work of Sengers<sup>[1]</sup>. Unfortunately, these models lack parameters that can be related to blend morphology and so, for properties like elongation at break poor fits are obtained.

Most commercial grades of these two blend types are made in co-rotating twin-screw extruders and/or internal mixers. Chapter 6 shows how the blend morphology evolves in these mixers during compounding. In both mixing equipments the morphology evolves very rapidly and the first changes are difficult to detect. For TPVs the morphology is fixed after dynamic vulcanization and does not undergo any further changes. Due to a process of homogenization, which occurs with increasing mixing time, particle size distribution becomes narrow. The morphology of SEBS/PP/oil blends however, are more susceptible to changes due to variations in the mixing time or alterations in the screw configuration of the twin-screw extruder. The degree of co-continuity of the SEBS phase is found to increase in transporting zones of the twin-screw extruder, where more coalescence and less break-up of the SEBS phase is observed. In the kneading zones of the twin-screw extruder, more break-up of the SEBS domains is observed leading to a lower degree of co-continuity of the SEBS phase.

Chapter 7 investigates the influences of several other possibilities that can be used to vary the morphology. The factors investigated are: (1) influence of crosslinking agent; (2) influence of the melt flow index of the PP; (3) influence of the speed of mixing; (4) effect of different oil-preblending methods and (5) effect of the temperature of mixing. The properties of the blends can be altered by all these factors even though the morphology is not visibly altered by most of them.

As a conclusion, the results reported in this thesis show that there are several important factors, which dominate the properties of thermoplastic elastomer blends. A summary is given in Table 8.1. Morphology is only one parameter among many others, which has an influence on the properties. Most of the properties measured at low strains, e.g. the hardness and E-moduli are rather insensitive to changes in blend morphology. So, it is not surprising that although the morphologies of the TPVs and SEBS/PP/oil blends are basically different, their properties are close enough for similar sorts of applications.

**Table 8.1 Summary of Properties and main Influencing factors**

Properties	Influencing factors
Morphology	(1) Base polymers; (2) composition; (3) method of production; (4) configuration of the mixing equipment: ex. kneading blocks vs. transporting blocks; (5) process conditions;
Hardness	(1) PP/(Rubber+oil) ratio;
E-moduli	(1) PP/(Rubber+oil) ratio; (2) oil distribution; (3) morphology (?)
Tensile strength	(1) PP/(Rubber+oil) content; (2) oil distribution; (3) morphology
Elongation at break	(1) Type of the rubber ; (2) morphology;
Elastic properties: (compression set, tension set)	(1) Crosslink density of the rubber phase; (2) PP/(rubber+oil) ratio
Thermal properties	(1) Crystallinity of the PP phase and (2) type of rubber;

## Reference

1. W. Sengers, PhD thesis, Technical University Delft, The Netherlands, to be published.

## ***Samenvatting***

---

Thermoplastische elastomeren zijn materialen, die onder omgevingscondities de eigenschappen van ge vulcaniseerde elastomeren combineren met de verwerkbaarheid van thermoplasten. Dit proefschrift beschrijft een studie naar de morfologie en mechanische eigenschappen van thermoplastische elastomeren gebaseerd op mengsels (blends) van polypropreen met twee verschillende rubbers. De eerste rubber is EPDM en de corresponderende blends worden EPDM/PP dynamische vulcanisaten (TPVs) genoemd. Dynamische vulcanisaten zijn een unieke categorie van de thermoplastische elastomeren, waarin de rubber-fase wordt gecrosslinkt gedurende het smelt-mengproces met de thermoplast. De tweede rubber is SEBS, een triblok-copolyme er waarin poly(etheen-buteen)-blokken geplaatst zijn tussen twee polystyreen eindblokken. SEBS zelf is reeds een thermoplastisch elastomeer. Bij kamertemperatuur clusteren de polystyreen-blokken samen en vormen op deze wijze een fysisch netwerk in dit materiaal. Deze blokken, die een typische grootte hebben van ongeveer 20 nm, verlenen elasticiteit aan het materiaal, zodat het zich gedraagt als een ge vulkaniseerd elastomeer. De polystyreen-blokken bereiken bij 100 °C de glasovergang temperatuur, waarboven het materiaal kan vloeien. Bij daling van de temperatuur clusteren de polystyreen-blokken weer samen en krijgt het materiaal zijn elastische eigenschappen terug.

Commerciële blends van EPDM/PP-TPVs en SEBS/PP worden vaak verder gemengd met paraffinische olie. De olie bevordert de verwerkbaarheid, maakt de blends zachter en verbetert tot op zekere hoogte de elastische eigenschappen. Vaak wordt er meer dan 100 phr (parts per hundred rubber) gebruikt, zodat de blend opgevat moet worden als bestaande uit 3 componenten: rubber, PP en olie.

Ternaire blends van rubber/PP/olie, zoals TPVs en SEBS/PP/olie, vertonen opmerkelijk vergelijkbare eigenschappen voor dezelfde soort toepassingen. Zo worden bijvoorbeeld beide blends gebruikt voor toepassingen onder de motorkap van auto's, "rack and pinion boots", airbag afdekkingen en vele 'soft touch' toepassingen. Dit is verrassend, omdat voorgaande studies hebben aangetoond dat beide blends een totaal verschillende morfologie hebben. Aangezien morfologie gezien wordt als de belangrijkste parameter, welke de eigenschappen van multi-fase polymere blends bepaalt, is deze paradox moeilijk te begrijpen. De beperkte publieke toegankelijkheid van informatie over dit soort blends vormt nog een probleem. Over TPVs is de meeste

informatie beschikbaar, maar de meeste studies over TPVs zijn uitgevoerd aan relatief harde monsters (meer dan 60 shore A) en zonder olie als derde component.

De vergelijkende studie aan EPDM/PP/olie-gebaseerde TPVs en SEBS/PP/olie-blends, waarover verslag wordt gedaan in dit proefschrift, is een poging om meer licht te laten schijnen op deze paradox. De ideale manier om dit probleem te benaderen is het verrichten van een dieptestudie naar de morfologie, rheologie en eigenschappen van deze systemen, zodat de relatie tussen deze parameters kan worden begrepen. In dit proefschrift worden alleen de morfologie-studies en de mechanische eigenschappen beschreven; de rheologische eigenschappen zullen worden beschreven in een gerelateerd aanvullend proefschrift<sup>[1]</sup>.

Recentelijk zijn allerlei microscopische technieken beschikbaar gekomen om de morfologie van polymere blends te bestuderen. Optische microscopie, Scanning Electron microscopy, Atomic Force microscopy en Confocal Scanning Laser microscopy worden allemaal veel gebruikt in de polymeer-wetenschap. Sommige van deze technieken zijn een aanvulling op andere. Sommige vereisen een ingewikkelde monstervooreibeding en zijn erg gevoelig voor de hoeveelheid olie, die in het monster aanwezig is. Een vergelijkende studie tussen verschillende microscopische technieken wordt beschreven in hoofdstuk 3 van dit proefschrift. Twee technieken, die bij uitstek toepasbaar blijken en veel gebruikt worden in dit proefschrift zijn: Low Voltage Scanning Electron microscopy (LVSEM) en Transmission Electron microscopy (TEM).

De meeste TEM-afbeeldingen van de blends blijken voldoende om een beeld te vormen van de morfologie. In sommige gevallen echter blijken TEM-afbeeldingen misleidend te zijn. Dit is in het bijzonder het geval, als de hoeveelheid rubber ten opzichte van de hoeveelheid PP relatief groot is, zoals in een 70/30 EPDM/PP-TPV. TEM-afbeeldingen van zulke blends laten vaak een elastomere fase zien, die aaneengesloten lijkt te zijn, wat niet verwacht mag worden vanwege de thermoplastische verwerkbaarheid. Een manier om dit probleem op te lossen is Electron Tomography, een techniek die veel gebruikt wordt in de biologie, maar nog niet in de materiaalwetenschap. In dit proefschrift wordt het gebruik van Electron Tomography beschreven voor het visualiseren van de driedimensionale morfologie van polymere blends.

De volgende stap na het optimaliseren van de microscopietechniek is het onderzoeken van de trek-rek eigenschappen van deze blends. Hoofdstuk 4 geeft een overzicht van de vergelijkende eigenschappen van deze blends. De eigenschappen

blijken te variëren met zowel de samenstelling als met de blend bereidings-methode, dat wil zeggen: mengen in een interne menger of in een dubbelschroefs-extruder. De trek-  
rek curven blijken meestal hetzelfde voor beide blend types, behalve bij grote rekken, waarbij de SEBS/PP/olie krommen duidelijk strain-hardening vertonen. De E-moduli zijn voor beide blend types min of meer gelijk, wat erop duidt dat zij weinig afhankelijk zijn van de morfologie. De waarden voor de treksterkte en de rek bij breuk vallen voor SEBS/PP/olie blends hoger uit dan voor de TPV-analogen. Het gel-gehalte van de TPVs blijkt hoger te zijn, wanneer deze bereid worden in de twin-screw extruder in vergelijking met de interne menger. Het gehalte aan kristalliniteit van de PP-fase wordt beïnvloed door de blend bereidingsmethode, maar correleert niet met de trek-rek eigenschappen.

De trek-rek eigenschappen blijken ook afhankelijk te zijn van de olie-verdeling tussen de PP- en de rubber-fase, zoals in hoofdstuk 5 wordt aangetoond. De waarden voor de E-moduli kunnen in feite verklaard worden door gebruik te maken van empirische modellen van Coran, Veenstra, Takayanagi en Kolarik, gebaseerd op de eigenschappen van tweeledige PP-olie en rubber-olie fases, en de olie verdeling in elk van beide fases. Helaas ontbreken in deze modellen parameters voor de blend-morfologie, zodat de berekende waarden voor treksterkte en rek bij breuk slecht overeenkomen met de experimentele waarden.

De meeste commercieel verkrijgbare blends van deze twee types worden gemaakt in een co-roterende dubbelschroefs-extruder en/of een interne menger. Hoofdstuk 6 laat zien hoe de blend-morfologie zich ontwikkelt in deze mixers gedurende het mengproces. In beide mengapparaten ontwikkelt de morfologie zich erg snel en de allereerste veranderingen zijn nauwelijks waar te nemen. Voor TPVs ligt de morfologie vast na dynamische vulkanisatie en deze verandert verder niet meer. Door het homogenisatieproces, dat plaatsvindt bij lange mengtijden, wordt de deeltjesgrootte-verdeling nauwer. De morfologie van SEBS/PP/olie blends daarentegen, is gevoeliger voor veranderingen in mengtijd of veranderingen in de schroefconfiguratie van de dubbelschroefs-extruder. De mate van co-continuïteit van de SEBS-fase blijkt hoger te zijn in de transport-zones van de dubbelschroefs-extruder, waar meer coalescentie en minder afbraak van de SEBS-fase wordt waargenomen. In de kneed-zones van de dubbelschroefs-extruder wordt meer afbraak van de SEBS-domeinen geconstateerd, wat leidt tot een lage co-continuïteit van de SEBS-fase.

In hoofdstuk 7 wordt het onderzoek beschreven naar verschillende andere mogelijke factoren, die de morfologie kunnen beïnvloeden. De onderzochte factoren zijn

(1) de invloed van de crosslinking agent; (2) de invloed van de melt flow index van PP; (3) de invloed van de mengsnelheid; (4) het effect van verschillende olie preblend-methoden en (5) het effect van de mengtemperatuur. De eigenschappen van de blends zouden kunnen veranderen door deze factoren, ook al wordt de morfologie door enkele niet veranderd.

De algehele conclusie uit dit proefschrift is dat er verschillende belangrijke factoren zijn, die de eigenschappen van thermoplastische elastomeren bepalen. Een samenvatting wordt gegeven in Tabel 8.1. Morfologie is slechts één parameter van de vele andere, die een invloed hebben op de eigenschappen. De meeste eigenschappen bij kleine rekken: bijvoorbeeld de hardheid en E-modulus, zijn nogal ongevoelig voor veranderingen in blend-morfologie. Het is dus niet verassend, dat ondanks de verschillen in morfologie van de TPVs en de SEBS/PP/olie blends, de eigenschappen voor vergelijkbare toepassingen dicht bij elkaar liggen.

**Tabel 8.1 Samenvatting van de eigenschappen en belangrijkste invloeds-factoren**

Eigenschappen	Factoren
Morfologie	(1) Soort polymeer; (2) samenstelling; (3) productiemethode; (4) configuratie van de mengapparatuur, bv. kneed-blokken vs. transport-blokken; (5) procescondities;
Hardheid	Afhankelijk van (1) PP/(rubber + olie) verhouding;
E-modulus	Afhankelijk van (1) PP/(rubber + olie) verhouding; (2) olie-verdeling; (3) morfologie (?);
Treksterkte	Afhankelijk van (1) PP/(rubber + olie) gehalte; (2) olie verdeling; (3) morfologie
Rek bij breuk	Afhankelijk van (1) rubber fase; (2) morfologie;
Elastische eigenschappen	Afhankelijk van (1) crosslink-dichtheid van de rubberfase; (2) PP/(rubber + olie) verhouding;
Thermische eigenschappen	Afhankelijk van (1) PP-fase; (2) het soort rubber;

**Referentie**

1. W. Sengers, Proefschrift Technische Universiteit Delft, in voorbereiding.

### List of symbols

$A$	Parameter inversely proportional to extent of interfacial bonding in Kolarik model
$a$	Parameter related to volume fraction of PP in Veenstra models C and D
$b$	Parameter related to volume fraction of rubber in Veenstra models C and D
$\Lambda$	Amount of continuous crystalline fraction in the blend as used in Takayanagi model
$\psi$	Dimensions of a unit cube in Veenstra model A and B
$\kappa$	Capillary number
$f$	Degree of co-continuity in the blend as used in Coran's model
$\mu$	Diffusion coefficient
$D$	Drop diameter
$E$	E-modulus
$n$	Fitting parameter used in Coran's model
$\delta$	Gap between rotor tip and mixing chamber in internal mixer
$\nu$	Interfacial tension
$M$	Any mechanical property e.g. E-modulus or tensile strength
$M_a$	Mechanical property of amorphous fraction of the blend as defined by Takayanagi model
$M_c$	Mechanical property of amorphous fraction of the blend as defined by Takayanagi model
$M(A)$	Mechanical property of the blend as calculated by Veenstra A model
$M(B)$	Mechanical property of the blend as calculated by Veenstra B model
$M(C)$	Mechanical property of the blend as calculated by Veenstra C model
$M(D)$	Mechanical property of the blend as calculated by Veenstra D model
$M_m$	Mechanical property of the matrix phase
$N$	Normal stress
$K$	Oil distribution coefficient
$P_e$	Peclet number
$S$	Rotor speed
$\dot{\gamma}$	Shear rate
$\sigma$	Stress
$TS$	Tensile strength
$\eta$	Viscosity
$\lambda$	Viscosity ratio
$\phi$	Volume fraction



### Abbreviations

AFM	Atomic force microscopy
BR	Polybutadiene rubber
BSE	Back scattered electrons
CCD	Charged coupled device
<sup>13</sup> C-NMR	Carbon Nuclear magnetic resonance spectroscopy
DCP	Dicumyl peroxide
DMA	Dynamic mechanical analysis
DOI	Design of experiments
DRS	Dielectric relaxation spectroscopy
DSC	Differential scanning calorimetry
EBM	Equivalent box model
ENB	Ethylidene norbornene
EPDM	Ethylene propylene diene rubber
ESR	Electron spin resonance
<sup>1</sup> H-NMR	Proton- nuclear magnetic resonance spectroscopy
LM	Light microscopy
LVSEM	Low voltage scanning electron microscopy
MFI	Melt flow index
MLR	Multiple regression analysis
NBR	Acrylonitrile butadiene rubber
NR	Natural rubber
ODT	Order-disorder temperature
PP	Polypropylene
RPM	Revolutions per minute
SBCs	Styrenic block copolymers
SBR	Styrene butadiene rubber
SBS	Styrene-butadiene-styrene triblock copolymer
SEBS	Styrene-(ethylene-butylene)-styrene triblock copolymer
SEM	Scanning electron microscopy
SEPS	Styrene-(ethylene-propylene)-styrene triblock copolymer
SIS	Styrene-isoprene-styrene triblock copolymer
TAC	Triallyl cyanurate
TEM	Transmission electron microscopy
TPA	Thermoplastic polyamides
TPEs	Thermoplastic polyesters
TPEt	Thermoplastic polyethers
TPO	Thermoplastic polyolefins
TPUs	Thermoplastic polyurethanes
TPVs	Thermoplastic vulcanizates
UV	Ultraviolet
WAXD	Wide angle X-ray diffraction

---

## Curriculum Vitae

---

Pratip Sengupta was born on the 9<sup>th</sup> February 1975 in Nagpur, a city in central India. After the initial 12 yrs school education in Nagpur, he moved to Calcutta, for Bachelors education. In 1995 he graduated with Chemistry honours from the University of Calcutta. After his graduation in chemistry he studied Polymer science for three years and in 1998, obtained a graduate degree (Bachelor of Technology) in Polymer science and Technology from the same university. In the two following years, he studied Rubber technology and obtained a Master's degree from Indian Institute of Technology (IIT) Kharagpur. During this study he received a DAAD scholarship from the German government through which he could do his master project work in Germany. He did this project in RWTH Aachen, under the guidance of Prof. B. Blümich, Institute of Makromolecular Chemie. This project that lasted for nine months, involved studying the interface between two different elastomer having different levels of curatives using NMR-imaging.

In 2000, he joined the Rubber technology group of Prof. J.W.M. Noordermeer, at the University of Twente, as a research fellow. In this project he investigated the structure-property relationship of Thermoplastic elastomer blends. The results of his research are described in this thesis.

Since 2004, he is working as a material development engineer in SABIC EUROPETROCHEMICALS B.V.

## Acknowledgements

---

I still remember the day I was interviewed by Prof. Noordermeer at DSM. I was staying in Aachen at that time, working on my Master's project. After some interviews, one of which even took place at the DSM canteen, I was offered a PhD position in his group. I knew very little at that time my future project and I was wondering how it would be to work under him? I had many questions in my mind...is he going to give me the personal freedom in the research? Can I work in a big project with many industrial partners ? Can I adjust in a Dutch society? Looking back, I feel very glad that I accepted his offer!!

Prof. Noordermeer, my first and foremost acknowledgement goes to you for offering me a PhD position in your group. I have always appreciated your knowledge, straightforwardness and honesty. You always encouraged me when things were not going well and directly criticized me whenever I was wrong. You have left a deep impression on me with your very high work standards, critical scientific evaluation and your aim for perfection. I must have given you a really hard time during the writing phase of my thesis due to my inconsistencies, but I never heard you complaining!!

Dear Auke, I am very grateful to you for finding all the time to correct my thesis in spite of your busy schedule. You corrected my chapters even during your vacation!! And Rabin (Kaku) - I am equally grateful to you for your suggestions and critical comments on my work.

Wilco (Sengers)- I highly acknowledge your continuous support to our project during these four years. I think we made an excellent team - you looking at the rheology and me looking at the morphology. We always shared each other's results and you were always available for suggestions, comments and discussions. I wish you **“good luck”** in finishing, your part of this project - without your thesis, mine will remain incomplete!!

I acknowledge Prof. Picken, Prof. Vansco, Prof. Poelsema and Dr. Jolly for being part of my PhD committee. The DPI committee members - Dr. A. Gotsis (TU Delft), Dr. M. van Duin (DSM Elastomers), Mr. A. Dozeman (DSM Elastomers), Dr. W. Zoetlief (DSM Elastomers), Mr. X. Muijldermans (Kraton Polymers), Mr. B. van Baarle (TNO), Mr. R. Sturme (Océ) and Dr. J. Jelenich (Akzo Nobel) are all acknowledged for their very active participation in this project, helping us with their materials, sample preparation and constant guidance.

Mark (Smithers) – Most of the images in this thesis are taken by you. Thanks a lot for helping me with the SEM and TEM experiments. I appreciate your corrections regarding the Chapter 3 of my thesis. I also want to thank Léon Segeren, Leon Beekmans, Martin and Clemens for helping me with the AFM experiments.

Special thanks goes to Dr. W. Geerts, molecular cell biology, University of Utrecht, for the Tomography experiments. Willie, I am really indebted to you for introducing me to the amazing

field of electron tomography. I went to you twice and on both occasions it took us the whole day before we could make some good tomography images. However, you did not even charge me for all those expensive measurements!! Moreover, you also corrected the Chapter 3 of my thesis. I am greatly indebted to you for everything you have done for me !!

I also want to thank Dr. P. Frederick from the department of electron microscopy, University of Maastricht, for teaching me the art of cryo-microtoming. After your training, I learnt to make 4-5 TEM samples per day while before that it used be only 2-3 and then I was even not sure about their quality. Douwe Wiebe...Special thanks to you for introducing me to optical microscopy and helping me with the microtome. You have been of constant help to me during this project and I have learnt a lot from you!!

My life at Twente would have been dull and boring without the ever-enthusiastic RBT group. It's an amazing cluster of funny, wonderful and lively young people within a single umbrella. Annemieke, Louis, Geert, Dries, Kinsuk, Jan, Wilma, Subhasda, Vipin, Alexej (bad that you left), Francesca, Montse, Richard, Wilco, Marek, Kuno, Joost, Nitu uncle, Kannika, Tony, Ray, Homey, Dorothea tall and Dorothea short - I have received help from everyone of you at one time or the other. I have so many pleasant memories from the movie evenings, occasional parties, borrels, dinner evenings and shooting sessions that it is impossible to narrate them here. Annemieke, I still remember you, trying to support me on my first skating adventure. I am looking forward to our next trip. Montse, why were you so angry at my chair everyday? It was really annoying when you hit it, but now I miss it! And Francesca, my chips eating buddy, I don't have words enough to thank you. The times that we have been together are all part of my sweet memories. Marek, sometimes I kicked at your door to scare you - SORRRY!! Wilco, Thanks for the Dutch translation of the summary!! You have to visit me again so that this time I can show you the caves of Valkenburg. Louis and Dries, you guys have helped me a lot during the initial experiments in the internal mixer. Geert, you always solved my computer problems. I felt ashamed when you gave me my concept thesis with your corrections! I really didn't see all those vital mistakes! And Gerda, I wonder how you can be so nice and co-operative towards me throughout these 4 yrs although I was also annoyed you along with others.

I want to acknowledge the special help that I received from the STEP and ATEX for my experiments in particular from Wilco, Dries Ype and Mathian. I could walk to their office anytime with my questions and they always had time for me. Edwin and Bas (PBM), I enjoyed organizing the triathlon and writing the Duursport with you. Dr. Gaymans, I am also grateful to you for your help and cooperation whenever I went to you with my questions.

I want to thank my colleagues and staff members (including Karin and Geneviève) from PBM, STEP and MTP especially Menno, Anne, Audre, Miechel, Joost, Marianne, Dirk, Piet (when shall we go to Githorn?) Zheng, Josien, Judith, Zhiyuan, Fenghua, Priscilla, Debby, Beata, Nina, Beata, Atila, Alex, Eva, Laura, Christine, Boon Hua, Ingrid, Mark A, Mark t B, Igor, Nikodem,

Monique, Wei Song and Zlata!! The coffee table was always a prime attraction for daily chit-chat, and spicy, harmless gossips. It was also a place of learning from each other's different national and cultural background. Then there were occasional social events like promotion parties, oliebollen, sinterklaas, wadlopen and of course the Triathlon. All together, it was a superb experience!!

This thesis would have been never complete without the co-operation of my new SABIC-colleagues. Klaas, Lada, Patrick, Peter, Rolf, Maria, Hans, Jacques, Rieky, Kathleen, Jos, Roel, Truus, Stuf and Harrie. You guys have helped me during the final stages of this thesis. Only because of your understanding, I could finish this work along with my day-to-day work at SABIC.

Next on my acknowledgement list comes my Indian friends and well-wishers. All of you are so close to me that I feel it too formal to say "Thank you". I always had the feeling that after office hours and during the weekends, I am back to Calcutta among my family. Kinsuk, Sankhoda, Saheli, Subhasda, Nitu kaku, Diptish, Richa, Kaushikda, Rituparna boudi, Rajada, Sharmisthadi, Parthoda, Moushumidi, Pranabda, Nelly, Swapanda, Anjana, Sumona kakima, Nikhilda and Rituparna boudi, I am absolutely flattered for all your love and affection for me. Needless to say, I share a very special tie with every one of you and I feel very proud about it.

My "paranimfen" Aandries and Sankhada – you guys are very special to me. I am indebted to both of you for your extraordinary help, support and friendship. I will feel very proud to see you around me during the defense.

My final acknowledgement goes to my family-my father, mother and sister- for their love and affection towards me which, helped me to finish this gigantic work.

*Pratip*